EVALUATION OF EFFECTS OF CYP450 DERIVED EICOSANOIDS IN CEREBRAL ISCHEMIA

By

Jafar Sadik Bhasha Shaik

Bachelor of Pharmacy (B. Pharm.), Birla Institute of Technology & Science, Pilani, INDIA 2002

Master of Pharmacy (M. Pharm.), Birla Institute of Technology & Science, Pilani, INDIA 2004

Submitted to the Graduate Faculty of

The School of Pharmacy in partial fulfillment

of the requirements for the degree of

Doctor of Philosophy

University of Pittsburgh

2013

UNIVERSITY OF PITTSBURGH

SCHOOL OF PHARMACY

This dissertation was presented

By

Jafar Sadik Bhasha Shaik

It was defended on

October 24, 2013

and approved by

Committee Members:

Raman Venkataramanan, Ph.D., Dept. of Pharmaceutical Science, School of Pharmacy

Regis R. Vollmer, Ph.D., Dept. of Pharmaceutical Sciences, School of Pharmacy

Steven H. Graham, M.D., Ph.D., Dept. of Neurology, School of Medicine

Philip E. Empey, Pharm.D, Ph.D., BCPS, Dept. of Pharmaceutical Sciences, School of Pharmacy

Samuel M. Poloyac, Pharm.D., Ph.D., Dept. of Pharmaceutical Sciences, School of Pharmacy

EVALUATION OF EFFECTS OF CYP450 DERIVED EICOSANOIDS IN CEREBRAL ISCHEMIA

Jafar Sadik Bhasha Shaik, M. Pharm., Ph.D.

University of Pittsburgh, 2013

Stroke and cardiac arrest (CA) both are characterized by severe fall in the cerebral blood flow (CBF) locally or globally at the onset of the event with subsequent prolonged reductions observed after initiation of reperfusion. These CBF derangements may lead to secondary neuronal damage and worse functional outcomes. Currently there is limited understanding of the causative factors of CBF dysregulation after cerebral ischemic injury. Among the many known vasoactive substances, CYP450 derived metabolites of arachidonic acid (AA), called CYP eicosanoids were shown to act as potent regulators of microvascular tone. The main objective of this research was to investigate the role of CYP eicosanoids in the cerebral ischemic injury using *in vitro* and *in vivo* models of ischemia. In order to characterize the regional and temporal distribution of CYP eicosanoids in the brain after ischemic injury, sophisticated lipidomics based analytical methods were developed and validated.

Studies in *in vitro* neuronal cultures indicated that 11,12-EET (vasodilatory) exhibited concentration-dependent neuroprotective effects whereas 20-HETE (vasoconstrictive) exhibited concentration-dependent toxic effects in a hypoxia-reoxygenation injury model. We have used two pharmacological inhibitors of CYP eicosanoid pathway for *in vivo* studies namely *t*-AUCB, an inhibitor of soluble epoxide hydrolase (sEH) that converts EETs to inactive DHETs (dihydroxyeicosatrienoic acid), and HET0016 that inhibits 20-HETE synthesis. The *in vivo* studies

in animal model of focal ischemia with *t*-AUCB showed the following key findings: i) significant reduction in the infarct size by specifically increasing the ratio of EET/DHET in the cortex; ii) significant improvement in the short-term functional outcome after acute administration; iii) marginal improvement in CBF around the infarcted area during the post-ischemic reperfusion, and iv) dose-dependent significant increase in the neuronal survival in a hypoxia-reoxygenation injury model of primary rat cortical neuronal cultures.

Our studies in animal model of global ischemia showed a specific pattern of CBF dysregulation during the reperfusion phase that is dependent on the duration of the initial injury itself. Our lipidomics analysis of regional and temporal distribution of AA metabolites in the rat brain revealed a significant imbalance in the tissue levels of these metabolites, and their association with the pathological changes in CBF in the cortex post resuscitation from different durations of CA. The studies with acute administration of HET0016 showed improvement in the cortical CBF during the early reperfusion phase after 12 min CA by selectively inhibiting 20-HETE levels in the cortex. Further, we showed significant reduction in neuronal death, and improved short-term behavioral performance after a single low dose administration of HET0016.

In conclusion, these results showed the evidence that CYP eicosanoids are associated with CBF dysregulation after ischemic injury in both focal and global ischemia, and that alteration of CYP eicosanoids levels in brain tissue with pharmacological inhibitors improves short-term functional outcome through vascular and non-vascular mechanisms. Further research is warranted in order to design an effective therapeutic strategy for administering pharmacological inhibitors of CYP eicosanoid pathway to rectify the CBF dysregulation and improve the long-term functional outcomes after stroke injury.

TABLE OF CONTENTS

LIST OF TABLES

LIST OF FIGURES

PREFACE

My decision to choose pharmacy as a discipline when I first began my undergraduation 15 years ago has given me a unique, and remarkable experience as I embarked on a research career in pharmaceutical sciences. Along this journey, my interactions with professors, researchers, students, friends, and family have influenced me in defining a set of personal goals for myself of which one of the greatest goals is to earn a Ph.D. degree in pharmaceutical sciences. There are many who have encouraged, and helped me in achieving this goal. It is difficult to thank everyone who has contributed to my success however, there are a few people who have played a major role in my achievements. So I would first like to express my sincere thanks and gratitude to my advisor Dr. Samuel Poloyac, who I had the privilege to work for and learn from in the last six years at University of Pittsburgh. His mentorship, dedication to work has motivated and stirred passion for research in me and shaped me in to an enthusiastic researcher. Under his guidance, I have developed skills such keen scientific thinking, and critical analysis that helped me in accomplishing my research goals. I would like express my sincere thanks and appreciation to my committee including Dr. Raman Venkataramanan, Dr. Steven Graham, Dr. Regis Vollmer, and Dr. Philip Empey for their mentorship, guidance, and scientific support over the past 5 years. I would like to thank Dr. Kevin Hitchens, Dr. Lesley Foley for their support in conducting MRI imaging studies. I would like to thank Dr. Wenjin Li, Dr. Muzamil Ahmad, and Dr. Marie Rose for their support in conducting cell culture studies and for surgical methods in rats. I would like to thank Dr. Bruce Hammock for his support by providing his compound for my research. Lastly, I would like to thank our collaborators at NIEHS who helped us in creating a transgenic mice, and providing us with tissues for further evaluation of the mice.

It truly has been a memorable learning and living experience for me here at University of Pittsburgh. I have always considered Pitt as my second home as it gave me an educational environment to evolve myself as a researcher, and a multicultural community to grow as an individual. I would like to thank the Dean, staff, fellow students, and colleagues from my lab at the school who have helped me through the years. I enjoyed interacting with and learning from them, and cherished my time as a graduate student researcher at Pitt. I also would like to thank my friends at the Islamic Center of Pittsburgh, and the Imam (leader) of the center, whose camaraderie made me feel at home and influenced my thinking and understanding of the greater purpose of the life. I'm proud to dedicate and share this achievement with my parents, my sister and her family, and my wife. Without the unconditional love and unwavering support of my parents, I would not have come this far in life and become what I'm today. Their faith in me and my capabilities has been highly instrumental in my growth as a person with values and principles and in reaching this stage of life. Words cannot explain the love and admiration I have for them. I would like to finish by thanking Almighty God for giving me this life, and for giving me such wonderful and lovely parents, and for giving me the knowledge and responsibility to benefit others by it.

ABBREVIATIONS

AA: arachidonic acid

AMPA:α-amino-3-hydroxy-5-methyl-4-isoxazole propionic acid

BBB: blood-brain barrier

CA: cardiac arrest

CBF: cerebral blood flow

$CMRO_2$: cerebral metabolic rate of O_2

CNS: central nervous system

COX: cyclooxygenase

CPP: cerebral perfusion pressure

CSF: cerebrospinal fluid

CPR: cardiopulmonary resuscitation

CVR: cerebrovascular resistance

CYP450: cytochrome P450

DHA: docosahexaenoic acid

DHET: dihydroxyeicosatrienoic acid

EDHF: endothelium derived hyperpolarizing factor

EET: epoxyeicosatrienoic acid

FA: fatty acid

FABP: fatty acid binding protein

FFA: free fatty acids

GPCR: G-protein coupled receptor

HETE: hydroxyeicosatetraenoic acid

HPβCD: hydroxypropyl-β-cyclodextrin

ICP: intracranial pressure

IL: interleukin

LDF: laser Doppler flow

LOX: lipoxygenase

LT: Leukotriene

MABP: mean arterial blood pressure

MCAO: middle cerebral artery occlusion

MRI: magnetic resonance imaging

NADPH: nicotinamide adenine dinucleotide phosphate

NDS: neurological deficit score

NMDA: N-methyl-D-aspartate

NO: nitric oxide

NOS: nitric oxide synthase

NV: neurovascular unit

OHCA: out of hospital cardiac arrest

OGD: oxygen-glucose deprivation

PARP: poly (adenosine diphosphate ribose) polymerase

PBS: phosphate buffered saline

PES: prostaglandin endoperoxide synthase

PG: prostaglandin

PK C: protein kinase C

PLA_2: phospholipase A_2

PND: post natal day

PPAR: peroxisome proliferator activated receptor

PUFA: poly unsaturated fatty acids

QC: quality control

ROS: reactive oxygen species

ROSC: return of spontaneous circulation

SAH: sub arachnoid hemorrhage

sEH: soluble epoxide hydrolase

SMC: smooth muscle cell

SP: Staurosporine

SPE: solid phase extraction

STAIR: stroke therapy academy industry roundtable

TBI: traumatic brain injury

TNF: tumor necrosis factor

TRP: transient receptor potential

TXA: thromboxane

VF: ventricular fibrillation

VSM: vascular smooth muscle

"The best of people are those that bring most benefit to the rest of mankind"

---- Prophet Mohammad (Peace be upon him) ---

1.0 INTRODUCTION AND BACKGROUND

1.1 STROKE AND CARDIAC ARREST

Stroke is the leading cause of long-term disability and third leading cause of death in the United States (Goldstein et al., 2001; Young et al., 2007). Each year almost 130,000 Americans die due to stroke. On average, one American dies from stroke every 4 minutes**.** Every year, more than 795,000 people in the United States have an incidence of stroke. About 610,000 of these are first or new strokes (Roger et al., 2012). Stroke costs the United States an estimated $38.6 billion each year, which includes the cost of health care services, medications, and missed days of work. Common stroke warning signs and symptoms include sudden numbness or weakness of the face, arm, or leg especially on one side of the body, sudden confusion, trouble speaking or understanding, sudden trouble seeing in one or both eyes, walking, dizziness, loss of balance or coordination, and sudden severe headache with no known cause. The risk of having a stroke varies with race, ethnicity, gender, and age. In general, stroke incidence and mortality rates are lower in premenopausal women relative to men of same age indicating that differences may exists in stroke risk and outcomes between men and women. However, some of these differences may be unrelated to sex hormones, and are inherent to gender differences at cellular level (Golomb et al., 2009; Lloyd-Jones et al., 2009). Key risk factors for stroke include high blood pressure, high LDL cholesterol, smoking, and lifestyle disorders such as diabetes, overweight and obesity, physical inactivity, and excessive alcohol use (Centers for Disease et al., 2011).

Out-of-hospital cardiac arrest (OHCA) is a leading cause of death among adults in the United States. Each year, approximately 300,000 persons in the United States experience an OHCA and approximately 92% of persons who experience an OHCA event die. An OHCA is defined as cessation of cardiac mechanical activity that occurs outside of the hospital setting and is confirmed

by the absence of signs of circulation. An OHCA can also occur from non-cardiac causes such as trauma, drowning, overdose, asphyxia, electrocution, primary respiratory arrests, and other non-cardiac etiologies (McNally et al., 2011). However, the most common cause of cardiac arrest (CA) in adults is ventricular fibrillation (VF). The majority of persons who experience an OHCA event do not receive bystander-assisted cardiopulmonary resuscitation (CPR) or other timely interventions that are known to improve the likelihood of survival to hospital discharge. It is estimated that 16,000 American children suffer a CA each year. Only 5% to 10% of patients survive OHCA and often with severe neurological complications whereas 27% of in-hospital arrest patients survive to discharge with 65% of them leaving with good neurological outcomes (Topjian et al., 2008). Pediatric arrests often occur as a complication of, or progression of respiratory failure, circulatory shock, or both (Sahu et al., 2010), which is one of the most common causes of non-traumatic brain injury in children. Return of spontaneous circulation (ROSC) is achieved in approximately 30% of children who suffer out-of-hospital CA, but only 12% of these survive to hospital discharge, and only 4% of these children have favorable neurologic outcome (Donoghue et al., 2005). In case of in-hospital CA the prognosis is comparatively better with 52% of the patients achieving ROSC, 27% survive to hospital discharge, and 15% have favorable neurological outcomes. Although respiratory failure is the major cause of CA in pediatric patients, ventricular fibrillation can also occur in 10 – 15% of the pediatric cases (Donoghue, et al., 2005; Young et al., 2004). Since pediatric CA are secondary to asphyxia rapid initiation of CPR to restore circulation is very crucial in improving survival as recommended by The International Liaison Committee on Resuscitation (ILCOR) (Herlitz et al., 2005; Hickey et al., 1995).

1.1.1 Classification and characterization

Approximately 15% of the stroke occurrences are of hemorrhagic nature due to rupture of a cerebral blood vessel in parenchyma or subarachnoid space, and 85% are of ischemic nature due to either thrombotic or embolic occlusion of a cerebral artery. There is a graded evolution of lesion in the tissue that is supplied by the occluded artery in ischemic stroke based on the residual blood cerebral blood flow (CBF). A focal or central region of rapid death called core (infarct) is characterized by marked reduction in CBF to less than 10% of baseline. It is surrounded by penumbral region (peri-infarct) with residual blood flow between 15 and 40% of baseline supplied from collateral arteries. Infarct region represents irreversible cell death whereas penumbral region represents cells at risk of death and is salvageable if blood flow is restored to normal levels in a timely manner. CA leads to global cessation of blood flow to brain causing global brain ischemia, which progressively changes the cellular architecture and physiology, rendering the cells susceptible to further damage following reperfusion. This condition of reduced nutritive supply of oxygen and glucose to brain due to decreased blood flow is termed as cerebral ischemia. Ischemia of cerebral tissue and cell death is common underlying mechanism in all forms of stroke including focal ischemia (embolic and/or thrombotic), and global ischemia (as in cardiac arrest). In addition, ischemia also overlaps with the underlying injury mechanisms of vascular complications in traumatic brain injury (TBI) and subarachnoid hemorrhage (SAH). Interestingly, there are remarkable differences in the underlying mechanisms of cell death between global and focal ischemia, and within the focal ischemia there are unique processes in the tissue that undergoes reperfusion (Smith, 2004). Understanding these injury type specific cell death mechanisms is critical in developing new therapeutic strategies for effectively reducing the ischemic complications of stroke and cardiac arrest.

1.1.2. Pathophysiology of cerebral ischemic injury

The energy needs of the brain are provided by metabolism of glucose and oxygen for the phosphorylation of ADP to ATP. Most of the ATP thus generated is used in the brain to maintain intracellular homeostasis and transmembrane ionic gradients. Cerebral ischemic injury mechanisms were well described in the literature. Although exact sequence of events is not determined, the sequence of events that follow after the injury are distinct and unique in different regions of the brain due to which they exhibit varied degrees of tolerance to ischemia. During ischemia within minutes brain tissue is deprived of glucose and oxygen. In the core infarct region, loss of glucose, and decrease in the pH due to accumulation of acidic products of metabolism severely decreases ATP production due to suppression of mitochondrial electron transport chain activity. Rapidly declining ATP levels affect energy dependent pumps like Na^+/K^+ ATPase, perturbing ionic gradients across membrane resulting in persistent depolarizations. This is exacerbated further due to high influx of Ca^{2+} owing to the failure of Na^+/Ca^{2+} exchanger resulting in massive sequestration of intracellular Ca^{2+}. At this point neurons in the infarct core region begin to fire repetitively releasing the excitatory neurotransmitters in the synapses such as glutamate, which was observed to increase in both focal (Hillered et al., 1989; Takagi et al., 1993) and global ischemia (Benveniste et al., 1984). A massively high intracellular Ca^{2+} is a key contributor of ischemic cell death as it initiates several events including activation of proteases that affect structural integrity of cytoskeleton, activation of phospholipases that affect membrane integrity. Increased intracellular Ca^{2+} also induces of nitric oxide synthase (NOS), which produces highly reactive free radical peroxynitrate capable of causing single stranded DNA breaks. This induces poly (adenosine diphosphate ribose) polymerase (PARP) activity, and together with other parallel mechanisms detailed above neurons eventually die due to necrosis.

However, depending on the degree and duration of ischemia these events describe above may be minimal and short lived resulting in temporary cellular dysfunction (Smith, 2004). In the penumbral region, cellular damage is mediated by different mechanisms. Since ATP levels and blood flow are marginally reduced in penumbra, ionic homeostasis, and transmembrane gradients are not fully impaired thus rendering neurons in this region functionally viable but electrically inactive. Increased levels of extracellular glutamate released from dying neurons of core region was found to be toxic to penumbral neurons, a phenomenon termed as excitotoxicity (Hugon et al., 1996; Kirino, 1994; Whetsell, 1996). Glutamate acts on ionotropic and metabotropic glutamate receptors, N-methyl-D-aspartate (NMDA), and α-amino-3-hydroxy-5-methyl-4-isoxazole propionic acid (AMPA) receptors resulting in elevated intracellular calcium [Ca^{2+}_i]. As shown in the **Figure 1-1**, moderate increases in Ca^{2+} activates phospholipases, cause lipid peroxidation, release fatty acids into cytosol, and increases release of cytochrome C from mitochondrial transition pore, which initiates apoptotic cell death by activating caspase activity.

Adding to the complexity, during reperfusion more free radicals are generated by mitochondria, creating oxidative stress, which accounts for much of neuronal damage. As such brain is particularly vulnerable to oxidative stress due to high concentrations of polyunsaturated fatty acids (PUFA), which are susceptible to lipid peroxidation and lower antioxidant defense compared to other organs. Specifically, neurons are more susceptible to damage by oxidative stress as they have lower levels of reduced glutathione (Dringen, 2000). These free radicals bind covalently to cellular proteins, nucleic acids, lipids and alter their function. Further, they also contribute to the inflammatory response by increasing the expression of cytokines, which in turn up-regulate

adhesion molecules, leukocytes, platelets that deposit over endothelium eventually damaging capillaries and worsening the ischemic injury.

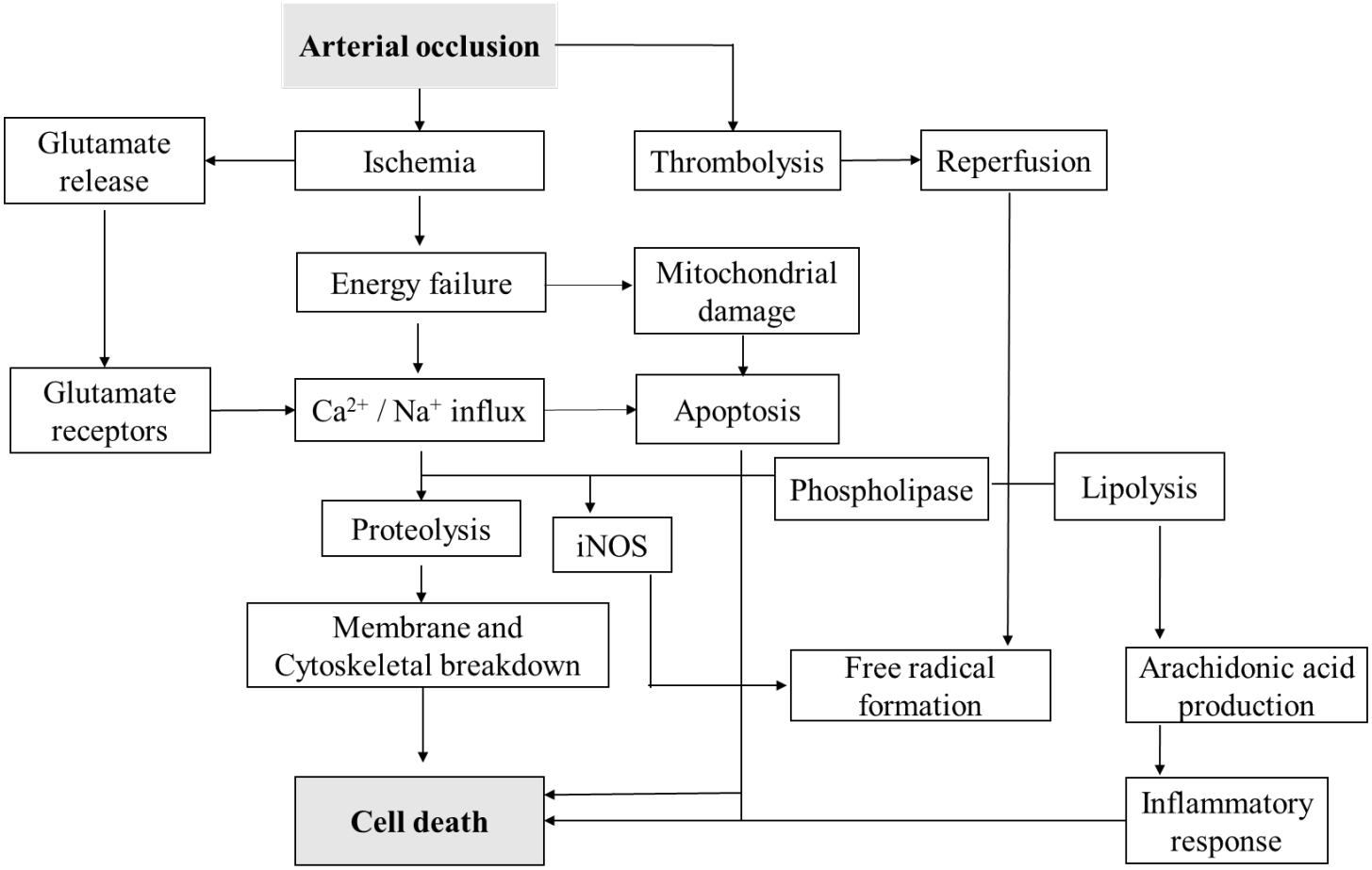

Figure 1-1. Pathways of cell death in cerebral ischemia

1.1.3. Phospholipases and free fatty acids in cerebral ischemia

1.1.3.1. Lipids and free fatty acids:

The central nervous system (CNS) has high concentration of lipids next to adipose tissue. Brain lipids are complex and consists of glycerophospholipids, sphingolipids, gangliosides, cholesterol,

and cholesterol esters. Glycerophospholipids are composed of two fatty acids (FA) attached to a glycerol backbone. A saturated FA is usually bound to sn-1 position, a polyunsaturated fatty acid (PUFA) in the sn-2 position, and a phosphate in the sn-3 position, covalently linked to a base group such as choline, serine, inositol, and ethanolamine (Tassoni et al., 2008). These phospholipids are important component of cell structure as they form bilayers that provide membrane fluidity, and structural integrity (Lenaz, 1979). In addition, they also serve as energy reservoirs, precursors to various secondary messengers such as arachidonic acid (AA), docosahexanoic acid (DHA), and phosphatidic acid. Lipids in the CNS plays a crucial role in cell signaling and tissue physiology. Knowledge of the phospholipid metabolism is critical to our understanding of the role they play in cell physiology under normal, and pathophysiological conditions since altered lipid metabolism in the CNS contributes to a variety of disorders of neurological origin such as stroke, Alzheimer's, schizophrenia, and Parkinson's (Adibhatla et al., 2006). Indeed, altered lipid metabolism is believed to be a key contributor to CNS injuries such as stroke.

One mechanism contributing to neuronal death after ischemic injury is the release of bioactive free fatty acids (FFA) from membrane phospholipids. Bazan et al first described the release of FFAs in brain during ischemia (Abe et al., 1987; Bazan, 1970; Bazan, 1976; Gardiner et al., 1981). Two pathways control release of FFA from membrane phospholipids. The first pathway is direct release from the hydrolysis of glycerophospholipids by various phospholipases, and the second pathway is the degradation of phosphatidylinositol by phospholipase C followed by formation of diacyglycerol, which is further metabolized to FFA by lipases such as diacylglyceride lipase (Sun et al., 1979). Accumulation of the saturated and polyunsaturated FFA (PUFA) may indicate regional lipid membrane damage, which further leads to progressive infarction after cerebral ischemia. It has been shown that the accumulation of FFAs after cerebral ischemia correlates

locally with the severity of the insult (Baskaya et al., 1996). In a study by Pilitsis, concentrations of FFAs measured in the cerebrospinal fluid (CSF) collected from ischemic and/or hemorrhagic stroke patients within 48 h of insult were found to be significantly higher than in the controls (Pilitsis et al., 2003; Pilitsis et al., 2001). Higher concentrations of PUFA in CSF obtained within 48 h of insult were correlated with lower admission Glasgow scores and worse outcomes at discharge. Of all the PUFA released in CSF of the patients, AA was released in the highest proportion followed by DHA. Initial elevation of FFA early after ischemic injury appear to return to control levels during the early phase of reperfusion. Particularly, levels of AA have been found to decrease faster than those of other FFA after recirculation (Shohami et al., 1982). Interestingly, a delayed increase in the FFA levels were also observed after three days of reperfusion in a gerbil model of ischemia (Nakano et al., 1990). It is postulated that decrease in the levels of all FFA during reperfusion phase is due to either vascular washout, reesterification or diffusion in to CSF. The cascade of events leading to ischemic-injury associated secondary brain damage due to accumulation of FFAs is mediated by direct and indirect mechanisms. Direct mechanisms include disruption of cellular energy metabolism, induction of blood-brain barrier breakdown, and edema formation (Chan et al., 1984; Rehncrona et al., 1979; Unterberg et al., 1987). Indirect mechanisms include generation of active oxygenated metabolites of liberated FFA that effect CBF and vascular tone. (Dempsey et al., 1986; Moncada et al., 1978).

1.1.3.2. Phospholipases:

In neural membranes, saturated fatty acids such as palmitic or stearic are usually esterified at sn-1 position of the glycerol backbone whereas PUFA such as arachidonic acid are esterified at the sn-2 position. The PLA_2 pathway is the primary pathway through which AA is released from phospholipids (Kudo et al., 2002; Perez-Chacon et al., 2009; Sun et al., 2004). PLA_1 and PLA_2

acts on the fatty acid ester bond at sn-1 and sn-2 positions respectively liberating a free fatty acid and a lysophospholipid. Lysophospholipids perturb membrane homeostasis and increase membrane fluidity and permeability (Caro et al., 2006). There are other types of phospholipases like PLB, PLC, and PLD as shown in **Figure 1-2**, that differ in their action on phospholipid hydrolysis position and subsequent lysophospholipid formed.

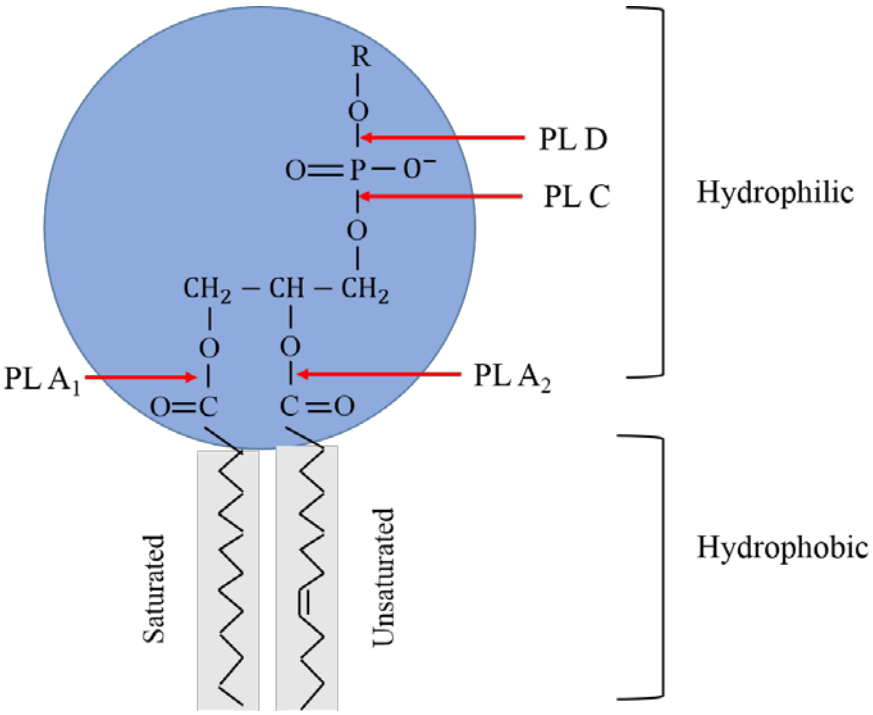

Figure 1-2. Free fatty acid release from membrane by phospholipases

PLA_1, A_2, C and D are all expressed in multiple forms in the brain tissue (Phillis et al., 2004). Within the brain, PLA_2 has been identified in different cell types such as neurons, astrocytes, microglial, and neuroblastoma cells. The PLA_2 can be categorized into three different families namely i) secretory ($sPLA_2$), ii) cytosolic or calcium dependent ($cPLA_2$), and iii) calcium independent ($iPLA_2$). Secretory PLA_2 does not exhibit specificity for any particular FA. Significant increases in the expression of $sPLA_2$ were observed in the hippocampus, and

neocortical areas in a transient forebrain ischemia model (Lauritzen et al., 1994). Calcium dependent PLA_2 exhibits specificity for arachidonic acid and its expression was identified in various brain regions including olfactory cortex, hippocampus, thalamus, and cerebellum. Increased intracellular Ca^{2+} (~ 100 – 500 nM) promotes translocation of $cPLA_2$ to intracellular membranes but Ca^{2+} as such is not needed for its catalytic activity. $iPLA_2$ represents dominant PLA_2 activity in the cytosol and function as housekeeping genes for the maintenance of membrane phospholipids. Similar to $sPLA_2$, it does not exhibit any particular substrate specificity and its expression was identified in all brain regions. $cPLA_2$ is implicated in various pathophysiological conditions such as ischemia/reperfusion injury (Hornfelt et al., 1999a; Hornfelt et al., 1999b; Kishimoto et al., 1999; Pepicelli et al., 2002).

In a rat model of focal ischemia, a biphasic increase in FFA was observed one early during ischemia and another at 16 h after reperfusion. FFA accumulation in early phase of focal ischemia was attributed to the action of $cPLA_2$ whereas in the late reperfusion phase it was attributed to upregulation of $sPLA_2$ in the reactive astrocytes of penumbral region (Zhang et al., 1995). Similarly, in global cerebral ischemia model also upregulation of $cPLA_2$ was observed (Pilitsis et al., 2002; Walton et al., 1997). Thus neuronal damage due to ischemic injury may activate $cPLA_2$, $sPLA_2$ depending on the cell type, time course, and type of ischemic insult. Neuronal excitation resulting from depolarization due to high concentrations of potassium, and stimulation with various excitatory neurotransmitter agonists such as AMPA, NMDA, glutamate, as well as muscarinic cholinergic agonists can stimulate release of AA, which plays an important role in cellular death by necrotic or apoptotic processes. Glutamate mediated excitotoxicity is accompanied with accumulation of intracellular Ca^{2+}, degradation of membrane phospholipids, and accumulation of FFA such as AA, and lipid peroxides implying the involvement of

phospholipases such as $cPLA_2$ (Lipton, 1999; Verity, 1993; Whetsell, 1996). AA can itself modulate ion channels (Kim et al., 1995), increase the mitochondrial permeability transition pore open time, affect release, uptake, and transport of several neurotransmitters, and activate many signaling pathways such as PKA, PKC, ERK, JNK, p38 MAPK, NADPH oxidase, diacylglycerol kinase, and Na^+/K^+ ATPase (Alexander et al., 2001; Katsuki et al., 1995). Different preclinical and clinical studies indicated that cytokines such as tumor necrosis factor-α (TNF-α), IL-1, and IL-6 are upregulated after stroke, which may be related to the release of AA during the initial periods of ischemia (Adibhatla et al., 2008).

1.1.4. Arachidonic acid metabolism

Arachidonic acid (C20:4, ω-6; AA) is one of the physiologically important PUFA that is required as a constituent of cell membrane phospholipids (Caro, et al., 2006). AA is accessible from dairy products and meat or can be synthesized *de novo* from linoleic acid, which is abundant in vegetable oils. As shown in **Figure 1-3**, Free AA release from phospholipid membranes is metabolized to various structurally different and biologically active products by cyclooxygenase (COX), lipoxygenase (LOX), and cytochrome P450 (CYP450) pathways (Liu et al., 2004; Panigrahy et al., 2010).

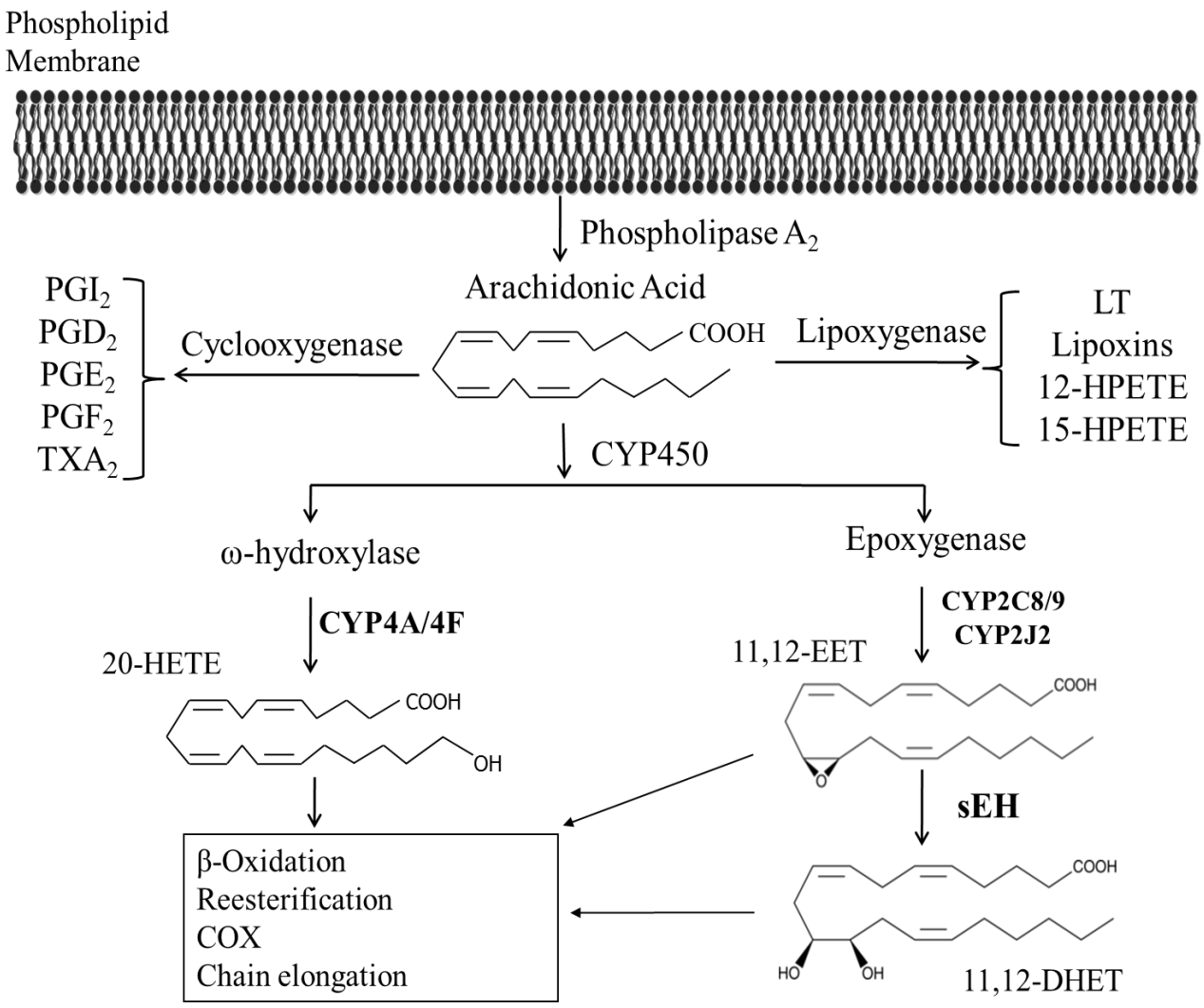

Figure 1-3. Pathways of arachidonic acid metabolism

Cyclooxygenase (COX): COX enzymes consists of a constitutive isoform (COX-1) and an inducible form (COX-2). Arachidonic acid is transformed into the cyclic endoperoxides by COX also known as prostaglandin endoperoxide synthase (PES). PES exhibit both cyclooxygenase and peroxidase activities (Samuelsson, 1987). The cyclooxygenase component of the enzyme introduces two molecules of oxygen into AA to yield a highly unstable endoperoxide product PGG_2, which is reduced by the peroxidase activity of the enzyme to form unstable PGH_2. PGH_2 is

further metabolized by various terminal tissue specific synthases, reductases, and isomerases to form prostaglandins (PG), prostacyclin (PGI_2), or thromboxanes (TXA_2) collectively referred as prostanoids. Isomerases catabolize PGH_2 into either PGD_2 or PGE_2. A- and B-series prostaglandins are derived from PGE_2 by sequential dehydration and isomerization. Prostaglandin $F_{2\alpha}$ ($PGF_{2\alpha}$) is generated via reduction of PGH_2. Prostacyclin and thromboxane (TX) synthases form PGI_2 and TXA_2, respectively. Hydrolysis of PGI_2 and TXA_2 yields inactive by-products (6-keto-$PGF_{1\alpha}$ and TXB_2) of much greater stability. Additional enzymes can interconvert the prostaglandins; for example, PGE_2 can be modified to $PGF_{2\alpha}$ by the action of PGE_2-9-ketoreductase.

Lipoxygenase (LOX): These cytosolic dioxygenases transform AA to hydroperoxides by introducing one molecule of oxygen at specific carbon position (e.g.: 5, 12, or 15) on AA. Leukocytes and mast cells are rich in 5-lipoxygenase. The 12-, and 15-lipoxygenase are predominant in platelets and respiratory tissues, respectively. Leukotrienes (LTs) are formed by the 5-lipoxygenase (5-LOX) pathway. AA is first metabolized by 5-LOX to 5-hydroperoxyeicosatetraenoic acid (5-HPETE), which is then either converted by a competing peroxidase to 5-HETE, or dehydrated into an unstable epoxide intermediate, LTA_4. Leukotriene A_4 is either hydrolyzed to form a dihydroxy derivative, LTB_4, or is linked with glutathione to create LTC_4. Further enzymatic process of LTC_4 yields LTD_4 and LTE_4. The other two LOX metabolizes AA into 12-HPETE, and 15-HPETE by 12-LOX, and 15-LOX respectively. These hydroperoxy products are rapidly reduced to their hydroxy analogues, 12-HETE and 15-HETE. 15-HETE is further subjected to the successive action of 5-LOX to form the tetraene trihydroxy lipoxins (LXs) (Samuelsson, 1987).

1.1.4.1 CYP450 enzymes: AA metabolism by COX and LOX enzymes were well characterized and studied for their role in various physiological and pathophysiological processes such as inflammation, vasoconstriction, vasodilation, thrombosis, mitogenesis, and allergic reactions. In the last few decades, CYP450 pathway emerged as third yet an important pathway of AA metabolism and ever since the interest in delineating the physiological significance of AA metabolites from this pathway has been steadily increasing in the lipid research field. Cytochrome P450 enzymes (CYP450) are members of a superfamily of membrane bound, heme-containing monooxygenases in a multienzyme system that also includes flavoprotein containing nicotinamide adenine dinucleotide phosphate (NADPH)-cytochrome P450 reductase, and cytochrome b_5. CYP450 enzymes originally considered as pigments were later discovered to contain iron-protoporphyrin IX complex. The reduced CO complex of this pigment absorbed light at 450 nm, which is unusual for heme containing proteins, thus they were named CYP450 (Omura et al., 1964; Omura et al., 1962). CYPs are membrane bound proteins, which are mainly found either in endoplasmic reticulum (ER) or in mitochondrial membrane (Hedlund et al., 2001). CYP450 enzymes metabolize cholesterol, steroids, fatty acids, vitamins, and numerous structurally diverse xenobiotics in an oxygen and NADPH-dependent manner. As shown in **Figure 1-4**, CYP450 typically introduces one oxygen atom to the substrate from molecular oxygen and incorporates the other incorporated into water. The first step in the process of catalysis is binding of the substrate to the apoprotein, which is non-covalently linked to the heme-protoporphyrin IX complex containing iron. The binding of substrate displaces the water molecule bound to iron above the plane of protoporphyrin-heme complex, facilitating the transfer of one electron from NADPH-CYP450 reductase and subsequent reduction of iron from ferrous (Fe^{3+}) to ferric (Fe^{2+}) state. This is in turn followed by binding of molecular oxygen forming [Fe^{3+}-$O_2^{\cdot}$] complex. Then another

electron is transferred either from NADPH-CYP450 reductase or cytochrome b_5 to the activated molecular oxygen forming a highly reactive nucleophilic iron-peroxo complex [Fe^{3+}-O_2^-]. This is followed by protonation from surrounding water to form reactive iron-hydroperoxo [Fe^{3+}-$OOH^{\cdot}$] complex. At this point molecular oxygen is dissected with the addition of one more proton forming one water molecule and electrophilic iron-oxo complex [Fe^{5+}-O] or [Fe^{4+}-OH]. The substrate, which is in the vicinity of this reactive electrophilic complex is oxidized to form monooxygenated metabolite, leaves the enzyme returning it back in Fe^{3+} state bound to water molecule (Meunier et al., 2004).

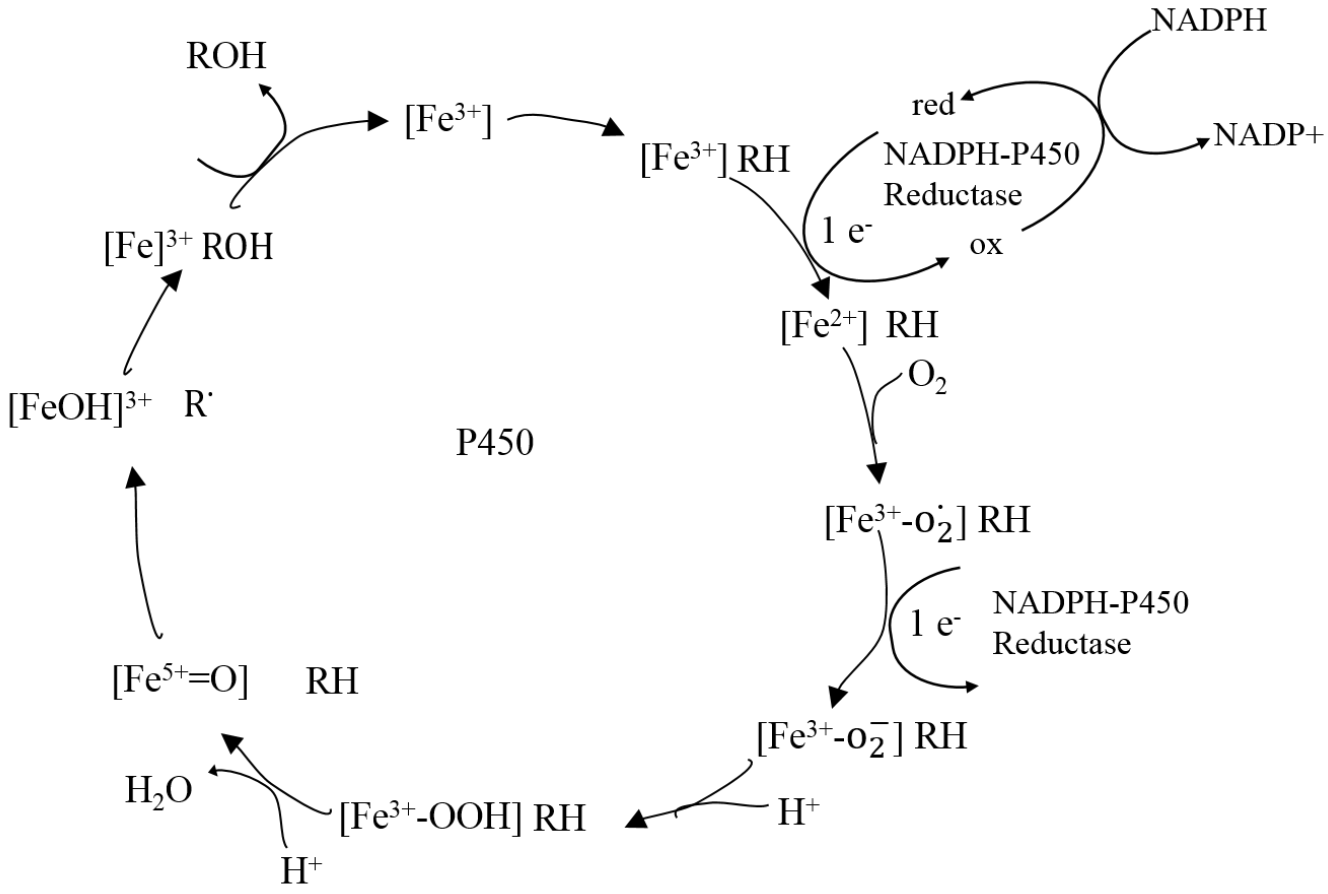

Fig 1-4. Cytochrome P450 catalytic cycle

CYP450 cycle can produced reactive oxygen species (ROS) like hydrogen peroxide, superoxide anion either by decomposition of the ferrous-dioxygen complex or by release from peroxyferric intermediates. The generation of ROS considerably varies depending on the P450, the presence or absence of substrate, nature of the substrate, and the action of cytochrome *b*5 (Zangar et al., 2004).

CYP expression in the brain is relatively lower than that of liver and kidney yet CYP enzymes in the brain perform specific function in fatty acid metabolism, which exerts diverse array of pharmacological actions (Warner et al., 1988). CYP enzymes from the family of CYP2B, CYP2C, CYP2D, CYP2E1, CYP2J, CYP4A, 4B, and 4F were shown to be involved in AA metabolism, and various orthologous isoforms in different species are expressed in liver, heart, lung, kidney, and brain with tissue specific expression profiles. For example, CYP2B, CYP2C11, CYP2E1, and CYP2J3 were found to have higher expression in the heart, while in the lung, CYP2B1, CYP2J3, and CYP4Fs were found to be highly expressed in rat (Zordoky et al., 2008). Genes encoding CYP1-4 families can be regulated at transcriptional level through one of the four receptor-dependent mechanisms. They are aryl hydrocarbon (AhR), constitutively active receptor (CAR), pregnane X receptor (PXR), and peroxisome proliferator activated receptor (PPAR). CAR, PXR, and PPAR belong to nuclear receptor superfamily, and they initiate transcription usually by binding as heterodimers with retinoid X receptor (RXR) to the respective response elements in target genes. Glucocorticoids, mineralocorticoids, progesterone, and fibrates activate PPARα inducing CYP4A and some CYP2C isoforms but downregulates the expression of CYP4F and CYP2C11 (Roman, 2002).

1.1.4.2. CYP450 eicosanoids: CYP450 enzymes metabolize AA by catalyzing hydroxylation, epoxidation or allylic oxidation reactions (Capdevila et al., 2000; Oliw et al., 1996)

producing an array of structurally diverse and physiologically active metabolites referred to as "CYP eicosanoids". Hydroxylation of AA results into a series of regioisomeric metabolites termed as hydroxyeicosatetraenoic acids (HETEs). Hydroxylation at subterminal positions forms 16-, 17-, 18-, and 19-HETE, which can occur as R- or S-enantiomers due to asymmetrical carbon atom whereas hydroxylation at terminal position forms 20-HETE. CYP isoforms 1A1, 1A2, and 2E1 are capable of carrying out ω-1 hydroxylation predominantly. However, in addition to 19-HETE these isoforms also can generate 18-HETE (CYP2E1) or 16-, 17-, and 18-HETE (CYP1A1 and 1A2) as minor products. CYP4A and 4F subfamilies predominantly carry out terminal hydroxylation of AA forming 20-HETE as major product.in the liver, kidney, brain, and cardiovascular system (Hardwick et al., 1987; Kroetz et al., 2005; Powell et al., 1998; Simpson, 1997). In rat, CYP4A1, 4A2, 4A3, and 4A8 are expressed in kidney, liver, and cerebral blood vessels (Gebremedhin et al., 2000; Helvig et al., 1998; Ito et al., 1998). CYP4F2, 4F3, 4F11, 4F12, and 4A11 are expressed in the liver and kidney of humans (Kikuta et al., 2000; Lasker et al., 2000). Among these, CYP4F2, CYP4A11, and CYP4F3B are the major 20-HETE synthesizing enzymes. However, these isoforms are also capable of ω-1 hydroxylation and form 19-HETE as a minor product. The orthologous isoforms of different species exhibit varied degree of regioselectivity in forming different HETEs for example, human CYP4A11 produces 20-HETE and 19-HETE in a ratio of 90:10, whereas mouse CYP4a12a forms in 87:13, and rat CYP4A1 forms in 93:7 proportions. Similarly, regioselectivity was also observed with the human CYP4F isoforms 4F2, 4F3A, and 4F3B (Konkel et al., 2011). In addition to the most common hydroxylation reactions at terminal and subterminal carbons of AA, certain CYP450 isoforms such as 2C8, 2C9 and 3A4 are also capable of performing allylic oxidation reactions, which form six regioisomeric hydroxy metabolites 5-, 8-, 9-, 11-, 12-, and 15-HETE containing a cis-trans conjugated dienol (Bylund et

al., 1998; Hornsten et al., 1996; Oliw, et al., 1996). These are referred to as mid-chain HETEs, which resemble the metabolites produced by lipoxygenases.

Epoxidation of AA at four unsaturated double bonds produces four regioisomeric cis-epoxyeicosatrienoic acids (5,6-, 8,9-, 11,12-, and 14,15-EET) , which can be either R,S- or S,R-enantiomers. Several mammalian CYP isoforms such as CYP1A, 2B, 2C, 2D, 2G, 2J, 2N, and CYP4A can produce EETs. They differ in selectivity for regioisomers, catalytic efficiency, inducibility, species, and organ distribution (Spiecker et al., 2005). CYP2C isoform produce the majority of EETs in human liver and kidney whereas CYP2J isoforms are predominant in EETs biosynthesis in rat and human heart. CYP2C and 2J isoforms also like CYP4A, 4F exhibit varied degree of regioselectivity in different species. For example, human CYP2C8 produces exclusively 14,15- and 11,12-EET in a ratio of 1.3:1 whereas CYP2C9 shows less regio and stereoselectivity. CYP2C3 in rat kidney produces 8,9-, 11,12-, and 14,15-EET in a ratio of 1:2:0.7. Similarly, regio and stereoselectivity was also observed with mouse CYP2C44, human CYP2J2.

1.1.4.3. CYP eicosanoids metabolism: Once produced the CYP eicosanoids (HETEs, EETs, and DHETs) are either reincorporated into membranes through esterification at sn-2 position by coenzyme A (CoA), forming membrane stores, which are readily released by the action of PLA_2 in response to the signaling pathways of hormones, cytokines, and growth factors or undergo further metabolism. CYP eicosanoids being fatty acid derivatives bind strongly to plasma proteins, which limit their biological activity in the circulation and restrict their distribution to plasma when administered directly through intravenous routes.

EETs: EETs are highly reactive and unstable. EETs are predominantly metabolized *in vivo* to less active dihydroxyeicosatrienoic acid (5,6-, 8,9-, 11,12- and 14,15-DHET) by soluble epoxide

hydrolase (sEH) enzyme (Chiamvimonvat et al., 2007; Newman et al., 2005; Spector et al., 2004), which is encoded by *EPHX2* gene. sEH expression was found in neurons, astrocytes, oligodendrocytes, endothelial cells, and VSM cells (Iliff et al., 2010). 5,6-EET is a poor substrate and 14,15-EET is a preferred substrate of sEH. sEH functions as a homodimer with each subunit consisting of two domains of different enzymatic activities. The carboxy terminal domain exhibits epoxide hydrolase activity and the amino terminal domain exhibits Mg^{2+} dependent lipid phosphatase activity. These two domains function independently, and inhibition of one activity does not affect the catalytic function of the other (Newman et al., 2003). EETs can bind to fatty acid binding protein (FABP), which modulates EETs incorporation into phospholipids and its availability to sEH for metabolism (Spector, et al., 2004; Spector et al., 2007). EETs can undergo β-oxidation forming 16-carbon epoxy derivatives, which accumulate in the extracellular fluid and they can also be chain-elongated to form 22-carbon derivatives that are incorporated into phospholipids. These two pathways take precedence in cells with low availability or activity of sEH. The other less common pathways of EETs metabolism include the terminal hydroxylation by ω-hydroxylases to form 20-hydroxy EETs, conjugation by glutathione-*S*-transferase, and metabolism by COX enzymes (Spector, et al., 2007).

HETEs: In an *in vitro* study of porcine coronary artery endothelial cells, 20-HETE was found to be esterified and stored in the phospholipids by the action of acylcoenzyme A synthase. 20-HETE is metabolized in the endothelial cells by β-oxidation to form short-chain 16-carbon derivatives, and by ω-oxidation to form 20-carboxy-arachidonic acid (20-COOH-AA) (Kaduce et al., 2004). 20-HETE is also metabolized to 20-hydroxy-PGG_2 and 20-hydroxy-PGH_2 by COX enzymes in the endothelium (Schwartzman et al., 1989).

1.1.5 Pharmacological effects and molecular mechanisms of CYP eicosanoids

CYP eicosanoids serve as lipid signaling molecules. They not only play a critical role in regulation of vascular, renal, and cardiac function (Hao et al., 2007; Imig, 2012) but also participate in various pathological conditions such as inflammation and ischemia/reperfusion injury. The extensively studied and characterized effects of CYP eicosanoids are their actions on vasculature of different organs as they regulate the vascular tone. Interestingly, some of the pharmacological actions of HETEs and EETs on vascular beds of different organs are diametrically opposite to each other.

1.1.5.1 HETE: 20-HETE, is most potent vasoconstrictor of HETEs in most vascular beds except for pulmonary and coronary circulation where it exhibits vasodilatory response in an endothelium and cyclooxygenase dependent manner (Birks et al., 1997; Pratt et al., 1998). Vasoconstrictive actions of angiotensin II, endothelin, and norepinephrine are mediated through 20-HETE signaling mechanism (Maier et al., 2001). 20-HETE induces vasoconstriction by inhibiting calcium activated large conductance potassium channels (BK_{Ca}), activating Rho-kinase, protein kinase C (PKC), and allowing Ca^{2+} entry by opening L-type Ca^{2+} channels (Kroetz, et al., 2005). Interestingly, 20-HETE though a potent vasoconstrictor of small arteries, and arterioles (< 100 μm) has little or no effect on the larger arteries (Roman, 2002). Vascular overproduction of 20-HETE is detrimental to endothelial function as it uncouples endothelial nitric oxide synthase (eNOS), and activates pro-inflammatory transcription factor NF-κB (Cheng et al., 2008; Ishizuka et al., 2008). Excessive formation of 20-HETE is also detrimental in ischemic organ injury in heart and brain (Miyata et al., 2005; Nithipatikom et al., 2004). 20-HETE mediates the signaling of mitogenic actions of growth factors and vasoactive agents (Muthalif et al., 1998), and promotes angiogenesis (Amaral et al., 2003) suggesting its important role in vascular cell growth. In addition

to controlling renal tone, 20-HETE also affects electrolyte excretion by inhibiting Na^+/K^+-ATPase, and Na^+/K^+-$2Cl^-$ cotransporter in the kidney (Maier, et al., 2001). In humans, increased urinary excretion of 20-HETE is associated with endothelial dysfunction. Several recent studies indicated that genetic polymorphisms in the genes encoding CYP4A11, 4F2 isoforms that form 20-HETE are associated with hypertension, coronary endothelial dysfunction, and stroke (Ding et al., 2010; Fava et al., 2008; Fu et al., 2008a; Fu et al., 2008b; Gainer et al., 2005; Zordoky et al., 2010).

20-HETE metabolite 20-COOH-AA also exhibits moderate vasodilatory effect in the porcine coronary microvessels (Kaduce, et al., 2004). The COX derived metabolites of 20-HETE also have shown vasoconstrictive effect in the rat aorta (Schwartzman, et al., 1989). Surprisingly, other subterminal hydroxylated AA metabolites such as 16-, 17-, 18-, and 19-HETE exert opposite pharmacological actions to that of 20-HETE. 19-HETE stereoselectively inhibits 20-HETE induced vasoconstriction and endothelial dysfunction (Alonso-Galicia et al., 1999). The pharmacological actions of mid-chain HETEs are less characterized and largely remain unknown.

1.1.5.2. EETs: EETs are potent vasodilators in most vascular beds except for pulmonary circulation where they exert opposite effects. Intracellular EETs can bind to FABP, interact with ion channels or transcription factors whereas EETs in membrane bound phospholipids can interact with other membrane proteins or phospholipid mediated signaling pathways. In several vascular beds, they function as the major endothelium derived hyperpolarizing factor (EDHF) because of their ability to dilate arteries (Campbell et al., 2007). EETs exert paracrine effects on vascular smooth muscle (VSM) by activating BK_{Ca} channels causing hyperpolarization of VSM cells and eventual relaxation and dilation. In addition, EETs also activate transient receptor potential (TRP) V4 channels, L-type Ca^{2+}, ATP sensitive potassium (K_{ATP}) and Na^+ channels, tyrosine kinase,

ERK1/2, p38 MAPK, and PI3 kinase signaling pathways in endothelial cells (Chen et al., 1998; Chen et al., 1999; Hoebel et al., 1998; Lee et al., 1999; Loot et al., 2008; Lu et al., 2001a). EETs unlike 20-HETE suppress the activation of NF-κB thus exerts anti-inflammatory properties (Spector, et al., 2007). They also promote endothelial cell growth but inhibit migration of VSM cells indicating their roles in angiogenesis and prevention of uncontrolled vascular remodeling (Fleming, 2007; Spiecker, et al., 2005). In humans, polymorphisms in genes encoding EET forming CYPs (CYP2C8, 2C9, and 2J2) and EET metabolizing sEH enzyme have been associated with increased risks for the development of hypertension, stroke, coronary artery disease, and myocardial infarction (Imig et al., 2009; Zordoky, et al., 2010). In various different studies looking at vasodilatory, anti-inflammatory, antioxidative, anti-migratory, and pro-fibrinolytic properties of EETs, 11,12-EET was found to be more efficacious than other regioisomers (Node et al., 1999; Sun et al., 2002; Wu et al., 1997).

1.1.5.3. DHET and sEH: DHETs are usually considered less active than EETs. Thus, inhibiting sEH is generally presumed not to be detrimental to any vital physiological processes. This view is supported by various studies that employed either genetic deletion of sEH (Sinal et al., 2000) or pharmacological inhibitors (Imig et al., 2005; Yu et al., 2000) reporting no toxicity associated with its inhibition or deletion. However, in recent studies vasodilatory activity of DHET in coronary circulation has been reported (Campbell et al., 2002; Lu et al., 2001b; Oltman et al., 1998). It is possible that they may be important in exerting vasodilatory effects under conditions of rapid EET metabolism to DHET. So far there is no conclusive evidence that any of the effects of DHET are essential in normal physiological function.

Although pharmacological actions and the underlying downstream mechanisms of CYP eicosanoids are well characterized, their primary targets on cells, which elicit these actions are not identified yet. Several explanations were proposed for the possible mode of action of CYP eicosanoids. Possibility of a membrane bound G-protein coupled receptor (GPCR) cannot be ruled out although unlike prostaglandins and leukotrienes, a putative receptor for CYP eicosanoids is yet to be identified. Another possible mode is direct interaction of CYP eicosanoids with intracellular or membrane bound targets. For example, EETs bind to and activate nuclear receptors PPAR, which are expressed endothelial cells and blood vessels (Cowart et al., 2002; Fang et al., 2006; Ng et al., 2007).

1.1.6. Animal models of cerebral ischemia

Various animal models were developed in the past in both small and large animals (e.g.: mice, rats, gerbils, rabbits, cats, dogs, pigs, sheep, and monkeys) to evaluate cerebral ischemia (Ahmed et al., 2000). Larger animals are easier to work with imaging techniques, physiological monitoring, measurement of CBF, and they have structural and functional similarity to human brain but on the down side they are very costly, labor intensive, need usage of different anesthetic regimens that may impact outcome. On the other hand, small animals especially rodents are less costly, genetically homogenous (especially mice), and sophisticated neurosensory and motor behavior assessments are well established to use with them. Despite of the many advantages they offer, the structural and functional differences to human brain limit their benefit in successfully translating the findings to humans. Yet they are routinely used as they can be physiologically controlled to get reproducible injury, studied for careful dissection of potential mechanisms of

injury, and neuroprotection, which greatly advance our understanding of the pathophysiology of the disease progression (Traystman, 2003).

Cerebral ischemia models can be characterized as global, focal, and multifocal ischemia models based on the extent of the tissue injured and as incomplete or complete based on the extent of reduction of CBF. In global model, CBF is reduced throughout most or all of the brain whereas in focal models CBF reduction occurs in specific region of the brain. In multifocal models, there is a patchy pattern of reduced CBF in the regions of the brain. With complete ischemia, global blood flow ceases completely whereas in incomplete it reduces severely to a level that is not sufficient enough to maintain cerebral metabolism and function. Most commonly used focal ischemia model for studying mechanisms of cell injury, and neuroprotection is middle cerebral artery occlusion (MCAO) using an intraluminal filament or suture (Longa et al., 1989). Reperfusion can be easily achieved in this model by withdrawing the suture, and the animals may survive for days to months depending on the severity of injury, enabling the functional outcome measures to be recorded thoroughly. Other commonly used models include MCAO + carotid occlusion, photochemical thrombosis, blood clot embolization, and electrocoagulation of MCA. Most commonly used global ischemia model is asphyxial cardiac arrest (Katz et al., 1995). Other routinely used models include neck cuff inflation, ventricular fibrillation, decapitation, forebrain ischemia models of 4-vessel (common carotid and vertebral arteries) occlusion, and 2-vessel occlusion. However, it is important to note that these models differ in terms of the extent and pattern of injury based on the strain and species used. Permanent and reperfusion models of ischemic stroke in animals are more relevant to human ischemic stroke. In animals region of the brain injured, termed as infarction is estimated through histological staining procedures whereas in human it can be visualized with diffusion-weighted magnetic resonance imaging (MRI) (Kelly et al., 2001).

1.2 CEREBRAL BLOOD FLOW REGULATION

1.2.1 Cerebral circulatory system

Arterial circulation can be broadly classified into macrocirculation and microcirculation based on the vessel size or intrinsic and extrinsic based on the location relative to parenchyma of brain. Large conductance arteries such as middle cerebral and pial arteries constitute macrocirculation and extrinsic system whose main function is conductance of blood whereas penetrating arterioles, capillaries, and venules constitute microcirculation and intrinsic system whose main function is regulation of flow, although definitive role of capillaries in regulation of flow is less characterized (Kulik et al., 2008). Neurons exert direct influence on CBF. Nerve fibers associated with cerebral vessels have been identified within both the macro and micro circulation (Hamel, 2006). Vascular reactivity of the vessels is conferred due to the contractile nature of VSM cells, which are not found in the capillaries. Capillaries instead contain specialized contractile cells pericytes. Regulation of flow at capillary level is dependent on the regulation at arteriole level (Kontos et al., 1978). Under physiological conditions, a significant proportion of cerebrovascular resistance (CVR) is located in the pial and penetrating arterioles. Thus in order to increase flow to intrinsic circulatory bed, the extrinsic vessels must dilate, otherwise a vascular shunting might occur.

A special feature of CNS is its redundancy of arterial supply (collateral circulation), which can protect brain in the event of focally restricted blood flow in a larger conductance vessel. Another unique feature of CNS is blood-brain barrier (BBB), which is formed by tight gap junctions of vascular endothelium. The BBB serves important regulatory function in maintaining ionic balance, transport of micro and macro nutrients and preventing toxic substances from blood to diffuse into

the parenchyma. The large conductance arteries, pial arteries, and penetrating arterioles all have a BBB (Roggendorf et al., 1977). Ischemic injury affects both smaller and larger arteries. In ischemic injury, leukocytes adherence to endothelial cell wall and platelet rupture leads to irreversible injury of BBB. During reperfusion phase injury is further aggravated as leukocytes interact with damaged abluminal endothelial wall and plug microvasculature causing a no-reflow phenomenon. In addition, release of inflammatory factors, cytokines, and free radicals worsen the injury (Chan, 2001).

1.2.2 Cerebral autoregulation of blood flow

The human brain comprises only 2% of the body mass yet it consumes 20% of the energy produced by the body at resting state. Since brain requires constant supply of glucose and oxygen, regulation of blood flow throughout the brain is vital for maintaining normal cognitive and motor functions. CBF varies directly with cerebral perfusion pressure (CPP), which is classically defined as difference between mean arterial pressure (MAP) and intracranial pressures (ICP), and inversely with the total CVR. Further, hemodynamics of blood flow is also affected by hematocrit, platelet aggregation, and plasma viscosity (Kee et al., 1984). The contribution of any given vessel to overall CBF is determined by its radius, length, blood viscosity, and pressure. Under physiological conditions, tissue perfusion in brain ranges from 50 to 55 mL/100 g/min. As blood perfusion decreases like in the example of ischemia, oxygen extraction from hemoglobin gradually increases so the decrease in oxidative metabolism can be less than the fall in CBF (Frykholm et al., 2000). Brain naturally develops autoregulatory mechanisms to maintain normal CBF in the face of rising blood pressure (myogenic tone) (Panerai, 2008). CBF is autoregulated over a range of arterial pressure from 70 to 120 mm Hg in normal brain. Autoregulation is governed by myogenic

regulation of precapillary blood vessels such as pial arteries and metabolic regulation at the level of small precapillary arterioles (Imig et al., 2011). In response to increases in arterial blood pressure, smooth muscle cells in vessels depolarize through the action of vasoconstrictive factors that increase intracellular Ca^{2+} resulting in vasoconstriction, thereby increasing the total CVR to maintain a constant CBF globally. Cerebral arteries originating from the circle of Willis and pial arteries on the surface of brain are highly myogenically active. The autoregulatory capacity is influenced by factors such as hematocrit, hemoglobin concentration, and blood levels of CO_2, O_2, H^+, brain temperature, cardiac output, and altitude. In certain chronic disease states such hypertension autoregulatory mechanisms may become dysfunctional due to which CBF passively changes with the changes in the MAP and ICP causing extreme fluctuations in the CBF eventually leading to vascular and organ damage over time.

1.2.2.1. Endothelium dependent relaxation:

Endothelium is involved in controlling the balance between vasoconstrictors (ET-1, $PGF_{2\alpha}$, and TXA_2), and vasodilators (NO, PGE_2, PGI_2, and EDHF) to help maintain a resting tone. In addition, it also plays important role in regulating local inflammatory and cell adhesion process, in vascular remodeling, platelet aggregation, and coagulation. A functioning endothelium is very essential in vascular adopting to the changes in the blood flow. Endothelial dysfunction is the underlying cause in the pathophysiology of many cerebrovascular and cardiovascular diseases (Cai et al., 2000; Iadecola et al., 2004; McIntyre et al., 1999; Widlansky et al., 2003). Circulating substances such as acetylcholine, bradykinin, and ATP that bind to specific endothelial surface receptors as well as mechanical stimuli such as fluid shear stress and pulsatile stretch activate the endothelium, which releases various vasoactive factors. Endothelium derived nitric oxide (NO) and prostacyclin (PGI_2) are well characterized endothelium derived relaxing factors that affect the

vascular tone. Despite the inhibition of NO and PGI_2 pathways, an endothelium dependent relaxation effect persisted in most vascular beds, which led to the identification of yet another endothelium derived hyperpolarizing factor (EDHF) (Chen et al., 1988; Taylor et al., 1988).

EDHF plays important role in the control of cerebral artery tone. EDHF exerts autocrine and paracrine effects by hyperpolarizing endothelial and VSM cell eventually leading to vasorelaxation. The underlying mechanisms include activation of BK_{Ca} on VSM cells promoting K^+ efflux and membrane hyperpolarization. Other mechanisms include activation of endothelial K_{Ca} channels of small (SK_{Ca}) and intermediate (IK_{Ca}) conductance, which release K^+ in to myoendothelial space. The released potassium either causes endothelial hyperpolarization, which is electrically transmitted through myoendothelial gap junctions into the smooth muscle cell (SMC) layer or activates the Na^+/K^+ ATPase and the inward rectifying potassium channels (K_{IR}) on the SMC inducing K^+ release, hyperpolarization of VSM and subsequent relaxation (Bellien et al., 2008). Though EDHF dependent relaxation is observed in both resistance and conduit arteries, its contribution appears to be prominent in small arteries and decreases inversely with the vessel size (Nagao et al., 1992). NO interacts with EDHF pathways by exerting a constant inhibition. Thus EDHF mediated relaxations are usually masked in the larger arteries and are evident only in the presence of NO inhibition or in conditions of low vascular availability of NO (Bauersachs et al., 1996).

1.2.3. Neurovascular coupling

As opposed to cerebral autoregulation of maintaining constant flow globally, in instances of increased neuronal activity blood flow is increased locally to match the metabolic demands of neurons through a phenomenon called neurovascular coupling or functional hyperemia (Filosa et

al., 2007; Imig, et al., 2011). Locally, cerebral blood vessels respond to changes in their physical (intraluminal pressure, longitudinal shear) and chemical (pH, partial pressures of O_2, and CO_2) environments but they can also sense and respond to increases in neuronal activity via a specialized system comprised of neurons, astrocytes, and blood vessels. Astrocytes, most abundant glial cell population in brain, serve as a key player in coupling neuronal activity to cerebral vessels. Fine perisynaptic processes extending from astrocyte cell body cover most synapses whereas terminal portion of large processes (endfeet) cover a major proportion of the abluminal vascular surface of capillaries, intracerebral arterioles, and penetrating arterioles (Simard et al., 2003). Thus they are ideally placed for sensing neuronal activity, and relaying that information to surrounding cerebral vessels by releasing vasodilatory mediators such as EETs. Thus together astrocytes, neurons, and cerebral blood vessels form a neurovascular (NV) unit (Attwell et al., 2010).

1.2.3.1. Neurogenic regulation: Neurovascular control of the cerebral circulation varies depending on the location and capacity of the vessels. Extracerebral vessels are in general innervated by peripheral nerves (extrinsic innervation) of sympathetic, parasympathetic, and sensory origin (Bleys et al., 2001). In contrast, parenchymal microvessels are primarily regulated by afferent fibers from subcortical pathways, local interneurons, and neuronal terminals from central origin (intrinsic innervation) (Hamel, 2006). Glutamate released from neuronal synapses during increased activity acts on ionotropic glutamate receptors or NMDA receptors on neurons increasing the intracellular Ca^{2+}. This in turn activates neuronal nitric oxide synthase (nNOS), which releases NO that is shown to dilate cerebral vessels in both *in vitro* and *in vivo* studies (Busija et al., 2007). However, in a study with mice deficient in eNOS, and nNOS no abnormalities in the normal CBF response to whisker stimulation were observed (Koehler et al., 2009; Lindauer et al., 1996; Ma et al., 1996) indicating that neurogenic control through NO may not be the only

mechanism in neurovascular coupling and that other compensatory mechanisms involving other vasodilators of neurogenic or non-neurogenic origin might be contributing to the hyperemic response.

1.2.3.2. Astrocyte regulation: Glutamate released from neurons also acts on the metabotropic glutamate receptors on astrocytes leading to an increase in intracellular Ca^{2+}. This transient increase in calcium levels either opens BK_{Ca} in astrocyte endfeet, which release K^+ onto microvessels or activate $cPLA_2$. Activated $cPLA_2$ increases free AA levels in cytosol, which is metabolized to form prostaglandins such as PGE_2 and EETs that dilate nearby arterioles (Peng et al., 2004; Zonta et al., 2003). However, an increase in intracellular Ca^{2+} in astrocytes also releases wide range of different vasoconstrictors (e.g. 20-HETE, $PGF_{2\alpha}$, thromboxane A_2, and endothelins) and vasodilators (e.g. NO, ATP, PGE_2, and EETs) depending on the type and duration of stimuli (Filosa, et al., 2007). Therefore, whether a rise in intracellular Ca^{2+}, causes dilation or constriction may in part be determined by the pre-existing tone of the vessel (Blanco et al., 2008). The relative importance of neuronal and astrocytic pathways in vasodilation remains unclear and is likely to differ across brain regions. It appears that NO, cyclooxygenase, and epoxygenase products are all important in mediating functional hyperemia in the cortex whereas NO is more dominant in the cerebellum (Yang et al., 1999). This implies that therapeutic modulation of the signaling pathways controlling CBF may have different effects in different brain regions and on different neuronal pathways in the same region. Adding to the complexity, interaction between different signaling pathways of vasodilation were also reported in the literature. For example, NO inhibits enzymes that forms 20-HETE and EETs, which explains the cyclic GMP independent vasodilatory effect of NO (Sun et al., 2000).

1.2.3.3. Endothelial regulation: Although the primary role of endothelium is to establish a resting tone of cerebral vessels through basal release of NO and set that tone as a background for other dilators and constrictors, its precise role in neurovascular coupling has not been clearly defined. However, it is speculated that neurogenic and astrocytic mediators released in response to increased neuronal activity, could traverse the VSM to stimulate receptors on the abluminal side of the endothelium to release various vasodilatory agents (Andresen et al., 2006). This was tested experimentally in different studies by applying dilator agents to the abluminal side of the endothelium although not in connection with neuronal activation (Dietrich et al., 1996; Faraci et al., 2004). Dilation of larger upstream arterioles and arteries along with the dilation of arterioles directly supplying to the capillary bed is required for maximizing the vascular control. Indeed, neuronal stimulation can dilate large upstream cerebral vessels. Vascular endothelium could play an important role in mediating upstream dilations by conducting a dilator response along the vessel to upstream arterioles possibly communicating via specialized gap junctions. In support of this, local application of ATP to penetrating arterioles induced both a local vasomotor response as well as an upstream dilation indicating that vascular endothelium could play an important role in mediating upstream dilations (Dietrich, et al., 1996; Horiuchi et al., 2002).

1.2.3.4. Regulation in disease states: Interestingly, impaired autoregulation and altered neurovascular coupling are both evident in several disease states and the interactions between the systems is poorly understood (Girouard et al., 2006; Krizanac-Bengez et al., 2004). In ischemia, functional hyperemia is observed in certain regions during the early reperfusion period, which is followed by long lasting periods of hypoperfusion. This inadequate matching of flow to the neuronal activity may produce damage to cells beyond that is caused by initial ischemic injury. This decreased flow or no-reflow phenomenon was attributed to different mechanisms. The first

one is reduction in the capillary diameter as a result of astrocyte endfoot swelling causing capillary blockage by blood cells and fibrin (Ames et al., 1968) whereas the other mechanism was failure of arteriole vasodilatory mechanisms (Kagstrom et al., 1983a; Wagerle et al., 1988).

1.2.4. CYP eicosanoids in CBF regulation

1.2.4.1. Role in cerebral autoregulation:

HETE: In an *in vitro* study with rat middle cerebral arteries, Gebremedhin et al., showed that elevating transmural pressure from 20 – 140 mm Hg produced a fourfold increase in 20-HETE levels. Inhibition of 20-HETE synthesis or antagonizing the vasoconstrictive actions of 20-HETE with synthetic structural analog 20-HEDE blocked pressure induced contraction of these vessels indicating that 20-HETE may be an essential component of the myogenic response in cerebral arteries. They also indicated that 20-HETE plays a critical role in determining the efficiency of autoregulation of CBF *in vivo*. Activation of PK C and Rho-kinase appears to be the key signaling mechanisms contributing to the myogenic response (Gebremedhin, et al., 2000; Strandgaard et al., 1984). It appears that endothelium derived factors could modulate the myogenic contraction by interfering with the actions of 20-HETE. For example, NO inhibits formation of 20-HETE by binding to CYP4A, 4F enzymes and it is reported in different studies that non cGMP dependent vasodilatory response of NO is due to the fall in 20-HETE levels in cerebral arteries (Sun, et al., 2000; Yu et al., 2002).

EETs: Exogenous application of EETs has been shown to dilate cerebral arteries in both *in vitro* (Gebremedhin et al., 1992) and *in vivo* (Ellis et al., 1990) studies. Alkayed et al., showed that inhibition of CYP epoxygenase decreases baseline blood flow suggesting that tonic release of

EETs participates in the maintenance of basal vascular tone in rat brain microcirculation (Alkayed et al., 1996). However, they measured EETs from cultured rat astrocytes and not from endothelium of cerebral vessels. In the previous section 1.2.2.1, I have described the role of endothelium, and especially EDHF in maintenance of basal vascular tone. Though, CYP derived EETs have been identified as EDHF in different vascular beds (Archer et al., 2003; Bellien et al., 2006; Fischer et al., 2007; Hillig et al., 2003) their role as EDHF in cerebral vasculature is not conclusively proved due to the limited evidence on expression of CYP epoxygenases in the cerebral blood vessels (Iliff, et al., 2010). Different studies showed that cerebral tone is markedly affected by EET production, although not from endothelium but astrocytes (Alkayed et al., 1997; Harder et al., 2000). However, EETs can functionally antagonize actions of 20-HETE by increasing the open state probability of K_{Ca} channels and activating Na^+-K^+-ATPase. In a study Imig et al., showed that inhibiting epoxygenase activity enhances arteriolar constriction when perfusion pressure is increased from 80 to 120 mm Hg (Imig et al., 1999). Thus, EETs can potentially impact the myogenic tone of cerebral arteries by counterbalancing the actions of 20-HETE in the blood vessels.

1.2.4.2. Role in neurovascular coupling:

EETs: In section 1.2.3.1, I have mentioned that the mice deficient in eNOS, and nNOS showed no abnormalities in the normal CBF response to whisker stimulation suggesting that NO may not be an essential component in neurovascular coupling (Koehler, et al., 2009). Consistent with this view different studies have showed that in response to glutamate released by neurons, astrocytes release EETs consequently increasing the CBF. EET antagonists or EET synthesis inhibitors were also shown to attenuate the increase in CBF on activation of the cerebral cortex (Filosa, et al., 2007; Koehler et al., 2006). These evidence prove that within neurovascular unit

EETs released from astrocytes function as sensors of neuronal activity in a feed forward manner and elicit functional hyperemia.

However, the role of EETs in neurogenic control of blood flow, especially in the large conduit arteries-perivascular nervous system was not elucidated until recently. Iliff et al, produced first evidence of CYP2J and sEH expression in the perivascular nerve fibers innervating the cortical surface vasculature including middle cerebral and basilar artery. This extrinsic perivascular innervation has population of vasodilatory neurons including parasympathetic fibers originating in the sphenopalatine ganglia (SPG), and otic ganglia, and sensory afferents that project to the trigeminal ganglia (TG). Expression of CYP2J and sEH in the sensory TG and parasympathetic SPG neurons (Iliff et al., 2009b) indicates that EETs may serve as a nerve derived vasodilatory factor in large cerebral conduit arteries. Electrical stimulation of efferent nerve fibers and chemical stimulation by capsaicin both showed EET mediated increase in cortical CBF, which was abolished by pretreatment of EET antagonist 14,15-EEZE. However, these fibers also release NO, vasoactive intestinal peptide (VIP) from parasympathetic nerve fibers, and calcitonin gene-related peptide (CGRP) from sensory fibers to mediate their vasodilatory effects. Based on their findings, Iliff et al postulated that EETs may interact with these other vasomotor pathways in three possible modes. One possible mode is release of EETs from nerves in additive manner with other neurotransmitters in response to stimuli to regulate vascular tone. A second possibility is that neurogenic EETs exert autocrine effects in releasing other neurotransmitters as VIP or CGRP. A third possible mode of interaction is that one or more releasable factors from parasympathetic or sensory perivascular neurons exert vasoactive effects via a vasomotor pathway dependent on endothelial EET signaling (Iliff, et al., 2009b).

20-HETE: 20-HETE does not exert any appreciable impact on the increase in cortical CBF in response to whisker barrel stimulation in rats or mice. Interestingly, an interaction between 20-HETE and EETs was observed when nNOS is inhibited whereby 20-HETE reduced the effects of EET in eliciting functional hyperemia (Liu et al., 2008).

1.2.5. Small molecule inhibitors of CYP eicosanoid pathway

Small molecule chemical inhibitors are best studied tools for delineating the pharmacological actions of CYP eicosanoids in various disease models. In this section, various pharmacological inhibitors used for studying the role of CYP eicosanoids in different *in vitro* and *in vivo* studies are summarized.

1.2.5.1. ω-hydroxylase pathway:

Mechanism based inhibitors: A single intraperitoneal injection of suicidal substrate 1-aminobenzotriazole (ABT) (50 mg/kg) selectively inhibited renal cortical 20-HETE formation in rats. However, chronic treatment with ABT inhibited both 20-HETE and EET formation in the rat kidney (Dos Santos et al., 2004; Su et al., 1998). A series of terminal acetylenic monocarboxylic fatty acids of varying length from 10 [10-undecynoic acid (10-UDYA)] to 17 [17-octadecynoic acid (17-ODYA)] carbons were tested as inhibitors of 20-HETE formation (Ortiz de Montellano et al., 1984; Reich et al., 1986). Of these, 17-ODYA was potent inhibitor of AA metabolism inhibiting both HETE and EET forming enzymes. Yet 17-ODYA was used in different *in vitro* and *in vivo* studies. A single dose administration of 10-undecynyl sulfate (10-SUYS), a structural analog of 10-UDYA decreased 20-HETE formation and reduced mean arterial blood pressure in spontaneously hypertensive rats (SHR) (Xu et al., 2002a).

Competitive and non-competitive inhibitors: An olefinic acyclic dibromide compound, N-methylsulfonyl-12,12-dibromododec-11-enamide (DDMS) reduced the pressure-induced vasoconstriction of isolated rat cerebral vessels, resulting in 24% increase in vessel diameter compared to control. In an *in vivo* study DDMS abolished the autoregulatory response in rat and increased the CBF corresponding to increases in arterial pressure (Gebremedhin, et al., 2000). A higher cerebrovascular 20-HETE levels were shown to contribute to oxidative stress and endothelial dysfunction, and increased susceptibility to ischemic brain damage (Dunn et al., 2008). Brain 20-HETE levels were found to be increased after ischemic stroke and chronic administration of a potent, selective 20-HETE synthesis inhibitor, N-hydroxy-N`-(4-butyl-2-methylphenyl)-formamidine (HET0016) decreased brain 20-HETE levels, attenuated the decrease in CBF during the reperfusion period, and reduced the infarct volume in a rat temporary MCAO model (Poloyac et al., 2006). Similarly, acute administration of HET0016 also reduced infarct size in a rat model of focal ischemia (Renic et al., 2009). HET0016 was also effective in reducing 20-HETE levels in CSF, and prevent the acute fall in CBF in the rat model of SAH (Cambj-Sapunar et al., 2003; Kehl et al., 2002). N-(3-Chloro-4-morpholin-4-yl) phenyl-N`-hydroxyimido formamide (TS-011), the most potent inhibitor of 20-HETE synthesis to date, has shown protection from hemorrhagic and ischemic stroke in rats by significantly reducing brain 20-HETE levels and improving functional outcomes (Marumo et al., 2010; Miyata, et al., 2005; Renic, et al., 2009). Recently, TS-011 was shown to improve defects in cerebral microcirculatory autoregulation near the infarct site thereby reducing cerebral damage following ischemia (Marumo, et al., 2010).

20-HETE antagonists: A stable structural analog of 20-HETE, 20-hydroxyeicosa-6(Z),15(Z)-dienoic acid (20-HEDE) blocked 20-HETE induced vasoconstriction of rat middle cerebral and basilar arteries, and attenuated 20-HETE mediated increases in intracellular Ca^{2+} in

an *in vitro* study and reduced the acute fall in CBF in a rat model of SAH (Gebremedhin, et al., 2000; Yu et al., 2004). 20-HETE antagonist also showed reduction in infarct size in a rat temporary MCAO model (Renic, et al., 2009).

1.2.5.2 Epoxygenase and sEH pathway: Miconazole and 17-ODYA have been used as epoxygenase inhibitors in the coronary and cerebral circulations (Harder et al., 1998). Miconazole significantly decreased baseline blood flow in the brain of rats (Alkayed, et al., 1996) and reduced glutamate induced increases in CBF (Harder, et al., 1998). Miconazole and N-methylsulfonyl-6-(2-propargyloxyphenyl) hexamide (MS-PPOH), a selective epoxygenase inhibitor blocked the functional hyperemic response to the activation of the whisker barrel cortex in rats (Bhardwaj et al., 2000). .

Since administering EETs is not a viable pharmacological approach as they rapid bind to plasma proteins or metabolized to less active DHETs, more metabolically stable analogs of EET (Sodhi et al., 2009) were developed in the past but most widely used approach for studying the effects of EETs has been increasing endogenous EET levels by inhibiting or genetically deleting sEH , which metabolizes EETs (Iliff et al., 2009a; Imig, et al., 2009). Different genetic studies have tested the association between the genetic polymorphisms in EPHX2 encoding sEH and the risk for ischemic stroke (Fornage et al., 2005; Gschwendtner et al., 2008; Koerner et al., 2007; Lee et al., 2010; Zhang et al., 2008a). There were conflicting findings in terms of the association with increased risk for stroke and/or cardiovascular diseases. However, pharmacological inhibition of sEH has consistently demonstrated effectiveness in reducing ischemic damage in rats and mice (Dorrance et al., 2005; Simpkins et al., 2009; Zhang et al., 2007; Zhang et al., 2008b). Different potent and specific sEH inhibitors were developed with better physicochemical properties (Kim et al., 2004; Morisseau et al., 1999; Morisseau et al., 2002). sEH inhibitor 12-(3-adamantan-1-yl-ureido)

dodecanoic acid (AUDA) protected against cerebral ischemia in spontaneously hypertensive and Wistakr-Kyoto rats. Both acute and chronic inhibition of sEH showed protection from ischemic injury irrespective of the time of administration of inhibitors and the protective effects appeared to be mediated by EETs as CYP epoxygenase inhibition by MS-PPOH abolished the protective effect of sEH inhibition (Zhang, et al., 2007; Zhang, et al., 2008b).

Despite the development of various chemical inhibitors targeting specific CYP450 eicosanoid pathways, most of the existing pharmacological inhibitors do not possess all favorable characteristics such as solubility, and permeability across BBB. Thus, there is a growing need to design new compounds with not just chemical stability but with selectivity and specificity to the CYP isoforms in the target organ, and with improved pharmacokinetic profile to achieve desired therapeutic concentrations in the brain, to test in animal models of cerebrovascular disease in order to develop effective therapeutic strategies to treat the debilitating neurological consequences of stroke and ischemic brain injury.

1.3. NEUROPROTECTIVE THERAPIES

1.3.1 Neuroprotective agents

Drugs used for acute ischemic stroke can be broadly classified into drugs that improve hemodynamics (thrombolytics, antiplatelet drugs, anticoagulants, and fibrinogen depleting agents) and others that target molecular and cellular pathways that mediate the injury, which are known as neuroprotective agents. In section 1.1.2 pathophysiology of cerebral ischemic injury was discussed. In this section, I will briefly review various therapeutic agents tested in clinical trials for ischemic stroke that target different cellular and molecular pathways of injury.

NMDA receptor antagonists were developed in the past as a putative neuroprotective therapy since they are primarily involved in mediating the excitotoxicity associated with glutamate release in ischemia. NMDA receptor competitive and non-competitive antagonists can reduce experimental ischemic volume as much as 30 – 50% (Lipton, 1999). MK-801, a potent non-competitive NMDA antagonist failed in the clinical trials due to unwanted serious side effects such as psychosis, hallucinations, and hypotension. A primary reason for the failure of many NMDA receptor antagonists was the therapeutic time window, which was as late as 6 h after stroke. This may be too late as glutamate release is highest in the initial few hours of ischemic injury. Ca^{2+} channel blockers were another class of drugs that attracted attention as they aim to decrease intracellular Ca^{2+}, which is key contributor in initiating many cell death pathways. However, these agents also reduce systemic blood pressure, and hypotension can increase infarct size by affecting the collateral flow, which can worsen the clinical outcome. Nimodipine, a calcium channel antagonist has only been effective in preventing ischemia from SAH associated vasospasm but not in focal ischemia. During reperfusion phase there is increased production of free radicals in penumbra. Free radical inhibitors were thought to be more beneficial as they offer longer therapeutic window than glutamate pathways. Spin-trap free radical inhibitors can dramatically reduce infarct volume in reperfusion models (Marshall et al., 2001; Sydserff et al., 2002). Free-radical inhibitors offer longer time window than that of glutaminergic pathways. Tirilazad, and NXY-059 both have failed in the clinical and currently Ebselen, an antioxidant that can react with peroxynitrite is undergoing phase III trials. Several other drugs were developed and tested in clinical trials that work through various known and unknown pathways (**Table 1-1**) but have not been successful (Smith, 2004; Xu et al., 2013). Currently the only approved medication by Food and Drug Administration (FDA) for improving clinical outcome in ischemic stroke is recanalization of the vessels using tissue

plasminogen activator (tPA) and even that has a narrow therapeutic index and must be administered within 3 hours of stroke onset (Fisher et al., 2003).

Table 1-1 List of neuroprotective agents tested for stroke (www.strokecenter.org/trials)

Mechanism	**Agent / Trial**	**Phase**	**Status**
Free radical scavenger / Antioxidant	Ebselen	III	On going
	Tirilazad	II	Completed
GABA agonist	Clomethiazole	II	Completed
Ca^{2+} channel blocker	Nimodipine	III	Completed
	Flunarizine	III	Completed
Ca^{2+} chelator	Dp-b99	II	On going
Glutamate antagonist			
AMPA antagonist	Zonampanel	II	Completed
	MPQX	II	Completed
Competitive NMDA antagonist	Selfotel	III	Completed
NMDA channel blocker	Aptiganel	III	Completed
	Traxoprodil	III	On going
	Magnesium	III	On going
Glycine site antagonist	Licostinel	I	On going
	Gavestinel	III	Completed
Growth factor	Fibroblast GF	III	Completed
Leukocyte adhesion inhibitor	Enlimomab	III	Completed
	Rovelizumab	III	Completed
Nitric oxide inhibitor	Lubeluzole	III	Completed
Opiod antagonist	Cervene	III	Completed
Phosphatidyl choline precursor	Citicoline	III	On going
Seretonin agonist	Repinotan	III	Completed
Sodium channel blocker	Fosphenytion	III	Completed
Potassium channel agonist	BMS-204352	III	Completed
Unknown mechanism	Piracetam	III	On going

There are probably several reasons for failure of most of the clinical trials that otherwise showed promise in preclinical testing. The reasons for the failure are complex and many including timing of administration of drug, window of opportunity, duration of ischemia, dose of the drug given, species, gender differences, age, and underlying diseases. There is a definite need to reassess the research paradigm in both preclinical and clinical stroke studies in order to improve successful translation of the animal studies to human. Perhaps appropriate model selection that accounts for factors like age, comorbid conditions; choice of anesthetics that have less confounding effects on neuroprotection; monitoring of physiological variables; assessing neurological damage in both permanent and temporary MCAO models; longer therapeutic time window; drugs that cross BBB may be some of the useful strategies. Further, as it is difficult to intervene early in stroke, preventing the ischemic cell death at later times by targeting the pathways leading to delayed ischemic cell death such as free radical damage may be useful as an adjuvant therapy along with recanalizing the vessels.

1.3.2 STAIR Recommendations

Lack of translation of therapies to human after ischemia has led to formation of an academy/industry joint roundtable "Stroke Therapy Academy Industry Roundtable" (STAIR) who made recommendations for appropriate conduct of preclinical trials of neuroprotective agents using stroke/ischemic models (STAIR, 1999). The following recommendations were made by them:

1. Adequate dose response curve: A full dose-response curve should be performed so that the minimum effective and maximum tolerated dose are clearly defined. Further, the studies should document that the drug in these range of concentrations is accessible to the target organ.

2. Therapeutic window: There is uncertainty about the relevance of therapeutic time window in animals to acute clinical stroke. Yet animal models appear to be relevant to address a therapeutic time window for thrombolytic and neuroprotective drugs. It is recommended to use penumbral imaging using perfusion/diffusion MRI mismatch to help identifying the therapeutic window in a particular model.

3. Outcome measures: Multiple endpoints are important and both histological and behavioral outcomes should be assessed. These assessments should include studies conducted at least 2 to 3 weeks or longer after stroke onset to demonstrate sustained benefit with emphasis on functional outcome in delayed survival studies.

4. Physiological monitoring: In many a focal ischemia models spontaneous reperfusion may occur leading to infarct size variability. Basic physiological parameters such as blood pressure, temperature, blood gases, and blood glucose should be routinely monitored. Temperature should be maintained within in the normal physiological range. It is suggested to monitor CBF using perfusion imaging or laser Doppler flow to document adequate sustained occlusion and to monitor reperfusion in temporary ischemia models.

5. Multiple species: Treatment efficacy should be established in at least 2 species using both histological and behavioral outcome measures. Rodents or rabbits are acceptable for initial testing and gyrencephalic primates or cats are desirable as second species.

6. Multiple models: The ischemia is usually reversible in animal models but this is occasionally the case in clinical trial subjects. Hence it is recommended to test efficacy of neuroprotective agents in both permanent and temporary focal ischemia models, and it is desirable for the agent to be effective in both models.

7. Infarction location: The infarction is mostly confined to the cortex in the rat models, while human ischemic strokes are often located in the white matter. Whether the ischemic area is located in grey or white matter impacts the outcome. Thus it is desirable to have neuroprotective agents show effectiveness for both cortical and subcortical infarctions.

8. Multiple targets: Protecting neurons *per se* is not enough. It is likely that glial cells and vascular elements in the brain also be protected from injury. The emerging concept of neurovascular unit emphasizes that all the multiple cell types in brain must be considered when identifying targets for developing neuroprotective agents.

1.4. NEW APPROACHES IN NEUROPROTECTION

1.4.1 Biomarker based approach

Secondary neuronal damage is commonly observed in both stroke and cardiac arrest after reperfusion/resuscitation. Identifying and measuring the key mediators of injury pathways, especially during the delayed death phase, may be of great prognostic value to identify patients at risk for developing secondary neuronal damage (Turner et al., 2013). These mediators commonly known as “biomarkers” are classically defined as a biological component that can be tangibly quantified to understand normal or pathological functioning in the body (Bettermann, 2011; Mayeux, 2004). They are useful in diagnosis, monitoring progress of disease, identify targets for intervention, and assessing the risk of pathology. One example is troponin-1 well known biomarker used in myocardial infarction. Previous studies have demonstrated differences in various markers that have potential to play a role in predicting outcomes, increase our understanding of pathophysiology of cerebral ischemia, and possibly provide targets for therapeutic intervention

(Denes et al., 2011; Navarro-Sobrino et al., 2011; Qian et al., 2012; Ramos-Fernandez et al., 2011). Historically, biomarker based studies have focused on single marker for diagnostic/prognostic purpose. However, in recent times there was transition towards identifying a panel of biomarkers that may improve sensitivity, specificity, and predictive values over time. Multiple biomarkers have been identified in literature for stroke. For example, matrix metalloproteinase (MMP-9) (Montaner et al., 2001), glial fibrillary acidic protein (GFAP) (Hasan et al., 2012), S100B (Montaner et al., 2012), D-dimer (Montaner et al., 2011). A vast number of clinical trials failed due to how stroke research was conducted (methodology) as well as the therapeutic targets selected. Thus, more research on biomarkers not only serve as diagnostic/prognostic tool but will also help in elucidating pathophysiology of cerebral ischemic injury.

1.5. SUMMARY AND RESEARCH HYPOTHESIS

Stroke and cardiac arrest are among the top three leading causes of death in adults with a common underlying mechanism of ischemic cell death although with differences in specific cellular and molecular pathways. Ischemic lesion evolution is the complex interplay of balance between various vasoactive factors, inflammatory mediators, and interaction between different injury pathways. Remarkable differences in the ischemic injury during interrupted blood flow and during reperfusion / resuscitation stress the need to understand these underlying pathways in order to design effective therapeutic strategies to minimize the debilitating consequences of stroke and cardiac arrest. Lipid metabolism, has taken the center stage in stroke research due to the plethora of actions these metabolites exert on regulation of CBF and tissue survival in a cell type specific manner. As discussed in this chapter, release of free fatty acids especially AA and its metabolites during the ischemic injury have been shown to play a critical role in the disease progression. In the past few decades, CYP450 enzymes have emerged as a third major pathway of AA metabolism with significant contribution to overall blood flow regulation in vascular beds of different organs. Pharmacological actions of CYP450 derived eicosanoids in different organs including kidney, lungs, and heart were well documented in the literature. However, interest in the delineating the significance of their role in cerebrovascular diseases such as stroke has gained momentum.

Studies outlined throughout this review have demonstrated significance of CYP eicosanoids in cerebral ischemic injury. Though these CYP eicosanoids affect CBF regulation, they also exert cytoprotective effects directly independent of blood flow modulation. The relative contributions of vascular and non-vascular mechanisms of neuroprotection by CYP eicosanoids have not been systematically elucidated. As discussed in this chapter, use of pharmacological inhibitors to inhibit

one pathway of AA metabolism may change levels of AA metabolites from other pathways due to shunting, which may or may not contribute to the overall neuroprotective effect observed. Thus, it is not only important to confirm the selectivity, and specificity of the pharmacological inhibitors but also it is equally important to quantify a whole array of AA metabolites in order to delineate the specific contribution of CYP eicosanoids in neuroprotection. The advanced and sophisticated analytical techniques to quantify lipids and their metabolic products, an approach called lipidomics is gaining wide spread use in lipid research however applications of this approach specifically in CYP eicosanoid research has been limited.

Pharmacological effects of CYP eicosanoids were traditionally evaluated from *in vitro* studies of microvessel diameter changes to *in vivo* studies of histological evaluation of infarct size. However, benefits of modulating CYP eicosanoid pathway in terms of improved outcomes was less emphasized. As recommended by STAIR, an assessment of short-term and long-term functional outcomes in addition to histological evaluation is warranted to advance pharmacological inhibitors of CYP eicosanoid pathway as a potential therapeutic intervention for treating cerebrovascular disorders like stroke. Further, understanding the relative contribution of components of neurovascular unit to the overall neuroprotection is important for developing therapeutic agents that modulate multiple targets in the neurovascular unit to achieve maximum therapeutic efficacy.

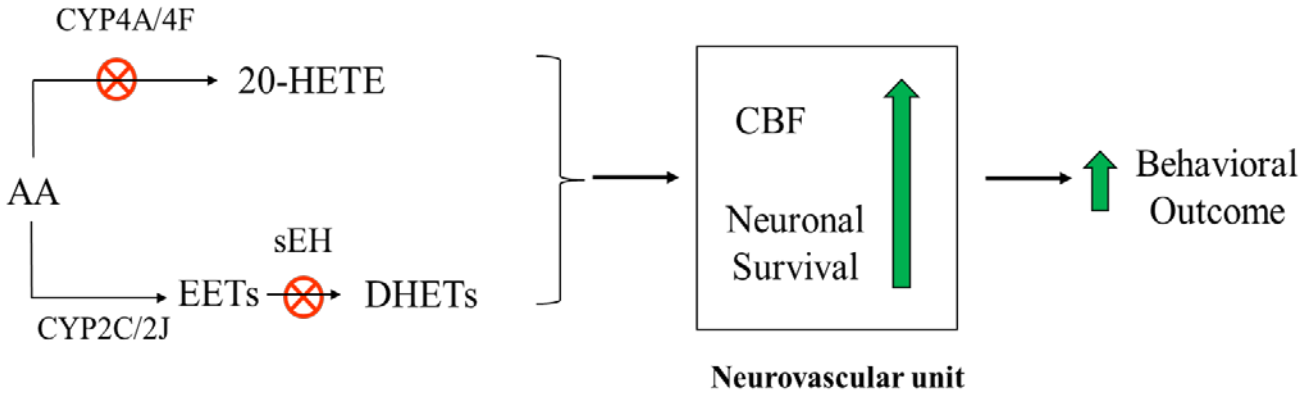

Figure 1-5. Schematic of research hypothesis

Therefore, the goal of this thesis research is to systematically evaluate the effects of CYP eicosanoids on neuronal death, CBF, and functional outcome in the context of neurovascular unit in experimental models of focal and global ischemia. As shown in **Figure 1-5**, we hypothesize that inhibiting the formation of 20-HETE and metabolism of the EETs by pharmacological inhibitors improves functional outcome by affecting the components of neurovascular unit such as neurons, and cerebral vessels (blood flow).

First objective of the study was to develop a comprehensive lipidomics analysis of tissue levels of prostanoids and CYP eicosanoids. This objective was achieved by using advanced analytical instruments and results are presented in Chapter 2. The second objective was to investigate the cytoprotective effects of CYP eicosanoids under normal and ischemic conditions. This objective was completed by using *in vitro* neuronal cultures and results are presented in Chapter 3. The third objective was to evaluate the effects of CYP eicosanoids in an experimental focal ischemia model. This was accomplished using advanced analytical assays, a rat MCAO model, state-of-the-art CBF assessment techniques, sophisticated neurobehavioral analysis, and *in vitro* neuronal cultures. The results are presented in Chapter 4. The fourth and final objective was to evaluate the CYP

eicosanoid effects in an experimental model of global ischemia. This was completed by using advanced analytical assays, pediatric asphyxial CA model, sophisticated CBF analysis, and neurological deficit analysis. The results are presented in Chapter 5.

2.0 ANALYTICAL METHOD DEVELOPMENT AND VALIDATION

[Jafar Sadik B Shaik, Tricia M. Miller, Steven H Graham, Mioara D. Manole, Samuel M Poloyac. "Rapid and simultaneous quantitation of prostanoids by UPLC-MS/MS in rat brain". Manuscript accepted for publication in *Journal of Chromatography B*]

2.1 INTRODUCTION

Many pharmacological inhibitors targeting different pathways of AA metabolism were developed in the past as a potential therapeutic intervention to treat various neurodegenerative and neuroinflammatory diseases. However, these inhibitors, while decreasing metabolites from a specific pathway, also lead to increase in the formation of metabolites of AA from other pathways due to shunting. Therefore, there is a need to analytically evaluate all AA metabolites to evaluate the total sum effect of interventions aimed at altering arachidonic acid metabolism. Analytical methods play a vital supportive role in drug discovery & development process from measuring the concentrations of drugs in biological fluids to measuring concentrations of biomarkers of diseases progression. In lipid research, identifying and measuring a panel of all AA metabolites in different tissues and biological fluids serves two main purposes: a) quantifying specific metabolites that may be elevated or reduced in various disease conditions; b) quantifying metabolites of a certain pathway as an indicator of target engagement for confirming the selectivity of pharmacological inhibitors. In addition to the above advantages, lipidomics based analytical methods also offer rapid throughput in bioanalysis. Therefore, for the purpose of this thesis research an UPLC-MS/MS method was developed and validated for rapid and simultaneous quantification of prostanoids and CYP eicosanoids in brain tissue. As discussed previously in **Chapter 1**, prostanoids are the cyclic lipid mediators produced from the cyclooxygenation of AA, a rate limiting step catalyzed by COX family of enzymes consisting of a constitutive (COX-1) and an inducible (COX-2) isoform (Gryglewski, 2008). As shown in **Figure 2-1**, these and other tissue specific terminal synthases convert AA to family of various structurally different prostanoid metabolites. These prostanoids bind to classes of GPCR designated EP (PGE_2), FP ($PGF_{2\alpha}$), DP

(PGD_2), IP (PGI_2), and TP (TXA_2) receptors that have various effects on cAMP and intracellular Ca^{2+} mobilization.

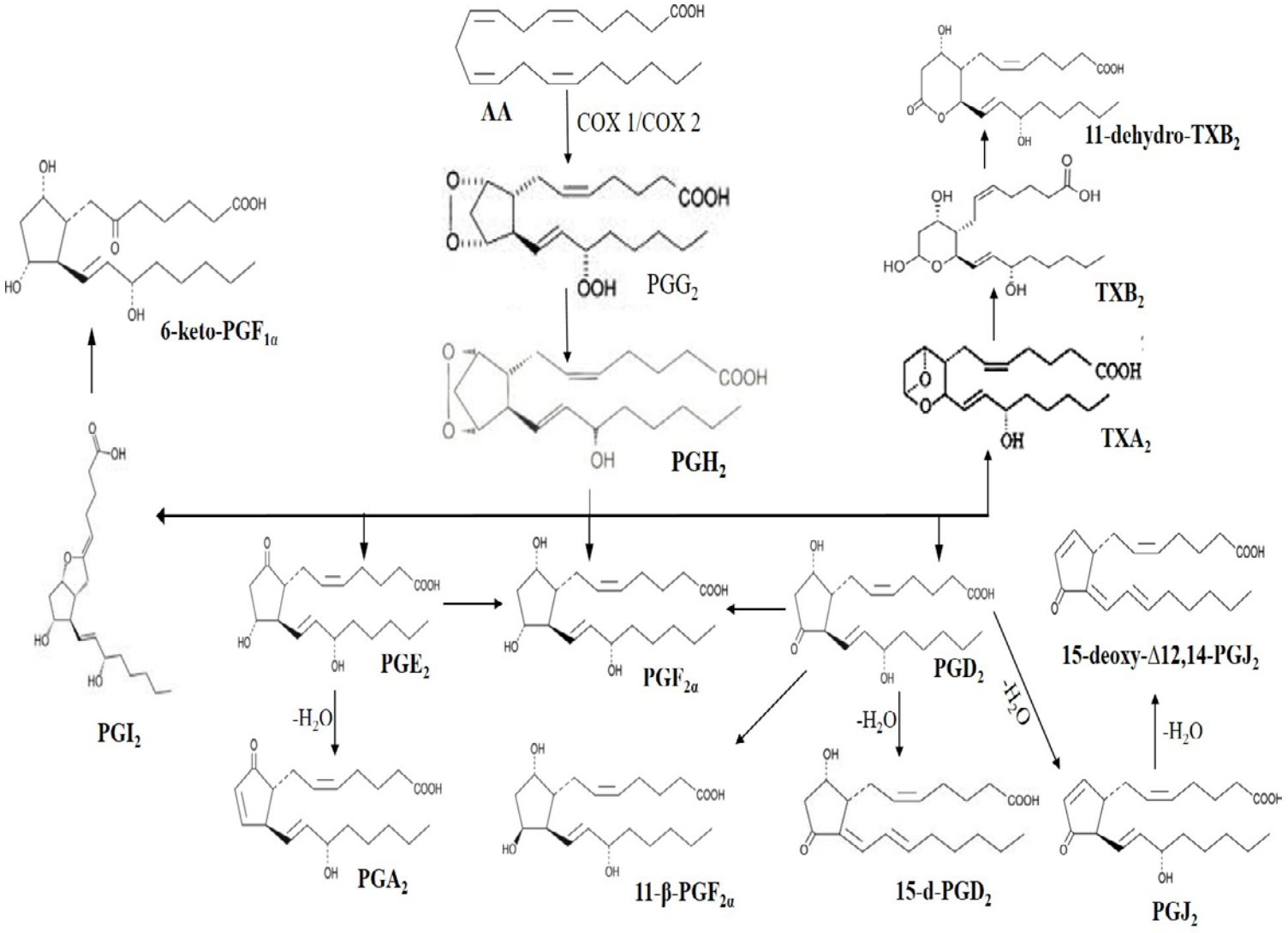

Figure 2-1. Cyclooxygenase pathway of AA metabolism. AA is converted to unstable cyclic endoperoxy metabolite (PGG_2), which is reduced to PGH_2. PGH_2 is further metabolized by tissue specific terminal isomerases (PGD_2 or PGE_2), reductases ($PGF_{2\alpha}$), prostacyclin synthase (PGI_2), and thromboxane synthase (TXA_2). Hydrolysis of PGI_2 and TXA_2 yields inactive by-products (6-keto-$PGF_{1\alpha}$ and TXB_2) of much greater stability.

2.1.1. Biological significance of prostanoids in CNS:

In previous chapter, I have discussed in detail on the biological significance of CYP eicosanoids in cerebral ischemia. In this section, the significance of prostanoids in various CNS disorders will be discussed. In the CNS, prostanoids have been implicated in various neuroinflammatory and neurodegenerative disorders (Lima et al., 2012). Prostanoid receptor signaling may elicit divergent pharmacological or pathological effects on tissue/cell viability depending on the type of injury. Previous studies showed that PGE_2 was neuroprotective in *in vitro* neuronal cultures (Akaike et al., 1994; Takadera et al., 2002) and in *in vivo* animal models of focal ischemia (Liu et al., 2005a; McCullough et al., 2004), conversely, PGE_2 was also shown to promote an inflammatory and neurotoxic effect in the lipopolysaccharide (LPS) model (Montine et al., 2002). Patients with probable Alzheimer Disease (AD) have higher CSF concentrations of PGE_2 than age-matched control subjects (Montine et al., 1999). Similarly, Parkinson's disease (PD) patients also have elevated PGE_2 concentrations in CSF (Mattammal et al., 1995). In addition, PGD_2 has been shown to be important in neuroinflammatory and neurodegenerative conditions (Rosenberger et al., 2004). PGD_2 synthase (PGDS) expression is localized in microglial cells surrounding senile plaques and DP_1 receptor (PGD_2 receptor) expression was observed in microglial cells and astrocytes within senile plaques in human AD brains (Iwamoto et al., 1989; Mohri et al., 2007). 15-deoxy-Δ12,14-PGJ_2 (15d-PGJ_2) and PGJ_2, non-enzymatic cyclopentenone metabolites of PGD_2, are increased in the rat brain after cerebral ischemia (Liu et al., 2011; Liu et al., 2013a). 15d-PGJ_2 mediates its effects through PPAR γ receptors. This prostanoid has been shown to exert neuroprotective effects in *in vitro* cell cultures by reducing microglial production of NO, IL-6, and TNF-α induced by Aβ40 (Takata et al., 2003).

$PGF_{2\alpha}$ has been shown to exacerbate hypoxic injury in rat primary neuronal culture (Li et al., 2008) as well as in *in vivo* models of ischemia with a FP agonist (Saleem et al., 2009). A prostacyclin receptor ligand has shown neuroprotective effects in a MCAO model (Takamatsu et al., 2002) and also in neuronal cultures by reducing expression of different inflammatory mediators such as TNF-α (Satoh et al., 1999). In addition to their role in neuroinflammation, prostanoids such as prostacyclin (PGI_2) and PGE_2 also alter vascular smooth muscle tone (Chapple et al., 1980; Greenberg et al., 1982; Lippton et al., 1979). Specifically, prostacyclin (PGI_2) and TXA_2 are potent vasodilators and vasoconstrictors of cerebrovasculature, respectively (Moncada et al., 1979). Collectively, these studies suggest that prostanoids produce a plethora of effects on CNS and are important mediators in the pathogenesis of neurodegenerative and neuroinflammatory diseases.

2.1.2. Analytical methods for quantifying prostanoids

Multiple methods have been developed for the detection and quantitation of prostanoid metabolites. Radio-immuno assays (Hofer et al., 1993), enzyme linked immunoassays (Pradelles et al., 1990), HPLC methods (Henden et al., 1993; Kiss et al., 1998; Moraes et al., 2004; VanderNoot et al., 2002), and gas chromatography-mass spectrometry methods (Baranowski et al., 2002; Nithipatikom et al., 2001) have been developed in the past for the quantitative analysis of these metabolites from many different matrices. Though these assays are useful, limitations of these methods include inadequate sensitivity, limited selectivity, narrow range of metabolites, and cross-reactivity. A significant issue in analysis of similar isomeric metabolites from complex biological matrices is the specificity. High performance liquid chromatography with tandem mass spectrometry (HPLC-MS/MS) methods have been successfully applied to quantify these metabolites from different matrices including cell cultures (Martin-Venegas et al., 2011;

Takabatake et al., 2002), biological fluids (Chappell et al., 2011; Ferreiro-Vera et al., 2011a; Ferreiro-Vera et al., 2011b; Komaba et al., 2009; Unterwurzacher et al., 2008), and tissues (Masoodi et al., 2006) but flow rate limitation common in HPLC systems has resulted in longer run times making most of these methods time-consuming and expensive. The shortest run time reported by these methods containing at least five different prostanoids is 25 min. A more efficient method would be the use of ultra-performance liquid chromatography (UPLC), which offers greater separation efficiency, higher sensitivity, and shorter run times.

Therefore, it was the purpose of this study to develop and validate a sensitive, accurate, and rapid high throughput UPLC-MS/MS method to simultaneously measure 11 prostanoid metabolites in rat brain tissue. In addition, we investigated the effects of the matrix on the reproducibility and reliability of the data as recommended by the Food and Drug Administrative (FDA) Quantitative Bioanalytical Methods Validation Report and other validation guidance documents (Matuszewski et al., 2003; Viswanathan et al., 2007). Furthermore, we applied the sample processing method employed in the prostanoid method development to our previously published CYP eicosanoid method (Miller et al., 2009) in order to measure them all from a single extracted sample of rat brain tissue rather than including all prostanoids and CYP eicosanoids in one single run, thereby compromising on sensitivity and analysis time. Therefore, development of this method is necessary for evaluation of these metabolites as potential quantitative biomarkers in order to elucidate their role in modulation of neuroinflammatory, neurodegenerative as well as vascular disorders.

2.2 EXPERIMENT AND METHOD VALIDATION

2.2.1 Chemicals and reagents

Stock standards of 6-keto-prostglandin $F_{1\alpha}$ (6-keto-$PGF_{1\alpha}$), 6-keto-prostaglandin $F_{1\alpha}$-*d4* (6-keto-$PGF_{1\alpha}$-*d4*), 11β-prostaglandin $F_{2\alpha}$ (11β-$PGF_{2\alpha}$), 11β-prostaglandin $F_{2\alpha}$-*d4* (11β-$PGF_{2\alpha}$-*d4*), prostaglandin $F_{1\alpha}$ ($PGF_{1\alpha}$), prostaglandin $F_{1\alpha}$-*d9* ($PGF_{1\alpha}$-*d9*), prostaglandin $F_{2\alpha}$ ($PGF_{2\alpha}$), prostaglandin $F_{2\alpha}$-*d4* ($PGF_{2\alpha}$-*d4*), prostaglandin E_2 (PGE_2), prostaglandin E_2-*d4* (PGE_2-*d4*), 11-dehydro-Thromboxane B_2 (11-d-TXB_2), 11-dehydro-Thromboxane B_2-*d4* (11-d-TXB_2-*d4*), prostaglandin D_2 (PGD_2), prostaglandin D_2-*d4* (PGD_2-*d4*), prostaglandin A_2 (PGA_2), prostaglandin J_2 (PGJ_2), 15-deoxy-Δ12,14-prostaglandin D_2 (15-d-PGD_2), 15-deoxy-Δ12,14-prostaglandin J_2 (15-d-PGJ_2), 15-deoxy-Δ12,14-prostaglandin J_2-*d4* (15-d-PGJ_2-*d4*) were purchased from Cayman Chemical Company (Ann Arbor, MI). High purity organic solvents were purchased from VWR (West Chester, PA) and all other chemicals were purchased from Sigma-Aldrich (St. Louis, MO).

2.2.2 Animals and treatment

Male postnatal day (PND) 16 to 18 Sprague-Dawley rats (between 30 to 45 g) were maintained on a 12-h light/dark cycle. Rats were initially subjected to anesthesia with the use of a spontaneous inhalational anesthesia system [Surgivet (Smiths Medical, Waukesha, WI) V7216 Isotec 4] containing 3% isoflurane / 50% N_2O & oxygen until unconscious and then the trachea was intubated with an 18-gauge angiocatheter and mechanical ventilation was initiated. Anesthesia was reduced to 2.5% isoflurane/50% N_2O & oxygen and femoral arterial and venous catheters were placed. Isoflurane was discontinued, and intravenous analgesia was initiated using fentanyl infusion at 50 µg/kg/h and neuromuscular blockade was obtained using vecuronium infusion at 5

mg/kg/h. Asphyxial cardiac arrest was induced by disconnecting the tracheal tube from the ventilator for 12 min. Resuscitation was initiated by reconnecting the ventilator, infusion of epinephrine 0.005 mg/kg and sodium bicarbonate 1 mEq/kg *i.v* and manual chest compressions until ROSC. Anesthesia and neuromuscular blockade were restarted at 30 min after ROSC. Animals were sacrificed by decapitation at 5 and 120 min after ROSC and brain cortical tissue was rapidly excised, snap frozen in liquid nitrogen and stored at -80 ºC. All animal procedures were approved by the University of Pittsburgh Institutional Animal Care and Use Committee.

2.2.3 UPLC-MS/MS method development

2.2.3.1 Chromatography and mass spectrometry

2.2.3.1.1 Prostanoids:

Liquid chromatography was performed using an Acquity ultra performance LC autosampler (Waters, Milford, MA). Prostanoids were separated on a UPLC BEH C-18, 1.7 µm (2.1 x 150 mm) reverse-phase column (Waters, Milford, MA) protected by a guard column (2.1 mm x 5 mm; Waters, Milford, MA) of the same packing material. Column temperature was maintained at 55 ºC. Mobile phases, delivered at a flow rate of 0.4 ml/min, consisted of 0.005% acetic acid, 5% acetonitrile in deionized water (A) and 0.005% acetic acid in acetonitrile (B) at an initial mixture of 65:35 A and B, respectively. Mobile phase B was maintained at 35% for 7.5 min and then increased to 98% in a linear gradient over 1.5 min, where it remained for 0.2 min. This was followed by a linear return to initial conditions over 0.1 min with a 2.7 min pre-equilibration period prior to the next sample run. Total run time per sample was 12 min and all injection volumes were 7.5 µl.

Mass spectrometric analysis of analyte formation was performed using a TSQ Quantum Ultra (Thermo Fisher Scientific, San Jose, CA) triple quadrupole mass spectrometer coupled with heated electrospray ionization source (HESI) operated in negative selective reaction monitoring (SRM) mode with unit resolutions at both Q1 and Q3 set at 0.70 full width at half maximum. Quantitation by SRM analysis on all prostanoid metabolites was performed by monitoring their respective m/z transitions. The SRM conditions for these analytes and their retention times are shown in **Table 2-1**. Parameters were optimized to obtain the highest $[M-H]^-$ ion abundance and were as follows: capillary temperature, 373 ºC, vaporizer temperature 340 ºC, spray voltage, 3500 kV, and a source collision-induced dissociation set at 0 V. Sheath gas, auxiliary gas, and ion sweep gas pressures were set at 60, 45, and 0, respectively. Scan time was set at 0.01 s and collision gas pressure was set at 1.5 mTorr. Analytical data was acquired and analyzed using Xcalibur software version 2.0.6 (Thermo Finnigan, San Jose, CA).

Table 2-1. SRM conditions for the prostanoid metabolites and the deuterated internal standards in negative electrospray ionization mode

Analyte	Precursor → Product (m/z)	Collision Energy	Retention time (min)
6-keto-$PGF_{1\alpha}$	369.3 → 245.1	28	1.61
6-keto-$PGF_{1\alpha}$-*d4*	373.2 →249.2	25	1.60
11β-$PGF_{2\alpha}$	353.1 → 193.1	26	2.30
11β-$PGF_{2\alpha}$-*d4*	357 → 197	27	2.29
$PGF_{1\alpha}$	355.1 → 311.1	23	2.63
$PGF_{1\alpha}$-*d9*	364 → 320.1	25	2.62
$PGF_{2\alpha}$	352.9 → 309.1	23	2.68
$PGF_{2\alpha}$-*d4*	357 → 313.1	23	2.66
PGE_2	351.1 → 271.1	20	2.90

PGE_2-*d4*	355.1 → 275.1	19	2.88
11-dehydro-TXB_2	367 → 305.1	22	3.00
11-dehydro-TXB_2-*d4*	371 → 309.1	20	2.98
PGD_2	351.1 → 271.1	20	3.30
PGD_2-*d4*	355.1 → 275.1	17	3.29
PGA_2	333 → 271.2	19	6.00
PGJ_2	333 → 271.2	19	6.42
15-deoxy-Δ12,14-PGD_2	333 → 271.2	19	9.32
15-deoxy-Δ12,14-PGJ_2	316 → 272	17	9.64
15-deoxy-Δ12,14-PGJ_2-*d4*	320 → 276	17	9.63

2.2.3.1.2 CYP eicosanoids:

CYP eicosanoids method development was described previously by our group (Miller, et al., 2009). Briefly, CYP eicosanoids were separated on a UPLC BEH C-18 column 1.7 µm (2.1 x 100 mm) reverse-phased column (Waters, Milford, MA) protected by a guard column (2.1 mm x 5 mm; Waters, Milford, MA) of the same packing material. Column temperature was maintained at 55 ºC. Mobile phases consisted of 0.005% acetic acid, 5% acetonitrile in deionized water (A) and 0.005% acetic acid in acetonitrile (B). CYP eicosanoids were separated by delivering mobile phase at 0.5 ml/min at an initial mixture of 65:35 A and B, respectively. Mobile phase B was increased from 35% to 70% in a linear gradient over 4 min, and again increased to 95% over 0.5 min where it remained for 0.3 min. This was followed by a linear return to initial conditions over 0.1 min with a 1.5 min pre-equilibration period prior to the next sample run. Total run time per sample was 6.4 min and injection volume was 7.5 µL. Mass spectrometric analysis of analyte formation was performed using a TSQ Quantum Ultra (Thermo Fisher Scientific, San Jose, CA) triple quadrupole mass spectrometer coupled with heated electrospray ionization (HESI) operated in negative

selective reaction monitoring (SRM) mode with unit resolutions at both Q1 and Q3 set at 0.70 full width at half maximum. Quantitation by SRM analysis on CYP eicosanoids was performed by monitoring their m/z transitions. Scan time was set at 0.01 s and collision gas pressure was set at 1.3 mTorr. Analytical data was acquired and analyzed using Xcalibur software version 2.0.6 (Thermo Finnigan, San Jose, CA).

2.2.3.2 Calibration standards and quality control samples

A stock solution of metabolites was prepared in 80:20 methanol:water to achieve a series of working solutions at 1 µg/ml, 100 ng/ml and 25 ng/ml concentrations. A solution of internal standard (IS) consisting of PGD_2-*d*4, 15-d-PGJ_2-*d*4, 6-keto-PGF_1-*d*4, 11β-PGF_2-*d*4, PGF_1-*d*9, 11-d-TXB_2-*d*4, PGE_2-*d*4, PGF_2-*d*4 was prepared in 80:20 methanol:water at a concentration of 1 µg/ml. Calibration standards and quality control (QC) samples were prepared from separate stock solutions by spiking appropriate amounts of the working solutions into deionized water. Calibration standards were prepared at 0.104, 0.208, 0.417, 0.83, 1.25, 1.67, 4.17, 8.33, 12.5, 16.7, and 33.3 ng/ml (6.25, 12.5, 25, 50, 75, 100, 250, 500, 750, 1000, and 2000 pg on column, respectively). QCs were prepared at 0.667, 7.50, and 20.83 ng/ml (40, 450 and 1250 pg on column, respectively).

2.2.3.3 Sample extraction procedure

Tissue samples were homogenized in deionized water containing 0.113 mM butylated hydroxytoluene (BHT) and centrifuged for 30 min at 10,000 rpm. The supernatant was removed for analysis. The metabolite concentrations in the tissue samples as well as in the calibration and quality control standards were all determined using a solid phase extraction (SPE) procedure.

Standards and tissue supernatants were spiked with 12.5 µL (containing 12.5 ng) of internal standard (IS) solution consisting of PGD_2-*d*4, 15-d-PGJ_2-*d*4, 6-keto-PGF_1-*d*4, 11β-PGF_2-*d*4, PGF_1-*d*9, 11-d-TxB_2-*d*4, PGE_2-*d*4, PGF_2-*d*4. The spiked samples were loaded onto Oasis hydrophilic-lipophilic balanced (HLB) (30 mg) SPE cartridges (Waters, Milford, MA) that were conditioned and equilibrated with 1 ml of methanol and 1 ml of water, respectively. Columns were washed with three 1 ml volumes of 5% methanol and were eluted with 100% methanol. Extracts were spiked with 15 µL of 1% acetic acid in methanol and dried under nitrogen gas at 37°C, and reconstituted in 125 µl of 80:20 methanol: water for further chromatographic analysis.

2.2.4 Method validation

Validation of the SPE assay was performed by using 11 standard concentrations of all prostanoid metabolites prepared in a 2 ml volume of the same deionized water used for sample dilution, and extracted via SPE using above method. The amount of metabolites in the standards ranged from 0.104 to 33.3 ng/ml (6.25 – 2000 pg on column). Four separate duplicate standard curves were prepared and analyzed over four consecutive days. Curves were calculated based on the peak area ratios between each metabolite to the IS and plotted against the amount of the metabolite injected onto the column.

2.2.4.1 Precision and accuracy

Precision and accuracy of the method was determined by the analysis of QC samples. Metabolites were spiked into deionized water to yield low, medium, and high QCs, corresponding to 0.667, 7.50, 20.83 ng/ml (40, 450, 1250 pg on column), respectively. Five samples at each level

were analyzed for two days, followed by 10 replicates of each on the final day of validation. The lower limit of detection (LLOD) was determined by the minimum value with a signal-to-noise (S/N) ratio of ≥ 3:1. The lower limit of quantitation (LLOQ) was determined by the minimum value with accuracy and precision within ±15% deviation of the nominal value. Accuracy was determined as the relative deviation in the calculated value (E) of a standard from that of its true value (T) expressed as a percentage. This accuracy, or relative standard error (RE%), was calculated using the equation RE%=(E−T)/T×100. Precision was evaluated and expressed as relative standard deviation (RSD %) of the mean concentrations using the equation RSD% = SD/M×100. The criteria for acceptability of data included accuracy and precision within ±15% deviation of the nominal value.

2.2.4.2 Analyte recovery determination

The extraction recovery (E.R.) efficiencies of the deuterated metabolites in deionized water were determined at 12.5 ng/ml (750 pg on column; n=6) by comparing the responses (area) of samples spiked before extraction to those spiked after extraction. The recovery samples were processed using SPE and concentrations of metabolites were determined by UPLC–MS/MS as described in section 2.2.3.3.

2.2.4.3 Matrix effects on prostanoids and CYP eicosanoids

Matrix effects (ME) were evaluated using 2 ml volume of the same deionized water (matrix) spiked with 0.113mM BHT used for processing rat cortical tissue samples. The matrix was extracted via SPE using the method described above, and the eluent was spiked with deuterated standards of prostanoids (PGD_2-*d*4, 15-d-PGJ_2-*d*4, 6-keto-PGF_1-*d*4, 11β-PGF_2-*d*4, PGF_1-*d*9, 11-d-TXB_2-*d*4, PGE_2-*d*4, PGF_2-*d*4) at 12.5 ng/ml. Similarly, the matrix effects on CYP

eicosanoids were measured by applying the current processing conditions to previously published CYP eicosanoids method (Miller, et al., 2009). The matrix was extracted via SPE and eluent was spiked with low and high concentrations of CYP eicosanoids (12-, 15-, and 20-HETE; 8,9-, 11,12-, and 14,15-EET; 5,6-, 8,9-, 11,12-, and 14,15-DHET) at 0.417 and 8.33 ng/ml, respectively and 20-HETE-*d*6 internal standard at 12.5 ng/ml. Neat samples containing the same concentration of deuterated prostanoid metabolites, CYP eicosanoids and 20-HETE-*d*6 were prepared in 80:20 methanol:water. Samples were analyzed using UPLC–MS/MS as described above. The ME for each prostanoid metabolite was calculated based on the area of the post-extraction spiked samples to the neat samples. The ME for each eicosanoid metabolite was calculated based on the area ratio (analyte/internal standard) of the post-extraction spiked samples to the neat samples. The ME values are expressed as average ± standard deviation (SD) with coefficient of variation (CV) (n=6). Values less than 1.00 indicate ion suppression and values greater than 1.00 indicate ion enhancement.

2.2.5 Statistical analysis

Statistical analysis was completed using GraphPad Prism software, version 5.0 (GraphPad Software, La Jolla, CA). In the matrix effect studies, IS-normalized matrix effect (ME) values for CYP eicosanoids in buffer and deionized water were compared using unpaired t-test and a $p < 0.05$ was considered significant. All data were represented as mean ± SD.

2.3. RESULTS

2.3.1 Development of UPLC-MS/MS Method

Acetonitrile and water mobile phases with acetic acid produced optimal chromatographic conditions and sensitivity for prostanoids detection. Addition of 15 µL of 1% (v/v) acetic acid in methanol to the eluent before the evaporation and reconstitution step increased sensitivity with a 2-fold increase in peak area. Under these experimental conditions, the representative chromatograms of a calibration standard at 0.417 ng/ml (25 pg on column) of prostanoids are depicted in **Figure 2-2**. The elution sequence was identified as 6-keto-$PGF_{1\alpha}$, 11β-$PGF_{2\alpha}$, $PGF_{1\alpha}$, $PGF_{2\alpha}$, PGE_2, 11-d-TXB_2, PGD_2, PGA_2, PGJ_2, 15-d-PGD_2, and 15-d-PGJ_2 as determined by comparison to injections of individual compounds and product fragments.

2.3.2 Linearity, accuracy and precision

Eleven calibration standards over a range of 0.104–33.3 ng/ml (6.25 – 2000 pg on column) were used to construct the curves for all metabolites except for 6-keto-$PGF_{1\alpha}$, $PGF_{2\alpha}$ and 11-d-TXB_2 , which ranged from 0.208 – 33.3 ng/ml. The weighting factor 1/Y typically provided the best fit of the plot as determined by visual inspection, correlation coefficient, and analysis of the residuals. All of the calibration standards fell within 15% deviation of back-calculated amounts from nominal spiked amounts for all levels and the correlation coefficients (R^2) were > 0.99 for each metabolite. The intra- and inter-day accuracy and precision for the assay were evaluated at three levels: 0.667, 7.50, and 20.83 ng/ml (40, 450 and 1250 pg on column, respectively), using the QC samples within the three validation runs. Ten replicates at each concentration within a single day of validation were used to determine the intra-day reproducibility. Inter-day reproducibility was determined over three separate days using n=5 at these concentrations.

Calculated values of the QCs were generated using the equation of linear regression obtained from the calibration curves run within the same sequence. Results were evaluated and are presented in **Table 2-2**. The %RSD for all metabolites fell within 15% indicating good reproducibility of the assay. The LLOQ was determined to be 0.104 ng/ml for all metabolites evaluated except for 6-keto-$PGF_{1\alpha}$, $PGF_{2\alpha}$ and 11-d-TXB_2, which was 0.208 ng/ml.

2.3.3 Recovery of analytes

The extraction recovery efficiencies for all deuterated prostanoid metabolites were determined at one level, 12.5 ng/ml (750 pg on column) (**Table 2-3**). The recovery ranged from 88.1 to 100.3%, with the 11β-$PGF_{2\alpha}$ having the lowest recovery. Similarly the extraction procedure of this method was applied to our previous CYP eicosanoids method. The recovery values for CYP eicosanoids from phosphate buffer at low (0.417 ng/ml) and high (8.33 ng/ml) concentrations ranged from 85.2 to 117% and 97.1 to 108%, respectively. Under new processing conditions E.R values from deionized water ranged from 92.0 to 111% and 98.1 to 112% at low and high concentrations respectively (**Table 2-5**). The recovery efficiency for all metabolites showed good reproducibility with a %RSD below 20.

Table 2-3 Extraction recovery efficiency of prostanoid metabolites in deionized water

Analyte	Extraction Efficiency (%)	RSD (%)
6-keto-$PGF_{1\alpha}$-*d4*	96.9	15.6
11β-$PGF_{2\alpha}$-*d4*	88.1	15.5
$PGF_{1\alpha}$-*d9*	100.3	13.5
$PGF_{2\alpha}$-*d4*	93.7	14.9
PGE_2-*d4*	91.6	16.3
11-dehydro-TXB_2-*d4*	89.8	18.0
PGD_2-*d4*	89.5	14.6
15-deoxy-Δ12,14-PGJ_2-*d4*	91.4	12.2

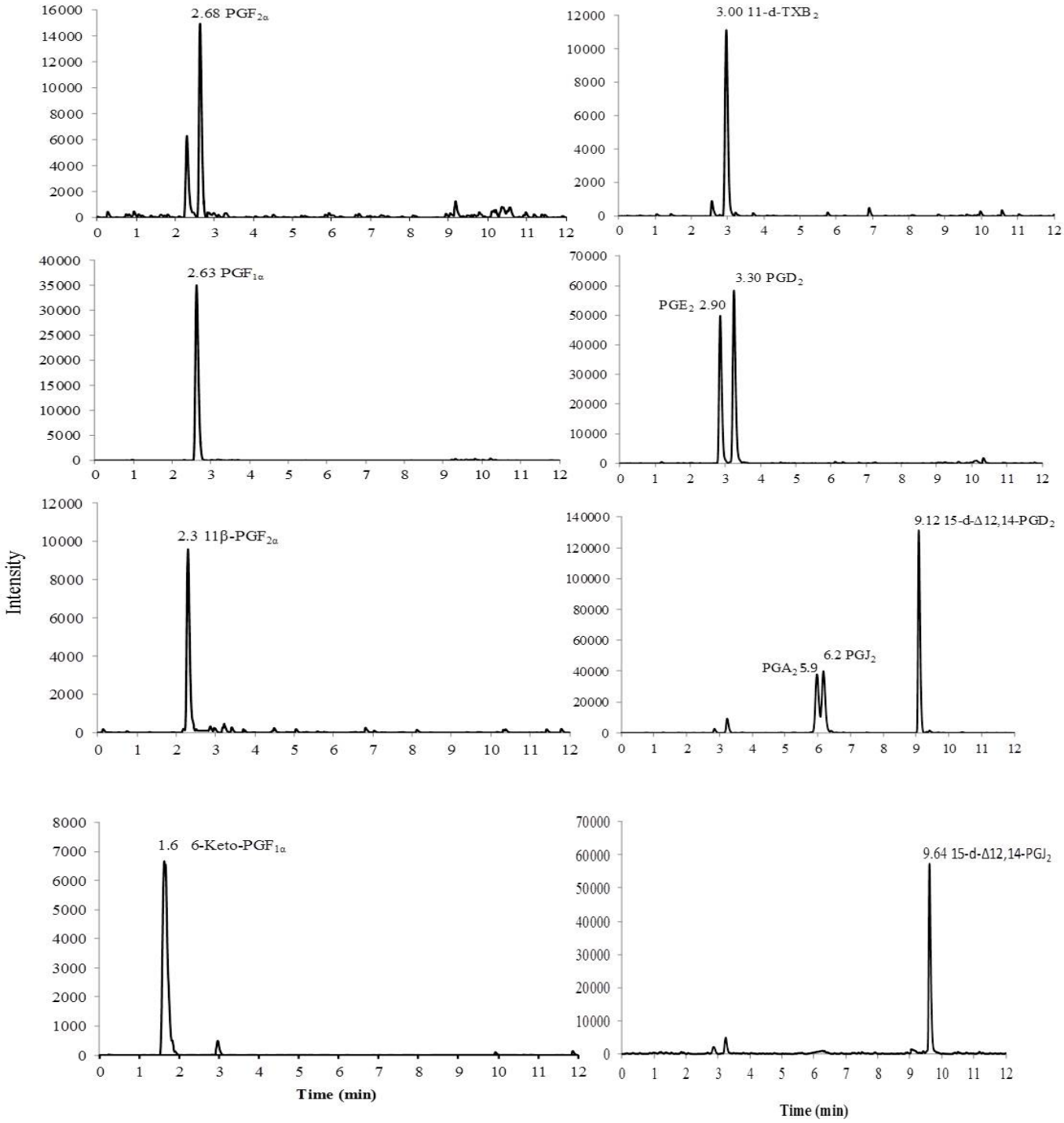

Figure 2-2. Chromatographic profiles, corresponding to 25 pg on column, depicting the separation of all prostanoids using a UPLC tandem MS/MS triple quadrupole mass spectrometer. Separation of metabolites was performed on a reversed-phase Acquity BEH C-18 column (2.1 x 150 mm; 1.7 µm i.d.). Metabolites were eluted at a flow rate of 0.4 ml/min over 12 min run time with a gradient from 35% acetonitrile containing 0.005% acetic acid to 98% acetonitrile containing 0.005% acetic acid.

Table 2-2. Accuracy and precision of assay for 11 prostanoid metabolites extracted in deionized water.

Analyte	Spiked amount (pg on column)	Intra-assay concentration (mean ± s.d) (pg on column)	RE%	RSD%	Inter-assay concentration (mean ± s.d) (pg on column)	RE%	RSD%
6-keto-$PGF_{1\alpha}$	40	38.7 ± 2.26	-3.01	5.82	40.7 ± 3.53	1.86	8.67
	450	437 ± 16.7	-2.83	3.82	449 ± 25.5	-0.21	5.69
	1250	1209 ± 34.2	-3.25	2.83	1241 ± 63.1	-0.72	5.08
11β-$PGF_{2\alpha}$	40	41.2 ± 2.91	3.00	7.06	40.9 ± 4.01	2.43	9.78
	450	435 ± 21.4	-3.12	4.91	437 ± 15.7	-2.80	3.58
	1250	1201 ± 52	-3.88	4.33	1228 ± 57	-1.71	4.64
$PGF_{1\alpha}$	40	37.7 ± 3.23	-5.72	8.56	39.5 ± 3.50	-1.28	8.86
	450	430 ± 15.3	-4.39	3.49	438 ± 11.1	-2.56	2.54
	1250	1216 ± 58.4	-2.68	4.80	1228 ± 64.5	-1.69	5.25
$PGF_{2\alpha}$	40	38.9 ± 4.65	-2.55	11.9	38.3 ±5.41	-4.25	14.1
	450	467 ± 47.7	3.90	10.2	455 ± 25.7	1.15	5.65
	1250	1249 ± 131	-0.06	10.5	1221 ± 67	-2.27	5.49
PGE_2	40	39.6 ± 1.58	-1.00	3.99	38.9 ± 1.24	-2.71	3.19
	450	413 ± 17.7	-8.11	4.29	439 ± 16.8	-2.23	3.83
	1250	1175 ± 44.8	-5.99	3.81	1209 ± 52	-3.26	4.30
11-dehydro-TXB_2	40	35.0 ± 1.88	-12.4	5.38	38.8 ± 4.05	-2.84	10.4
	450	407 ± 26.5	-9.41	6.50	446 ± 31.4	-0.88	7.04
	1250	1314 ± 61.2	5.14	4.66	1363 ± 77.8	9.05	5.71
PGD_2	40	39.7 ± 3.12	-0.74	7.85	39.9 ± 1.89	-0.02	4.71
	450	412 ± 5.97	-8.24	1.45	436 ± 17.8	-3.03	4.09
	1250	1206 ± 49.2	-3.46	4.08	1238 ± 21.7	-0.91	1.76
PGA_2	40	37.6 ± 2.94	-5.83	7.80	39.0 ± 2.67	-2.36	6.83
	450	409 ± 22.6	-9.03	5.53	434 ± 30.7	-3.54	7.08
	1250	1192 ± 112	-4.57	9.41	1228 ± 69.6	-1.71	5.67
PGJ_2	40	41.1 ± 2.72	2.87	6.60	39.5 ± 2.09	-1.18	5.28
	450	455 ± 11.2	1.25	2.46	443 ± 24.7	-1.38	5.57
	1250	1267 ± 47.6	1.37	3.76	1237 ± 56.7	-1.01	4.59
15-deoxy-PGD_2	40	38.1 ± 4.11	-4.58	10.7	39.8 ± 2.50	-0.40	6.26
	450	430 ± 35.5	-4.22	8.24	442 ± 28.6	-1.72	6.47
	1250	1206 ± 113	-3.44	9.44	1249 ± 76.1	-0.02	6.09
15-deoxy-PGJ_2	40	42.0 ± 3.54	5.18	8.41	41.6 ± 2.96	4.11	7.10
	450	443 ± 17.9	-1.54	4.05	449 ± 13.9	-0.08	3.10
	1250	1216 ± 95.6	-2.72	7.86	1253 ± 40.6	0.27	3.25

2.3.4 Analysis of matrix effects

2.3.4.1 Prostanoids

The effects of the deionized water (matrix) on the reproducibility of the assay to measure metabolites were determined. **Table 2-4** shows the coefficient of variation (CV) of the peak area of each deuterated metabolite of the post-extraction spike in deionized water along with the CV of neat samples prepared in 80:20 methanol:water (n=6). The % CV values for all metabolites were below 16%, demonstrating good precision and reliability of the assay. **Table 2-4** also shows the average matrix effect (M.E.) values of each metabolite as mean and CV (n=6). The average M.E. ranged from 0.86 to 0.97. A M.E. of 1 signifies no matrix effects. A M.E value less than 1 signifies ion suppression while a value greater than 1 signifies ion enhancement or analyte loss in the absence of matrix. The % CV of the M.E. values for most of the metabolites was below 15%, which demonstrates minimal effects of the deionized water (matrix) on the precision and reliability of the assay.

Table 2-4 Assessment of matrix effects of the deionized water on the reproducibility of the assay and the matrix effect factor for the deuterated metabolites.

Analyte	Precision (%CV)		Matrix Effect (M.E)	
	Neat	Deionized Water	Mean	%CV
6-keto-$PGF_{1\alpha}$-*d4*	1.28	15.8	0.89	14.7
11β-$PGF_{2\alpha}$-*d4*	8.50	11.0	0.94	13.7
$PGF_{1\alpha}$-*d9*	12.8	14.2	0.97	18.4
$PGF_{2\alpha}$-*d4*	12.4	9.1	0.91	15.0
PGE_2-*d4*	7.03	11.7	0.94	12.7
11-dehydro-TXB_2-*d4*	5.38	13.8	0.86	13.9
PGD_2-*d4*	8.02	10.9	0.87	13.0
15-deoxy-Δ12,14-PGJ_2-*d4*	6.16	7.61	0.93	9.96

2.3.4.2 CYP eicosanoids

The matrix effects of the phosphate buffer and deionized water (matrix) on the CYP eicosanoids were determined at low (0.417 ng/ml) and high (8.33 ng/ml) concentrations, respectively. **Table 2-5** shows the average IS-normalized M.E. as mean and CV (n=5). The average IS-normalized M.E. values in buffer ranged from 0.80 to 1.11 and 0.90 to 1.07 at low and high concentrations, respectively whereas in deionized water the values ranged from 0.99 to 1.17 and 0.95 to 1.07 at low and high concentrations, respectively. The % CV of the M.E. values for all of the metabolites was below 18%, which demonstrates minimal effects of the deionized water (matrix) on the precision and reliability of the assay. Overall, matrix effect seems to be minimal on CYP eicosanoids when deionized water was used as compared to microsomal incubation buffer.

Table 2-5 Effects of deionized water on the reproducibility and extraction efficiency of CYP eicosanoids

Medium	Analyte	Amt (pg)	M.E		E.R	
			Mean	%C.V	Mean	%C.V
Buffer	20-HETE	25	0.94	11.2	113.5	18.7
	12-HETE	25	0.80	12.2	108.4	10.1
	15-HETE	25	0.93	8.3	85.2	12.8
(n=5)	8,9-EET	25	1.09	13.4	98.3	16.2
	11,12-EET	25	0.92	13.8	104.2	11.6
	14,15-EET	25	0.91	8.5	111.4	13.7
	5,6-DHET	25	1.03	2.4	104.0	17.6
	8,9-DHET	25	1.01	5.9	107.0	12.6
	11,12-DHET	25	0.97	7.3	117.0	5.2
	14,15-DHET	25	1.11	4.8	115.7	5.9
Water	20-HETE	25	1.08	5.6	104.6	10.7
	12-HETE	25	1.06	15.6	95.8	14.7
	15-HETE	25	1.00	8.4	92.4	10.4
(n=5)	8,9-EET	25	1.04	10.8	104.3	10.0
	11,12-EET	25	1.03	16.9	103.3	15.0
	14,15-EET	25	0.99	10.8	98.7	18.2
	5,6-DHET	25	1.02	4.5	111.2	19.7
	8,9-DHET	25	1.17	6.3	92.0	12.5
	11,12-DHET	25	1.01	6.6	109.5	9.9
	14,15-DHET	25	1.06	8.9	105.4	17.0
Buffer	20-HETE	500	1.04	6.0	99.2	10.6
	12-HETE	500	0.90	14.4	103.5	10.3
	15-HETE	500	0.93	11.7	97.6	9.8
	8,9-EET	500	0.97	16.0	97.1	12.2
(n=5)	11,12-EET	500	0.95	15.8	101.5	9.1
	14,15-EET	500	0.97	14.8	99.8	12.3
	5,6-DHET	500	0.99	15.3	105.3	12.6
	8,9-DHET	500	0.98	10.7	106.2	9.5
	11,12-DHET	500	1.02	12.4	106.9	12.0
	14,15-DHET	500	1.07	7.7	108.3	6.6
Water	20-HETE	500	0.95	7.8	103.2	5.0
	12-HETE	500	1.06	10.8	98.1	7.0
	15-HETE	500	1.03	7.5	98.9	7.8
(n=5)	8,9-EET	500	1.05	6.8	101.1	6.6
	11,12-EET	500	1.07	11.2	101.6	3.5
	14,15-EET	500	1.03	7.6	99.4	5.2
	5,6-DHET	500	1.02	1.1	111.0	5.6
	8,9-DHET	500	1.03	8.1	112.1	4.5
	11,12-DHET	500	1.06	7.9	104.6	6.3
	14,15-DHET	500	1.07	1.9	105.5	3.3

2.3.5 Analysis of rat brain tissue samples

Rat brain cortex tissue samples (n=6) collected at 5 min post resuscitation were analyzed from animals subjected to 12 min of asphyxial cardiac arrest to determine prostanoid and eicosanoid metabolite concentrations using the standard calibration curves of each metabolite and results are shown in **Figure 2-3** and **2-4**. Quantitative amounts of all prostanoids were measured in these tissue samples and values ranged from 10.2 to 937 pmol/g wet tissue. The levels measured in the order of abundance were PGD_2, PGJ_2, PGE_2, 15-d-PGD_2, PGA_2, 15-d-PGJ_2, $PGF_{2\alpha}$, $PGF_{1\alpha}$, 11β-$PGF_{2\alpha}$ at 937±305, 36.9±10.7, 35.5±12.3, 32.7±14.8, 24.2±11.8, 18.4±0.80, 14.4±7, 13.9±7.7, 10.2±3.2 pmol/gm wet tissue (Figure 3). Detectible amounts of 6-keto-$PGF_{1\alpha}$, and 11-d-TXB_2 were also seen in these samples. Similarly, quantitative amounts of all CYP eicosanoids measured in the same tissue sample range from 2.23 to 793 pmol/g wet tissue. The levels measured in the order of abundance were 12-HETE, 15-HETE, 14,15-EET, 8,9-EET, 11,12-EET, 20-HETE, 14,15-DHET, 11,12-DHET at 793±161, 143±50.8, 44.6±3.78, 39.4±2.63, 20.8±1.46, 6.79±2.30, 4.17±0.21, 2.23±0.16 pmol/gm wet tissue (Figure 4). Detectible amounts of 8,9- and 5,6-DHET were also seen in these samples. These results imply that multiple arachidonic acid metabolites (prostanoids and CYP eicosanoids) in rat brain cortex can be quantified reliably using this method.

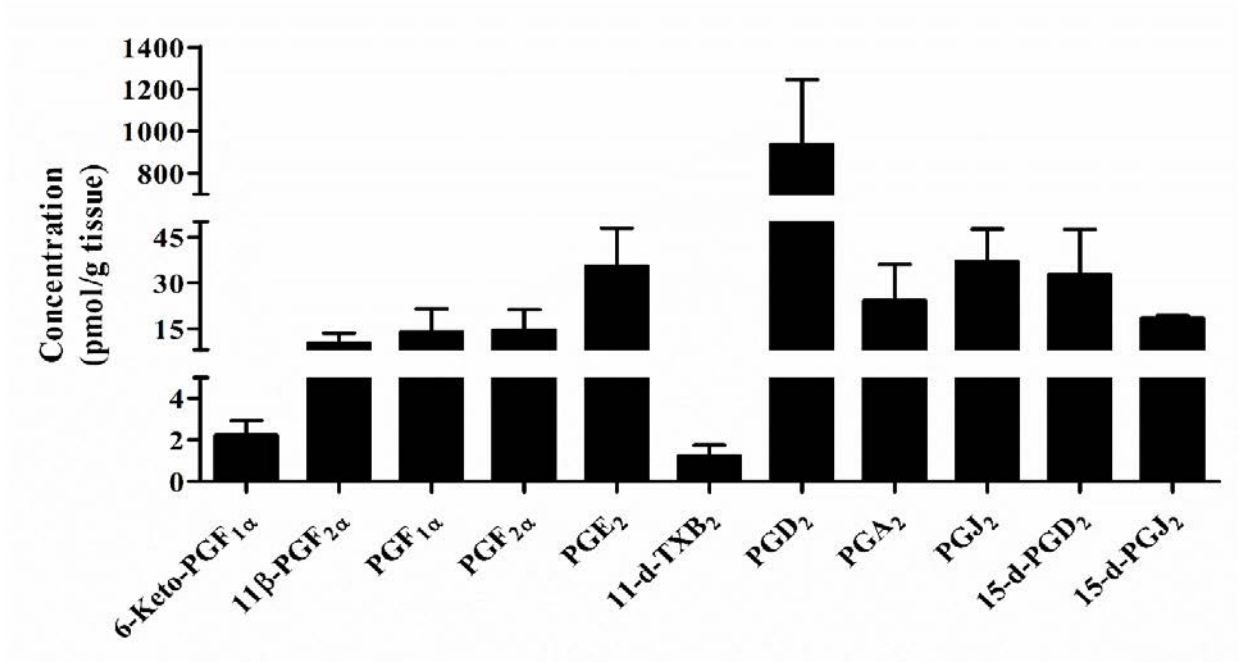

Figure 2-3. Concentrations of prostanoid metabolites detected in brain cortical tissue of pediatric rats at 5 min post resuscitation after being subjected to 12 min of asphyxial cardiac arrest.

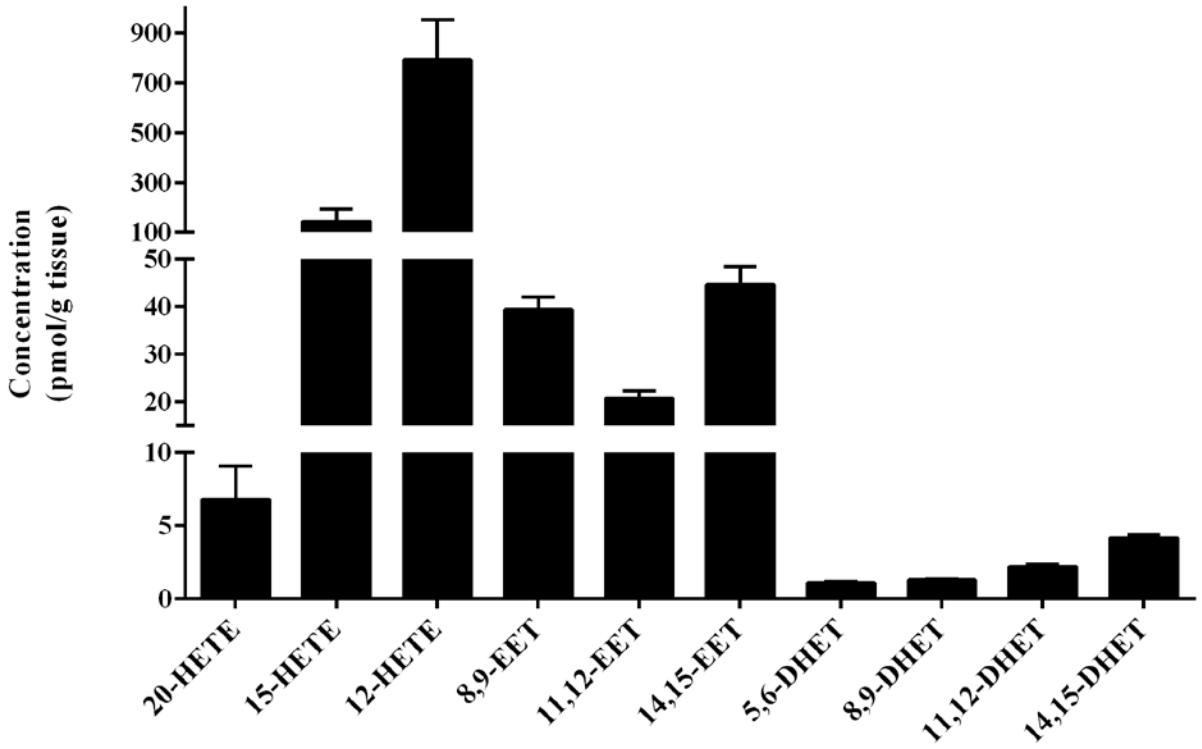

Figure 2-4. Concentrations of eicosanoid metabolites detected in brain cortical tissue of pediatric rats at 5 min post resuscitation after being subjected to 12 min of asphyxial cardiac arrest. These CYP eicosanoids were analyzed from same tissue extracts used for prostanoids measurement.

2.4. DISCUSSION

In this study we report a robust method to measure 11 prostanoid metabolites in rat brain cortical tissue. This is the first validated method reporting quantification of cyclopentenone metabolites in rat brain tissue. These compounds were simultaneously detected, identified and quantified using a validated UPLC-MS/MS method. Furthermore, we have successfully applied the processing conditions and extraction procedure of this method to our previously published method for CYP eicosanoid quantification in rat brain extracts with different MS/MS conditions (Miller, et al., 2009). With this approach we achieved an overall improvement in extraction recovery of CYP eicosanoids and reduction in matrix effects. This gave us the unique advantage of detecting and quantifying both the prostanoid and eicosanoid metabolites from the same extracted sample by two MS injections. Collectively, these results suggest that our validated UPLC-MS/MS method is an accurate and sensitive method and can be used successfully to quantify a wide range of arachidonic acid metabolites in rat brain tissue.

We have performed the validation of linear calibration curves ranging from 0.104 to 33.3 ng/ml (6.25 to 2000 pg on column) for all prostanoid metabolites except for 6-keto-$PGF_{1\alpha}$, $PGF_{2\alpha}$ and 11-d-TXB_2, which ranged from 0.208 to 33.3 ng/ml (12.5 to 2000 pg). The inter-day and intra-day variance was less than 15% with extraction efficiency greater than 88%. We demonstrated that matrix effect of deionized water did not significantly affect the reliability and reproducibility of the assay. In our previously validated CYP eicosanoid method we used microsomal incubation buffer as our matrix. In this study, we used the same matrix (deionized water) for both the prostanoid and CYP eicosanoid methods to test the extraction recovery and matrix effects at low and high concentrations for all CYP eicosanoids. The addition of 15 µl of 1%

acetic acid to the eluent before evaporation and reconstitution resulted in significant increase in extraction recovery for 15-HETE and significant reduction in matrix effect for 12-HETE at low concentrations while recovery and matrix effects largely remain unchanged at high concentrations for all CYP eicosanoid metabolites.

Concentrations of prostanoid metabolites were measured in rat brain tissue extracts. These include PGD_2, PGJ_2, PGE_2, 15-d-PGD_2, PGA_2, 15-d-PGJ_2, $PGF_{2\alpha}$, $PGF_{1\alpha}$, 11β-$PGF_{2\alpha}$, 6-keto-$PGF_{1\alpha}$, and 11-d-TXB_2. Several of these metabolites have been previously detected in different matrices such as cell cultures (Martin-Venegas, et al., 2011; Takabatake, et al., 2002), plasma/serum (Ferreiro-Vera, et al., 2011a; Ferreiro-Vera, et al., 2011b; Komaba, et al., 2009), urine (Chappell, et al., 2011; Masoodi, et al., 2006), and rat kidney (Blewett et al., 2008). Masoodi et al. (Masoodi, et al., 2006) and Yue et al. (Yue et al., 2007) reported measurements of prostanoids in rat brain or cortical tissue. Masoodi et al. measured prostanoids in uninjured rat brain whereas Yue et al. measured them in sham and traumatic brain injured rats. Yue et al. reported concentrations of only PGE_2 and PGD_2 from ipsi-lateral 72 h post-injured brains as 11.3 ± 0.61 and 4.99 ± 0.64 pmol/g tissue, respectively, and PGJ_2 and $PGF_{2\alpha}$ were not detected in their method. Although a direct methodological comparison cannot be determined given the differences in the animal and injury model, the levels of PGE_2 measured from a 5 min post resuscitation pediatric rat brain cortex using our method was comparable to the results reported by Yue *et al* (Yue, et al., 2007). We were able to detect all of the prostanoid metabolites of our assay, in the pediatric rat brain cortex post-injury indicating good specificity and sensitivity of our method. In addition, we successfully quantified CYP eicosanoids with different MS/MS conditions (as reported in our previous method) from the same tissue extracts. Together, our method is capable of measuring a

total of 21 arachidonic acid metabolites including prostanoids and CYP eicosanoids from a single extracted sample in a combined run time of 18 minutes.

The results from our method are similar to other studies that have reported the detection of similar metabolites in different matrices. Ferreiro-Vera et al. described simultaneous measurement of different inflammation biomarkers from human serum and human plasma and reported concentrations of $PGF_{2\alpha}$ and PGE_2 as 10.3 and 0.17 ng/ml in plasma (Ferreiro-Vera, et al., 2011a), and 0.11 ng/ml for PGE_2 (Ferreiro-Vera, et al., 2011b) in serum, which are within our standard calibration range of 0.104 - 33.3 ng/ml. LOQs reported in their method as 46, 138 and 188 pg (on column) for $PGF_{2\alpha}$, PGE_2 and PGD_2 were however found to be higher than our method. In addition, Unterwurzacher et al. described a method for measurement of hydroxyeicosatetraenoic acid, hydroxyoctadecadienoic acid (HODE), leukotrienes, and prostanoids by HPLC-MS/MS in human plasma (Unterwurzacher, et al., 2008). The LOQ from this method is reported as 0.352, 0.264, 1.42, and 1.85 ng/ml for PGD_2, PGE_2, $PGF_{2\alpha,}$ and 6-keto-$PGF_{1\alpha,}$ respectively. Similarly, Blewett et al. reported simultaneous measurement of several arachidonic acid metabolites by HPLC-MS in rat kidney (Blewett, et al., 2008). The LOQ from this method were 14.4, 25.3, 20.6 pg (on column) for $PGF_{2\alpha}$, PGE_2, $PGD_{2,}$ respectively. The LOQ for all metabolites measured in our method was 0.104 ng/ml (6.25 pg on column) except for 6-keto-$PGF_{1\alpha,}$ $PGF_{2\alpha}$ and 11-d-TXB_2, which was 0.208 ng/ml (12.5 pg on column) and is comparable to the values reported by Unterwurzacher et al. (Unterwurzacher, et al., 2008) and Blewett et al. (Blewett, et al., 2008). Also, our UPLC-MS/MS prostanoid method reports a shorter run time of 12 minutes as compared to the 60 and 30 minute run times reported by the HPLC-MS or HPLC-MS/MS methods described by Blewett et al. and Ferreiro-vera et al. (Blewett, et al., 2008; Ferreiro-Vera, et al., 2011b). The advantages of the method described in this article are: 1) the shorter run time and comparable LOQ for

measurement of various prostanoid metabolites in biological matrices, and 2) the ability to reliably quantify a wide range of physiologically important metabolites of arachidonic acid metabolism from COX and CYP450 pathway in a shorter run time from a single extracted sample of rat brain tissue.

2.5. CONCLUSIONS

A solid phase extraction procedure coupled with a UPLC-MS/MS method was validated, and successfully applied for simultaneous extraction of 11 prostanoids including cyclopentenone metabolites. This method was optimized to provide high resolution and sensitivity for the detection of these analytes in rat brain tissue with an analysis time of 12 minutes per sample. Quantitative amounts of majority of the prostanoids were found in rat brain cortical tissue, and they were within the validated linear range of 0.104 - 33.3 ng/ml. We determined that the matrix did not significantly affect the reliability and reproducibility of the assay. In addition, we have also demonstrated that applying the processing and extraction procedure of this method to our previously validated CYP eicosanoid method improves overall extraction efficiency and reduces matrix effects on CYP eicosanoids. We have successfully quantified CYP eicosanoids from the same extracted sample of rat brain tissue with different MS/MS conditions as reported previously. Collectively, these data demonstrate that our method can be used to effectively quantitate these metabolites with reliability, reproducibility, and rapid analysis time. The increased throughput of analyzing these metabolites should help to evaluate effects of shunting on total sum arachidonic acid metabolism, and advance our understanding of their role as potential therapeutic targets and/or biomarkers of inflammatory and cerebrovascular disorders.

3.0 IN VITRO EVALUATION OF CYTOPROTECTIVE EFFECTS OF CYP EICOSANOIDS

3.1 INTRODUCTION

Previous two chapters have discussed the biological significance of CYP eicosanoids and prostanoids in cerebrovascular disorders evaluated in different *in vitro* and *in vivo* studies. Particularly, the molecular mechanisms underlying the pharmacological effects of CYP eicosanoids were discussed in detail in **Chapter 1**. In addition to their effects on cerebral vasculature, CYP eicosanoids also interact with different intracellular signaling pathways that may affect tissue/cell survival in cerebral ischemia. This is important as the neuroprotective effects of CYP eicosanoids may in part be mediated through both vascular as well as non-vascular effects. This view is supported by findings from different *in vivo* studies that indicated the possibility of a non-vascular effect of CYP eicosanoids. Inhibition of 20-HETE synthesis reduced infarct volume in experimental models of focal cerebral ischemia (Miyata, et al., 2005; Omura et al., 2006; Poloyac, et al., 2006; Tanaka et al., 2007) without producing any intra-ischemic vasodilation (Cao et al., 2009; Renic, et al., 2009). Further, CYP 4A expression was detected in the cortical neurons after ischemia (Omura et al., 2006) indicating that 20-HETE may exert effects directly on neurons, and contribute to the overall neuroprotection independently from the effects on CBF. Similarly, ischemic preconditioning protects against ischemic cell death in a MCAO model by increasing the expression of P450 epoxygenases in brain. Further, pharmacological inhibition of sEH has also shown neuroprotection against focal ischemia in the absence of changes in CBF (Zhang, et al., 2007) suggesting that EETs may exert cytoprotective effects independent of their effects on CBF. Together, these findings suggest a possible role for non-vascular effects of CYP eicosanoids in the neuroprotection.

3.1.1 Non-vascular effects of CYP eicosanoids

Findings from some *in vitro* studies have indicated the presence of a non-vascular mechanism of neuroprotection by CYP eicosanoids in ischemia. Renic et al, recently have shown that 20-HETE synthesis inhibition reduces injury from oxygen-glucose deprivation (OGD) in hippocampal slice cultures (Renic et al., 2012). Similarly, Terashvili et al, showed protective effect of 14,15-EET against hydrogen peroxide (H_2O_2) induced cell death in astrocyte-dopaminergic neurons co-culture. In the same study, they showed that neurons were more vulnerable than astrocytes as basal endogenous levels of 14,15-EET was higher in astrocytes than neurons. Further, sEH inhibition by AUDA protected cells from H_2O_2 induced cell death (Terashvili et al., 2012). In yet another study, application of exogenous EETs (Liu et al., 2005b) or overexpression of CYP2J2 protected rat primary astrocytes against ischemic cell death in an *in vitro* OGD model (Li et al., 2012). CYP2J2 overexpression also showed protection against hypoxia-reoxygenation injury in cultured bovine aortic endothelial cells. Koerner et al showed that 14,15-EET protected primary rat cortical neurons against ischemic cell death in an *in vitro* OGD model. However, this effect was seen only in the cultures transduced with human sEH variants expressing functional polymorphisms that altered enzyme's hydrolase activity. In this study, naïve rat primary cortical neuronal cultures were not protected from ischemic death either by exogenous EET administration or pharmacological inhibition of sEH (Koerner, et al., 2007). Similar observation was made in another study by Fairbanks et al, who showed gender differences in neuronal susceptibility to ischemic cell death that are linked to sEH expression, and possibly to hydrolase activity but showed no protective effect of sEH pharmacological inhibition either in male or female primary rat cortical neurons in an *in vitro* OGD model (Fairbanks et al., 2012).

3.1.2 Rationale for the *in vitro* study

The findings of recent studies detailed above do not provide conclusive evidence on the role of CYP eicosanoids in mediating direct cytoprotective effects in hypoxia or ischemia. To date, there has been only one study that reported the effects of 20-HETE under *in vitro* ischemic conditions (Renic et al., 2012) but this was evaluated in organotypic hippocampal slices. Typically, CYP4A expression is found high in VSM but the observation of increased CYP4A expression in cortical neurons after ischemia (Omura et al., 2006) still poses the question on the role of 20-HETE in these cortical neurons. Similarly, astrocytes and neurons both express CYP epoxygenases with astrocytes being major source of forming and releasing EETs. Exogenous administration of EETs or sEH inhibition or CYP epoxygenase expression have all shown protective effects in primary rat astrocyte cultures in both OGD as well as H_2O_2 induce cell death but protective effects of EETs were not seen in primary rat cortical neurons. In the studies that used cortical neurons, both EET and sEH inhibitor were administered at a single dose and no dose response was established. Further, it may be possible that sEH inhibition is protective by mitigating toxic effects of DHET. There was only one study that evaluated effects of 14,15-DHET on cortical neuronal survival in OGD model that showed no toxicity for 14,15-DHET (Koerner et al., 2007).

As discussed above, many *in vitro* studies have used either hippocampal slices or cultures for studying the injury mechanisms, and evaluating protective effects of different neuroprotective agents under OGD induced ischemic conditions. There have been limited number of *in vitro* studies that used primary cortical neuronal cultures to evaluate neuroprotective effects of CYP eicosanoids under hypoxic (lack of O_2) or ischemic (lack of O_2 and glucose) conditions. Therefore, the purpose of this study is to evaluate the cytoprotective effects of 20-HETE, EETs and DHETs

over a wide range of concentrations in an *in vitro* neuron-enriched rat primary cortical neuronal cultures under normoxic and hypoxic conditions.

3.2 EXPERIMENTAL METHODS AND PROCEDURES

All animal studies were conducted in accordance with the principles and procedures outlined in the National Institutes of Health Guide for the Care and Use of Laboratory Animals and were approved by the University of Pittsburgh Institutional Animal Care and Use Committee.

3.2.1 Rat neuronal cell culture

Rat primary cortical neurons were prepared as described previously (Li, et al., 2008). Briefly, cortical primary neuronal cultures were prepared from embryonic day 17 (E17) fetal rats (Sprague-Dawley, Charles River, Wilmington, MA). Brains were removed and cortices dissected out, freed of meninges and trypsinized for 30 min in 0.25% trypsin in Dulbecco's modified Eagle medium (DMEM). After centrifuging at 1,000 x g for 3 min, the supernatant was removed and the tissue was triturated in culture medium to produce a single-cell suspension. The cells were then plated at a density of 6×10^4 cells/well in a 96-well plate coated with poly-D-lysine (100 μg/ml) and maintained in a humidified incubator in air with 5% CO_2 (Forma Scientific, Morijetta, Ohio). The neurons were grown in neurobasal medium without phenol red, supplemented with 2% B27 (Invitrogen, Carlsbad, CA), 1% Glutamax (Invitrogen), and 1% penicillin/streptomycin (Invitrogen). The medium was replaced the following day and every 3 days thereafter with Neurobasal A medium (Invitrogen). The cultures were used for experiments after 10 days as the cultures were considered to be mature and stable at this time. This is a neuron-enriched primary culture as it contains > 95% neurons.

3.2.2 Cell culture treatment with CYP eicosanoids

On the 11th day, neuronal cultures were used for evaluating protective effects of CYP eicosanoids under normoxic conditions. Stock vials of CYP eicosanoids 20-HETE, 11,12-EET, 14,15-EET, 11,12-DHET, and 14,15-DHET (Cayman Chem, Ann Arbor, MI) were gently evaporated under nitrogen to remove ethanol and the residue was dissolved in phosphate saline buffer (PBS), pH 7.4. All working stock solutions were prepared by diluting the mother stock in neurobasal medium. A different plate was used for each eicosanoid. Each well (n=6/treatment) was added with 100 μL of medium containing CYP eicosanoids at a final concentration ranging from 0.05 to 50 μM as shown in the Figure 3-1. This range of concentrations were selected to account for possible losses due to chemical instability, degradation, metabolism during cellular uptake, non-specific binding to cellular components. Cultures were then incubated (Forma Scientific) for 24 h under normoxic conditions. Staurosporine (Sigma-Aldrich, St. Louis, MO), a 100% cell death internal standard in which almost all cells appear dead at 24 h when observed under light microscopy, and MK-801 (Cayman Chem, Ann Arbor, MI), an internal cell survival standard in, which almost all cells survive were used as positive and negative controls in the assay. Cell death measurements were taken at the end of 24 h incubation.

	SP	**MK-801**	**Med**	**0.05**	**0.1**	**0.5**	**1.0**	**5**	**10**	**50**	

Figure 3-1. Schematic of 96-Well Plate Design for CYP eicosanoids experiment

For hypoxia experiments, on the 11th day the cells were either pre-treated for one hour with vehicle (neurobasal medium) or with CYP eicosanoids (20-HETE, 11,12-EET, and 14,15-EET) each diluted in neurobasal medium at a final concentration ranging from 0.1 to 50 μM (n=6 well / treatment). After pre-treatment the culture plates were placed into a hypoxic glove box (Coy Laboratories, Grass Lake, MI, USA) and flushed for 5 min with 95% argon and 5% CO_2. The culture medium was removed, washed twice with degassed medium and replaced with degassed medium containing CYP eicosanoids. The culture plates were then subjected to hypoxia for varied durations (for each eicosanoid) ranging from 2 to 4 h in the chamber at 37 ºC. At the end of hypoxia, culture plates were removed, degassed medium was replaced with pre-warmed culture medium, and returned to the incubator to allow reoxygenation for 24 h. This duration of anoxia followed by reoxygenation produces ~ 40 –60% neuronal death in untreated cultures compared to cultures treated with 20 μM Staurosporine (SP). Cell death measurements were taken at the end of 24 h incubation.

3.2.3 Cell death measurements

Cell death was quantitatively assessed by measuring lactate dehydrogenase (LDH) release into the culture medium 24 h after hypoxia. LDH release signifies both cell death and loss of membrane integrity. LDH activity was measured from the reduction of NAD^+ after the oxidative conversion of $_L$-lactate to pyruvate. For LDH measurement, medium from cell culture plates was collected into a different plate and each well was mixed with 150 μl of reaction mixture prepared according to kit directions (Pointe Scientific Inc., Canton, MI). The sample plate was then measured at 340 nm using a plate reader (Spectramax, Molecular Devices, Sunnyvale, CA). Cell

death in all treatment groups was normalized to that of SP treated group and reported as % cell death.

3.2.4 CYP eicosanoid measurement from medium and cell lysates

Stability of the CYP eicosanoids in the culture medium under normal incubation conditions was evaluated at different concentrations. At the end of incubation, cell culture medium was removed and cells were washed twice with PBS. The cells were then lysed with RIPA lysis buffer (Sigma-Aldrich, St. Louis, MO) and lysates was collected to measure the cellular uptake of CYP eicosanoids. Both lysates and culture medium were extracted and analyzed by UPLC-MS/MS method for quantifying CYP eicosanoids as follows:

The cell lysates and culture medium were spiked with 12.5 µL (containing 12.5 ng) of 20-HETE-d_6 as internal standards (IS). The spiked samples were loaded onto Oasis hydrophilic-lipophilic balanced (HLB) (30 mg) solid phase extraction (SPE) cartridges (Waters, Milford, MA) that were conditioned and equilibrated with 1 ml of methanol and 1 ml of water, respectively. Columns were washed with three 1 ml volumes of 5% methanol and were eluted with 100% methanol. Extracts were dried under nitrogen gas at 37°C, and reconstituted in 125 µl of 80:20 methanol/deionized water for chromatographic analysis as described in **Chapter 2**.

3.2.5. Statistical Analysis

Significant differences between treatment groups (excluding positive and negative controls) were assessed by one-way ANOVA and Dunnett's post-hoc test was used to compare means with control (medium) treated cells. A *$p<0.05$ was considered significant. All data were represented as mean ± SD.

3.3 RESULTS

3.3.1 Normoxic conditions

3.3.1.1 11,12-DHET:

Under normoxic incubation conditions, 11,12-DHET did not show any significant decrease in cell death when tested at concentrations ranging from 0.05 to 1 µM. However, there was an increase in % cell death as the concentration was increased, and at 1 µM there was a non-significant decrease in cell death as compared to control (medium) treated cells (76.5 ± 7.7% vs 61.1 ± 9.3%; n=6; p=0.07) (**Figure 3-2**).

3.3.1.2 14,15-DHET:

Under normoxic incubation conditions, 14,15-DHET did not show any significant decrease in cell death when tested at concentrations ranging from 0.05 to 5 µM. There was no concentration related changes in cell death (**Figure 3-3**).

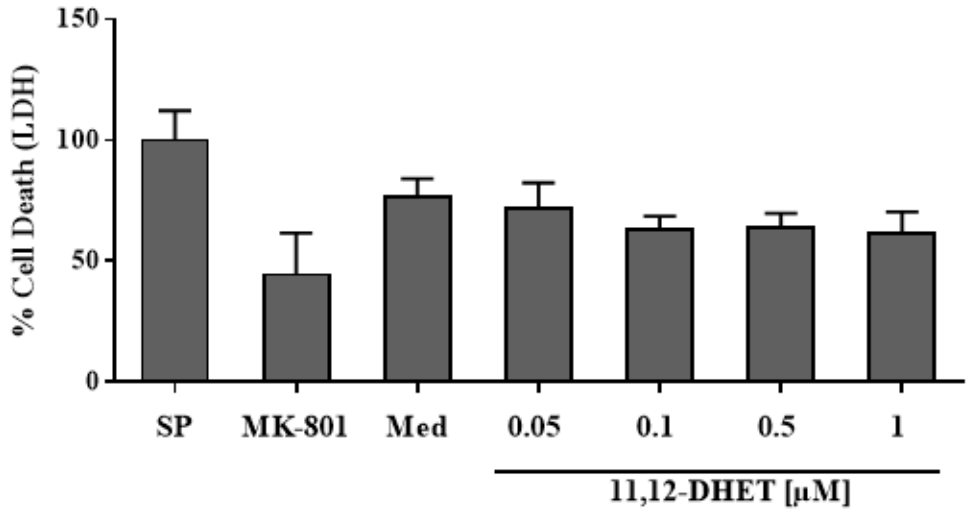

Figure 3-2 Effect of 11,12-DHET under normoxic incubation conditions. No significant differences were observed between different treatment groups of 11,12-DHET when compared to control (medium) group (n=6 wells/treatment).

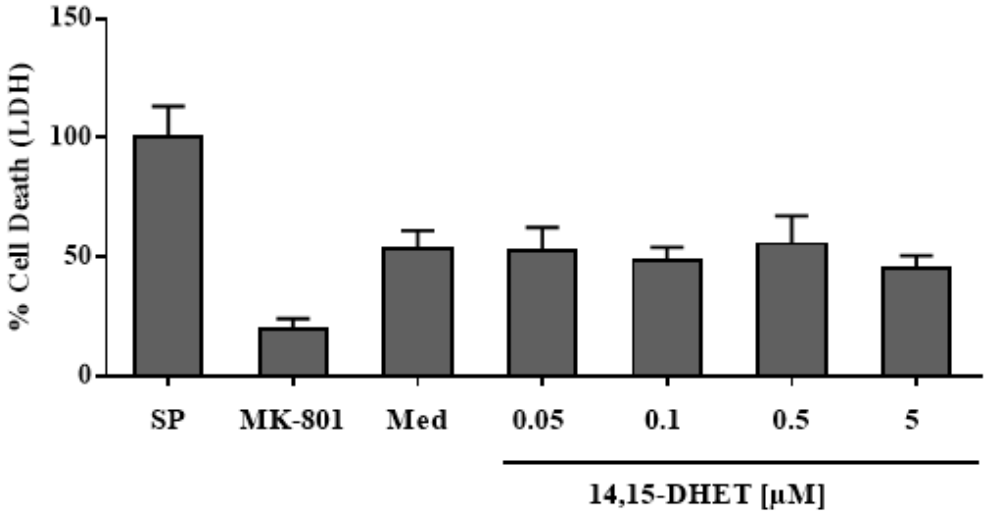

Figure 3-3 Effect of 14,15-DHET under normoxic incubation conditions. No significant differences were observed between different treatment groups of 14,15-DHET when compared to control (medium) group.

3.3.1.3 20-HETE:

20-HETE showed no significant decrease in cell death when tested at a wider concentration range from 0.1 to 50 µM under normoxic conditions. There was a flat concentration-effect over the tested range (**Figure 3-4**).

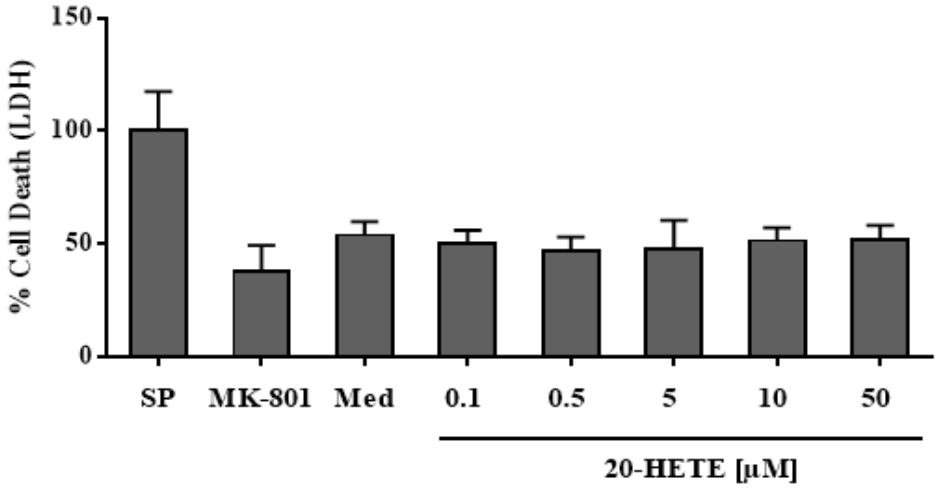

Figure 3-4 Effect of 20-HETE under normoxic incubation conditions. No significant differences were observed between different treatment groups of 20-HETE when compared to control (medium) group.

3.3.1.4 11,12-EET:

11,12-EET showed decrease in the cell death over a concentration range of 0.1 to 50 µM. At high concentration 10 µM, there was a non-significant decrease in cell death compared to vehicle group (51.3 ± 11.2% vs 34.8 ± 9.5%; n=6; p=0.059). However at even higher concentration 50 µM, there was a significant decrease in cell death compared to vehicle (51.3 ± 11.2% vs 31.1 ± 11.5%; n=6; *p<0.05) (**Figure 3-5**).

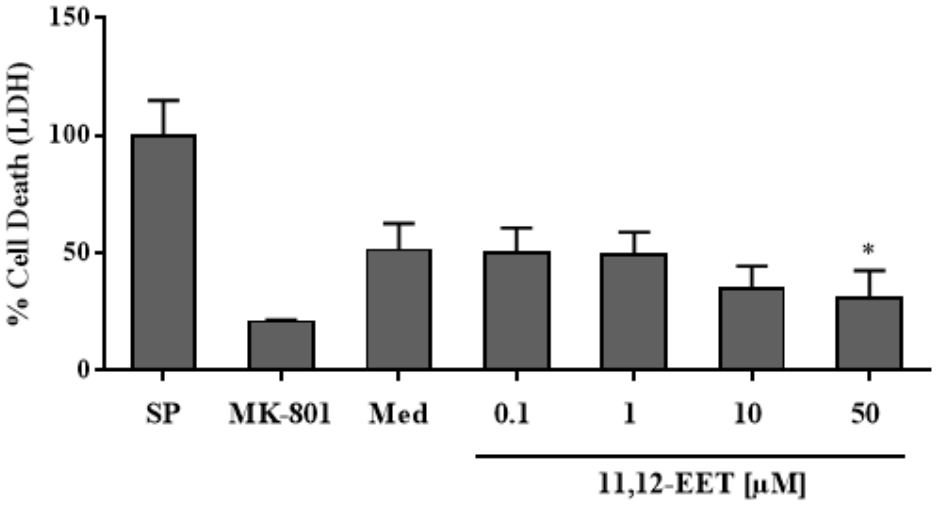

Figure 3-5 Effect of 11,12-EET under normoxic incubation conditions. Significant differences of treatment groups compared to vehicle (medium) group were denoted by *p<0.05.

3.3.1.5 14,15-EET:

14,15-EET showed no significant decrease in cell death when tested over a concentration range from 0.1 to 50 µM. There was a flat concentration-effect observed over the tested range (**Figure 3-6**).

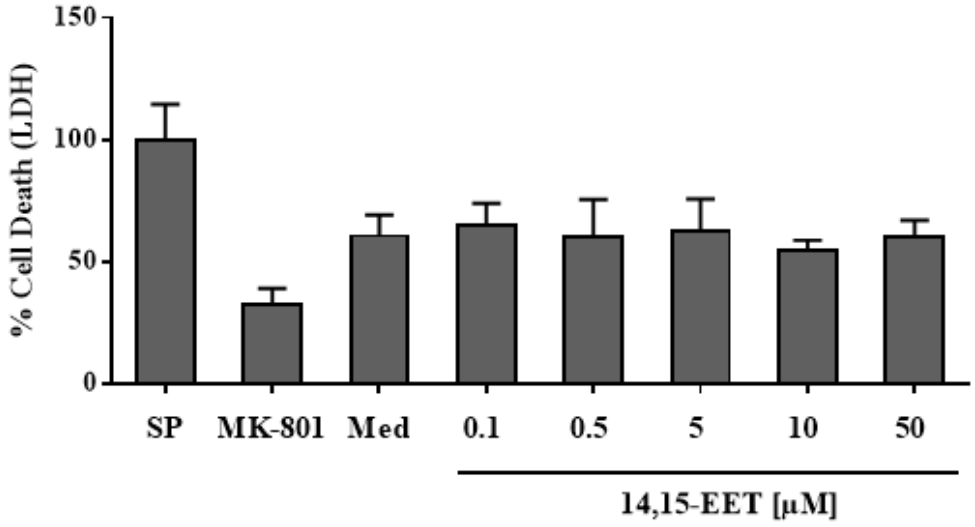

Figure 3-6 Effect of 14,15-EET under normoxic incubation conditions. No significant differences were observed between different treatment groups of 14,15-EET when compared to control (medium) group.

3.3.2 Hypoxic conditions

3.3.2.1 20-HETE:

Under hypoxic conditions, 20-HETE showed an increase in the cell death over a concentration range of 0.1 to 50 µM. There was a non-significant increase in cell death when compared to vehicle group (45.7 ± 5.1%) at 5 µM (56.5 ± 6%; n=6; p=0.073). However, there was a significant increase in cell death compared to vehicle group (45.7 ± 5.1%) at higher concentrations 10 µM (58.8 ± 6.1%; n=6; *p<0.05), and 50 µM (64.3 ± 12.2%; n=6; *p<0.001) (**Figure 3-7**).

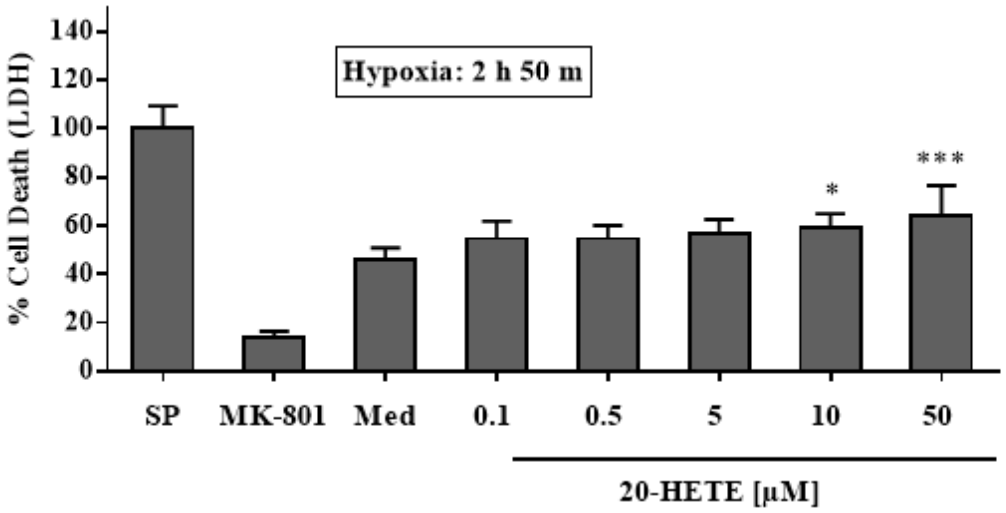

Figure 3-7 Effect of 20-HETE under hypoxic conditions. Significant differences of treatment groups compared to vehicle group (n=6 wells/treatment) were denoted by *p<0.05, **p<0.01.

3.3.2.2 14,15-EET:

Under hypoxic conditions, 14,15-EET showed decrease in the cell death at 10, and 50 µM. There was a non-significant decrease in cell death when compared to vehicle group (48.2 ± 6.2%) at 50 µM (36.5 ± 3.8%; n=6; p=0.079) (**Figure 3-8**).

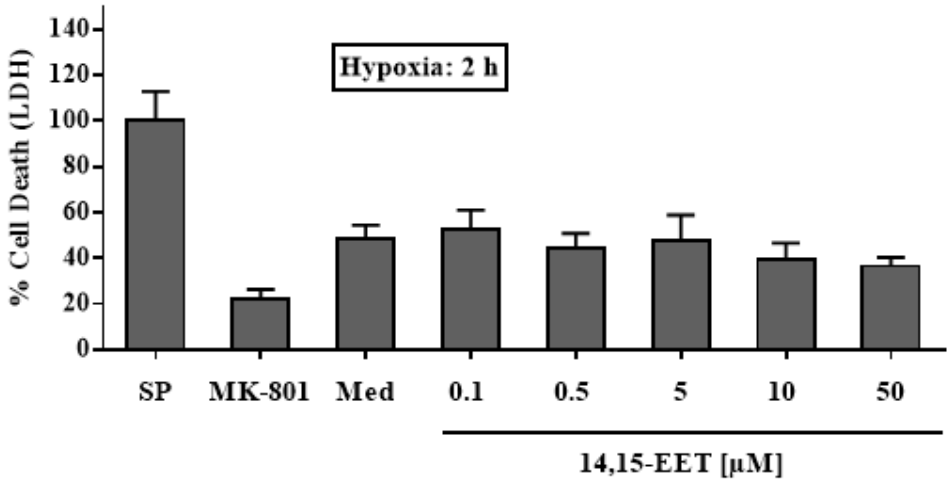

Figure 3-8 Effect of 14,15-EET under hypoxic conditions. No significant differences were observed between different treatment groups of 20-HETE when compared to control (medium) group.

3.3.2.3 11,12-EET:

11,12-EET showed decrease in the cell death over a concentration range of 0.1 to 50 µM. There was a significant decrease in cell death when compared to vehicle group (51.5 ± 14%) at 5 µM (34.3 ± 4.3%; n=6; *p<0.05), 10 µM (35.1 ± 7.4%; n=6; *p<0.05), and 50 µM (32.9 ± 6.4%; n=6; *p<0.05) (**Figure 3-9**).

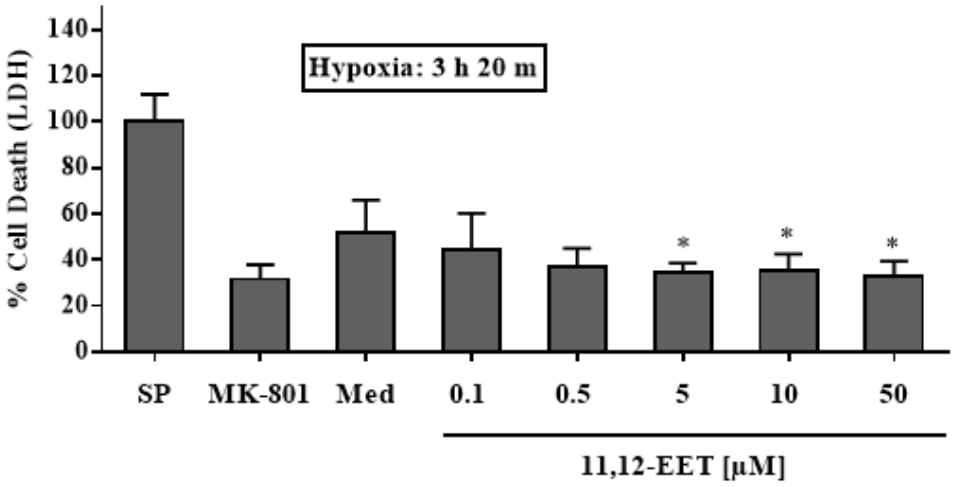

Figure 3-9 Effect of 11, 12-EET under hypoxic conditions. Significant differences of treatment groups compared to vehicle (medium) group were denoted by *p<0.05.

3.3.3 Stability of CYP eicosanoids in culture medium

As shown in **Table 3-1**, 20-HETE was stable in the culture medium after 24 h under normoxic incubation conditions (5% CO_2, 37 ºC) at low, medium, and high concentrations (0.5, 10, and 50 µM; n=6). When incubated with live cells for 24 h, 20-HETE concentrations in the culture medium decreased in a concentration dependent manner. 20-HETE was readily taken up by live cells as measured from cell lysates at the end of 24 h. 11,12-EET was relatively less stable than 20-HETE at medium, and high concentrations (10, and 50 µM; n=6) in the culture medium after 24 h under normal incubation conditions. The concentrations of 11,12-EET in the culture

medium decreased more rapidly than 20-HETE when incubated with live cells. However, no concentrations of 11,12-EET were detected in the cell lysates.

Table 3-1 Stability of CYP eicosanoids under incubation conditions

Analyte	Conc (μM)	Incubation Time (min)	Pure medium (% rem)	Live cells	
				Culture medium (% rem)	Lysates (% control)
20-HETE	0.5	24	101.7 ± 3.6	53.8 ± 17.6	ND
	10	24	95.3 ± 5.3	36.4 ± 5.6	0.47 ± 0.02
	50	24	90.7 ± 12.2	33.2 ± 6.5	0.33 ± 0.06
11,12-EET	0.5	24	112 ± 7.7	24.5 ± 4.0	ND
	10	24	69.4 ± 7.5	7.58 ± 1.6	ND
	50	24	73.1± 5.7	19.1 ± 2.3	ND

Conc = Concentration; ND = not detected; % rem = % remaining

3.4 DISCUSSION

In this study, we investigated the neuroprotective effects of CYP eicosanoids over a wider concentration range under normoxic and hypoxic conditions. Specifically, we found that 11,12-EET at high concentrations is protective even under normoxic conditions. Under hypoxic conditions, 20-HETE was found to be toxic to neurons at high concentrations whereas 11,12-EET protects neurons in a dose dependent manner. Collectively, these data suggest that CYP eicosanoids exert a direct cytoprotective or cytotoxic effect on neurons under normal and hypoxic conditions.

In this study, we have used neuron-enriched rat primary cultures for *in vitro* evaluation of CYP eicosanoids effects. Primary neuronal cultures prepared from same source can be maintained and differentiated identically over long-term to examine cell death signaling mechanisms in mature, synaptically integrated cortical neurons. Further, potentially confounding factors such as neuromodulators from glial or other types of neighboring cells can be obviated making it a simple system to test the direct effects of hypoxia. Hypoxia of sufficient duration or severity can alter neuronal function and cell morphology, and can lead to cell injury or death. A number of studies have shown that *in vitro* hypoxia causes neuronal alterations that may reflect the actual processes under ischemia *in vivo* (Goldberg et al., 1986; Nieber, 1999). Indeed, the cerebral cortex has been shown to be more vulnerable to global ischemia and is a major site of neurodegeneration after hypoxia-ischemia, and stroke (Martin et al., 1998; Martin et al., 1997). Neurons of the hippocampus and cortex are the most vulnerable targets in the CNS to hypoxia. However, some studies suggested that neocortical brain regions are more vulnerable to hypoxia than the hippocampus (Bachevalier et al., 1996). Further, hypoxic-ischemic injury in neonatal piglets preferentially damages primary somatosensory and forebrain motor systems. Neocortical neurons in humans and rat have shown minor differences in the cellular properties and large similarities in cell morphology and electrophysiological properties between the two species (Jiang et al., 1992). Thus, neuron-enriched rat primary cortical neuronal cultures used in this study are a suitable system to evaluate neuroprotective effects of CYP eicosanoids under hypoxic conditions.

Our findings of 20-HETE effect on toxicity of neurons under hypoxic conditions is consistent with the recent data reported in an OGD model of hippocampal neurons in which a 20-HETE mimetic, 20-hydroxyeicosa-5(Z),14(Z)-dienoic acid (5,14-20-HEDE) potentiated the ischemic injury, and

20-HETE synthesis inhibition protected neurons from ischemic death (Renic, et al., 2012). In this study, for the first time we report a dose dependent increases in neuronal cell death by 20-HETE at high concentrations 10, and 50 μM. Interestingly, under non-hypoxic conditions, 20-HETE did not show any toxic effect over the same concentration range tested. Though there are differences in the *in vitro* model used in both studies, together these findings suggest that 20-HETE's effects are potentiated only after a hypoxic-ischemic event and that the toxic effects are concentration dependent, which can be reversed by 20-HETE antagonists or synthesis inhibitors.

We also found that pretreatment of 11,12-EET protected neurons from hypoxic cell death. Neuroprotective effects of EETs were previously reported in pure astrocytes (Terashvili, et al., 2012), and astrocyte-dopaminergic neuron co-cultures (Liu, et al., 2005b) in both H_2O_2 and OGD models. There was one study that reported protective effects of EETs in cortical neuronal cultures (Koerner, et al., 2007) transduced with human sEH variants expressing functional polymorphisms in an OGD model. In this study, we showed for the first time that 11,12-EET protects cortical neurons from hypoxic cell death in a dose dependent manner. Interestingly, 11,12-EET also showed protection under normoxic conditions at higher concentrations. However, 14,15-EET did not show any protective effect at all concentrations tested either under normoxic or hypoxic conditions. In the study by Koerner et al., 14,15-EET did not show any protective effect in rat primary cortical neurons in OGD model. This could be due to increased metabolism of 14,15-EET by sEH during the hypoxic-ischemic event as it is a preferred substrate of the sEH. Together, these findings suggest that 11,12-EET, a potent regioisomer of the EETs protects different cells of CNS such as neurons, and astrocytes from hypoxia-ischemic as well as oxidant induced cell death.

In our study, we did not find any effects of DHETs on cortical neurons under normoxic and hypoxic conditions. We determined the stability of 20-HETE, and 11,12-EET under the normoxic incubation conditions and found that 20-HETE is more stable than 11,12-EET in the culture medium under the incubation conditions. Both 20-HETE and 11,12-EET are readily taken up by neurons from the culture medium however 11,12-EET concentrations declined rapidly from culture medium than 20-HETE. However, when we measured cellular levels of 20-HETE and 11,12-EET at the end of incubation with exogenous administration to neurons, we only detected low levels of 20-HETE in cell lysates and 11,12-EET could not be detected. This could be due to re-esterification or rapid metabolism of these CYP eicosanoids in the neurons. Together, these data suggests that CYP eicosanoids can be administered exogenously to neurons for studying their effects *in vitro* under different conditions of cell death as they are relatively stable under moderate incubation conditions, and are readily up taken by cells.

There are possible limitations to this study. We did not study the specific cellular signaling mechanisms activated by CYP eicosanoids after hypoxia-reoxygenation injury. As discussed in Chapter 1, CYP eicosanoids interact with different intracellular signaling pathways. Delineating specific cellular pathways involved will help gaining mechanistic insight into neuroprotective effects of CYP eicosanoids and also helps to validate these pathways as potential therapeutic targets to treat cerebral ischemic disorders. We have used one measure of cell death in this study. Since ischemic injury is progressive and time dependent, one type of cell death assay may not be representative of different modes of cells death such as apoptosis and necrosis. Hence, different measures of cell death or viability should be used to strengthen the findings, and also to establish full dose-response of the CYP eicosanoids. Though exogenous administration of CYP eicosanoids

are protective in hypoxic injury, these compounds are not suitable for chronic administration as these lipid derivatives are rapidly metabolized both *in vitro* and *in vivo*. Future studies employing inhibitors of formation of 20-HETE and metabolism of 11,12-EET in the *in vitro* cultures should be done to evaluate the effects of CYP eicosanoids in more severe and chronic conditions of hypoxia. Often, hypoxia is accompanied by lack of glucose. Glutamate-mediated neurotoxicity is an important factor under conditions when the neurons are deprived of both oxygen and glucose since removal of glucose from the medium results in a stronger hypoxic depolarization. Thus, further studies should be done in different models of ischemic cell death like OGD to evaluate the sensitivity of neurons and the potency of CYP eicosanoids in different types of ischemic injury that may have overlapping cellular mechanisms.

3.5 CONCLUSIONS

In summary, in the current study we have for the first time demonstrated the neuroprotective effects of CYP eicosanoids on rat primary cortical neuronal cultures in a hypoxia-reoxygenation injury model. Further, we have showed dose dependent effects of 20-HETE and 11,12-EET in hypoxic injury. We demonstrated that the CYP eicosanoids can be exogenously administered to neuronal cultures under hypoxic conditions as they are moderately stable, and readily taken up by neurons. These findings suggest a possible role of the non-vascular mechanism of neuroprotection mediated by CYP eicosanoids in ischemic injury. The understanding of relative contributions of vascular and non-vascular effects of CYP eicosanoids in mediating neuroprotection is critical for developing therapeutic agents that modulate cellular pathways specific to each mechanism in order to maximize the neuroprotective benefits of CYP eicosanoids.

4.0 EVALUATION OF EFFECTS OF CYP EICOSANOIDS IN FOCAL ISCHEMIA

[Jafar Sadik B Shaik, Ahmad M, Li W, Rose ME, Foley LM, Hitchens TK, Graham SH, Hwang SH, Hammock BD, Poloyac SM. “Soluble epoxide hydrolase inhibitor trans-4-[4-(3-Adamantan-1-yl-ureido)-cyclohexyloxy]-benzoic acid (*t*-AUCB) is neuroprotective in rat model of ischemic stroke”. *American Journal of Physiology. Heart and Circulatory Physiology* Article in Press]

4.1 INTRODUCTION

Previous chapter has evaluated the CYP eicosanoids in *in vitro* cultures to test the non-vascular mechanisms of neuroprotection. Specifically, we showed that 11,12-EET was effective in protecting neurons in a dose-dependent manner in hypoxia-reoxygenation injury. Together with their vascular and non-vascular effects, EETs appear to play a significant role in protecting cerebral tissue from ischemia-reperfusion injuries. This pattern of injury is produced in an experimental models of focal and global ischemia with subsequent reperfusion. This chapter will evaluate the *in vivo* protective effects of EETs in a focal ischemia model. Since administering EETs is not a viable pharmacological approach as they rapidly bind to plasma proteins or metabolized to less active DHETs, metabolically stable analogs of EETs were developed in the past but most widely used approach for studying the effects of EETs has been increasing endogenous EET levels in the tissue by inhibiting sEH, which is the primary route of degradation of EETs. The inhibitors of sEH have been shown to be neuroprotective, however no studies have evaluated if acute administration of sEH inhibitors can improve neurofunctional outcomes after ischemic stroke. These data are essential to add to the growing data to establish if sEH inhibitors meets the STAIR criteria for further clinical development (Fisher et al., 2009). Therefore, the primary goals of this study were to evaluate the effect of acute sEH inhibition by *t*-AUCB on infarct volume, functional outcome and changes in CBF using a transient MCAO model in rats.

4.2 EXPERIMENTAL METHODS AND PROCEDURES

All animal experiments were approved by the University of Pittsburgh Institutional Animal Care and Use Committee (IACUC) and performed in accordance with the NIH Guide for the Care and Use of Laboratory Animals.

4.2.1 Animals and experimental design

Male Sprague-Dawley rats (250-300g) (Hilltop Laboratory Animals Inc., Scottsdale, PA) were maintained on a 12-h light/dark cycle and were given food and water *ad libitum*. The rats were randomly assigned to either vehicle (lyophilized hydroxypropyl-β-cyclodextrin (HPβCD), 15%), or treatment (lyophilized *t*-AUCB in HPβCD, 0.5 mg) groups. MCAO was performed on all rats. All HPβCD lyophilized complexes (vehicle or *t*-AUCB) were reconstituted in PBS, pH=7.2, and filtered prior to administration. Treatment group rats received a single *t*-AUCB 0.9 mg/Kg bolus dose via the femoral vein at the time of MCAO. As shown in the **Figure 4-1**, five experiments were performed: 1) effect of *t*-AUCB on cerebral infarct volume after MCAO (n=9/group); 2) *t*-AUCB inhibitory potential on brain cortical sEH activity (n=6/group); 3) acute *t*-AUCB effect on short-term behavioral outcome after MCAO (n=9/group); 4) changes in CBF during and after MCAO with *t*-AUCB treatment were determined with ASL-MRI (n=7/group); and 5) effect of *t*-AUCB on primary neuronal cultures after hypoxic injury (n=6 wells/group). A power analysis was conducted at $\beta = 0.80$ to detect significant difference between the treatment groups with an effect size of 15% (for experiments 1, 3, 4, and 5) and an effect size of two-fold change in the ratio (for experiment 2). The surgeon and individuals involved in all above experiments were blinded to all treatment groups.

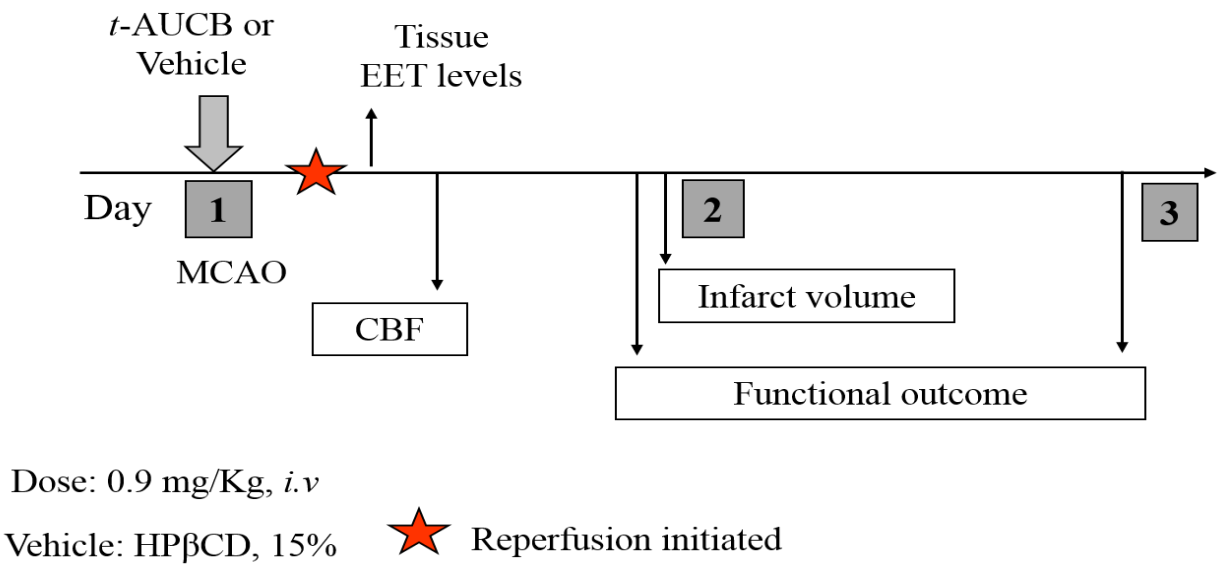

Figure 4-1 Schematic of the experimental design in a focal ischemia model

4.2.2 Middle cerebral artery occlusion in rats

Rats received MCAO for 90 minutes followed by reperfusion as described previously (Shimizu et al., 2001). Briefly, rats were anesthetized via nose cone with 1-2% isoflurane, 50/50 N_2O/O_2 throughout surgery. The left common carotid artery (CCA) was exposed and the external common carotid artery was isolated and ligated using 5-0 silk (Ethicon). MCAO was achieved by inserting a 5-0 nylon suture (with tip coated with silicon ~280 µm diameter) into the internal carotid artery (ICA) a distance of 16 - 19 mm from the bifurcation of the CCA and ICA. The wound was closed and the animals were allowed to recover with the suture in place. After 90 minutes, the rats were re-anesthetized and the suture removed, initiating reperfusion. Sham surgeries were performed in the same manner as MCAO surgeries but without insertion of suture. Throughout the surgical procedure core temperature was maintained at 37±0.5 °C using a thermo regulated heating pad.

4.2.3 Infarct volume determination

Rats (n=9/group) were sacrificed at 24 h after reperfusion and infarct volume was assessed by staining with 2,3,5-triphenyl-tetrazolium chloride (TTC, Sigma, St. Louis, MO, 2% in PBS). Brains were placed in a rat brain matrix (ASI Instruments, Warren MI) and were sliced into 1 mm sections. The sections were immersed in the TTC for 30 min at room temperature. The sections were transferred to formalin and photographed. Infarct volume was measured using image analysis (MCID, St Catharines, Ontario, Canada). To minimize the effect of edema on the quantification of infarct size the method of Swanson *et al.*, was used (Swanson et al., 1990). The percentage infarct volume was calculated by dividing infarct volume by contralateral hemisphere volume.

4.2.4 Tissue extraction and chromatographic analysis of CYP eicosanoids

Concentrations of CYP eicosanoids and prostanoids were determined from brain cortical tissues of vehicle and *t*-AUCB (0.9 mg/kg i.v; n=6/group) treated rats that underwent MCAO surgery using solid phase extraction, and UPLC-MS/MS analysis as described in C**hapter 2** previously.

4.2.5 Functional outcome assessment

Functional outcome experiments were aimed at evaluating motor activity (primary motor cortex), and somatosensory activity of rats that underwent MCAO surgery. Behavioral deficits (functional outcome evaluation) in rats (n=9/group) were examined at 24 and 48 h after reperfusion. A simple neurological scoring system was used to assess neurological damage following MCAO surgery as follows: 0 = no neurological deficit; 1 = failure to extend left forepaw fully & torso turning to ipsilateral side when held by tail (a mild focal neurologic deficit); 2 =

circling to the effected side (a moderate focal neurologic deficit); 3 = unable to bear weight on the effected side (a severe focal deficit); 4 = no spontaneous locomotor activity. Behavioral deficits were determined using the arm flexion and sticky tape test as described previously (Aronowski et al., 1996). The arm flexure test was conducted once daily by lifting rats by their tails so that their ventral surface was exposed for observation. The cumulative duration of asymmetrical arm flexure during a ten second period after tail lifting was recorded using a stop watch. In the tape test, self-adhesive labels (1-cm-diameter circles) were placed on each forepaw to assess the time required for the rat to touch and remove each label. In addition, the order (contralateral versus ipsilateral) of removal was also used to determine ipsilateral asymmetry. Preference for a given wrist was accounted for by affixing larger labels to the wrist less preferred and correspondingly smaller labels to the other wrist. The larger the ratio between surface of ipsilateral versus contralateral patches (from 1:1 to 1/8:15/8) the more extensive the damage (scored on a scale from 1 to 7 in the increasing order of severity of damage). One trial per day was conducted at 24 hours and 48 hours after reperfusion.

4.2.6 Cerebral blood flow assessment using ASL-MRI imaging

CBF measurements were assessed by arterial spin labeled (ASL) MRI (**Figure 4-2**). Rats (n=7/group) underwent femoral artery catheterization and were placed in a prone position on the cradle. MRI was performed using a 4.7-Tesla, 40 cm bore Bruker BioSpec AVI system (Billerica, MA, USA), equipped with a 12-cm shielded gradient insert. A 72-mm volume coil with 2.5 cm actively-decoupled brain surface coil was used for imaging. Continuous ASL was used to quantify CBF (Detre et al., 1992; Williams et al., 1992). A single shot SE-EPI sequence was used with a TR = 2 s, 64 x 64 matrix, FOV = 2.3 cm, 2-s labeling pulse. The labeling pulse for the inversion

plane was positioned ± 2 cm from the perfusion detection plane. For each experiment, a map of the spin-lattice relaxation time of tissue water (T_{1obs}) was generated from a series of spin-echo images with variable TR (FOV = 2.3 cm, 4 averages, 64 x 64 matrix) (Hendrich et al., 1999). CBF was assessed at three time points, at baseline, 70 min (during the occlusion period), and at 270 min (three hours after reperfusion). Blood gases were sampled at each time point and analyzed (Radiometer, Westlake, OH, USA). For the duration of the experiment mean arterial blood pressure (MABP) and EKG were continuously monitored. Rectal temperature was maintained at 37°C using a warm air system (SA Instruments, Stony Brook NY, USA).

Figure 4-2 ASL-MRI imaging unit

4.2.7 Primary neuronal cultures and hypoxia study

Rat primary cortical neurons were prepared as discussed in Chapter 2. The cultures were used for hypoxia experiments after 10 days. On the 11th day, the cells were either pre-treated for

one hour with vehicle (neurobasal medium) or *t*-AUCB diluted in neurobasal medium at a final concentration of 0.1 and 0.5 μM. These concentrations were selected to be 50 to 100 folds above the IC_{50} of *t*-AUCB (Tsai et al., 2010) to account for possible losses due to metabolism during uptake, non-specific binding to cells, degradation/instability under assay conditions. After pre-treatment the culture plates were placed into a hypoxic glove box (Coy Laboratories, Grass Lake, MI, USA) flushed with argon for a period of 3 h, resulting in ~50% cell death after 24 h of reperfusion under normal incubation conditions. Staurosporine (20 μM) and MK801 (1 μM) were used as positive and negative controls respectively. Cell death was quantitatively assessed by CytoTox-Fluor kit (Promega, Madison, WI, USA) following manufacturer's protocol, and by Propidium Iodide (PI) staining (Molecular Probes Inc., OR, USA) in two different experiments. For PI assay, cell were stained with 0.1 μg/mL PI (a red fluorescent dye that permeates dead cells) and 0.1 μg/mL Hoechst (a blue fluorescent dye that stains chromatin in live and dead cells) and fixed with 2% formaldehyde in PBS 24 h after hypoxia. PI and Hoechst stained cells were photographed with a Leica DMIRB fluorescence microscope at 20X, then counted by a blinded observer from 10 to 12 fields of at least three cultures. Cell death in all treatment groups was normalized to that of Staurosporine (SP) treated group.

4.2.8 Statistical analysis

Significant differences between treatment groups in experiments measuring infarct volume were assessed by Student's t-test and for brain sEH activity and *in vitro* neuronal culture experiments one-way ANOVA with Dunnett's post-hoc test was used. Significant differences for ASL-MRI blood flow measurements, and functional outcome assessments were determined via repeated measures ANOVA analysis. A $*p<0.05$ was considered significant. All data were represented as mean ± SD.

4.3 RESULTS

4.3.1 Effect of *t*-AUCB on infarct volume

The effect of acute *t*-AUCB pre-treatment on infarct volume after MCAO was evaluated and compared against vehicle. **Figure 4-3** depicts representative rat brain sections stained with TTC. A significant reduction in percentage infarct volume was observed in *t*-AUCB as compared to vehicle treated (14.5±2.7% vs 41.5±4.5%;***p<0.001) rats (**Figure 4-3**).

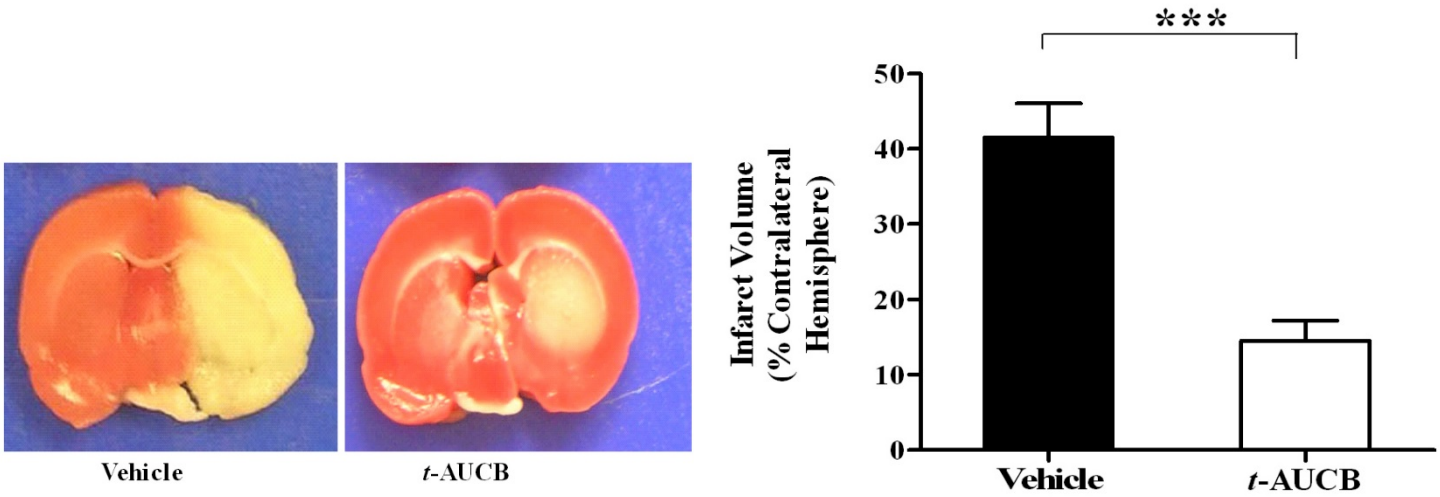

Figure 4-3 Effect of acute *t*-AUCB treatment on brain infarct volume after MCAO in rats. *t*-AUCB significantly reduced infarct volume upon acute administration at the time of MCAO as compared to vehicle treated group (n=9).

4.3.2 Effect of *t*-AUCB administration on brain sEH activity

The effect of acute sEH inhibition by *t*-AUCB in brain cortex after MCAO was assessed by measuring concentrations of various HETEs, EETs and DHETs as well as various PGs to verify the specificity of *t*-AUCB inhibition. A significant increase in the ratio of cumulative EETs (11,12- & 14,15-EET) to DHETs (11,12- & 14,15-DHET) was observed in *t*-AUCB as compared to

vehicle treated (4.40±1.89 vs 1.97±0.85;*p<0.05) rats (**Figure 4-4A**). No significant differences were observed in the concentrations of representative metabolites from the HETE and PG family such as 20-HETE (**Figure 4-4B**: vehicle: 6.39±0.92 vs *t*-AUCB: 6.80±1.7 pmol/gm tissue; p=0.62), 6-keto-$PGF_{1\alpha}$, a metabolite of prostacyclin (**Figure 4-4C**: vehicle: 22.3±4.35 vs *t*-AUCB: 24.9±6.21 pmol/gm tissue; p=0.41), and $PGF_{2\alpha}$ (**Figure 4-4D**: vehicle: 57.7±9.92 vs *t*-AUCB: 64.7 ± 13.7 pmol/gm tissue; p=0.35) in the cortex of *t*-AUCB and vehicle treated rats. Control values of these metabolites (without stroke) were also depicted in respective figures. Representative LC/MS chromatograms depicting the levels of EET, 20-HETE before and after treatment with t-AUCB was shown in **Figure 4-5**.

4.3.3 Effect of *t*-AUCB treatment on functional outcome

The effect of *t*-AUCB pre-treatment on short-term behavioral deficits after MCAO was evaluated in arm flexion and sticky tape behavioral tests. Rats receiving *t*-AUCB treatment showed significantly improved outcome in the arm flexure test on days 1 and 2 as compared to the vehicle treated group (day 1: 3.28±0.5 s vs 7.50±0.9 s, ***p<0.001; day 2: 1.71±0.4 s vs 5.28±0.5 s,***p<0.001) (**Figure 4-6A**). Similarly *t*-AUCB treatment significantly lowered neurological deficit scores on days 1 and 2 compared to the vehicle treated group (day 1: 1.71±0.9 vs 2.75±0.4, *p<0.05; day 2: 1.14±0.3 vs 2.14±0.3, ***p<0.001) (**Figure 4-6B**). Sticky tape tests also revealed a significant impact of *t*-AUCB on days 1 and 2 compared to the vehicle treated group (**Figures 4-6C and 4-6D**). Time to remove (in sec) sticky tape from the contralateral arm was 140.4±15 s vs 92.8±3.5 s on days 1 and 2, respectively in the vehicle group, which was significantly reduced in the *t*-AUCB group on both days 1 and 2 (98.1±6 s, and 64.6±8 s,***p<0.001). Tape surface area ratio of contralateral to ipsilateral arm in the vehicle group was 6.96±0.77 vs 5.97±1.2 on days 1

and 2, respectively. This was significantly reduced with *t*-AUCB treatment on both days (2.53±0.6 vs 1.19±0.2, ***p<0.001).

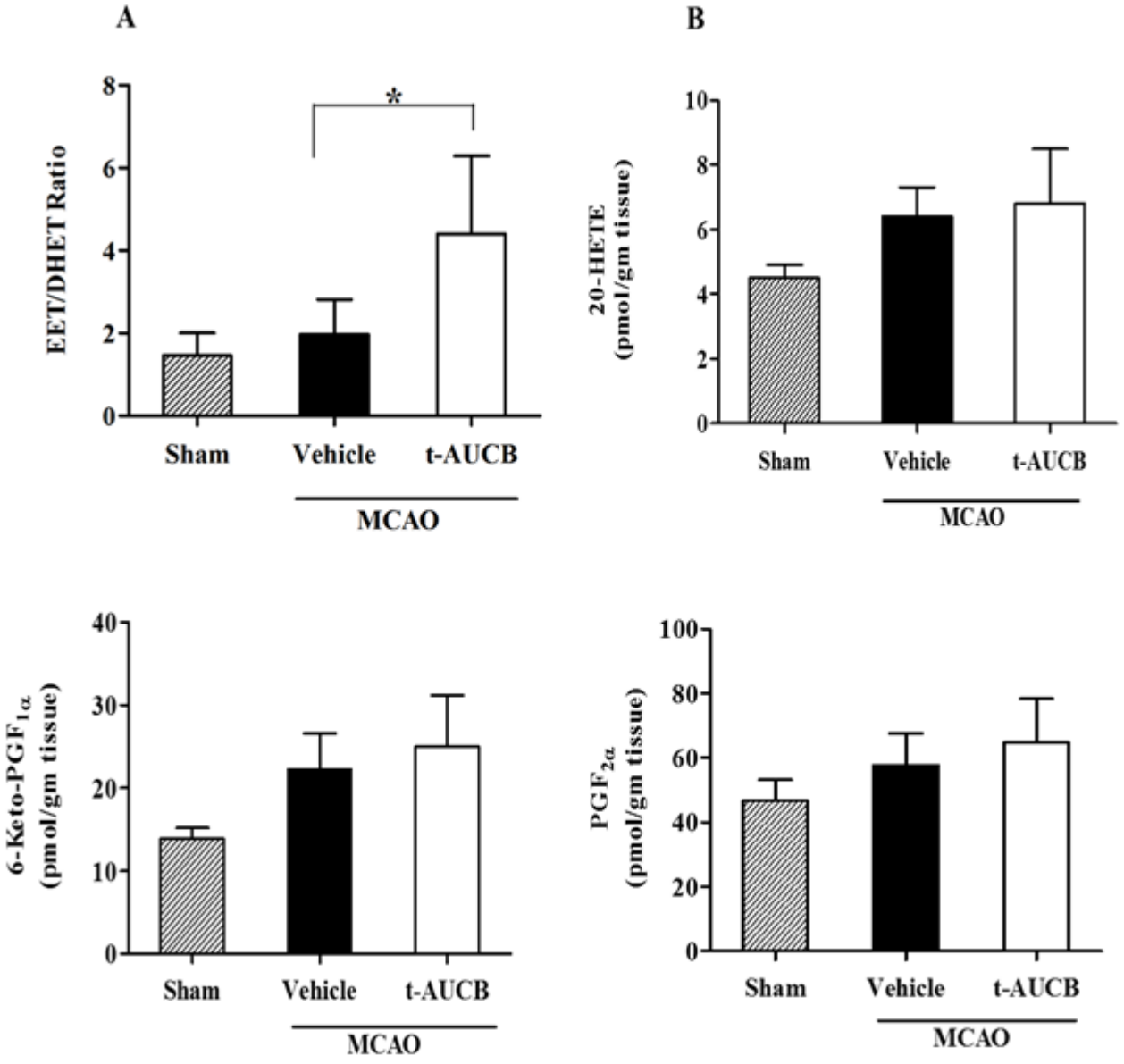

Figure 4-4 The effect of acute *t*-AUCB treatment on brain cortical sEH activity after temporary MCAO in rats (n=6). Brain cortices were collected at 6 hours after *t*-AUCB dosing. Significant differences were only seen in the levels of cumulative EET/DHET ratio in the cortex of *t*-AUCB treated rats compared to vehicle.

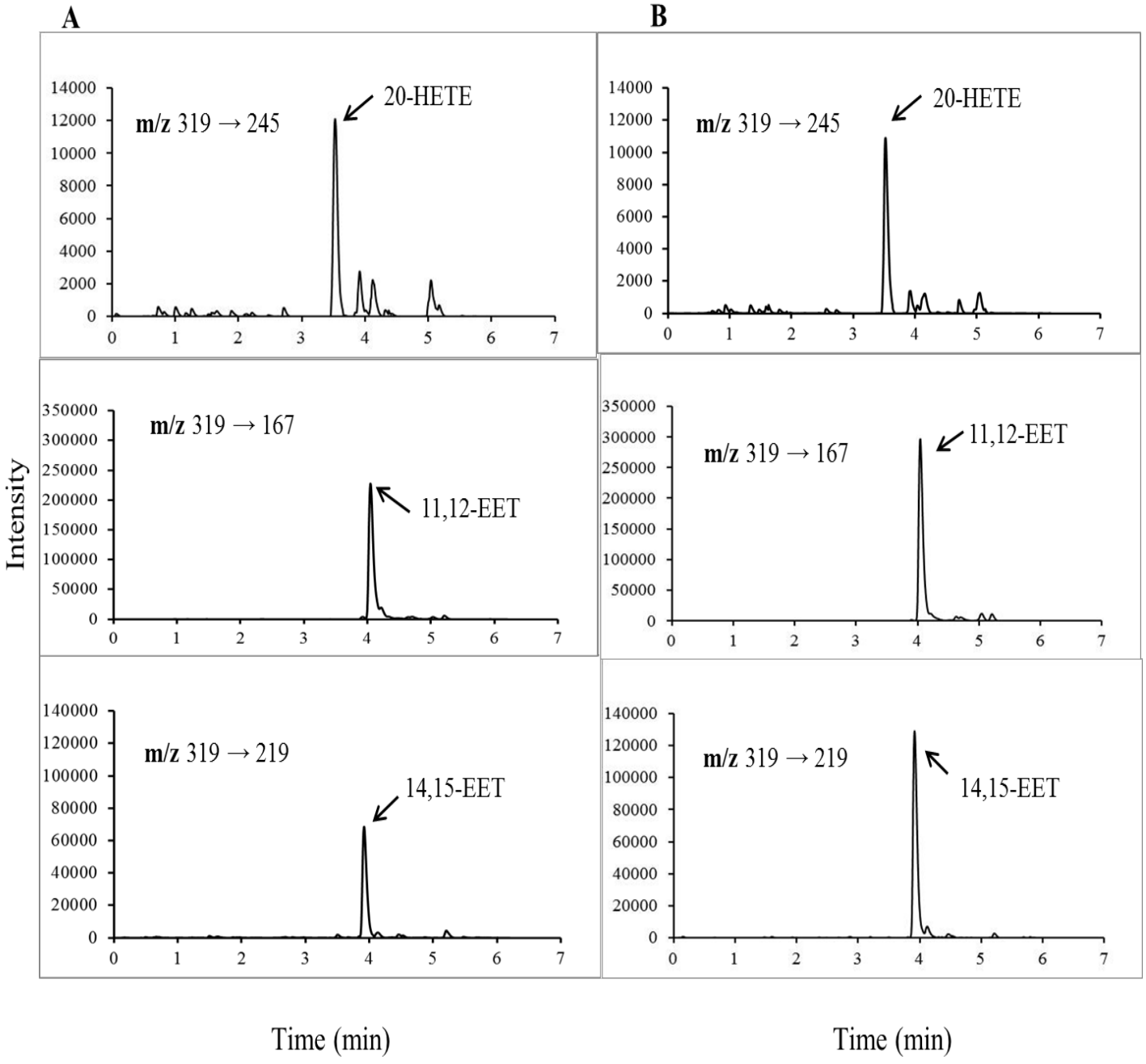

Figure 4-5 Representative LC/MS chromatograms of rat brain cortical sample showing EETs, and 20-HETE A) before and B) after treatment with *t*-AUCB

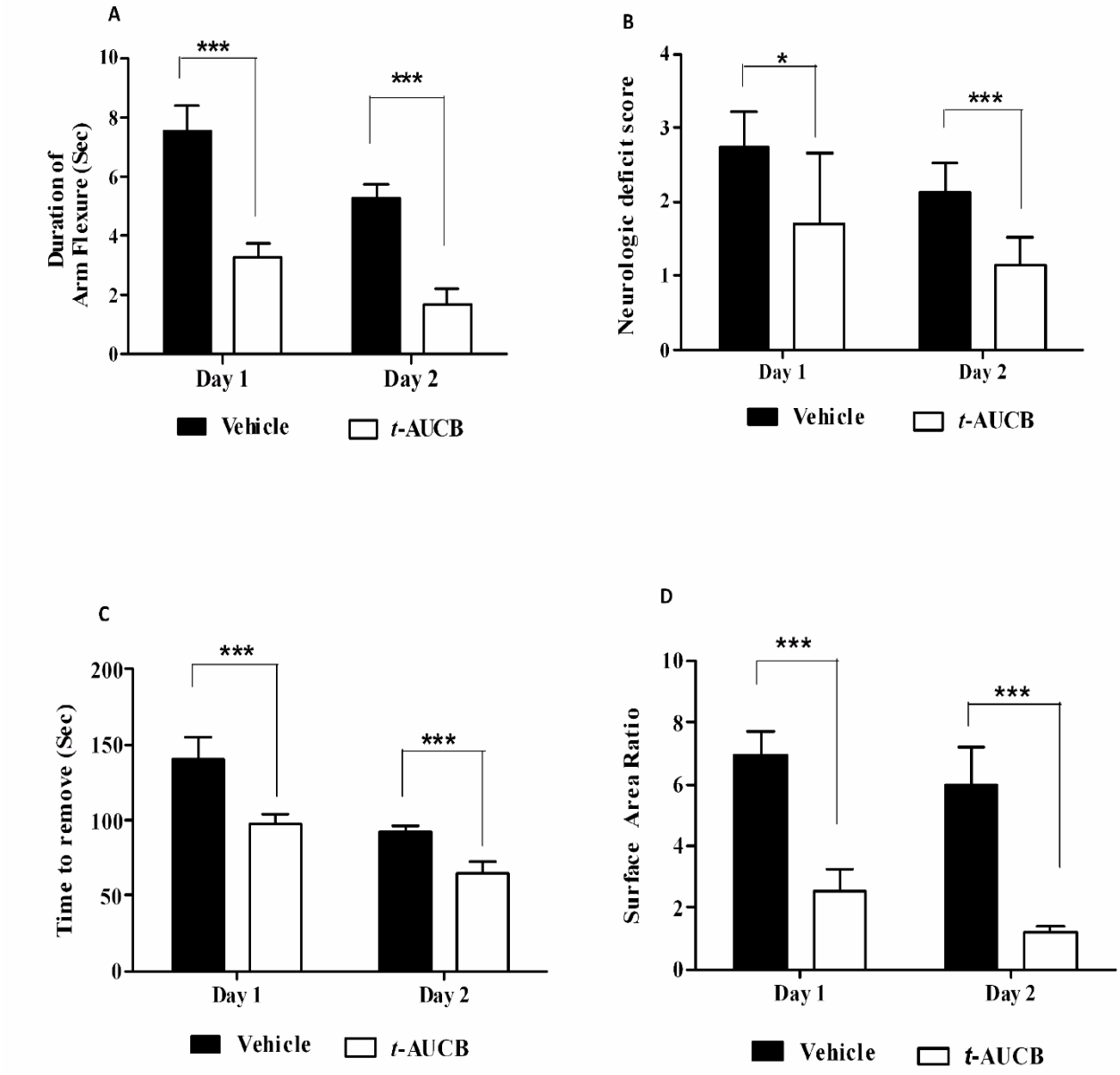

Figure 4-6 The effect of acute *t*-AUCB on functional outcome in a rat temporary MCAO model (n=9). Rats treated with *t*-AUCB showed significant improvement in A) arm flexure, B) neurological deficit score, C) time to remove tape, and D) tape surface area ratio compared to vehicle treated group on both days 1and 2.

4.3.4 Effect of *t*-AUCB treatment on cerebral blood flow changes

The effect of *t*-AUCB treatment on changes in CBF during and after ischemic injury was assessed with ASL MRI. Representative brain perfusion maps of rats treated with *t*-AUCB or vehicle at three different time points are shown in **Figure 4-7**. There is mild to moderate improvement in perfusion around the infarcted tissue during the post-ischemic hypoperfusion period (270 min MRI scan) in *t*-AUCB treated rats. CBF values calculated from perfusion and T_{1obs} maps, revealed no differences in the CBF values between the two groups at baseline and during ischemic injury (**Figure 4-8**). However, a non-significant increase in CBF was seen during the post-ischemic hypoperfusion period (180 min after reperfusion) in *t*-AUCB treated rats compared to vehicle control (**Figure 4-8**; *t*-AUCB: 73.3±35 vs vehicle: 42.2±17 ml/100 g/min; p=0.079). No statistically significant differences between physiological variables such as MABP, and pCO_2 were observed between the two treatment groups (**Figure 4-9**).

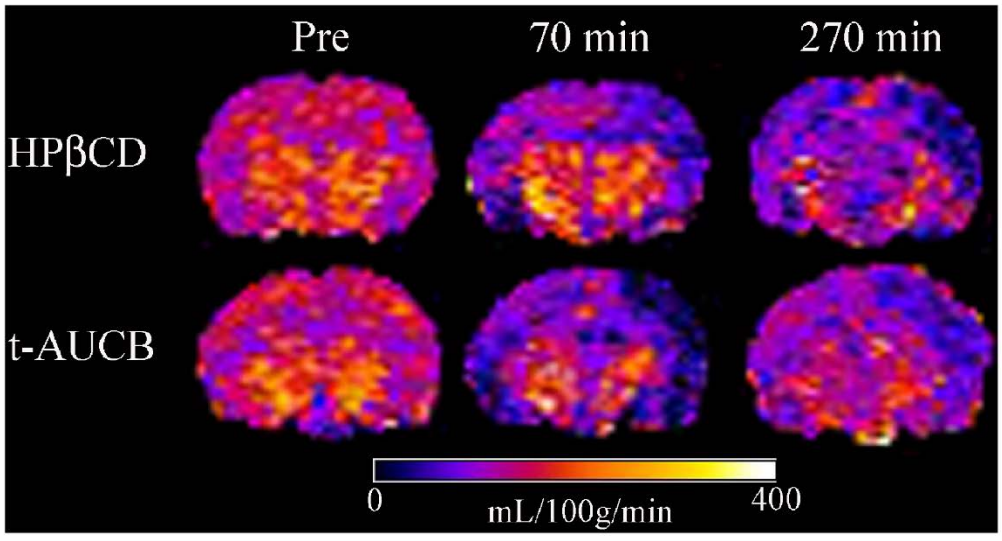

Figure 4-7 Representative brain CBF maps of rats treated with vehicle or *t*-AUCB before MCAO (pre), during MCAO (70 min) and after post-ischemic reperfusion (270 min). Dark blue regions indicate regions of low perfusion as seen at 70 and 270 min maps of both treatment groups.

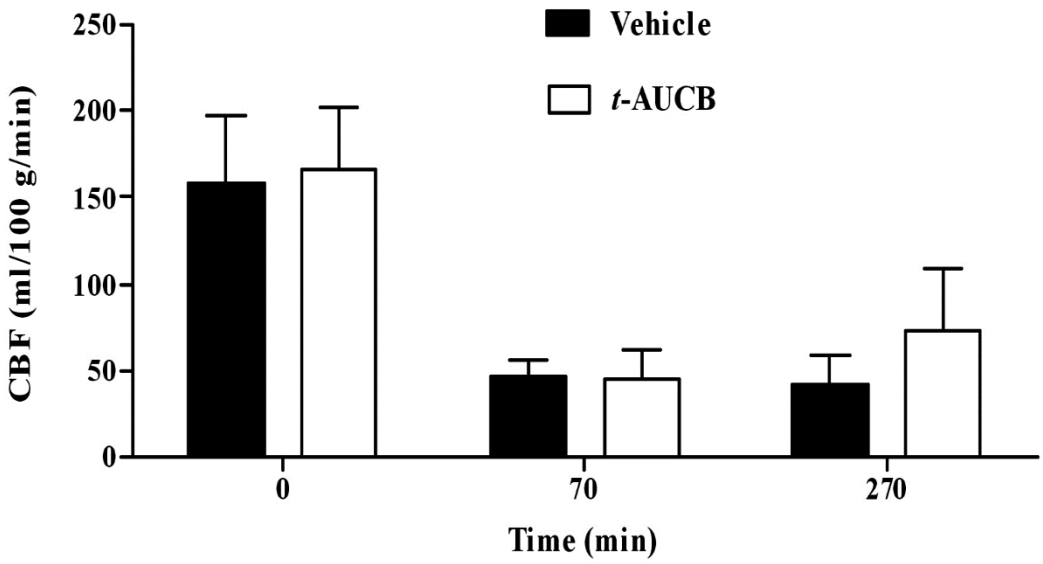

Figure 4-8 Comparison of CBF values (reported as ml/100 g tissue/min) in the cerebral cortex ipsilateral to infarct of vehicle and *t*-AUCB treated rats (n=7). There was a non-significant trend towards increase in CBF in *t*-AUCB treated rats as compared to vehicle treated group.

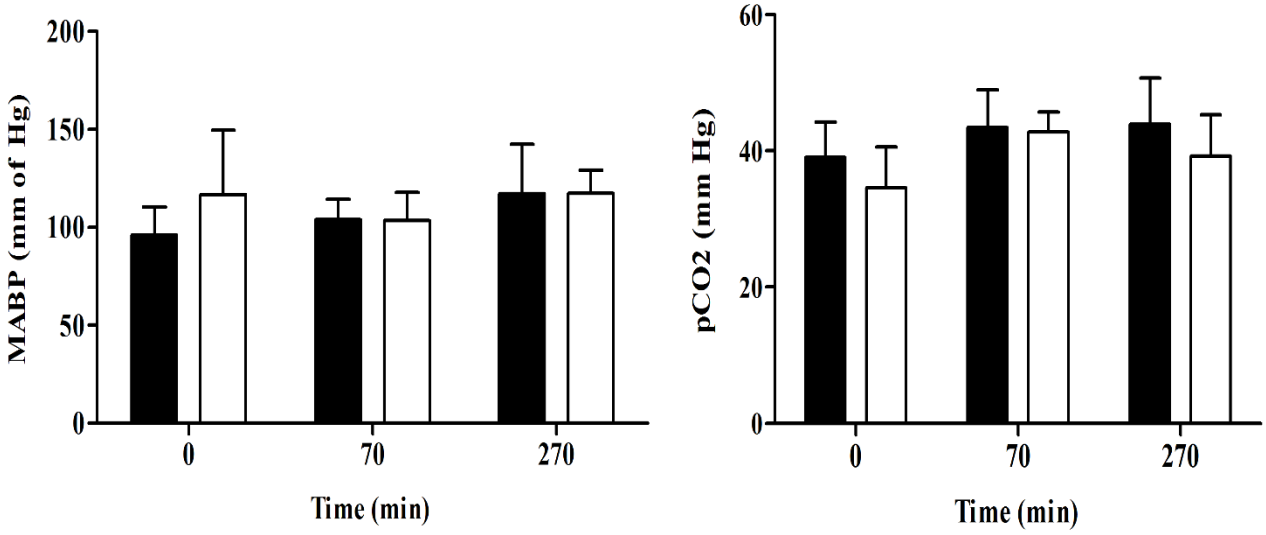

Figure 4-9 Comparison of physiological parameters in the vehicle and *t*-AUCB treated rats. No significant differences were observed between the physiological parameters of vehicle and t-AUCB treated rats.

4.3.5 Effect of *t*-AUCB on cytotoxicity of neuronal cultures under hypoxic conditions

The effect of *t*-AUCB on cytotoxicity of rat primary cortical neuronal culture was assessed by treating neurons with 0.1 and 0.5µM *t*-AUCB followed by hypoxic injury. Pre-treatment prior to hypoxic injury resulted in a non-significant reduction in cell death at 0.1 µM (% cell death: vehicle: 67±11.6 vs *t*-AUCB: 56.91±7; p=0.057) and significant reduction at 0.5 µM (% cell death: vehicle: 67±11.6 vs *t*-AUCB: 48.5±9.5; **p<0.01) compared to their respective vehicle treated groups as assessed by the CytoTox-Fluor kit assay (**Figure 4-10**). Under non-hypoxic conditions of incubation *t*-AUCB did not alter neuronal survival compared to vehicle treated group (% cell death: vehicle: 45.6±9.4; *t*-$AUCB_{0.1\mu M}$: 44.1±7.5; *t*-$AUCB_{0.5\mu M}$: 52.0±6.1; p=0.124) when tested at the same concentration range. In another experiment, neurons treated with *t*-AUCB at 0.1 and 0.5 µM prior to hypoxic injury were imaged under a fluorescent microscope for Hoechst (Blue) and PI (Red) staining (**Figure 4-11**). *t*-AUCB pre-treatment prior to hypoxic injury resulted in significant reduction in cell death in a concentration-dependent manner (% PI positive cells: vehicle: 70.9±7.1 vs *t*-$AUCB_{0.1\mu M}$: 58±5.11; vs *t*-$AUCB_{0.5\mu M}$: 39.9±5.8; ***p<0.001) compared to the vehicle treated group (**Figure 4-12**).

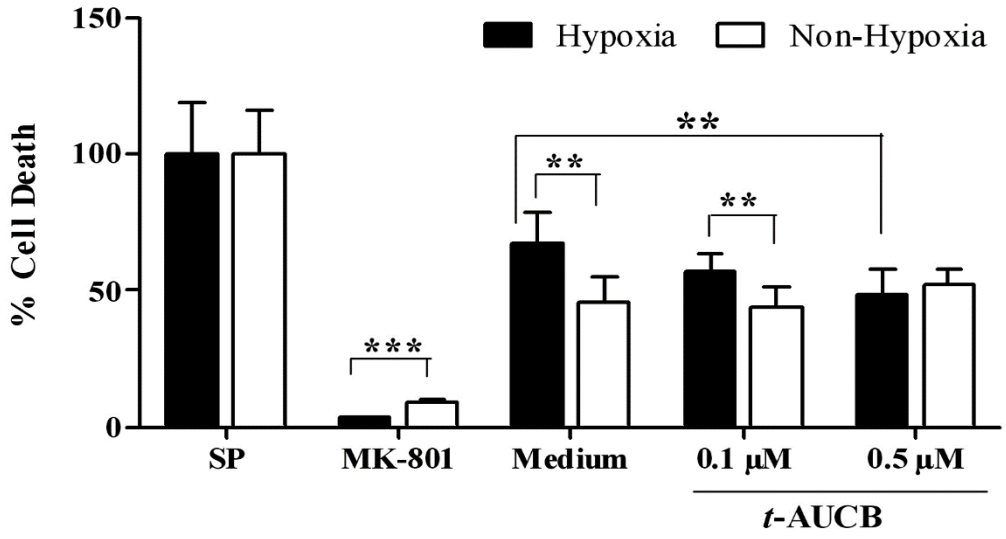

Figure 4-10 The effect of *t*-AUCB on cytotoxicity of primary rat cortical neuronal cultures. % Cell death with *t*-AUCB or vehicle treatment under hypoxic and non-hypoxic conditions. *t*-AUCB showed significant reduction in cell death at 0.5 µM under hypoxic conditions as compared to vehicle group.

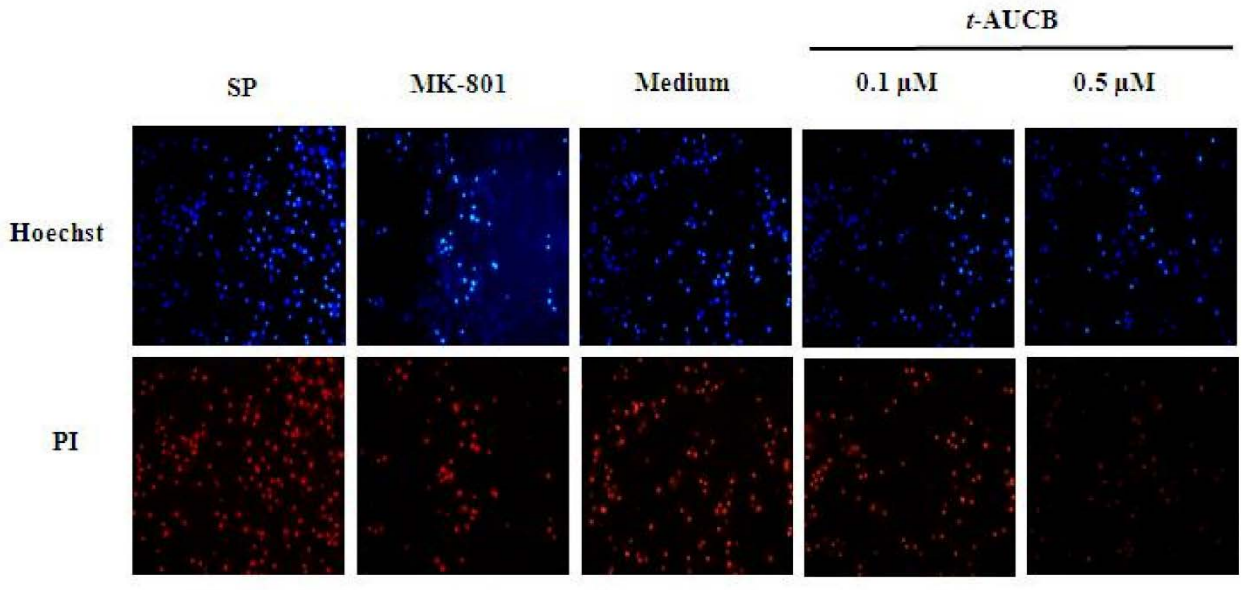

Figure 4-11 Representative images of rat primary cortical neuronal cultures imaged under fluorescence microscope after Hoechst (Blue) and PI (Red) staining.

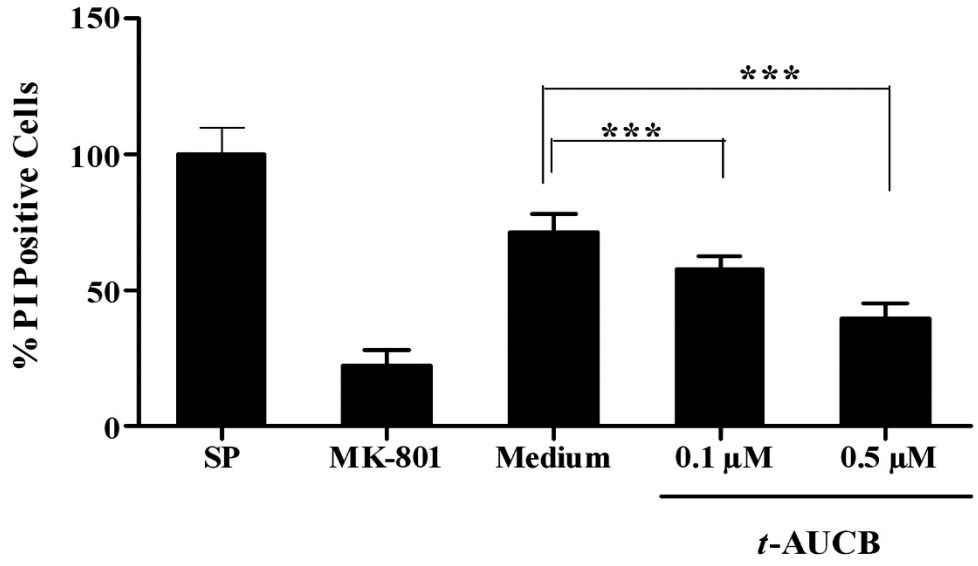

Figure 4-12 The effect of *t*-AUCB on cytotoxicity of primary rat cortical neuronal cultures. Cytotoxicity assessment after hypoxic injury by PI staining. *t*-AUCB treatment showed concentration-dependent decrease in cell death as compared to medium treated group.

4.4 DISCUSSION

In this study, we investigated the neuroprotective effects of acute sEH inhibition with a single low dose, *t*-AUCB (0.9 mg/kg, *iv*) in focal ischemic stroke and the factors contributing to the neuroprotection. Specifically we have established causative relationship between acute sEH inhibition, EETs concentrations and neuroprotection. Furthermore, this study is the first to report the impact of acute sEH inhibition on behavioral performance using a comprehensive behavioral tests evaluating motor and somatosensory activity. The major findings of this study are that a single low dose administration of *t*-AUCB i) significantly decreases infarct volume and elevates brain cortical EETs concentrations, ii) significantly improves short-term functional outcome, iii) does not significantly alter CBF as determined by ASL-MRI, and iv) significantly increases neuronal survival under hypoxic conditions. Collectively, these data suggest that acute inhibition of sEH by

t-AUCB offers neuroprotection primarily through a direct cytoprotective effect on neurons with a minor contribution from alterations in CBF.

Our finding of significant reduction in infarct volume after MCAO is consistent with the previous data reported using urea-based derivative 12-(3-adamantan-1-yl-ureido)-dodecanoic acid butyl ester (AUDA-*n*BE) in a mouse (10 mg/kg,ip) (Dorrance, et al., 2005; Iliff, et al., 2009a; Zhang, et al., 2007), and rat (2 mg/day) (Simpkins, et al., 2009) model of ischemic stroke. Also our results are consistent with other non-urea based sEH inhibitors such as 4-Phenyl Chalcone Oxide (4-PCO) that have been shown to produce neuroprotection in stroke models (Iliff, et al., 2010). This study with the urea based inhibitor for the first time showed that infarct volume reduction was associated with a two-fold elevation of the cumulative EETs/DHETs ratio in brain cortex with *t*-AUCB treatment. Analysis of brain cortices by our validated UPLC-MS/MS method demonstrated no significant changes in the levels of metabolites produced from CYP4A, CYP4F, and the COX pathway, thereby indicating the specificity and selectivity of sEH inhibition by *t*-AUCB. Together, these findings suggest that low dose *t*-AUCB selectively alters EETs concentrations and significantly reduces infarct volume after a single dose administration in the rat MCAO model.

Based on these results, we delineated the impact acute sEH inhibition had on behavioral performance. Our findings suggest that acute administration of *t*-AUCB significantly improved behavioral performance following post-ischemic reperfusion. Behavioral tests used in this study are relevant to evaluate the damage produced by MCAO. MCA, the largest branch of the internal carotid, supplies a portion of the frontal lobe and the lateral surface of the temporal and parietal lobes, including the primary motor and sensory areas of the face, throat, hand and arm. Therefore, we have used behavioral tests that evaluate motor and sensory systems deficits. Further, these

behavioral tests to assess MCAO damage have been shown to correlate with the duration of ischemia and relate to the degree of behavioral deficit (Aronowski, et al., 1996). Acute treatment with *t*-AUCB at the time of ischemic injury exerted beneficial effects on days 1 and 2 following reperfusion. The data from these behavioral performance tests suggest that the extent of cortical damage was more severe in vehicle treated rats after MCAO when compared with *t*-AUCB treated animals, and that the rats recovered significantly from cortical damage and sensory neglect after acute *t*-AUCB administration. Taken together, these data demonstrate that selectively increasing brain cortical EETs concentrations by acute sEH inhibition may not only reduce infarct volume, but also improves the neurofunctional outcome in rats after MCAO, thereby providing additional evidence in support of sEH inhibitors as potential therapeutic intervention for neuroprotection after ischemic injury.

The data from infarct volume and behavioral performance assessments led us to investigate the factors contributing to the neuroprotective effects of *t*-AUCB. We employed a non-invasive ASL-MRI imaging technique to evaluate real-time CBF analysis. We found that acute *t*-AUCB treatment produced a non-significant trend towards improved CBF around the infarcted area during the post-ischemic hypoperfusion period with no major differences in CBF observed either during or after ischemia. Our findings after ischemic injury were similar to the results reported previously showing no significant differences in regional CBF rates as measured by [^{14}C] iodoantipyrene [IAP] autoradiography between AUDA-*n*BE and vehicle treated groups (Zhang, et al., 2007). Conversely, in another study, Zhang, et al reported that brain tissue perfusion was significantly higher in sEH null mice (sEH$^{-/-}$) compared to WT mice during and after vascular occlusion by Laser-Doppler perfusion and [^{14}C] IAP autoradiography (Zhang, et al., 2008b). One

of the likely explanations for the contradictory findings between sEH$^{-/-}$ phenotype and chemical sEH inhibition is related to acute chemical sEH inhibition versus chronic loss of activity in sEH$^{-/-}$ mice producing differential effects on CBF. It is also possible that developmental differences or loss of phosphatase activity in the sEH$^{-/-}$ animals may explain the observed CBF effects. Interestingly, this discrepancy in the pharmacological inhibition versus gene deletion of sEH is not unique to CBF effects as several studies have reported differences in other phenotypes that are independent of CBF effects. For example, in a study Keseru *et al.*, observed increased right heart hypertrophy and pulmonary artery muscularization in sEH$^{-/-}$ mice subjected to chronic hypoxia than the wild type mice treated chronically with sEH inhibitors (Keseru et al., 2010). Similarly, Fairbanks et al. also reported gender differences in neuronal susceptibility to ischemic cell death in *in vitro* OGD model and linked it to sEH expression and possibly to hydrolase activity. In this study of primary cortical neuronal cultures made from male and female rats, acute sEH inhibition by 4-PCO did not abolish the gender differences in ischemic death but knock out of sEH eliminated differences in sensitivity to OGD between neurons from male and female mice (Fairbanks, et al., 2012). Collectively, these studies support that the phenotype differences exist between sEH chemical inhibition and sEH$^{-/-}$ animals. More studies focusing on CBF changes should be completed to elucidate the underlying mechanisms of these phenotypic differences and to better understand the degree to which changes in CBF within microvessels contribute to overall neuroprotection within the neurovascular unit.

Given that acute administration did not significantly affect CBF in the rat MCAO model, we sought to determine if *t*-AUCB directly protects neurons from ischemic damage *in vitro*. Our *in vitro* experiments with naïve rat primary cortical neurons showed that *t*-AUCB significantly reduced

neuronal cell death in a concentration-dependent manner after hypoxic injury, thereby suggesting a direct neuroprotective effect of *t*-AUCB treatment under hypoxic conditions. In our assay, negative control MK-801, a potent NMDA receptor antagonist prevented neuronal death significantly after hypoxic injury, suggesting that involvement of excitotoxic mechanisms for neuronal death, however it is unknown if the protective mechanisms of the EETs are identical *in vivo* vs *in vitro*. Future studies comprehensively evaluating the protective mechanisms will help understand the similarity of *in vitro* protective mechanisms to the *in vivo* mechanisms. In a study, Koerner, et al reported protective effects of exogenous administration of 14,15-EET or sEH inhibition by 4-PCO at low concentration in an *in vitro* OGD study with primary rat cortical neurons transduced with human sEH variants expressing functional polymorphisms that alter hydrolase activity of sEH (Koerner, et al., 2007). However, these protective effects were not observed in naïve rat cortical neurons. In this study, for the first time we reported significant neuroprotective effects of sEH inhibition by *t*-AUCB in rat primary cortical neurons after hypoxia-reoxygenation injury. Though in this experiment we did not measure cellular levels of EETs after sEH inhibition, our findings of protective effect of exogenous 11,12-EET administration from **Chapter 3** indicate that EETs exert direct neuroprotective effects in ischemic injury. In addition to the protective effect on neurons, EETs also appear to exert beneficial effects on other brain cells in ischemia as reported by Liu *et al* who showed cytoprotective effects of exogenous administration of EETs on cortical astrocyte culture in an OGD model (Liu, et al., 2005b).

Although, we studied the neuroprotective mechanisms *in vitro* and CBF changes *in vivo*, we observed significant improvements in infarct volume reduction and behavioral performance in the absence of a significant CBF improvement suggesting that the protective effects may be due to both direct effect on neurons and additional contributions from CBF changes. Future studies

evaluating EET agonists and antagonists that evaluate microvascular flow will aid in the elucidation of the mechanisms of neuroprotection. Furthermore, evaluating the effect of sEH inhibition on oxidative stress and inflammation accompanying ischemic damage of cerebral tissue will elucidate underlying effector mechanisms involved in the pathogenesis. Although we did not observe significant changes in the levels of key prostaglandin metabolites across treatment groups, future studies evaluating the levels of key oxidative stress markers such as 8-isoprostane will help in elucidating the underlying mechanisms of pathogenesis of ischemic injury. Collectively, these data suggest that altering EETs levels by acute inhibition of sEH is likely to produce the largest benefits by affecting multiple components of neurovascular unit such as astrocytes, neurons, and microvascular flow.

There are possible limitations to this study. One of the limitations is the administration of *t*-AUCB at the time of initiation of ischemia. Due to the difficulty in administering *t*-AUCB post ischemic injury in our MCAO model in CBF assessment experiments by ASL-MRI, we administered *t*-AUCB immediately prior to initiation of ischemic injury in all of our experiments. Future direction of our work includes evaluating the neuroprotective effects of *t*-AUCB administered with the same dosing regimen (0.9 mg/Kg, *i.v*) during the post-ischemic reperfusion period. A second limitation is that we evaluated the protective effects after acute administration of a single dose of *t*-AUCB. Additional studies are need in future to establish a dose-response curve as *t*-AUCB has favorable pharmacokinetic profile due to good solubility and permeability across tissues, and longer half-life (Tsai, et al., 2010), and to evaluate the impact of chronic administration during the post-ischemic reperfusion phase on the regional CBF and long-term functional outcome. Third limitation of our study was that in our *in vitro* cell culture experiments, we used high

concentrations of *t*-AUCB (0.5 µM) to account for possible loss due to non-specific binding to cells and metabolism after uptake. This concentration may not be reflective of intracellular concentrations achieved with our dosing regimen (Tsai, et al., 2010). Future goals of our work will aim at assessing the *in vitro* neuroprotective efficacy of *t*-AUCB over a wider concentration and time exposure range. Fourth limitation of our study was that *t*-AUCB neuroprotection was evaluated in male rats alone. A previous study has showed that sEH expression in females was lower than males and that the gene deletion of sEH did not reduce infarct volume in females presumably due to lower sEH expression (Zhang et al., 2009). Additional studies in future evaluating acute and/or chronic sEH inhibition in female rats will help to understand if gender difference plays a crucial role in sEH mediated neuroprotective effects.

4.5 CONCLUSIONS

In summary, in the current study we have demonstrated the neuroprotective effects of *t*-AUCB in a rat MCAO model at a low dose and have produced the first evidence that *t*-AUCB alters EETs/DHETs ratio without significant changes in other AA metabolites from CYP4A, CYP4F, and COX pathways. In addition, these data are first to demonstrate improved short-term behavioral performance by *t*-AUCB; thereby, providing evidence that sEH inhibitors meet the STAIR criteria of improved functional outcome in the rat. Further, we demonstrated that the neuroprotection by *t*-AUCB is likely due to direct neuronal effects with minor contributions from alterations in CBF. Chronic sEH inhibition by pharmacological inhibitors is an area of the future study to better elucidate long-term behavioral performance and evaluate sEH inhibitors as a potential novel intervention for focal ischemic insults.

5.0 EVALUATION OF EFFECTS OF CYP EICOSANOIDS IN GLOBAL ISCHEMIA

[Jafar Sadik B Shaik, Samuel M Poloyac, Henry Alexander, Robert SB Clark, Patrick M Kochanek, Mioara D Manole. "20-HETE inhibition by HET0016 offers neuroprotection by increasing cortical CBF during post-resuscitation in a pediatric rat asphyxial cardiac arrest model." *Manuscript prepared*]

5.1 INTRODUCTION

Previous chapter has investigated the effects of CYP eicosanoids on neuroprotection, CBF changes and short-term functional outcomes in focal ischemia model. As mentioned in the earlier chapter, CBF dysregulation is commonly observed after reperfusion from ischemic stroke or cardiac arrest (CA). In the introduction, I've discussed on adult and pediatric CA. Ventricular fibrillation is main cause of adult CA. In children common cause for CA is respiratory failure due to asphyxiation with 10 – 15% cases attributed to ventricular fibrillation. In addition to poor prognosis and clinical outcomes after CA in children, limited knowledge of the developmental differences in ion channels, receptor subtype expression in pediatric population curtails our understanding of pathophysiology of global ischemic injury in pediatric CA as compared to adult CA. Further, these developmental differences in ion channels could raise an issue in using general anesthetics blocking GABA with high risk for excitotoxicity. For this reason, we chose pediatric asphyxial CA model to elucidate the pathophysiology of global ischemic injury after CA in pediatrics. Like in focal ischemic models, resuscitation after CA may produce secondary neuronal damage as a result of global ischemic brain injury (Buunk et al., 2000). Thus, restoration of CBF following CA is critical in determining neuronal survival. (Manole et al., 2008; Shaffner et al., 1999; Xu et al., 2002b). The CBF derangements after CA are well documented in adult animals describing a typical phasic pattern. During the first phase that corresponds to the CPR maneuvers there is no flow, followed by low flow at the end of CPR. Immediately after reperfusion there is a transient global increase in CBF (hyperemia) (Fischer et al., 1995; Shaffner et al., 1998) followed by a prolonged post-ischemic hypoperfusion (hyporemia) (Liachenko et al., 2001). In a clinically relevant pediatric rat asphyxial CA model, similar pattern of CBF changes after CA were observed with a transient hyperemia in subcortical regions followed by prolonged hypoperfusion in cortical

regions (Manole et al., 2009; Manole et al., 2012). There have been conflicting opinions regarding the relationship between CBF changes, and neurological outcome after CA. It was hypothesized that early hyperemia after CA is beneficial and hypoperfusion is detrimental for neuronal survival (Della Corte et al., 1993; Snyder et al., 1975); however, other studies indicated that early hyperemia may lead to poor neurological outcome (Cohan et al., 1989; Pignataro et al., 2008). Currently there are no therapeutic treatments that have shown efficacy in improving neurological outcomes after CA except for hypothermia (Bernard et al., 2002; Weigl et al., 2005). The mechanisms implicated in the pathogenesis of CBF derangements after resuscitation from CA are not fully elucidated. Increases in the levels of endogenous catecholamines, nitric oxide production in cerebral vessels are attributed to early hyperemia post ROSC. Other mechanisms such as vascular resistance, cerebral edema, coagulation, lipid peroxidation and neuronal apoptosis or necrosis are also attributed to the ischemia / reperfusion injury (Gando et al., 1997; Nitatori et al., 1995; Traystman et al., 1991). Therefore, a thorough pathophysiological investigation of regional dynamic changes in CBF during the early and late period after resuscitation should be done to gain insight into the mechanisms leading to secondary neuronal damage.

Ischemic injury following CA increases PLA_2 mediated release of AA into the cytosol, which is metabolized further to form prostanoids, CYP eicosanoids, and leukotrienes. Prostanoids are potent regulators of vascular tone and mediate their effects through various membrane receptors of GPCR family (Wright et al., 2001). Specifically, prostacyclin (PGI_2) and TXA_2 are potent vasodilator and vasoconstrictor of cerebral vasculature. Other prostanoids such as PGE_2, and $PGF_{2\alpha}$ also induce either vasoconstriction or vasodilation depending on the type of receptor activated (Moncada, et al., 1978). As discussed in **Chapter 1**, CYP eicosanoids are also potent

regulators of cerebrovascular tone and blood flow. Thus, an imbalance in the levels of prostanoids, and CYP eicosanoids may serve to limit the CBF recovery during the reperfusion phase after CA. Role of prostanoids in the ischemic brain damage has been well characterized and studied. The neuroprotective effects of different prostanoids in *in vitro* and *in vivo* models of ischemia were summarized in **Chapter 2**. Similarly, role of CYP eicosanoids in the pathogenesis of ischemic injury after focal ischemia (Iliff, et al., 2009a; Miyata, et al., 2005; Omura, et al., 2006; Poloyac, et al., 2006; Zhang, et al., 2007) is well characterized. However, their role in global ischemia is poorly understood. Hitherto, there is only one published report that investigated the role of 20-HETE in global ischemia or neonatal hypoxia-ischemia (Yang et al., 2012). Therefore, the primary goals of this study were to measure the brain tissue levels of CYP eicosanoids and prostanoids, to evaluate the changes in CBF, and to evaluate the effect of acute inhibition of 20-HETE synthesis by HET0016 on CBF, and functional outcome in a pediatric rat asphyxial cardiac arrest model.

5.2 EXPERIMENTAL METHODS AND PROCEDURES

All animal experiments were approved by the University of Pittsburgh Institutional Animal Care and Use Committee (IACUC) and performed in accordance with the NIH Guide for the Care and Use of Laboratory Animals.

5.2.1 Animals and experimental design

Mixed litter, male PND 16 to 18 Sprague-Dawley rats (30 to 45 g) were used. The rats were randomly assigned to receive either 9 min or 12 min of asphyxial arrest or sham surgery. Sham control rats underwent anesthesia and surgery without asphyxial arrest or resuscitation. Initial experiments were performed to assess CBF changes at serial time intervals (5, 10, 30 and

60 min) following resuscitation from CA. Rats were sacrificed by decapitation at 5 and 120 min after ROSC, and brain tissue was rapidly excised, snap frozen in liquid nitrogen and stored at -80 ºC until further analysis to measure levels of CYP eicosanoids and prostanoids in the cortex and the midbrain. In a separate study, rats were randomly assigned to either vehicle (lyophilized HPβCD, 15%), or treatment (lyophilized HET0016 in HPβCD, 0.5 mg) groups. All rats were subjected to either sham surgery or 12 min of CA. All HPβCD lyophilized complexes (vehicle or HET0016) were reconstituted in PBS, pH=7.2, and filtered prior to administration. Four experiments were performed: 1) effect of HET0016 on cerebral blood flow changes after CA (n=6/group); 2) CYP eicosanoids and prostanoids levels in the cortex and the midbrain at 5 min after ROSC following HET0016 or vehicle treatment (n=6/group); 3) acute HET0016 effect on short-term neurological deficits at 24 and 48 h after resuscitation from CA (n=6/group); and 4) effect of HET0016 on neuronal survival after CA (n=6/group). For experiments 1and 2 a single bolus dose of HET0016 at 0.9 mg/Kg was administered via the femoral vein at the time of resuscitation from CA. For experiments 3 and 4 multiple doses of HET0016 at 0.9 mg/Kg were administered intravenously at every 6 hours over a period of one day since the time of resuscitation. Sample size was determined based on the power analysis of detecting a significant difference between treatment groups with an effect size of 20% and 2 fold increase in the ratios at 80% power. The surgeon and individuals involved in all above experiments were blinded to all treatment groups.

5.2.2 Asphyxial cardiac arrest in pediatric rats

Rats underwent asphyxial CA for 9 or 12 minutes followed by resuscitation as described previously (Fink et al., 2004). A schematic diagram illustrating the CA model was shown in **Figure**

5-1. Briefly, the rats were initially anesthetized via nose cone with 3% isoflurane, 50/50 N_2O/O_2 in a Plexiglas chamber until unconscious and then the trachea was intubated with an 18-gauge angiocatheter and mechanical ventilation was initiated. $PaCO_2$ was maintained between 35 to 45 mm Hg by adjusting ventilation rate and tidal volumes. During surgery, anesthesia was reduced to 2.5% isoflurane, 50/50 N_2O/O_2 & oxygen and femoral arterial and venous catheters were placed. Isoflurane was discontinued and intravenous analgesia was initiated using fentanyl infusion at 50 µg/kg/h and neuromuscular blockade was obtained using vecuronium infusion at 5 mg/kg/h. Prior to recording baseline CBF, a 30 min duration of isoflurane washout was performed to minimize the effect of inhaled anesthetics on CBF. Asphyxial cardiac arrest was induced by disconnecting the tracheal tube from ventilator and maintained until 9 or 12 min. Resuscitation was initiated by reconnecting the ventilator, infusion of epinephrine 0.005 mg/kg and sodium bicarbonate 1 mEq/kg *i.v.*, and manual chest compressions until ROSC. Anesthesia and neuromuscular blockade were restarted at 30 min after ROSC until the end of experiment. MABP and heart rate were continuously monitored via femoral arterial and venous catheters. Arterial blood gases were measured at baseline, during CA and post resuscitation till the end of experiment. Rectal temperature was continuously monitored and maintained at 37 ºC via a heater water blanket system throughout the surgery.

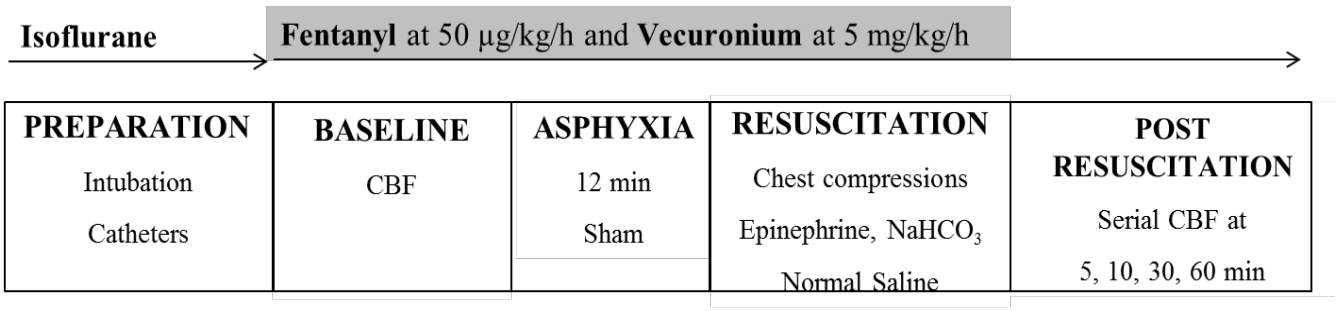

Figure 5-1 A schematic diagram illustrating the asphyxial CA model in pediatric rats.

5.2.3 Tissue extraction and chromatographic analysis of AA metabolites

Concentrations of various metabolites including CYP eicosanoids, and prostanoids were determined from cortex and midbrain of vehicle and HET0016 (0.9 mg/kg i.v; n=9/group) treated rats that underwent either sham surgery or asphyxial cardiac arrest using solid phase extraction and UPLC-MS/MS analysis as described in **Chapter 2**.

5.2.4 Cerebral blood flow assessment using laser-speckle photometry

Cortical CBF was measured using laser-speckle photometer from Perimed (PeriCam PSI, Perimed, Switzerland) **(Figure 5-2)**. During anesthesia, rats were placed into a standard stereotaxic frame and the skull was exposed with a midline scalp incision skin. The skull area was cleaned to remove any traces of blood. Rats were placed under a PeriCam PSI system, which utilizes a built-in 70 mW laser diode to illuminate the cortical surface. PeriCam PSI laser head was adjusted to a distance of 15 cm and at an angle of 90 degree to the imaging plane such that the laser beam falls in the center of the imaging area. The Imaging area was set to 2 X 2 cm. The perfusion imaging was recorded continuously at a frame rate of 10 images/sec and resolution of 0.14 mm throughout the experiment. Measurement events were marked at regular intervals starting from baseline, during CA, after CA till the end of the experiment. CBF perfusion maps were obtained at baseline and at 5, 10, 30, 60 min after ROSC. CBF perfusion values in the regions of interest (ROI) in cortex were computed from perfusion images using PIMSoft software (Perimed, Switzerland).

Figure 5-2 Perimed laser speckle perfusion imaging unit

5.2.5 Neurological deficit assessment

Neurological deficits in rats (n=6/group) from vehicle, and HET0016 groups at 3, 24, and 48 h after resuscitation from CA or from sham group were examined by a modified neurological deficit score (NDS) system as described previously (Neumar et al., 1995). Parameters assessed in in the NDS were listed in **Table 5-1**. Briefly, various parameters including general consciousness, cranial nerves, motor, sensory, and coordination response were each scored individually. Cumulative score obtained is normalized to maximum test score and represented as % NDS score. A NDS score of 0-10% is considered normal and 100% is considered maximum neurological damage.

Table 5-1 Neurologic deficit scoring system for assessing behavioral performance of pediatric rats subjected to asphyxial CA

Parameter	Score scale
General	
Consciousness	0 / 50 / 100
Respiration	0 / 50 / 100
Total points	200
Clinical nerves	
Olfactory	0 / 10 / 20
Vision	0 / 10 / 20
Corneal reflex	0 / 10 / 20
Whisker movement	0 / 10 / 20
Hearing	0 / 10 / 20
Total points	100
Motor	
Left forepaw	0 / 5 / 10
Right forepaw	0 / 5 / 10
Left hindpaw	0 / 5 / 10
Right hindpaw	0 / 5 / 10
Tail	0 / 5 / 10
Total points	50
Sensory	
Left forepaw	0 / 5 / 10
Right forepaw	0 / 5 / 10
Left hindpaw	0 / 5 / 10
Right hindpaw	0 / 5 / 10
Tail	0 / 5 / 10
Total points	50
Coordination	
Travel ledge	0 / 5 / 10 / 15 / 20 / 25
Placing test	0 / 15 / 25
Righting reflex	0 / 15 / 25
Stop table edge	0 / 15 / 25
Total points	100
Total Score	500
Percent NDS	0 – 100 %

5.2.6 Neuronal survival assessment after global ischemic injury

Effect of acute HET0016 treatment on neuronal survival after asphyxial CA was assessed by FluoroJade-B (Schmued et al., 1997), and hematoxylin and eosin (H&E) staining. At 48 h from resuscitation after CA, rats receiving either HET0016 or vehicle treatment were anesthetized with 3% isoflurane and 50% N_2O / balance O_2 followed by transcardial perfusion with 250 mL of ice-cold heparinized saline and 250 ml of 4% paraformaldehyde. The brains were removed and fixed in 4% paraformaldehyde. Coronal sections of the paraffin embedded brains were cut at 5 µm using a cryotome, and 5 to 6 systematic random sections were obtained. Separate sections were further processed and stained with FluoroJade-B for identifying degenerating neurons, and with H&E for evaluating gross ischemic cellular changes.

For FluoroJade-B staining, coronal sections were washed sufficiently with xylene to remove paraffin, then immersed in 100% ethanol and 1% sodium hydroxide for 90 sec, followed by another 30 sec treatment with 70% ethanol. Slides with coronal brain sections were mixed with 0.06% potassium permanganate for 10 min on a shaker and subsequently washed in distilled water before immersion in a 0.006% working solution of Fluoro-Jade B with 4,6-diamidino-2-phenylindole (DAPI) for 30 min. Slides were then washed with distilled water multiple times, drained and placed on a slide warmer at 50°C for 10 min, then cover-slipped with DPX mounting medium. Cells stained positively in the primary motor and sensory cortex were counted under microscope from multiple sections by an observer blinded to experimental condition.

5.2.7 Statistical analysis

Primary hypothesis in the experiments with HET0016 was to evaluate changes in the levels of 20-HETE with or without HET0016 administration. Hence, primary statistical comparisons were done to evaluate significant changes in 20-HETE levels with subsequent secondary analysis performed to evaluate significant changes in other metabolites. Significant differences between treatment groups in experiments measuring CYP eicosanoid and prostanoid levels, and neuronal survival one-way ANOVA with Dunnett's post-hoc test was used. Significant differences between groups in CBF changes at regular intervals after ROSC, neurological deficit assessments, and physiological variables were determined via repeated measures ANOVA analysis. A *$p<0.05$ was considered significant. All data were represented as mean ± SE.

5.3 RESULTS

5.3.1 Effect of CA duration on CBF in the cortex in pediatric rat asphyxial cardiac arrest model

Changes in the cortical blood flow during early and late reperfusion period after asphyxial cardiac arrest were evaluated in a 9 and 12 min CA models. Blood flow changes in the cortex, represented as % of baseline, throughout the reperfusion phase exhibited same pattern in both models of CA with a rapid decline until 30 min and sustained low flow till 120 min (**Figure 5-3**). However there was significant decrease in CBF early at 5 min after ROSC in 12 min group (77.8 ± 1.7%) as compared to 9 min CA (86.3±1.2%; *$p<0.05$). During the late reperfusion period, CBF in 12 min CA group was significantly low at 60 (56±2.5% vs 63.1±1.2%; *$p<0.05$) and 120 min (55.4±1.8% vs 64.4±2.7%; *$p<0.05$) after ROSC as compared to 9 min CA group.

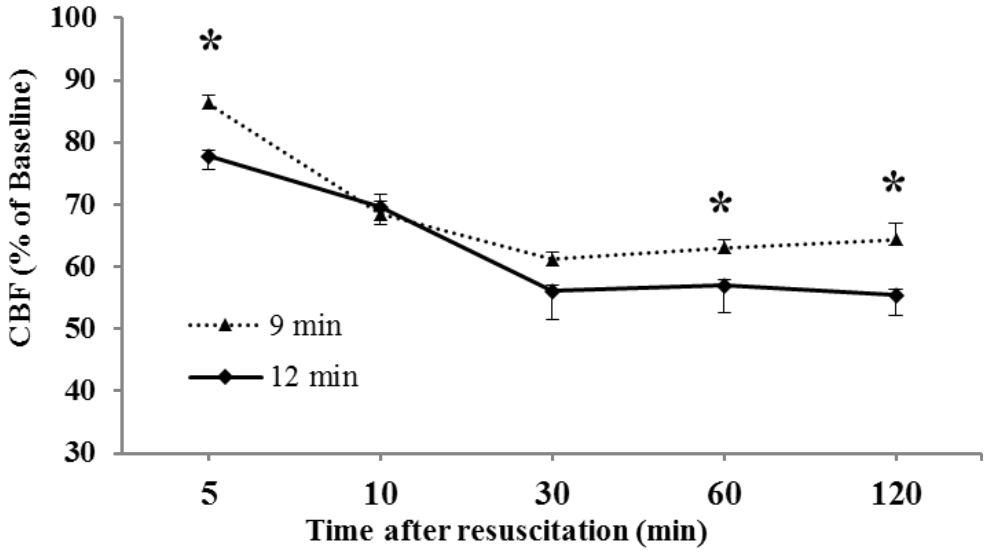

Figure 5-3 Effect of duration of CA on cortical blood flow after resuscitation from CA. CA (independent of duration) produced a trend of initial steep decrease in CBF followed by sustained low flow post resuscitation. 12 min CA showed significant reduction in CBF at 5, 60, and 120 min compared to 9 min CA in the post-ischemic reperfusion period.

5.3.2 Effect of CA duration on the prostanoid levels in the cortex after ROSC in pediatric asphyxial cardiac arrest

Prostanoid levels in the cortex at 5 and 120 min after ROSC were evaluated in both 9 and 12 min CA models. In 9 min CA model, 5 min after ROSC significant increases in the levels (pmol/g tissue) of 6-Keto-$PGF_{1\alpha}$ (3.22±0.2 vs 2.24±0.2; *$p<0.05$), 11β-$PGF_{2\alpha}$ (16.1±2.2 vs 3.34±0.71; *$p<0.001$), $PGF_{2\alpha}$ (58.5±10.9 vs 15.8±1.92; *$p<0.001$), PGE_2 (122±20.9 vs 12.8±2.0; *$p<0.001$), 11-d-TXB_2 (11.7±2.3 vs 1.37±0.4; *$p<0.01$), PGD_2 (1029±82 vs 351±90.7; *$p<0.001$), 15-d-PGD_2 (34.2±5.7 vs 27.6±7.9; *$p<0.05$), 15-d-PGJ_2 (53.0±9.4 vs 12.8±2.2; *$p<0.01$), and significant decrease in the levels of $PGF_{1\alpha}$ (3.3±0.7 vs 16.5±2.2; *$p<0.001$) were observed in cortex as compared to sham rats (**Table 5-2**). However fold changes in the levels of PGE_2 with respect to sham were higher than all other metabolites. At 120 min after ROSC, concentrations of

most of the metabolites decreased to sham or below sham levels. In 12 min CA model, during the early reperfusion at 5 min, significant increases in the levels of 6-Keto-$PGF_{1\alpha}$ (14.5±1.9 vs 2.24±0.2; *p<0.001), 11β-$PGF_{2\alpha}$ (10.2±1.3 vs 3.34±0.7; *p<0.001), $PGF_{2\alpha}$ (131±12.5 vs 15.8±1.9; *p<0.001), PGE_2 (35.5±5.0 vs 12.8±2.0; *p<0.001), PGD_2 (937±125vs 351±90.7; *p<0.001), 15-d-PGJ_2 (18.4±0.4 vs 12.8±2.2; *p<0.05) and significant decreases in the levels of $PGF_{1\alpha}$ (2.6±0.39 vs 16.5±2.2; *p<0.05) were observed in cortex as compared to sham rats. However fold change in the levels of 6-Keto-$PGF_{1\alpha}$, and $PGF_{2\alpha}$ relative to sham in the early phase of reperfusion was higher in 12 min CA as compared to 9 min CA. At 120 min the levels of 6-Keto-$PGF_{1\alpha}$ (13.5±1.67 vs 2.24±0.2; *p<0.001) was still significantly higher than sham whereas PGJ_2 (1.81±0.43 vs 36.9 ± 4.80; *p<0.001), 15-d-PGD_2 (2.06± 0.4vs 27.6±7.9; *p<0.01), and 15-d-PGJ_2 (5.36±1.1vs 12.8±2.2; *p<0.01) have decreased significantly compared to sham rats. In contrast to 9 min CA model, levels of PGA_2 were not detected at either 5 or 120 min after ROSC in the 12 min CA model. Fold changes in the levels of all prostanoids in the cortex with respect to sham at 5 and 120 min after ROSC in 9 and 12 min CA was depicted in a polar plot (**Figure 5-4**). Each spike represents a prostanoid, and the radius of the circle represents fold changes normalized to sham. Prostanoids with significant changes compared to sham were separately shown in **Figure 5-5**.

5.3.3 Effect of CA duration on the prostanoid levels in the midbrain after ROSC in pediatric asphyxial cardiac arrest

Prostanoid levels in the midbrain at 5 and 120 min after ROSC were evaluated in both 9 and 12 min CA models. In 9 min CA significant increases were only observed in the levels of $PGF_{2\alpha}$ (39.5±3.4 vs 20.8±2.1; *p<0.001) whereas significant decreases were observed in the levels of 11β-$PGF_{2\alpha}$ (10.3±1.8 vs 21.9±4.8; *p<0.05), $PGF_{1\alpha}$ (3.58±0.4 vs 20.9±2.9; *p<0.001), PGA_2

(2.37±0.91 vs 18.4±4.6; *p<0.001),15-d-PGD_2 (25.6±5.1 vs 62.2±0.8; *p<0.001) at 5 min after ROSC in the midbrain compared to sham rats (**Table 5-3**). At 120 min, significant increases were only seen in the levels of $PGF_{1\alpha}$ (12.0±1.70 vs 20.9±2.97; *p<0.05) whereas significant decreases were observed in the levels of 11β-$PGF_{2\alpha}$ (9.41±2.12 vs 21.9±4.81; *p<0.05), $PGF_{2\alpha}$ (8.66±0.77 vs 20.8±2.1; *p<0.001), PGD_2 (171±36 vs 479±147; *p<0.05), PGJ_2 (8.02±1.8 vs 22.7±4.5; *p<0.05), 15-d-PGD_2 (16.9±2.9 vs 62.2±0.85; *p<0.001) compared to sham rats. In 12 min CA model, during the early reperfusion at 5 min, significant increases in the levels of 6-Keto-$PGF_{1\alpha}$ (7.83±0.71 vs 1.80±0.5; *p<0.001), $PGF_{2\alpha}$ (57.8±5.4 vs 20.8±2.1; *p<0.001) and significant decreases in the levels of $PGF_{1\alpha}$ (1.31±0.21 vs 20.9±2.97; *p<0.001), PGE_2 (19.8±2.37 vs 159±35.7; *p<0.05), 11-d-TXB_2 (1.55±0.3 vs 7.68±1.7; *p<0.01), 15-d-PGD_2 (16.7±1.41 vs 62.2±0.85; *p<0.001), 15-d-PGJ_2 (10.7±1.4 vs 44.8±6.6; *p<0.001) were observed in the midbrain compared to sham rats. At 120 min, the levels of 6-Keto-$PGF_{1\alpha}$ was still significantly higher whereas PGE_2, 11-d-TXB_2, PGD_2, PGJ_2, 15-d-PGD_2, and 15-d-PGJ_2 were still significantly lower compared to sham rats. At 120 min, there were no levels of 11β-$PGF_{2\alpha}$, $PGF_{1\alpha}$, and PGA_2 detected in the midbrain. Fold changes in the levels of all prostanoids in the midbrain with respect to sham at 5 and 120 min after ROSC in 9 and 12 min CA was depicted in a polar plot (**Figure 5-6**). Each spike represents a prostanoid, and the radius of the circle represents fold changes normalized to sham. Prostanoids with significant changes compared to sham were separately shown in **Figure 5-7**.

Table 5-2 Effect of CA duration on temporal profile of prostanoid levels (pmol/g tissue) in brain cortex after ROSC. Five minutes after ROSC there were significant increases in the prostanoids which returned to sham or below sham levels at 120 min after ROSC.

Analyte	CA	Sham	9 min		12 min	
	ROSC(min)		5	120	5	120
6-Keto-$PGF_{1\alpha}$		2.24 ± 0.2	3.22 ± 0.2*	2.68 ± 0.3	14.5 ± 1.9*	13.5 ± 1.7*
11β-$PGF_{2\alpha}$		3.34 ± 0.7	16.1 ± 2.2*	3.61 ± 0.8	10.2 ± 1.3*	1.37 ± 0.3
$PGF_{1\alpha}$		16.5 ± 2.2	3.3 ± 0.7*	7.4 ± 1.4*	2.6 ± 0.4*	-
$PGF_{2\alpha}$		15.8 ± 1.9	58.5 ± 11*	13.2 ± 1.8	131 ± 12.5*	13.2 ± 2.3
PGE_2		12.8 ± 2.0	122 ± 20.9*	88.8 ± 23.9*	35.5 ± 5.0*	9.71 ± 2.2
11-d-TXB_2		1.37 ± 0.4	11.7 ± 2.3*	3.93 ± 1.1	1.25 ± 0.2	0.86 ± 0.2
PGD_2		351 ± 90.7	1029 ± 82*	180.3 ± 41.4	937 ± 125*	57.4 ± 12.4
PGA_2		24.2 ± 5.3	20.8 ± 4.8	3.53 ± 0.4*	-	-
PGJ_2		36.9 ± 4.8	50.6 ± 10.8	11.9 ± 2.1	33.8 ± 5.3	1.81 ± 0.4*
15-d-PGD_2		27.6 ± 7.9	34.2 ± 5.7	9.33 ± 2.1	27.0 ± 2.5	2.06 ± 0.4*
15-d-PGJ_2		12.8 ± 2.2	53.0 ± 9.4*	20.2 ± 4.1	18.4 ± 0.4*	5.36 ± 1.1*

Table 5-3 Effect of CA duration on temporal profile of prostanoid levels (pmol/g tissue) in the midbrain after ROSC. Five minutes after ROSC there were significant increases in the prostanoids which returned to sham or below sham levels at 120 min after ROSC

Analyte	CA	Sham	9 min		12 min	
	ROSC(min)		5	120	5	120
6-Keto-$PGF_{1\alpha}$		1.80 ± 0.5	1.50 ± 0.2	2.66 ± 0.4	7.83 ± 0.7*	9.90 ± 1.2*
11β-$PGF_{2\alpha}$		21.9 ± 4.8	10.3 ± 1.8*	9.41 ± 2.1*	5.62 ± 0.7*	-
$PGF_{1\alpha}$		20.9 ± 2.9	3.58 ± 0.4*	12.0 ± 1.7*	1.31 ± 0.2*	-
$PGF_{2\alpha}$		20.8 ± 2.1	39.5 ± 3.4*	8.66 ± 0.7*	57.8 ± 5.4*	7.16 ± 0.9*
PGE_2		159 ± 35.7	88.6 ± 17.4	84.9 ± 12.2	19.8 ± 2.4*	6.02 ± 0.8*
11-d-TXB_2		7.68 ± 1.7	9.16 ± 1.6	9.43 ± 2.1	1.55 ± 0.3*	1.43 ± 0.2*
PGD_2		479 ± 147	569 ± 53	171 ± 36*	522 ± 53.9	28.4 ± 4.04*
PGA_2		18.4 ± 4.6	2.37 ± 0.9*	2.94 ± 0.7*	-	-
PGJ_2		22.7 ± 4.5	31.7 ± 4.2	8.02 ± 1.8*	18.0 ± 2.2	1.13 ± 0.1*
15-d-PGD_2		62.2 ± 0.8	25.6 ± 5.1*	16.9 ± 2.9*	16.7 ± 1.4*	2.10 ± 0.4*
15-d-PGJ_2		44.8 ± 6.6	55.7 ± 7.3	49.5 ± 8.1	10.7 ± 1.4*	3.22 ± 0.7*

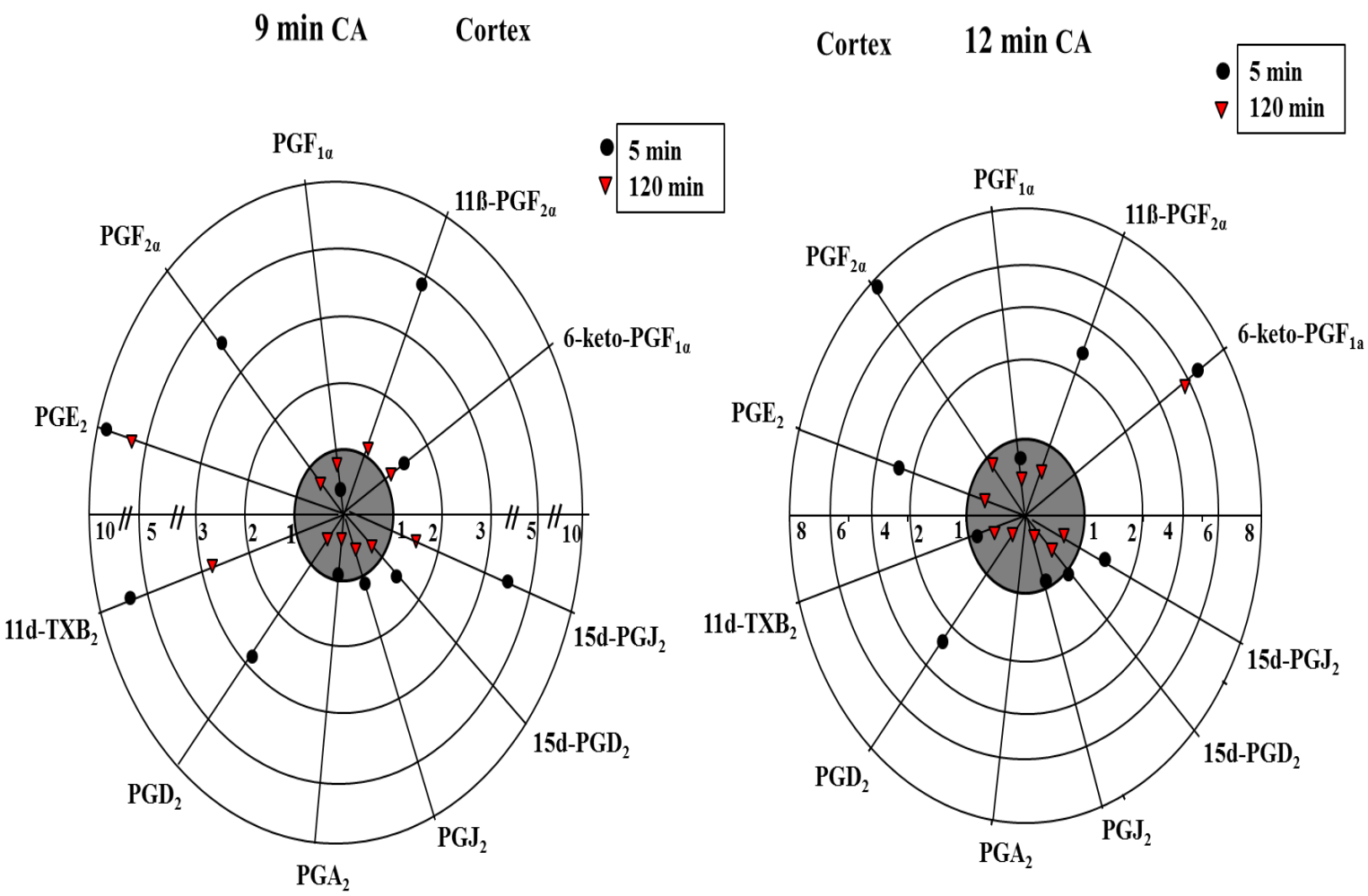

Figure 5-4 Polar plot representing changes in prostanoid levels of cortex normalized to sham at 5 and 120 min after ROSC in 9 and 12 min CA models. Significant changes were observed in the cortical levels of prostanoids at 5 min after ROSC in both 9 and 12 min CA groups. At 120 min majority of the prostanoids returned to sham or below sham levels in both groups.

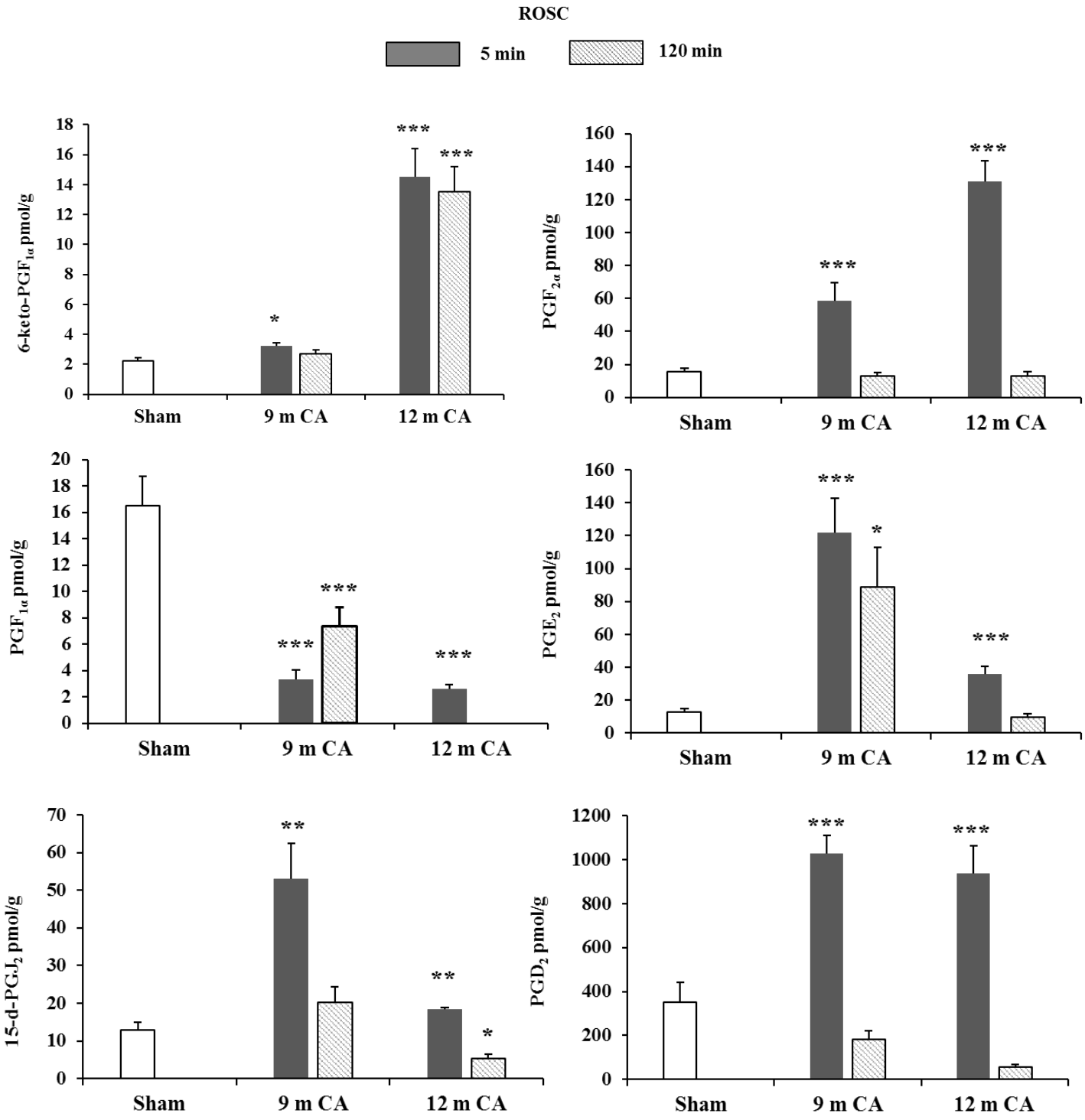

Figure 5-5 Significant changes in the prostanoids levels in the cortex at 5 and 120 min after ROSC in 9 and 12 min CA models. At 5 min ROSC 6-keto-$PGF_{1\alpha}$, and $PGF_{2\alpha}$ significantly increased in 12 min CA group whereas PGE_2, and 15-d-PGJ_2 levels decreased significantly. At 120 min majority of prostanoids decreased significantly in 12 min CA group except 6-keto-$PGF_{1\alpha}$.

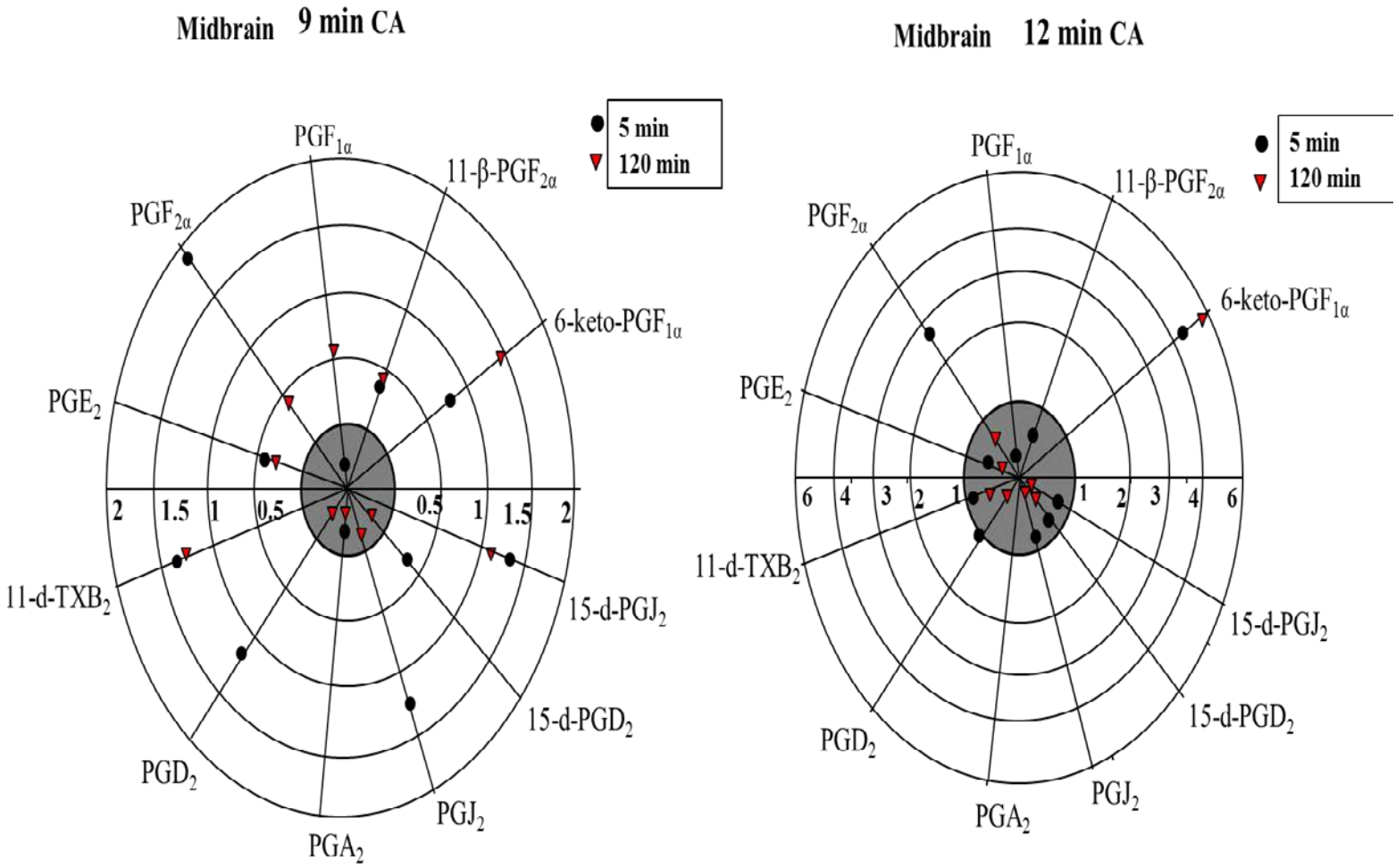

Figure 5-6 Polar plot representing changes in prostanoid levels in midbrain normalized to sham at 5 and 120 min after ROSC in 9 and 12 min CA models. Significant changes were observed in the levels of prostanoids in midbrain at 5 min after ROSC in 9 min CA group. At 120 min majority of the prostanoids returned to sham or below sham levels in both groups.

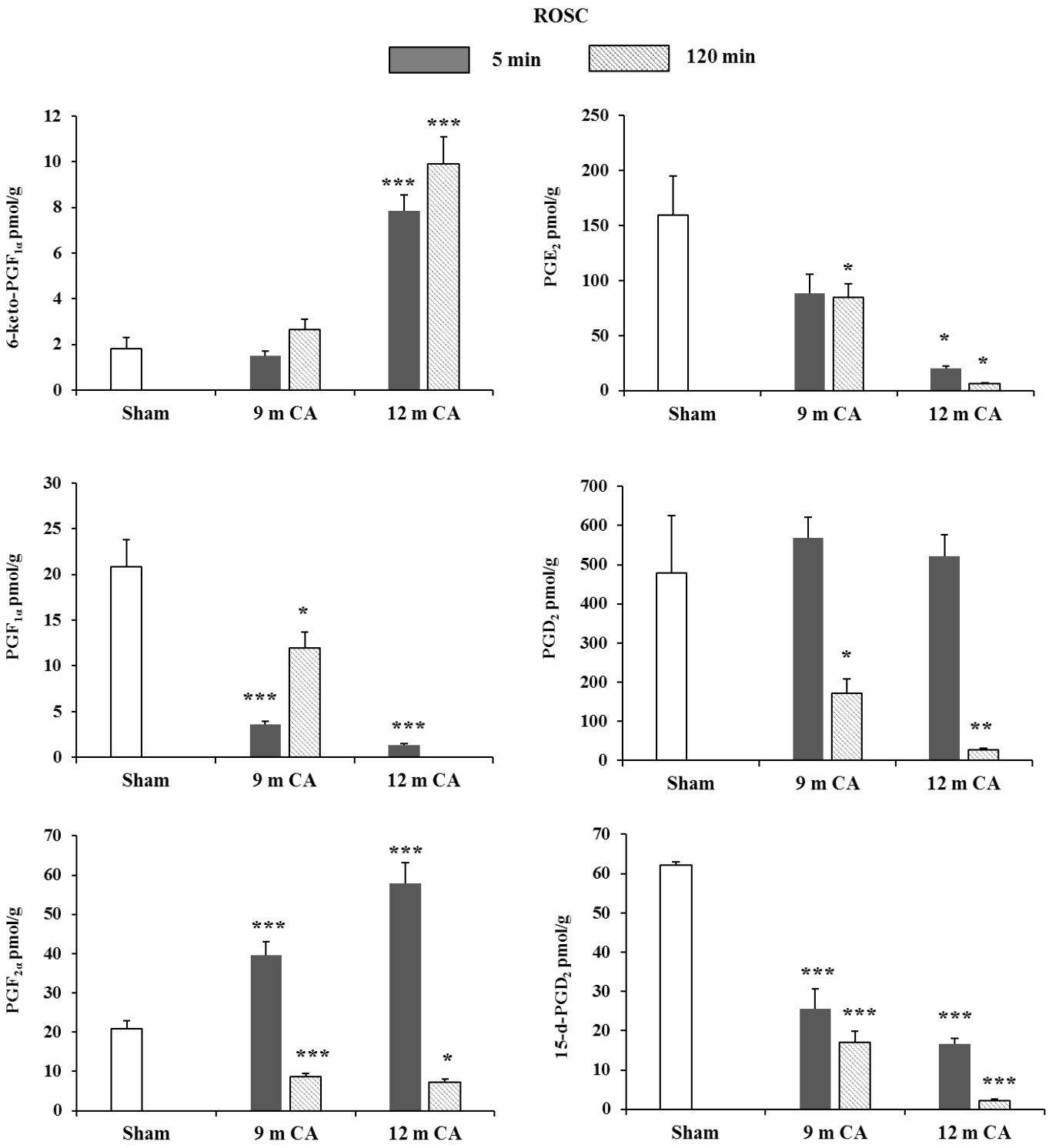

Figure 5-7 Significant changes in the prostanoids levels in the midbrain at 5 and 120 min after ROSC in 9 and 12 min CA models. At 5 min ROSC 6-keto-$PGF_{1\alpha}$, and $PGF_{2\alpha}$ significantly increased in 12 min CA group whereas PGE_2, $PGF_{1\alpha}$, and 15-d-PGD_2 levels decreased significantly. At 120 min majority of prostanoids decreased significantly in 12 min CA group except 6-keto-$PGF_{1\alpha}$.

5.3.4 Effect of CA duration on the CYP eicosanoid levels in the cortex after ROSC in pediatric asphyxial cardiac arrest

CYP eicosanoid levels in the cortex and midbrain at 5 and 120 min after ROSC were evaluated in both 9 and 12 min CA models. In 9 min CA model, 5 min after ROSC significant increases in the levels (pmol/g tissue) of 20-HETE (6.79±1.4 vs 3.78±0.4; *p<0.05), 8,9-EET (39.3±9.3 vs 2.66±0.34; *p<0.01), 14,15-EET (44.6±13.3 vs 7.43±2.8; *p<0.01) and the corresponding DHET metabolites 8,9-DHET (1.31±0.2 vs 0.86±0.1; *p<0.05), 14,15-DHET (4.17±0.7 vs 1.41±0.2; *p<0.001) were observed in cortex as compared to sham rats (**Table 5-4**). However fold changes in the levels of 8,9-EET and 14,15-EET with respect to sham were higher than that of 20-HETE. At 120 min after ROSC, 20-HETE levels decreased whereas 15-HETE levels (291±51 vs 173±27; *p<0.05) significantly increased in cortex as compared to sham rats. Though 8,9-EET and 14,15-EET levels decreased at 120 min they were still higher than sham but were not statistically significant. In 12 min CA model, during the early reperfusion at 5 min, significant increases in cortex were only observed in the levels of 20-HETE (12.8±2.8 vs 3.78±0.41; *p<0.01), and 14,15-DHET (3.39±0.73 vs 1.41±0.2; *p<0.05) as compared to sham rats. However, fold change in 20-HETE levels relative to sham in the early phase of reperfusion was higher in 12 min CA as compared to 9 min CA. At 120 min, there were no significant increases in the levels of any metabolites. Fold changes in the levels of all CYP eicosanoids in the cortex with respect to sham at 5 and 120 min after ROSC in 9 and 12 min CA was depicted in a polar plot (**Figure 5-8**). Each spike represents a CYP eicosanoid, and the radius of the circle represents fold changes normalized to sham. CYP eicosanoids with significant changes compared to sham were separately shown in **Figure 5-9**.

5.3.5 Effect of CA duration on the CYP eicosanoid levels in the midbrain after ROSC in pediatric asphyxial cardiac arrest

Similarly, in 9 min CA no significant increases in 20-HETE levels were observed at 5 min after ROSC in the midbrain but an increase in 8,9-EET (80.3±21.1 vs 2.31±0.5; *p<0.01), 14,15-EET (46.5±12.8 vs 14.6±6.0; *p<0.05), and 8,9-DHET (4.14±0.9 vs 1.59±0.3; *p<0.05) were observed as compared to sham rats (**Table 5-5**). At 120 min, only 15-HETE (375±44 vs 154±14; *p<0.05) levels significantly increased in the midbrain. No significant changes in the levels of any metabolites were observed in midbrain in 12 min CA. Fold changes in the levels of all CYP eicosanoids in the midbrain with respect to sham at 5 and 120 min after ROSC in 9 and 12 min CA was depicted in a polar plot (**Figure 5-10**). Each spike represents a CYP eicosanoid, and the radius of the circle represents fold changes normalized to sham. CYP eicosanoids with significant changes compared to sham were separately shown in **Figure 5-11**.

Table 5-4 Effect of CA duration on temporal profile of CYP eicosanoid levels (pmol/g tissue) in brain cortex after ROSC

Analyte	CA	Sham	9 min		12 min	
	ROSC(min)		5	120	5	120
20-HETE		3.78 ± 0.4	6.79 ± 1.4*	4.14 ± 0.5	12.8 ± 2.8*	5.35 ± 0.6
15-HETE		173 ± 27.2	143 ± 19.2	291 ± 51.1*	211 ± 31.5	171 ± 61.6
12-HETE		1649 ± 366	793 ± 61	1379 ± 191	1732 ± 275	1453 ± 478
8,9-EET		2.66 ± 0.3	39.3 ± 9.3*	15.9 ± 6.6	2.74 ± 0.3	2.81 ± 0.6
11,12-EET		11.8 ± 4.3	20.9 ± 5.2	13.9 ± 4.9	3.79 ± 0.3	5.18 ± 0.8
14,15-EET		7.43 ± 2.8	44.6 ± 13.3*	17.8 ± 6.7	5.78 ± 1.6	3.86 ± 0.6
5,6-DHET		0.63 ± 0.05	1.10 ± 0.1	0.82 ± 0.1	0.84 ± 0.2	0.91 ± 0.2
8,9-DHET		0.86 ± 0.1	1.31 ± 0.2*	0.95 ± 0.1	1.03 ± 0.1	0.81 ± 0.1

11,12-DHET	1.29 ± 0.2	2.23 ± 0.6	1.18 ± 0.2	1.90 ± 0.1	1.34 ± 0.4
14,15-DHET	1.41 ± 0.3	4.17 ± 0.7*	1.36 ± 0.3	3.39 ± 0.7*	1.38 ± 0.3

Table 5-5 Effect of CA duration on temporal profile of CYP eicosanoid levels (pmol/g tissue) in the midbrain after ROSC

Analyte	**CA**	**Sham**	**9 min**		**12 min**	
	ROSC (min)		**5**	**120**	**5**	**120**
20-HETE		4.58 ± 0.8	6.34 ± 1.0	5.05 ± 0.6	7.75 ± 0.8	6.30 ± 1.2
15-HETE		154 ± 14	258 ± 39	375 ± 44*	144 ± 20	119 ± 35
12-HETE		1440 ± 170	974 ± 79	1263 ± 346	1207 ± 173	1141 ± 307
8,9-EET		2.31 ± 0.5	80.3 ± 21*	41.1 ± 7.93	3.27 ± 0.6	3.05 ± 0.4
11,12-EET		20.2 ± 7.7	51.4 ± 15.1	35.1 ± 6.6	4.48 ± 0.8	3.66 ± 0.9
14,15-EET		14.6 ± 6.0	46.5 ± 12.8*	33.4 ± 5.7	4.19 ± 0.7	2.53 ± 0.2
5,6-DHET		1.11 ± 0.1	1.88 ± 0.3	1.33 ± 0.2	1.32 ± 0.1	1.15 ± 0.13
8,9-DHET		1.59 ± 0.3	4.14 ± 0.9*	3.20 ± 0.5	1.18 ± 0.2	1.13 ± 0.04
11,12-DHET		1.89 ± 0.5	2.94 ± 0.6	4.07 ± 0.9	1.42 ± 0.2	1.32 ± 0.1
14,15-DHET		2.56 ± 0.3	2.40 ± 0.2	2.79 ± 0.5	2.32 ± 0.3	1.71 ± 0.5

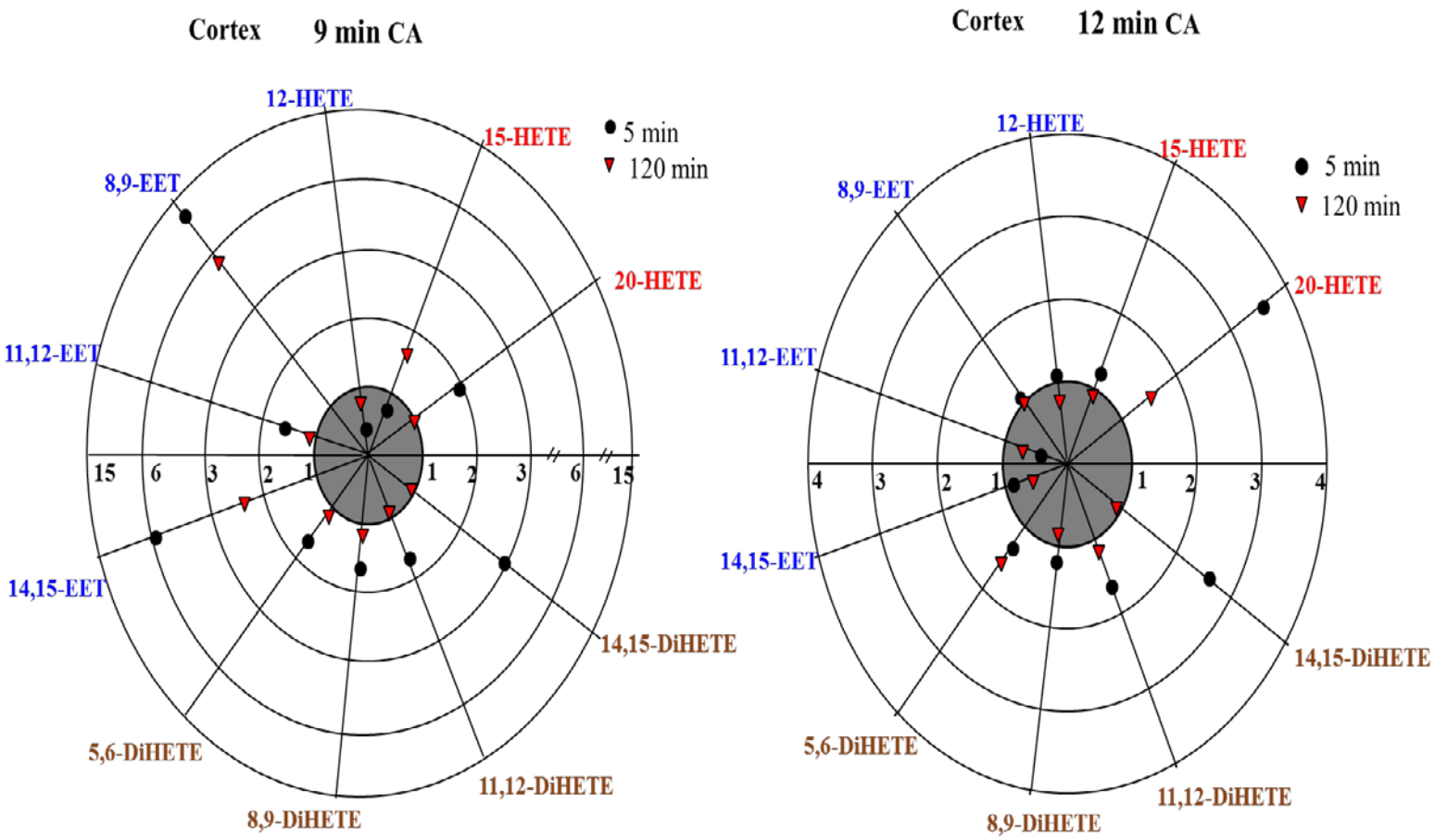

Figure 5-8 Polar plot representing changes in CYP eicosanoid levels of cortex normalized to sham at 5 and 120 min after ROSC in 9 and 12 min CA models. 8,9-EET and 14,15-EET levels were significantly elevated in 9 min CA at 5 min ROSC which decreased at 120 min. In 12 min CA group 20-HETE levels were significantly elevated compared to 9 min CA group and the levels were still above sham levels at 120 min ROSC.

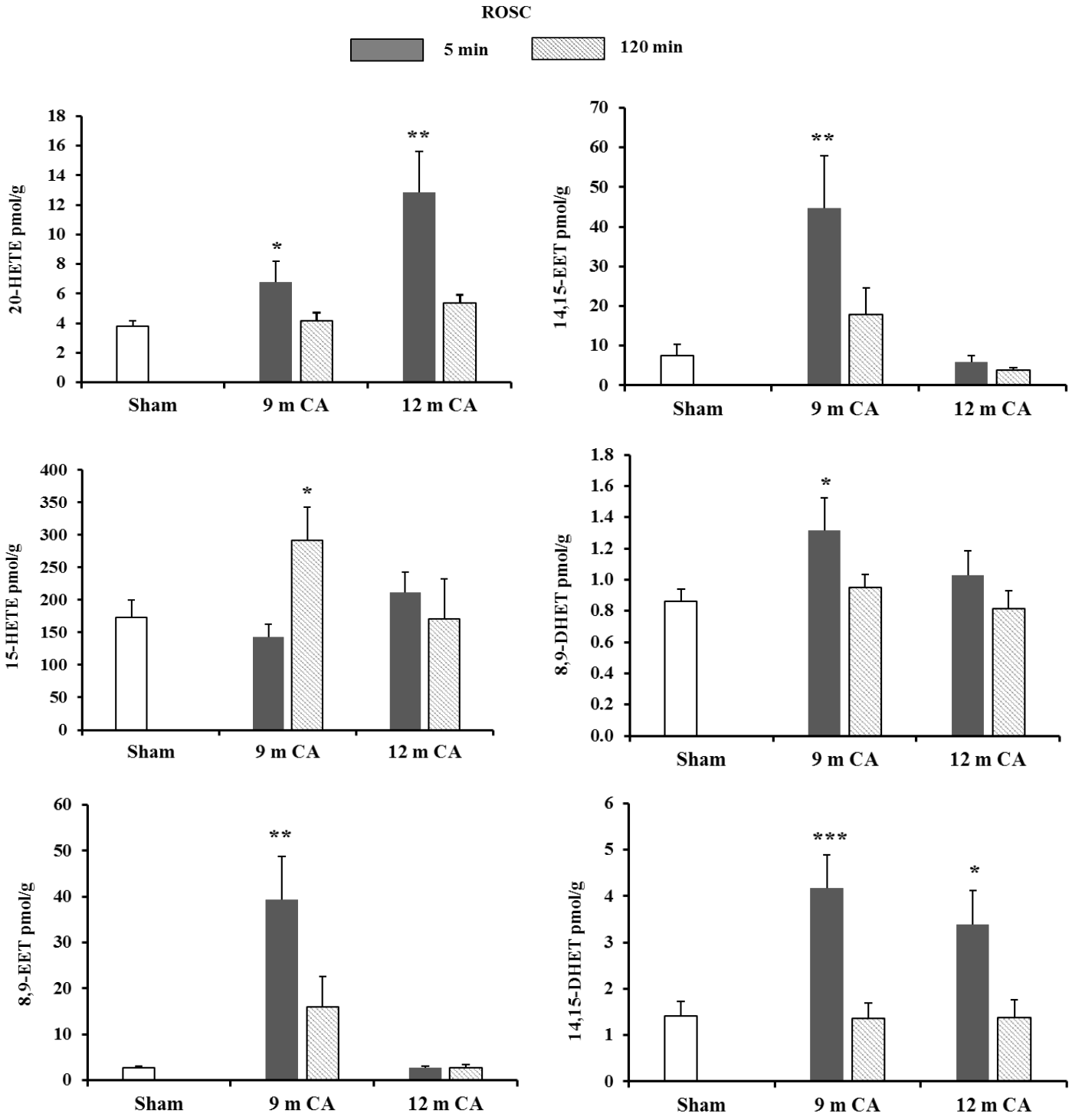

Figure 5-9 Significant changes in the CYP eicosanoids levels in the cortex at 5 and 120 min after ROSC in 9 and 12 min CA models. At 5 min ROSC 20-HETE levels significantly elevated in 12 m CA as compared to 9 min whereas 8,9-EET and 14,15-EET were significantly elevated in 9 m CA group. At 120 min ROSC EET levels significantly decreased in 12 min group whereas 20-HETE levels were above sham.

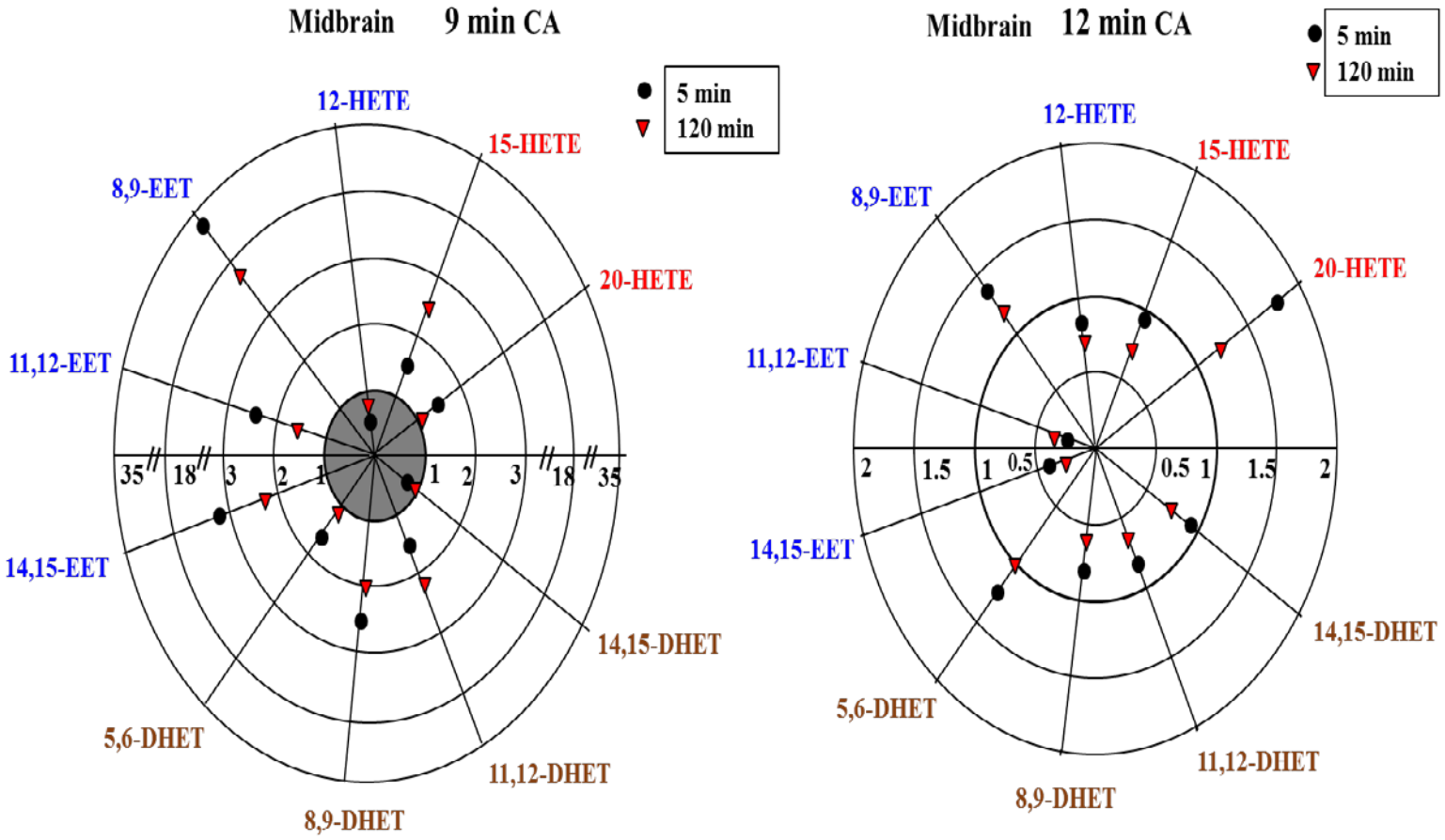

Figure 5-10 Polar plot representing changes in CYP eicosanoid levels of midbrain normalized to sham at 5 and 120 min after ROSC in 9 and 12 min CA models. EETs and DHETs were significantly elevated at 5 min ROSC in 9 min CA group which decreased significantly in 12 min CA. 20-HETE levels were significantly elevated in 12 min CA group at 5 min ROSC. At 120 min ROSC, EET levels returned to normal in 12 min CA group whereas they were above sham levels in 9 min CA group.

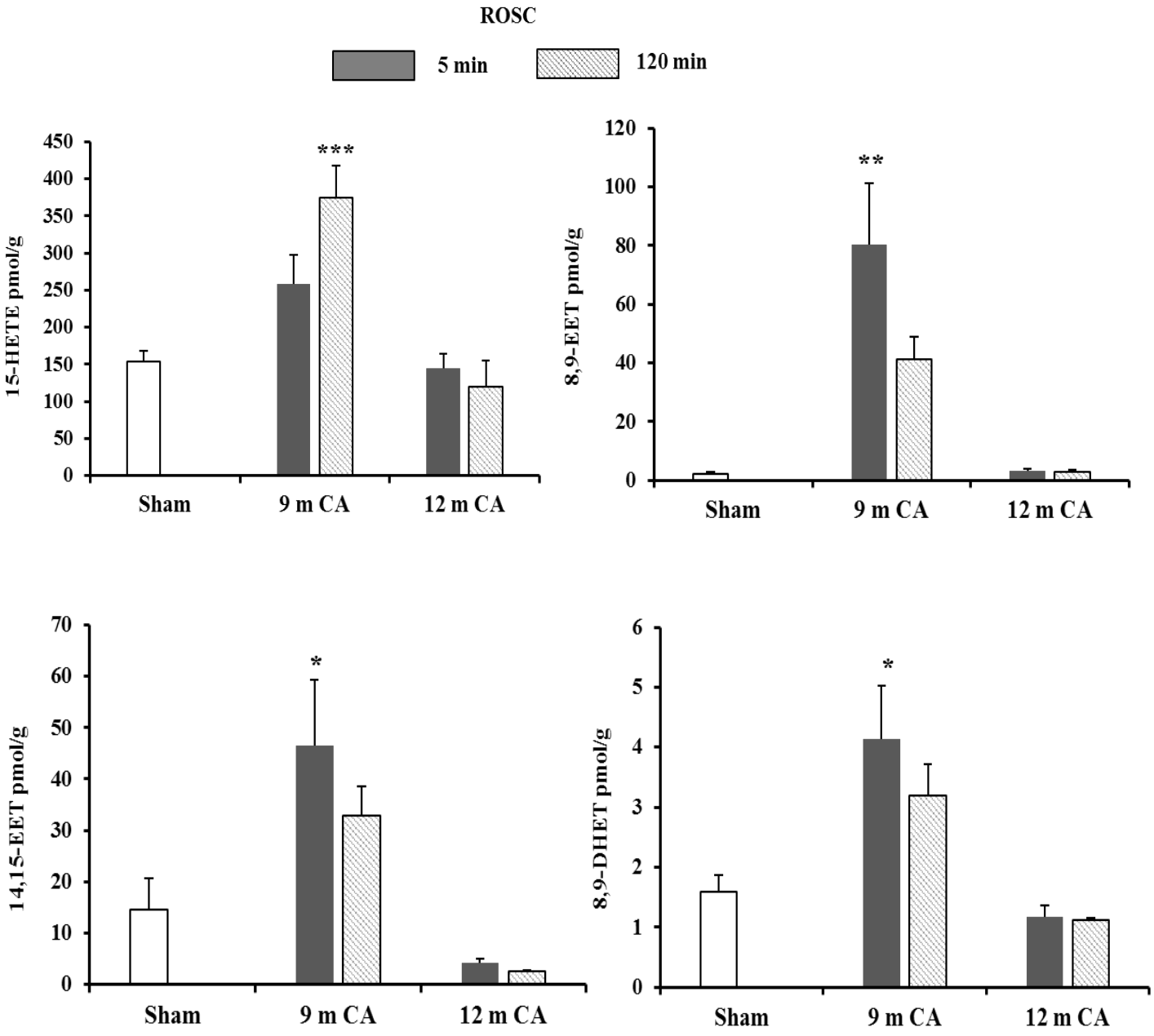

Figure 5-11 Significant changes in the CYP eicosanoids levels in the midbrain at 5 and 120 min after ROSC in 9 and 12 min CA models. At 5 min ROSC 8,9-EET, 14,15-EET, and 8,9-DHET levels were significantly elevated in 9 min CA group and decreased significantly in 12 min CA group. At 120 min ROSC, EET and DHET levels were above sham levels in 9 min CA group whereas they decreased to sham levels in 12 min CA group.

5.3.6 Effect of HET0016 treatment on cerebral blood flow in cortex after ROSC in pediatric asphyxial cardiac arrest

The effect of acute HET0016 treatment on CBF at 5, 10, 30, and 60 min after ROSC in a 12 min CA was evaluated and compared against vehicle. Cortical CBF in vehicle treated rats rapidly declined to 77.8 ± 4.2% of baseline at 5 min post resuscitation and continued to decline sharply till 30 min to 56.1 ± 2.5 % of baseline and sustained from there onwards till 60 min (**Figure 5-12**). A significant increase in the cortical CBF was observed at 5 min and 10 min after resuscitation from 12 min CA in HET0016 as compared to vehicle treated rats (% CBF at 5 min: 101 ± 12.5% vs 77.8 ± 4.2%; at 10 min: 91.6 ± 14.2% vs 69.5 ± 4.6%; *p<0.05) rats.

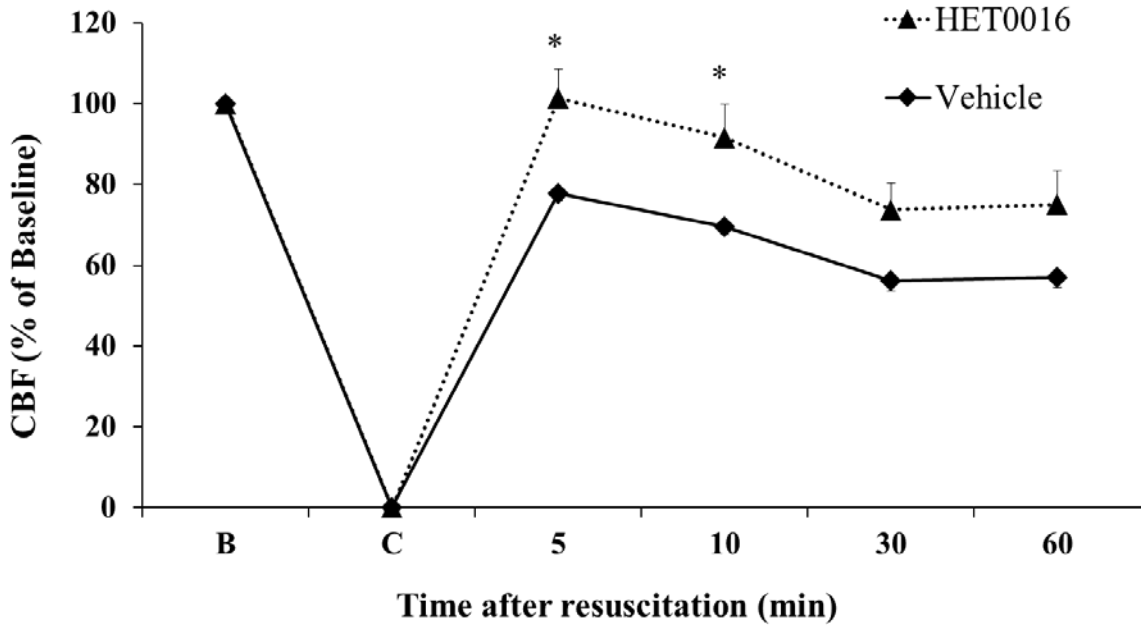

Figure 5-12 Effect of HET0016 treatment on cortical blood flow after ROSC in 12 min CA. Acute HET0016 administration significantly increased CBF at 5 and 10 min post resuscitation as compared to vehicle treated group.

5.3.7 Effect of HET0016 treatment on CYP eicosanoid and prostanoid levels in cortex and midbrain after ROSC in pediatric asphyxial cardiac arrest

The effect of acute dosing of HET0016 at the time of resuscitation on the levels of CYP eicosanoids and prostanoids in cortex and midbrain was evaluated at 5 min after ROSC in a 12 min CA model. HET0016 treatment significantly reduced 20-HETE levels (1.99 ± 0.20 vs 8.06 ± 1.33 pmol/g tissue; *$p<0.001$) in cortex and midbrain (3.18 ± 0.22 vs 6.44 ± 0.89 pmol/g tissue; *$p<0.05$) but did not change the levels of other eicosanoid metabolites as compared to vehicle treated group (**Table 5-6**). Fold changes in the levels of all CYP eicosanoids after HET0016 treatment in the cortex with respect to sham at 5 min after ROSC in 12 min CA was depicted in a polar plot (**Figure 5-13**). HET0016 treatment did not change the levels of the prostanoids in the cortex and midbrain as compared to vehicle treated group (**Table 5-7)**. A summary of the physiological variables (mean arterial pressure, $paCO_2$, pO_2 and pH) at baseline and post resuscitation in rats treated with either vehicle or HET0016 is presented in **Table 5-8**. Treatment of HET0016 itself did not significantly change the physiological variables when compared to vehicle group at each time point after resuscitation.

Table 5-6 Effect of HET0016 treatment on the levels of CYP eicosanoids (pmol/g tissue) in the cortex and the midbrain at 5 min after ROSC in 12 min CA model

Analyte	CA (12 min)			
	Cortex		Midbrain	
	Vehicle	HET0016	Vehicle	HET0016
20-HETE	8.06 ± 1.3	1.99 ± 0.2*	6.44 ± 0.9	3.18 ± 0.2*
15-HETE	473 ± 118	352 ± 42	495 ± 125	336 ± 78
12-HETE	3698 ± 725	2953 ± 251	3932 ± 965	2753 ± 539
8,9-EET	6.24 ± 1.0	5.66 ± 1.0	5.62 ± 0.7	6.82 ± 0.8
11,12-EET	4.32 ± 0.6	4.39 ± 0.4	3.56 ± 0.4	4.70 ± 0.6
14,15-EET	6.93 ± 0.9	6.55 ± 0.7	5.65 ± 0.8	6.64 ± 0.5
5,6-DHET	0.64 ± 0.1	0.67 ± 0.1	0.98 ± 0.1	0.93 ± 0.1
8,9-DHET	1.89 ± 0.2	2.00 ± 0.3	2.56 ± 0.3	2.08 ± 0.4
11,12-DHET	1.82 ± 0.1	1.54 ± 0.1	2.09 ± 0.2	2.00 ± 0.2
14,15-DHET	2.88 ± 0.4	2.15 ± 0.2	3.09 ± 0.2	2.29 ± 0.1

Table 5-7 Effect of HET0016 treatment on the levels of prostanoids (pmol/g tissue) in the cortex and the midbrain at 5 min after ROSC in 12 min CA model

Analyte	CA (12 min)			
	Cortex		Midbrain	
	Vehicle	HET0016	Vehicle	HET0016
6-Keto-$PGF_{1\alpha}$	11.5 ± 0.9	11.9 ± 1.3	7.78 ± 0.7	7.32 ± 1.1
11β-$PGF_{2\alpha}$	11.2 ± 1.2	12.4 ± 1.9	11.4 ± 1.1	9.75 ± 1.3
$PGF_{1\alpha}$	1.88 ± 0.3	1.7 ± 0.3	1.92 ± 0.2	1.51 ± 0.2
$PGF_{2\alpha}$	113 ± 10	116 ± 12	79.2 ± 7.9	71.1 ± 7.6
PGE_2	20.7 ± 2.6	19.1 ± 2.6	12.1 ± 0.7	11.2 ± 1.5

11-d-TXB_2	0.50 ± 0.1	0.42 ± 0.1	0.93 ± 0.2	0.71 ± 0.1
PGD_2	820 ± 81	834 ± 88	661 ± 53	630 ± 51
PGA_2	0.73 ± 0.1	0.82 ± 0.1	1.16 ± 0.3	1.22 ± 0.1
PGJ_2	27.8 ± 5.2	20.49 ± 3.6	17.8 ± 2.3	20.2 ± 5.3
15-d-PGD_2	20.1 ± 2.1	14.2 ± 1.4	18.3 ± 1.6	15.0 ± 1.8

Table 5-8 Physiological variables after treatment with either vehicle or HET0016 12 min CA model

	Baseline	**10 min**	**30 min**	**60 min**
MAP				
Vehicle	72.2 ± 4.7	84.7 ± 4.8	57.5 ± 3.7*	69.2 ± 5.2
HET0016	71.0 ± 4.2	79.0 ± 4.8	50.0 ± 2.2*	58.3 ± 2.5
$PaCO_2$				
Vehicle	33.9 ± 1.7	31.5 ± 4.3	30.03 ± 1.9	36.4 ± 1.9
HET0016	32.5 ± 0.8	28.6 ± 1.8	29.7 ± 1.9	41.9 ± 2.1*
PaO_2				
Vehicle	209 ± 12	432 ± 19*	443 ± 11*	378 ± 53*
HET0016	224 ± 1.9	423 ± 12*	402 ± 25*	414 ±20*
pH				
Vehicle	7.42 ± 0.01	7.29 ± 0.05*	7.46 ± 0.01	7.46 ± 0.03
HET0016	7.43 ± 0.01	7.31 ± 0.02*	7.41 ± 0.03	7.40 ± 0.03

MAP, Mean arterial pressure

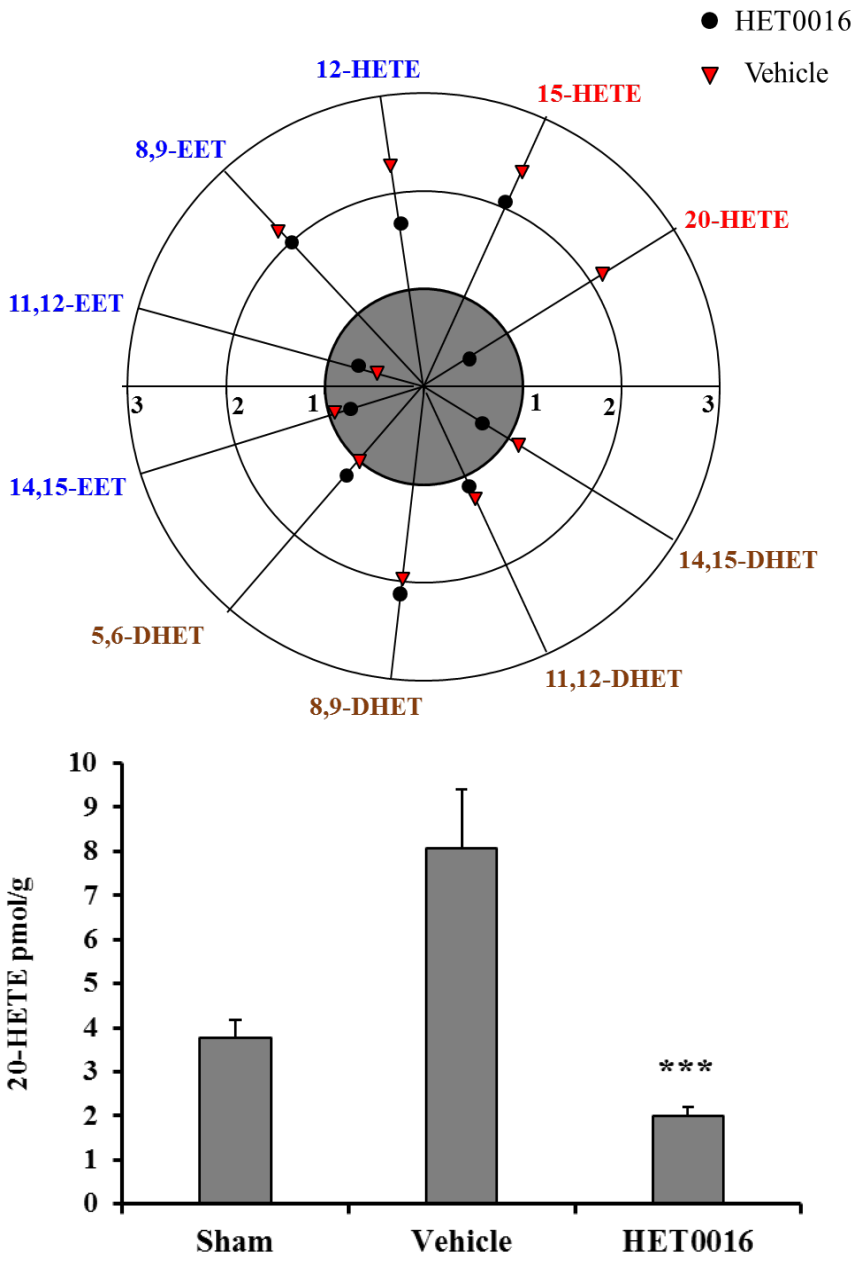

Figure 5-13 Polar plot representing changes in CYP eicosanoid levels in the cortex normalized to sham at 5 min after ROSC in 12 min CA model. Significant changes in the CYP eicosanoids levels are shown in separate plot (bottom panel). HET0016 administration significantly reduced cortical 20-HETE levels at 5 min after ROSC as compared to vehicle treated group in a 12 min CA model.

5.3.8 Effect of HET0016 treatment on neurological deficit after asphyxial cardiac arrest

The effect of acute HET0016 treatment on short-term neurologic deficits were evaluated at 3, 24, and 48 h after resuscitation from 12 min CA and compared against vehicle and sham groups. There was a time and treatment effect on the neurological outcome in vehicle and HET0016 treatment groups. At 3 h after ROSC there was moderate to severe neurological damage in rats receiving vehicle, which was significantly reduced by HET0016 treatment (52.2 ± 4.8% vs 37.5 ± 9.9%; **p<0.01). Rats in both treatment groups showed recovery from neurological damage over time. At 24 h vehicle treated rats showed mild neurological damage as compared to HET0016 group, which was significantly reduced by HET0016 (10.4 ± 4.9% vs 2.8 ± 0.8; **p<0.001). At 48 h vehicle treated rats still exhibited residual neurological damage whereas HET0016 treated rats did not show any signs of neurological damage indicating full recovery (**Figure 5-14**). Rats receiving sham surgery showed no signs of any neurological damage except very little at 3 h

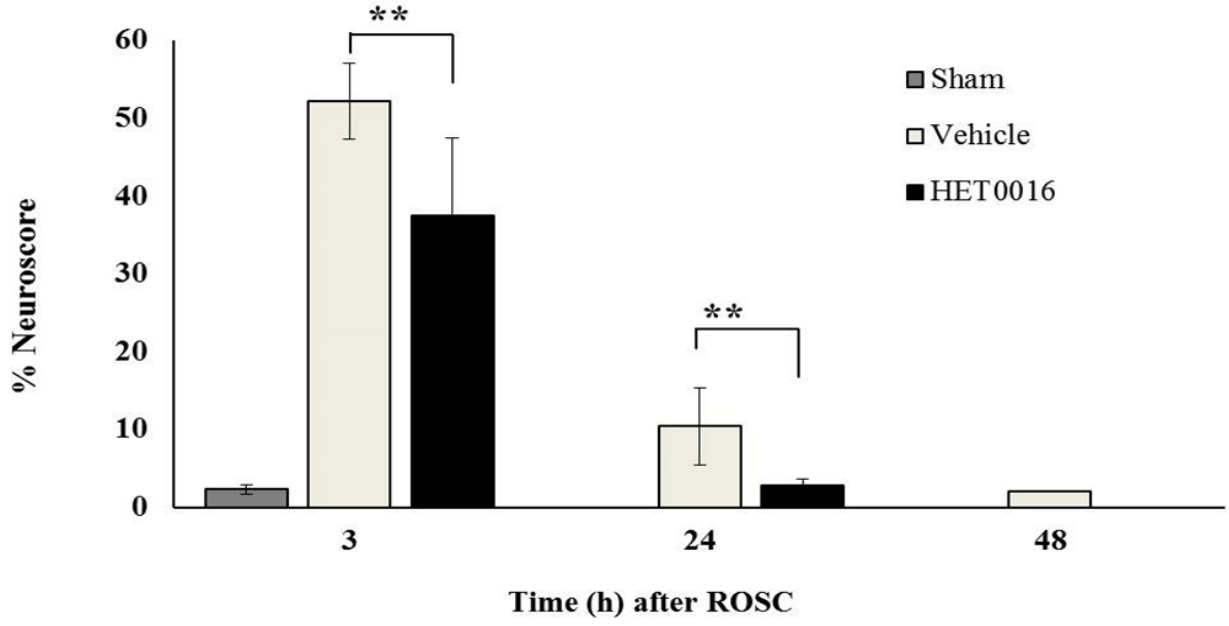

Figure 5-14 Effect of HET0016 treatment on short-term neurologic deficit after 12 min CA. HET0016 administration significantly decreased neurological deficit at 3 and 24 h after reperfusion as compared to vehicle treated group in a 12 min CA model.

5.3.9 Effect of HET0016 on neuronal death after asphyxial cardiac arrest

The effect of HET0016 treatment on neuronal survival at 48 h after ROSC from 12 min CA was evaluated by FluoroJade-B and H&E staining. The 12 min CA induced significant neuronal death in vehicle treated rats as compared to sham operated rats (average no.of FluoroJade +ve cells: 41.4±9.6 vs 4.6±2.0; ***$p<0.001$), which was significantly reduced by HET0016 treatment (22.8±6.9; **$p<0.01$). Similarly, H&E staining also revealed significant neuronal death in vehicle treated rats compared to sham (average no.of H&E +ve cells: 45.2±9.8 vs 5.0±1.8; ***$p<0.001$), which was significantly reduced by HET0016 treatment (24.8±7.2). (**Figure 5-15**). Representative sections of brain from vehicle and HET0016 treated rats photographed under microscope with FluoroJade-B (green) and H&E staining (purple red) were also depicted (**Figure 5-15**).

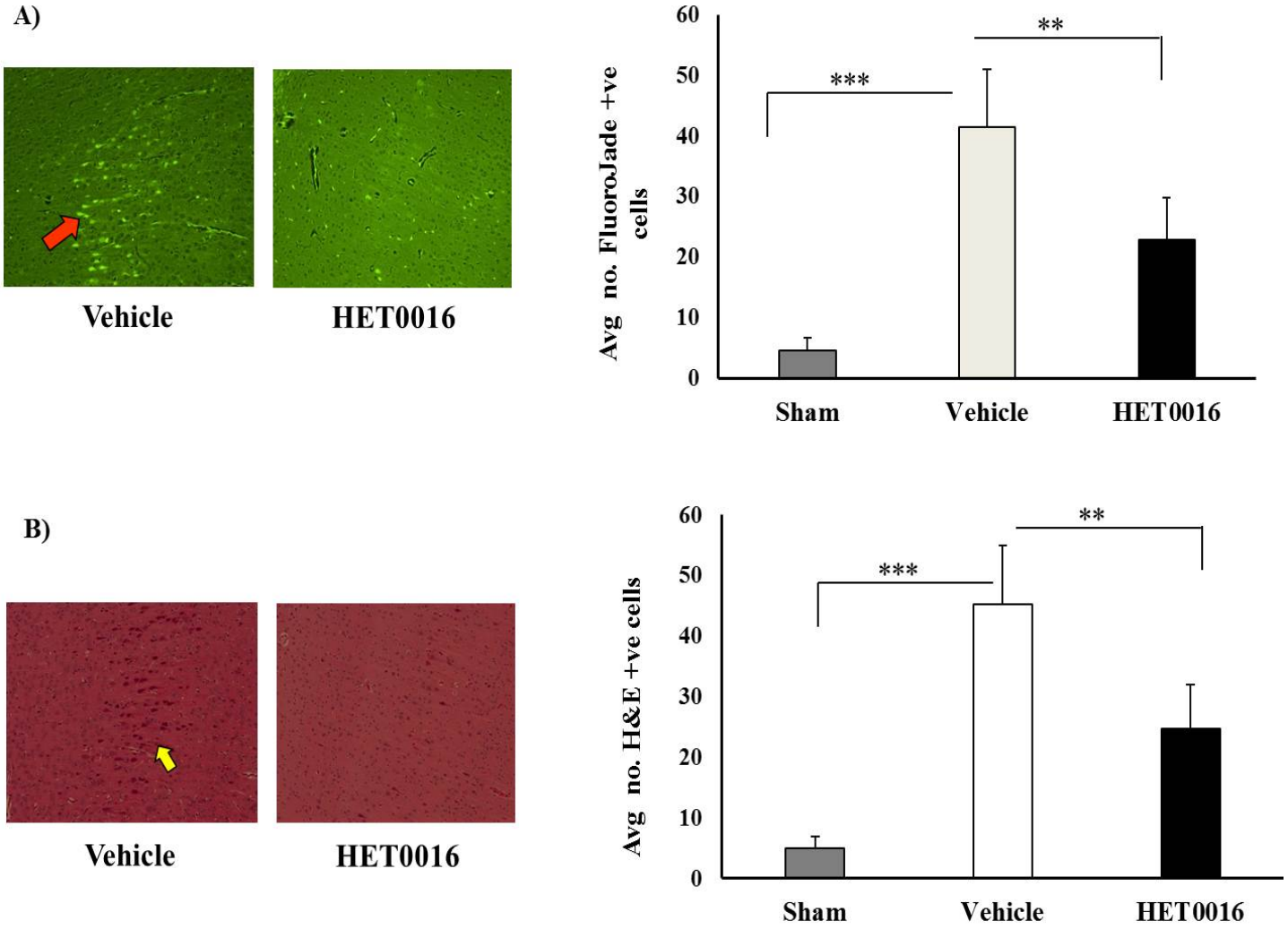

Figure 5-15 Effect of HET0016 treatment on neuronal death at 48 h after ROSC in a 12 min CA model. Top panel (A) shows degenerating neurons stained positively by Fluorojade-B and bottom panel (B) shows cells stained with H&E. Acute administration of HET0016 significantly decreased degenerating neuronal population as measured at the end of 48 h after reperfusion from 12 min CA when compared to vehicle treated group.

5.4 DISCUSSION

The major findings of this study are i) reduction in the cortical CBF post resuscitation from cardiac arrest during both early and late reperfusion period increases significantly with the duration of the cardiac arrest, ii) significant changes in the levels of vasoconstrictive and vasodilatory prostanoids and CYP eicosanoids occurred in the early reperfusion period after 9 and 12 min CA, iii) acute administration of HET0016 significantly increased cortical CBF in the early reperfusion period after 12 min CA by significantly decreasing 20-HETE levels in the cortex, iv) administration of HET0016 significantly decreased neuronal death and increased short-term functional outcome following resuscitation from a 12 min CA. Collectively, these data suggest that CBF dysregulation in the cortex after resuscitation is dependent on the duration of ischemic injury and is related to the imbalance in the levels of vasoactive AA metabolites in cortex and that the acute administration of 20-HETE synthesis inhibitor, HET0016 improves short-term functional outcome by significantly increasing CBF.

In previously reported experimental studies of CA, various techniques such as microspheres, Laser Doppler Flow (LDF) technology (Brown et al., 1986; Nozari et al., 1999; Nozari et al., 2000), Xenon-washout (Cohan, et al., 1989), MRI (Manole, et al., 2009; Xu, et al., 2002b), and PET imaging (Heiss et al., 1998; Mortberg et al., 2007) were used to measure CBF before and after ROSC. LDF is not suitable to study inter-regional or global CBF, microspheres have disadvantage of non-homogenous mixing in blood, MRI, and PET are expensive and time consuming. In this study we measured CBF by laser speckle photometry, which is relatively inexpensive, fast, and allows accurate measurements of regional blood flow in the cortex. Our findings of CBF measurement with this technique suggest that CBF dysregulation during

reperfusion after global ischemic injury is dependent on the duration of the injury itself. Specifically, we observed that longer duration of asphyxia leads to immediate or delayed hypoperfusion in the cortex without any hyperemia. Further, we observed prolonged exposure of decreased CBF beginning as early as 30 min after resuscitation from CA in both 9 and 12 min CA models with the latter exhibiting significant reduction in CBF in the low perfusion phase compared to the 9 min injury. Previous studies in experimental animal models investigating reperfusion patterns after CA produced variable results with regards to hyperemia in cortex. While some studies indicated the presence of early hyperemia in cortex after CA in adult rats (Liachenko, et al., 2001), and young pigs (Mortberg, et al., 2007) other studies indicated absence of hyperemia in new born pigs (Goplerud et al., 1989; Leffler et al., 1989). The pattern of CBF changes after CA in pediatric rats is consistent with previously published data reporting hyperemia in subcortical structures and hypoperfusion in the cortex (Manole, et al., 2009; Manole, et al., 2012). This observation of post-ischemic hypoperfusion is consistent with previous animal studies in adult rats (Bottiger et al., 1997; Liachenko et al., 1998), young pigs (Mortberg, et al., 2007), and dog (Shaffner, et al., 1998). Together, these findings suggest the presence of a delayed post-ischemic hypoperfusion in cortex that is dependent on the severity of ischemic injury.

Based on our findings from CBF analysis, we set out to investigate the vascular pathways of pathological CBF changes after resuscitation. Therefore, we quantified regional (cortex and midbrain), and temporal (5 and 120 min after ROSC) profile of prostanoids and CYP eicosanoids levels in the post-ischemic brain following CA. We have employed a lipidomics approach using our validated UPLC-MS/MS method to quantify a panel of various vasoactive AA metabolites. Our lipidomics analysis showed that both moderate and severe CA significantly increased the

concentrations of majority of prostanoids in the cortex at 5 min after reperfusion as compared to sham rats. However, concentrations in the midbrain were significantly lesser compared to sham rats at 5 min after reperfusion. In both regions, concentrations decreased at 120 min after reperfusion. However, 12 min CA has produced rapid decline in prostanoid levels than 9 min CA group at 120 min after reperfusion. The most abundant prostanoid in the cortex and midbrain of control rats in this study was PGD_2, which increased following ischemic injury. This is consistent with the previous findings reporting prostaglandin concentrations in the ischemic brain of rat and gerbil (Kempski et al., 1987; Narumiya et al., 1982). Also, the order of the abundance of prostanoid levels measured in control rats in this study is consistent with the recent data measuring prostanoids at different intervals in hippocampus and cortex of sham pediatric rats (Liu et al., 2013b). Together, these data shows that ischemia and reperfusion injury produces differential changes in prostanoid levels that are region, time dependent, and prostanoid-specific.

The effects of prostanoids on CBF regulation under normal and pathophysiological conditions are more complex to delineate as the net resultant effect depends not only on local concentrations but also on receptor subtype expression in the cerebral vasculature and the interaction with other vasoactive factors with overlapping signaling mechanisms. However, in this study changes in cortical blood flow during early and late reperfusion period after CA were correlated with ratio of cumulative vasoconstrictive (11β-$PGF_{2\alpha}$, $PGF_{1\alpha}$, $PGF_{2\alpha}$, 11-d-TXB_2, PGA_2) to vasodilatory (6-keto-$PGF_{1\alpha}$, PGE_2, PGD_2, PGJ_2, 15-d-PGD_2, 15-d-PGJ_2) prostanoids in the cortex. We found that moderate CA (9 min) favored a shift towards a net vasodilatory effect at 5 min after reperfusion although no hyperemia was observed whereas more severe CA (12 min) abolished such response in the cortex. This is consistent with our CBF findings observed at 5 min

after reperfusion where 12 min CA has significantly lower CBF than the 9 min CA group. This is further supported by steep increases in the vasodilatory PGD_2, PGE_2 prostanoids at 5 min after reperfusion in 9 min CA compared to 12 min CA. However, at 120 min after reperfusion there was a shift towards net vasoconstrictive effect, which was more pronounced in 12 min CA group as compared to 9 min CA. This is consistent with CBF response at 120 min, which is significantly lower in 12 min CA group. This is supported by rapid decline in the concentrations of prostanoids in 12 min CA than in 9 min. Though we did not measure blood flow in subcortical regions, our observation of prostanoid changes at 5 and 120 min in both 9 and 12 min CA groups are supportive of the findings of CBF in the thalamus as measured by ASL-MRI (Manole, et al., 2009). In this study Manole et al, reported hyperemia in the thalamus at 5 min after reperfusion and hypoperfusion at 120 min. Consistent with this findings, we found a decrease in the ratio of vasoconstrictor to vasodilatory prostanoids indicating a shift towards net vasodilatory effect at 5 min and an increase in the ratio at 120 min indicating a shift towards net vasoconstrictive effect. Together, these findings suggest that CBF dysregulation in the post-ischemic phase are in part related to the imbalances in the ratio of vasoactive prostanoids that are injury severity, and reperfusion time dependent.

Prostanoids exert diverse array of pharmacological actions sometimes functionally antagonizing depending on the membrane receptor they bind to and activate. For example, PGE_2 induces vasoconstriction through EP1 and EP3 receptors but induces vasodilation through EP2 and EP4 receptors. This explains the PGE_2 induced vasoconstriction and relaxation effects on MCA of adult baboon, adult cat basilar and MCA, and adult human pial and basilar arteries (Jadhav et al., 2004). (Thornhill et al., 1999). Further, vascular responses to PGE_2 seems to be age

dependent as the expression of EP receptor subtypes may vary. For example, in newborn pigs, PGE_2 dilates pial and intraparenchymal microvessels but in adults the same are constricted (Armstead et al., 1989; Li et al., 1994) whereas in premature and newborn baboons, PGE_2 relaxes MCA, but in adults the same are constricted (Hayashi et al., 1985). Thus, PGE_2 response seems to be preferential vasodilation in the new born, and a preferential vasoconstriction in adults. In our study, we found significant increases in the PGE_2 levels in the cortex of PND 17 rats following ischemic injury. It may be possible that PGE_2 in these rats exert vasodilatory effects preferentially but such conclusions need further investigations of receptor subtype expression in these rats under normal and ischemic conditions. Another surprising finding in our study was the levels of 6-keto-$PGF_{1\alpha}$, a stable metabolite of prostacyclin (PGI_2) in the cortex and midbrain of especially 12 min CA group where the levels were significantly higher at both 5 and 120 min post reperfusion. It would be expected that vasodilatory effects of prostacyclin dominate the net response but interestingly CBF in 12 min CA group at both 5 and 120 min are significantly lesser than 9 min CA group. One possible explanation suggested for this could be activation of IP and TP (thromboxane receptor) receptor by prostacyclin, which are functionally antagonistic. In a recent study, Liu et al described that COX-1 generated endothelial PGI_2 dilator activity mediated by IP receptors can be compromised by a concomitant TP receptor activation (Liu et al., 2012). It may be possible that high concentrations of prostacyclin as seen in the cortex and midbrain in our study, activate both IP and TP receptors thus diminishing the overall dilatory effect of prostacyclin. Further investigations are needed to thoroughly understand relative contributions of specific receptor subtypes of prostanoids and the net effect on the cerebral vasculature under physiological and pathophysiological conditions.

The findings from prostanoid analysis suggest that an imbalance in tissue levels of these vasoactive prostanoids may be associated with the observed hypoperfusion during the post-ischemic reperfusion phase. However, caution need to be exercised in extrapolating these findings to correct the CBF dysregulation using COX or specific prostanoid receptor inhibitors. Many different studies have evaluated the neuroprotective effects of COX or specific prostanoid receptor inhibitors in different ischemic models with contradictory findings on CBF enhancements. For example, prostacyclin infusion given at 2 h after reperfusion did not improve global CBF as measured by ^{133}Xe clearance during the delayed post-ischemic hypoperfusion in a cat global cerebral ischemia model (van den Kerckhoff et al., 1983). In another study, inhibition of thrombaxane synthase did not decrease the hypoperfusion in the post-ischemic brain after global ischemia. Interestingly, TXA_2 inhibition increased production of PGI_2 in post-ischemic cerebral blood vessels (Prough et al., 1986). These studies concluded that PGI_2 and TXA_2 may not play a significant role in hypoperfusion after global ischemia and that further increasing the physiological levels of PGI_2 may not dilate the cerebral vessels. In another study, Nishida et al reported that COX inhibitor diclofenac modulated fetal CBF response to hypoxia through systemic changes by decreasing MAP rather than affecting CVR and cerebral vascular tone (Nishida et al., 2006). However, administration of indomethacin along with the infusion of PGI_2 attenuated the post-ischemic hypoperfusion in a dog model of global ischemia (Hallenbeck et al., 1982). On the other hand, PGD_2 DP1 receptor knockout mice showed increased infarct size in a focal cerebral ischemia model however, no differences in CBF (measured by LDF) were observed during ischemia or 1 h post reperfusion between WT and $DP1^{-/-}$ mice. In yet another study, EP1 receptor knockout mice has significantly improved CBF *in vivo* after focal ischemia and increased neuronal survival in *in vitro* neuronal cultures (Saleem et al., 2007). Though we found association between imbalances in

vasoactive prostanoids, and CBF dysregulation in the post-ischemic brain cortex, together these findings suggest that prostanoids alone may not explain all of the observed phenotype of hypoperfusion in the cortex after CA. This is could likely be due to more prominent effects of prostanoids on larger cerebral arteries with minimal effects on the resistance vessels, and the total CVR. Vasoactive properties of prostanoids in general on cerebral vasculature was largely evaluated in large cerebral arteries such as MCA, basilar, and pial arteries of different species. However, their effects on resistance microvessels, total CVR, and changes in CBF during pathological conditions such as ischemia needs further investigation in order to fully elucidate the role of prostanoids in pathophysiological regulation of CBF.

We further quantified the CYP eicosanoids from the same tissue used for prostanoids measurement. Our lipidomics analysis showed that the vasoactive CYP eicosanoids are formed early after CA and returned to normal levels during the late reperfusion period in both 9 and 12 min CA. Specifically, we observed that during early reperfusion period there is prominent increases in vasodilatory EET metabolites and their breakdown products DHETs in the brain cortex of rats subjected to shorter duration of asphyxia and prominent increase in vasoconstrictive 20-HETE in longer duration of asphyxia. The ratio of 20-HETE and EETs indicated that in the early reperfusion period eicosanoid equilibrium is shifted towards a vasodilatory effect in shorter ischemic insult and towards a vasoconstrictive effect in longer ischemic insult. This is consistent with CBF observation in 12 min CA, which is significantly lower than in 9 min CA group. Interestingly, there was no hyperemia observed in the cortex with shorter asphyxial arrest even though EETs levels were elevated higher than that of 20-HETE. This could be due to the rapid degradation of EETs to DHETs as evident in 9 min CA group. In the midbrain, during the early

reperfusion period after 9 min CA there was massive increase in the levels of EETs in the absence of any changes in 20-HETE, favoring towards a significant vasodilatory effect. This is consistent with the findings of Manole et al., who reported hyperemia in the thalamus at 5 min after reperfusion as measured by ASL-MRI (Manole, et al., 2009). During late reperfusion period, concentrations of most of the metabolites in cortex and midbrain returned to at or below baseline levels irrespective of duration of asphyxia with the exception of 15-HETE, which was significantly elevated in the cortex and midbrain of rats subjected to 9 min CA. This could be likely due to either substrate or enzyme depletion, or further metabolism to other substances. Hypoperfusion in the cortex was seen in both 9 and 12 min CA with the effect being more pronounced in longer insult. This phenomenon is consistent with previously published data from different animal models (Bottiger, et al., 1997; Liachenko, et al., 1998; Mortberg, et al., 2007; Shaffner, et al., 1998). Together, these findings suggest that vasculature in the cerebral cortex may be especially vulnerable to impaired vascular patency in global ischemia and that no-reflow phenomenon can occur as a result of impaired vascular patency, which is in turn dependent on the duration of the global ischemia (Fischer, et al., 1995; Kagstrom et al., 1983b). It has been shown previously that cerebral cortex is more vulnerable to global ischemia (Geraghty et al., 2006; Martin, et al., 1997). In a study by Buunk et al, they reported high endothelin levels, decreasing nitrate levels, increasing cGMP levels in comatose patients resuscitated from cardiac arrest suggesting the presence of active cerebral vasoconstriction due to an imbalance in local vasoconstrictors and dilators (Buunk et al., 1996). In yet another study, CBF was improved by abolishing the abnormal vasoconstriction using endothelin type-A antagonist in a rat CA model (Krep et al., 2000; Krep et al., 2003). To our knowledge, there is no study published so far evaluating the impact of vasoconstrictors of microvasculature on the CBF changes during the reperfusion phase in a global ischemic brain

injury model. The preset findings of our study produce the first evidence of an imbalance in the levels of vasoconstrictive and vasodilatory CYP eicosanoids and their possible link to the delayed hypoperfusion in the cortex after global cerebral ischemia.

Our findings from CBF assessment and CYP eicosanoid levels measurement suggested a prominent role of vasoconstriction in the early and delayed hypoperfusion in a 12 min CA model. Thus, we set out to delineate the role of 20-HETE by using synthesis inhibitor HET0016 on CBF changes in a 12 min CA model. Our results showed that acute treatment of low dose HET0016 at the time of resuscitation significantly increased CBF in the cortex consistent with the significant reduction of 20-HETE levels during the early reperfusion period when compared to vehicle treatment. There was no change in the levels of other CYP eicosanoids and prostanoids due to HET0016 treatment as compared to vehicle indicating the specificity of the inhibition at the given dose. Further, HET0016 treatment did not significantly change physiological variables such as MAP, $paCO_2$, pO_2, and pH at any time after resuscitation when compared to vehicle treated group. Our findings of HET0016 effect on CBF is similar to our previous data showing significant reduction in the attenuation of CBF in post-ischemic hypoperfusion phase in a rat focal ischemia model (Poloyac, et al., 2006) but contradictory to the data by Yang et. al, (Yang, et al., 2012) who reported no significant changes in CBF measured by LDF in a neonatal piglet hypoxia-ischemia model. This could be due to different reasons such as i) different animal model, ii) difference in the CBF measurement technique, iii) different time of administration of HET0016 (during resuscitation versus 5 min after resuscitation), and v) different doses of HET0016 (0.9 mg/kg vs 10 mg/kg). In our study we observed significant elevation of 20-HETE at 5 min after resuscitation and corresponding significant decreasing in CBF, thus we chose to administer HET0016 during resuscitation. Further, higher dose of HET0016 may produce concentrations in brain beyond its

selectivity index for CYP4A/4F enzymes, inhibiting CYP2C/2J enzymes that form vasodilatory EETs. Thus, we acutely administered a lower dose of HET0016 in our pediatric rat asphyxial CA model. Together, these findings suggest that HET0016 significantly improves cortical CBF during early reperfusion phase after 12 min CA by significantly reducing 20-HETE levels in the cortex.

The findings of HET0016 treatment on cortical CBF and eicosanoid levels in the cortex led us to investigate the impact of HET0016 on neuronal survival and short-term functional outcome. Our data indicated that the 12 min CA produced moderate to severe neurological damage during early reperfusion phase, which was significantly reduced by HET0016. Rats showed recovery from damage over time, however, HET0016 showed full recovery by 48 h after reperfusion whereas vehicle treated rats still exhibited residual neurological damage as assessed by functional outcome experiments. Further, staining of brain sections collected at 48 h from reperfusion by FluoroJade-B for degenerating neurons (green) indicated that our injury model produced moderate neuronal death, which was significantly reduced by HET0016 treatment. Our findings of neuroprotective effects of HET0016 are consistent with the data published by Yang et al in a neonatal piglet hypoxic-ischemia model. Further, Yang et al, showed that 20-HETE increases the phosphorylation of NMDA receptor NR1 subunit selectively at protein kinase-C sensitive sites indicating a direct effect of 20-HETE in mediating excitotoxicity (Yang, et al., 2012). Our studies showed the evidence of increased CBF after HET0016 treatment indicating a possible role of vascular mechanism whereas data from Renic et al, on protective effect of HET0016 on hippocampal slice cultures from oxygen-glucose deprivation (Renic, et al., 2012), neuronal localization of CYP4A in putamen of pig (Yang, et al., 2012), and in post-ischemic cortical neurons of adult rat (Omura, et al., 2006) suggest possible activation of neuronal signaling

cascade indicating role of a non-vascular mechanisms of neuroprotection. Future studies need to be completed evaluating the degree to which microvascular flow changes contribute to neurovascular protection in global cerebral ischemia. Together, these data suggest that neuroprotection by 20-HETE inhibition may likely be mediated by both blood flow changes and direct cytoprotective effects on neurons.

There are possible limitations to this study. One of the limitations is that regional and temporal distribution of CYP eicosanoids and prostanoids was done over relatively shorter duration of post-ischemic reperfusion period. Future studies will include temporal profiling of AA metabolites from different brain regions over longer time intervals extending into one week after ischemic injury for fully characterizing the time they peak and return to basal levels. This will help in determining the therapeutic window of time for administering small molecule inhibitors like HET0016, which has relatively shorter half-life *in vivo* (Mu et al., 2008). In this study, we administered HET0016 acutely as it has shorter half-life and at low dose as high concentrations can inhibit EET synthesis. A future direction of this study includes continuous infusion of low dose HET0016 at different intervals during post-ischemic reperfusion to achieve target concentrations in the selectivity range in order to evaluate effects of chronic inhibition on long-term functional outcomes, and on the regional CBF in the extended period of post-ischemic reperfusion. Additional studies with the antagonists of 20-HETE will confirm if the protective effects of HET0016 are direct or mediated through 20-HETE inhibition. Another future direction includes administering COX inhibitor individually and along with HET0016 to elucidate the relative contributions of prostanoids and CYP eicosanoids on pathological CBF regulation in the cortex during post-ischemic reperfusion. A second limitation is that we did not evaluate the direct neuroprotective effects of HET0016 in

in vitro neuronal cultures. Future studies will evaluate the neuroprotective efficacy of HET0016 over a wider concentration under ischemic conditions.

5.5 CONCLUSIONS

In summary, in the current study we have described the pattern of CBF dysregulation during the post-ischemic reperfusion phase after different durations of CA and first time reported full profile of regional and temporal distribution of CYP eicosanoids and prostanoids in the rat brain after global ischemic injury. Further, we have produced the first evidence of an imbalance in the tissue levels of vasoactive CYP eicosanoids and their relationship to pathological changes in cortical blood flow during post-ischemic reperfusion. Further, we have showed that HET0016 improves cortical CBF during the early reperfusion phase after 12 min CA by selectively inhibiting 20-HETE levels in the cortex. In addition to CBF improvements, we showed significant reduction in neuronal death and improved short-term behavioral performance after a single low dose administration of HET0016.

6.0 CONCLUSIONS AND FUTURE DIRECTIONS

6.1 Summary and conclusions

The main objective of this research was to investigate the role of CYP eicosanoids in the cerebral ischemic injury. This was achieved by studying the effect of CYP eicosanoids on the individual components of neurovascular unit in *in vitro* and *in vivo* models of ischemia by using small molecule pharmacological inhibitors. In order to systematically evaluate the effects, *in vitro* primary neuronal cultures, a focal and global ischemic rat models were utilized. In addition, advanced analytical assays and sophisticated blood perfusion imaging systems were used in this research to further understand the relationship between CYP eicosanoids, and CBF changes. Finally, modulation of specific CYP eicosanoid pathways by pharmacological inhibitors were assessed for their potential impact on improving neurofunctional outcome, a necessary criteria suggested by STAIR for translating preclinical findings from a relevant animal model to clinical stroke research. Several key findings are made from this research, which are summarized in the following section.

In the first part of this research, we have developed and validated a robust and rapid UPLC-MS/MS assay for quantitating a wide range of AA metabolites including CYP eicosanoids and prostanoids from same tissue extract. Further, this is the first validated method to report quantification of cyclopentenone prostanoid metabolites (PGA_2, PGJ_2, 15-d-PGJ_2) in rat brain tissue. In this and other Chapters of this research, we have successfully applied this method not only to profile regional and temporal distribution of the AA metabolites in the rat brain after cerebral ischemic injury but also to test the specificity of the pharmacological inhibitors. This lipidomics based method offers a potential advantage in identifying potential biomarkers that may be critical in

disease progression and may be viable therapeutic targets for mitigating secondary neuronal damage after ischemic injury.

In the second part of this research, we evaluated the neuroprotective effects of CYP eicosanoids over a wide concentration range in *in vitro* rat primary cortical neuronal cultures under normoxic and hypoxic conditions. We verified that the CYP eicosanoids are relatively stable and readily taken up by neurons under the incubation conditions and that they can be exogenously administered to neuronal cultures. We demonstrated three novel findings from this study. First, 11,12-EET is protective even under normoxic conditions at relatively high concentrations. Second, 20-HETE exhibited concentration dependent toxic effects and these effects are potentiated only after a hypoxic-ischemic event. Third, 11,12-EET showed concentration dependent neuroprotective effects in hypoxic injury. These findings from Chapter 3, suggest a possible role for the non-vascular mechanism of neuroprotection by CYP eicosanoids in ischemic injury.

In the third part of the study, we have evaluated the *in vivo* protective effects of CYP eicosanoids in a focal ischemia model of rat MCAO using *t*-AUCB, a pharmacological inhibitor of sEH. We have demonstrated the neuroprotective effects of *t*-AUCB at a low dose. This study is the first to report that acute *t*-AUCB administration increases cumulative EETs/DHETs ratio in the cortex and is associated with the observed neuroprotective effects. Further, we have applied our lipidomics method and showed that *t*-AUCB did not change the levels of other AA metabolites from CYP4A, CYP4F, and COX pathways indicating the specificity of sEH inhibition. In addition, these data are the first to demonstrate improved short-term behavioral performance by *t*-AUCB by evaluating motor and somatosensory behavior. Functional outcome improvements is one of the

important criteria suggested by STAIR for successfully translating preclinical drug candidates to further clinical development in stroke research, and our findings provide evidence that *t*-AUCB meets this criteria. We have also demonstrated for the first time that exogenous *t*-AUCB administration to primary cortical neuronal cultures significantly increases their survival in a concentration dependent manner in a hypoxia-reoxygenation injury model. Further, we have showed that acute sEH inhibition by *t*-AUCB has marginal improvements in CBF around the infarcted area during the post-ischemic hypoperfusion period. These findings from Chapter 4 suggest that altering EETs levels by acute inhibition of sEH is likely to produce the largest benefits by affecting multiple components of neurovascular unit.

In the final part of this study, we have evaluated the *in vivo* protective effects of CYP eicosanoids in a global ischemia model of pediatric asphyxial CA using HET0016, a pharmacological inhibitor of CYP4A/4F. We have described the pattern of CBF dysregulation during the post-ischemic reperfusion phase after different durations of CA. We have for the first time described a comprehensive profile of regional and temporal distribution of CYP eicosanoids and prostanoids in the rat brain after global ischemic injury. Further, we have produced the first evidence of an imbalance in the tissue levels of these vasoactive AA metabolites and their possible association with pathological changes in CBF in the cortex post resuscitation from different durations of CA. We have selected HET0016, inhibitor of synthesis of 20-HETE, a potent constrictor of microvasculature and showed that acute HET0016 administration improves cortical CBF during the early reperfusion phase after 12 min CA by selectively inhibiting 20-HETE levels in the cortex. We confirmed the selectivity of this inhibition using our validated analytical method. In addition to CBF improvements, we showed significant reduction in neuronal death and improved short-

term behavioral performance after low dose administration of HET0016. These findings from Chapter 5 suggest that correcting the imbalance in the tissue levels of vasoactive CYP eicosanoids improves CBF at least during the initial phase of reperfusion and improves short-term functional outcome.

6.2 Clinical relevance

1) Several clinical studies have shown that polymorphisms in the genes encoding CYP enzymes that result in altered levels of AA metabolites are associated with increased risk for stroke in some specific patient population. The findings of this study also showed that modulation of CYP pathway of AA metabolism in ischemic injury by small molecule inhibitors affects multiple components of neurovascular unit and improves functional outcome. These findings help us to gain a better insight into the role of brain CYP450 enzymes in endogenous fatty acid metabolism particularly of AA and their relationship to cerebrovascular diseases such as stroke.

2) This research facilitates the understanding of the CYP eicosanoids role in the progression of cerebral ischemic injury. We showed that duration and severity of CBF reduction in the cortex of post-ischemic brain is dependent on the tissue levels of CYP eicosanoids. Several clinical studies have also shown the evidence of increased levels of AA and CYP eicosanoids in the CSF of stroke patients. Thus, CYP eicosanoids can serve as potential biomarkers for assessing the severity of CBF reductions during the reperfusion phase of the post-ischemic brain and thereby identifying patients at risk for secondary neurological complications of stroke.

3) In the last two decades of stroke research, several therapeutic agents have failed in the clinical trials. From the drug development perspective, the failures could be ascribed to the lack of efficient target engagement due to poor permeability across BBB and/or to the lack of assessing target engagement. The research paradigm applied in this study addresses the first problem by improvising drug delivery using formulations made of HPβCD, and the second problem by using lipidomics analysis to quantify an array of biomarkers to ensure target engagement. This approach has potential clinical value in designing therapeutic strategies for optimum dosing in order to maximize the efficacy of the therapeutic agents by achieving relevant drug concentrations in the brain.

6.3 Future directions

The findings of this work provides the basis and foundation for future preclinical studies and opens up avenues to further investigate the mechanistic underpinning of the CYP eicosanoids effects in cerebral ischemia. These future studies can generate additional evidence in support of the primary findings of this research. There are several future directions to this body of work, which are listed in the following section.

The lipidomics method developed and used in this work is applicable to measure tissue levels of CYP eicosanoids and prostanoids. However, additional studies are needed in future to develop and validate the method for measuring these metabolites in biological fluids such as plasma or CSF in order to extend its scope for clinical applications. We have performed *in vitro* evaluations in pure neuronal cultures alone under hypoxic conditions. However, further studies in pure astrocytes or mixed neuron-astrocytic cultures are needed in future to evaluate the neuroprotective effects of CYP eicosanoids in the context of neurovascular unit. For example, adding the media from

astrocyte cultures treated with CYP eicosanoids to neuronal cultures will help in teasing out the effects of CYP eicosanoids on individual cell types and/or in mixed cultures. Additionally, more *in vitro* studies are warranted to investigate the signaling pathways activated by CYP eicosanoids after ischemic injury. For example, electrophysiology experiments evaluating direct effect of individual CYP eicosanoids on different ion channels that are linked to excitotoxicity and Ca^{2+} overload will help in differentiating the protective mechanisms of CYP eicosanoids. At present, a putative 20-HETE or EET receptor has not been identified. Thus, there is need for identifying CYP eicosanoid receptor in order to gain an insight into the molecular mechanisms of neuroprotection.

Throughout this study, ischemia was assessed by measuring CBF changes alone after the stroke and/or CA. However, it is observed that oxygen and glucose extraction increase as the blood flow is reduced. So the decrease in the oxidative metabolism can be less than the fall in CBF, which means even during the hypoperfusion period neurons in selective regions might survive as long as the oxidative metabolism remains above a certain threshold. Thus, another future direction to this work includes cerebral metabolic rate of oxygen ($CMRO_2$) assessments along with CBF measurements to better serve as a predictor of neuronal survival after ischemic injury. Additional studies assessing the extent of autoregulatory dysfunction after ischemic injury in global and focal ischemia models will aid in developing small molecule inhibitors that can restore autoregulation of CBF.

Reperfusion after initial ischemic event burdens the system with free radicals increasing the oxidative stress and initiating inflammatory response. Thus, another future direction to this work includes measurement of the markers of oxidative stress such as 8-isoprostanes and pro-inflammatory cytokines such as IL-6 to elucidate underlying effector mechanisms involved in the

pathogenesis of ischemic damage. The regional and temporal distribution of CYP eicosanoids and prostanoids was done over relatively shorter duration of post-ischemic reperfusion period. Further studies are needed to describe temporal profile of AA metabolites from different brain regions over longer time intervals extending as long as one week after ischemic injury for characterizing the time they peak and return to basal levels. In addition, CBF measurement should be taken over the same interval in order to correlate with tissue levels.

In this work acute administration of low doses of HET0016 and *t*-AUCB were individually evaluated for their protective effects in different animal models of ischemia. Though both HET0016 and *t*-AUCB showed neuroprotection in this study, HET0016 showed evidence of neuroprotection through both vascular and non-vascular mechanisms. Also, sEH inhibitors may not be preferable to use in chronic conditions with comorbid diseases such as cancer due to the potential angiogenic effects of EETs. Thus their use may be limited to acute applications. Thus, HET0016 appears to be a good candidate for further clinical development. A future direction of this work includes administering the inhibitor at different intervals after reperfusion to establish the therapeutic time window of neuroprotection. Additional studies are warranted for establishing a dose-response curve and chronic dosing to evaluate the impact on the regional CBF in the extended post-ischemic reperfusion phase and on long-term functional outcome. Another possible future direction to this work includes, a synergistic combination of both pharmacological inhibitors to maximize the neuroprotection however the dosing strategy must be optimized to ensure that there is no cross-inhibition to nullify the protective effects of each other. Another future direction includes antagonists of CYP eicosanoids to confirm if the protective effects of these inhibitors are direct or mediated through CYP eicosanoids. Another potential strategy in the development of pharmacological inhibitors would be repurposing clinically approved medicines for other

indications with potential effect on CYP eicosanoid system. For example, Fingolimod, a sphingosine-1-phosphate receptor modulator is clinically used for treating multiple sclerosis. Fingolimod is a major substrate for CYP4F2 which could probably be used as a competitive inhibitor of AA metabolism to reduce 20-HETE levels. Such approaches will help in advancing clinical development of pharmacological inhibitors of CYP eicosanoid pathway.

Some of the major disadvantages of pharmacological inhibitors are that sometimes they may not offer required selectivity at the *in vivo* concentrations achieved, and may exert off-target effects that are unavoidable. Genetic tools such as transgenic mice overexpressing a particular CYP or knockout animals devoid of a particular CYP are indispensable tools to investigate the underlying molecular mechanisms of CYP enzymes in cerebral ischemic injury. We have created a humanized mouse overexpressing CYP4F2 under the Tie2 promoter of vascular endothelium. Initial experiments of functional characterization were performed. Future *in vivo* studies with these transgenic animals are needed to be done to investigate the role of 20-HETE produced from CYP4F2 in cerebral ischemia after stroke or cardiac arrest. These studies will corroborate the findings from pharmacological inhibitor studies and also give more insight into the effects of overexpressed CYP4F2 and its AA metabolite 20-HETE under normal and ischemic conditions. Further, these transgenic animals could also be used to investigate the role of CYP4F2 generated 20-HETE in other diseases of cardiovascular, and renal system.

In conclusion, the results of the work performed throughout this thesis research could have important clinical implications, since altered tissue levels of CYP eicosanoids are related to CBF dysregulation, ischemic brain injury, and worse functional outcomes. Pharmacological inhibitors could potentially mitigate or reduce the ischemic injury and associated long-term complications.

Further research is warranted in order to design an optimum dosing strategy for single or combination small molecule inhibitors of CYP eicosanoid pathway to rectify the CBF dysregulation, and improve long-term functional outcomes after stroke injury.

APPENDIX A:

Tie2-CYP4F2 transgenic mice functional characterization

A.1 Tie2-CYP4F2 vector creation:

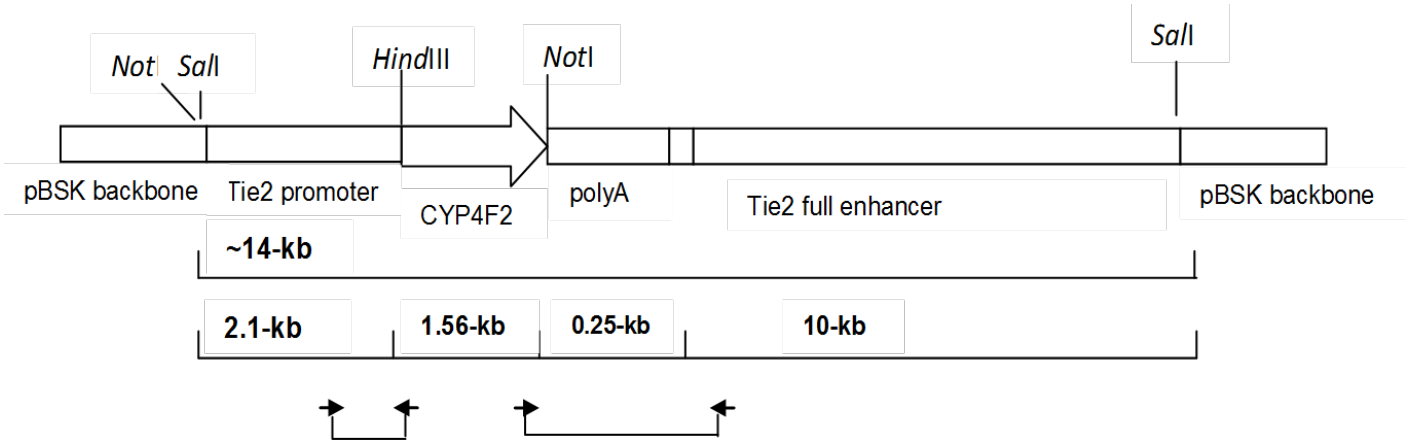

Fig A-1: Map of Tie2-CYP4F2 insert in pBSK(+) vector. CYP4F2 is expressed in vascular endothelium under Tie2 promoter with full enhancer sequence. Transgenic mice were created on C57BL/6 strain.

A.2 CYP4F2 mRNA expression in the Tie2-CYP4F2 transgenic mice:

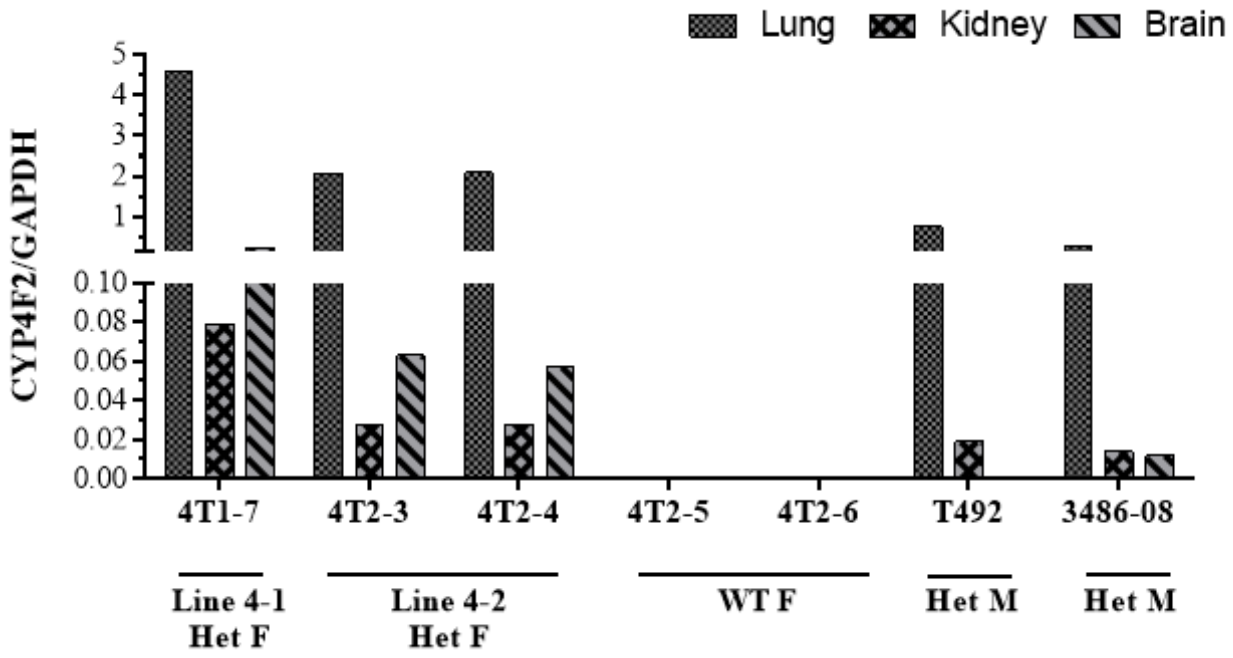

Fig A-2: mRNA expression levels of CYP4F2 in different tissues of WT and heterozygous transgenic mice from different lines. Highest expression was observed in lung, brain followed by kidney.

A.3 Microsomal yield from different batches of transgenic mice:

Table A-1: Protein estimation of microsomes from batch-1Tie2-CYP4F2 mice

				Liver		Kidney		Lung		Heart		Brain	
S.No	**Sample**	**Gender**	**GT**	**Wt (g)**	**Conc. (µg/µL)**	**Wt (g)**	**Conc. (µg/µL)**	**Wt (g)**	**Conc. (µg/µL)**	**Wt (g)**	**Conc. (µg/µL)**	**Wt (g)**	**Conc. (µg/µL)**
1	4T1-7	F	Het	0.336	2.20	0.082	1.13	0.035	0.212	0.049	3.57	0.1813	10.40
2	4T2-3	F	Het	0.324	3.35	0.096	1.35	0.029	0.334	0.047	4.05	0.1669	10.47
3	4T2-4	F	Het	0.383	5.05	0.106	1.49	0.027	0.389	0.033	2.59	0.1976	10.44
8	T492	M	Het	0.437	2.69	0.111	2.13	0.059	0.659	0.041	4.38	NA	-
10	3468-08	M	Het	0.273	2.75	0.137	2.79	0.0790	1.062	NA	-	0.2067	10.50
4	4T2-5	F	WT	0.397	3.50	0.103	1.56	0.032	0.383	0.048	4.03	0.1963	10.76
5	4T2-6	F	WT	0.399	3.51	0.092	1.38	0.029	0.248	0.038	3.01	0.1930	10.91
6	4T3-4	F	WT	0.344	2.88	0.114	1.64	0.038	0.352	0.064	5.18	0.1931	10.55
7	4T3-5	F	WT	0.295	3.04	0.119	1.84	0.044	0.464	0.042	5.44	0.2439	10.27
9	MH78-2	M	WT	0.332	2.88	0.115	2.12	0.096	1.003	0.044	4.66	NA	-

GT: genotype; Het: heterozygous; WT: Wild type

A.3 Microsomal yield from different batches of transgenic mice:

Table A-2: Protein estimation of microsomes from batch-2 Tie2-CYP4F2 mice

				Liver		Kidney		Lung		Brain		Heart	
S.No	Sample	Gender	GT	Wt (g)	Conc. (µg/µL)	Wt (g)	Conc. (µg/µL)	Wt (g)	Conc. (µg/µL)	Wt (g)	Conc. (µg/µL)	Wt (g)	Conc. (µg/µL)
1	4T12-6	F	WT	0.1120	3.03	0.0588	3.28	0.0393	1.65	0.2625	6.48	0.0565	10.87
2	4T13-1	M	Het	0.0838	2.86	0.0756	3.43	0.0416	1.64	0.3020	6.88	0.0614	13.08
3	4T13-2	M	WT	0.1534	4.52	0.1030	3.88	0.0438	1.95	0.3359	6.98	0.0626	20.62
4	4T13-3	F	Het	0.1529	3.51	0.0615	2.12	0.0400	1.75	0.3326	6.78	0.0743	13.74
5	4T13-4	F	Het	0.1596	3.45	0.0736	4.15	0.0394	1.86	0.3535	9.85	0.0643	18.62
6	4T13-5	F	WT	0.1471	3.72	0.0578	2.60	0.0344	1.89	0.3574	9.09	0.0443	12.04

GT: genotype; Het: heterozygous; WT: Wild type

A.4 Functional activity evaluation of different batches of transgenic mice:

Table A-2: Functional activity evaluation in different tissues of from batch-1 Tie2-CYP4F2 mice

				Liver			Kidney			Lung			Brain			Heart		
				20-HETE Velocity (pmol/mg/min)			20-HETE Velocity (pmol/mg/min)			20-HETE Velocity (pmol/mg/min)			20-HETE Velocity (pmol/mg/min)			20-HETE Velocity (pmol/mg/min)		
S.No	Line	Gender	GT	Avg	SD	% C.V	Avg	SD	% C.V	Avg	SD	% C.V	Avg	SD	% C.V	Avg	SD	% C.V
1	4T1-7	F	Het	217.7	26.2	12.0	19.4	2.3	11.7	5.0			3.40	0.41	12.1	0.6	0.04	8.0
2	4T2-3	F	Het	243.6	7.9	3.2	13.2	0.5	3.8	14.1	0.3	2.4	2.27	0.26	11.6	0.4	0.02	5.2
3	4T2-4	F	Het	217.1	33.8	15.6	12.5	1.1	8.6	7.8	1.6	20.7	2.53	0.24	9.4	0.4	0.01	2.8
4	4T2-5	F	WT	219.5	25.1	11.4	2.9	0.8	26.8	7.6	1.0	13.0	3.05	0.16	5.3	NF		
5	4T2-6	F	WT	355.5	27.8	7.8	10.7	1.3	12.1	14.5			2.43	0.44	18.0	NF		
6	4T3-4	F	WT	266.7	13.4	5.0	15.4	0.7	4.5	13.4	1.4	10.5	1.87	0.14	7.7	0.3		
7	4T3-5	F	WT	265.2	27.0	10.2	11.8	0.7	6.2	12.5	1.3	10.6	2.26	0.08	3.7	NF		
8	T492	M	Het	203.4	18.2	8.9	18.8	0.5	2.7	34.4	1.5	4.3	**Not collected**			0.4	0.1	4.0
9	MH78-2	M	WT	289.3	31.1	10.7	16.1	1.5	9.5	27.1	1.8	6.5				NF		
10	P3468-8	M	Het	188.1	23.8	12.6	40.0	3.9	9.9	18.1	1.1	6.2	5.26	0.90	17.19	**Not collected**		

GT: genotype; Het: heterozygous; WT: Wild type

20-HETE formation was highest in liver, followed by kidney, and lungs and brain. 20-HETE detection was negligible in heart microsomes of WT

A.4 Functional activity evaluation of different batches of transgenic mice:

Table A-3: Functional activity evaluation in different tissues of from batch-2 Tie2-CYP4F2 mice

				Liver			Kidney			Lung			Brain			Heart		
				20-HETE Velocity (pmol/mg/min)			20-HETE Velocity (pmol/mg/min)			20-HETE Velocity (pmol/mg/min)			20-HETE Velocity (pmol/mg/min)			20-HETE Velocity (pmol/mg/min)		
S.No	Line	Gender	GT	Avg	SD	% C.V	Avg	SD	% C.V	Avg	SD	% C.V	Avg	SD	% C.V	Avg	SD	% C.V
1	4T12-6	F	WT	612.3	42.4	6.9	83.7	16.0	19.1	12.0	1.6	13.0	2.75	0.27	9.8	NF		
2	4T13-2	M	WT	459.2	42.3	9.2	156.4	3.6	2.3	6.6	0.0	0.1	1.62	0.20	12.5	NF		
3	4T13-5	F	WT	499.3	68.1	13.6	39.5	1.1	2.7	6.8	2.1	31.7	1.87	0.23	12.2	NF		
4	4T13-1	M	Het	506.7	70.0	13.8	120.1	11.1	9.2	18.1	0.0	0.0	4.00	0.54	13.5	0.05	0.004	8.66
5	4T13-3	F	Het	525.1	49.2	9.4	51.6	0.7	1.3	14.8	2.5	16.6	2.01	0.30	14.9	0.07	0.002	3.20
6	4T13-4	F	Het	588.8	30.3	5.1	36.1	1.2	3.3	14.6	2.0	13.9	1.62	0.04	2.6	0.05	0.000	0.00

GT: genotype; Het: heterozygous; WT: Wild type

20-HETE formation was highest in liver, followed by kidney, and lungs and brain. 20-HETE formation was not detected in WT heart microsomes

BIBLIOGRAPHY

1. **Abe K, Kogure K, Yamamoto H, et al.** (1987) "Mechanism of arachidonic acid liberation during ischemia in gerbil cerebral cortex". *J Neurochem* **48**: 503-509.

2. **Adibhatla RM, and Hatcher JF**. (2008) "Altered lipid metabolism in brain injury and disorders". *Subcell Biochem* **49**: 241-268.

3. **Adibhatla RM, Hatcher JF, and Dempsey RJ**. (2006) "Lipids and lipidomics in brain injury and diseases". *AAPS J* **8**: E314-321.

4. **Ahmed SH, Shaikh AY, Shaikh Z, et al.** (2000) "What animal models have taught us about the treatment of acute stroke and brain protection". *Curr Atheroscler Rep* **2**: 167-180.

5. **Akaike A, Kaneko S, Tamura Y, et al.** (1994) "Prostaglandin E2 protects cultured cortical neurons against N-methyl-D-aspartate receptor-mediated glutamate cytotoxicity". *Brain Res* **663**: 237-243.

6. **Alexander LD, Cui XL, Falck JR, et al.** (2001) "Arachidonic acid directly activates members of the mitogen-activated protein kinase superfamily in rabbit proximal tubule cells". *Kidney Int* **59**: 2039-2053.

7. **Alkayed NJ, Birks EK, Hudetz AG, et al.** (1996) "Inhibition of brain P-450 arachidonic acid epoxygenase decreases baseline cerebral blood flow". *Am J Physiol* **271**: H1541-1546.

8. **Alkayed NJ, Birks EK, Narayanan J, et al.** (1997) "Role of P-450 arachidonic acid epoxygenase in the response of cerebral blood flow to glutamate in rats". *Stroke* **28**: 1066-1072.

9. **Alonso-Galicia M, Falck JR, Reddy KM, et al.** (1999) "20-HETE agonists and antagonists in the renal circulation". *Am J Physiol* **277**: F790-796.

10. **Amaral SL, Maier KG, Schippers DN, et al.** (2003) "CYP4A metabolites of arachidonic acid and VEGF are mediators of skeletal muscle angiogenesis". *Am J Physiol Heart Circ Physiol* **284**: H1528-1535.

11. **Ames A, 3rd, Wright RL, Kowada M, et al.** (1968) "Cerebral ischemia. II. The no-reflow phenomenon". *Am J Pathol* **52**: 437-453.

12. **Andresen J, Shafi NI, and Bryan RM, Jr.** (2006) "Endothelial influences on cerebrovascular tone". *J Appl Physiol* **100**: 318-327.

13. **Archer SL, Gragasin FS, Wu X, et al.** (2003) "Endothelium-derived hyperpolarizing factor in human internal mammary artery is 11,12-epoxyeicosatrienoic acid and causes relaxation by activating smooth muscle BK(Ca) channels". *Circulation* **107**: 769-776.

14. **Armstead WM, Mirro R, Busija DW, et al.** (1989) "Vascular responses to vasopressin are tone-dependent in the cerebral circulation of the newborn pig". *Circ Res* **64**: 136-144.

15. **Aronowski J, Samways E, Strong R, et al.** (1996) "An alternative method for the quantitation of neuronal damage after experimental middle cerebral artery occlusion in rats: analysis of behavioral deficit". *J Cereb Blood Flow Metab* **16**: 705-713.

16. **Attwell D, Buchan AM, Charpak S, et al.** (2010) "Glial and neuronal control of brain blood flow". *Nature* **468**: 232-243.

17. **Bachevalier J, and Meunier M**. (1996) "Cerebral ischemia: are the memory deficits associated with hippocampal cell loss?". *Hippocampus* **6**: 553-560.

18. **Baranowski R, and Pacha K**. (2002) "Gas chromatographic determination of prostaglandins". *Mini Rev Med Chem* **2**: 135-144.

19. **Baskaya MK, Prasad MR, Donaldson D, et al.** (1996) "Enhanced accumulation of free fatty acids in experimental focal cerebral ischemia". *Prostaglandins Leukot Essent Fatty Acids* **54**: 167-171.

20. **Bauersachs J, Popp R, Hecker M, et al.** (1996) "Nitric oxide attenuates the release of endothelium-derived hyperpolarizing factor". *Circulation* **94**: 3341-3347.

21. **Bazan NG** (1976) "Free arachidonic acid and other lipids in the nervous system during early ischemia and after electroshock". *Adv Exp Med Biol* **72**: 317-335.

22. **Bazan NG, Jr.** (1970) "Effects of ischemia and electroconvulsive shock on free fatty acid pool in the brain". *Biochim Biophys Acta* **218**: 1-10.

23. **Bellien J, Iacob M, Gutierrez L, et al.** (2006) "Crucial role of NO and endothelium-derived hyperpolarizing factor in human sustained conduit artery flow-mediated dilatation". *Hypertension* **48**: 1088-1094.

24. **Bellien J, Thuillez C, and Joannides R**. (2008) "Contribution of endothelium-derived hyperpolarizing factors to the regulation of vascular tone in humans". *Fundam Clin Pharmacol* **22**: 363-377.

25. **Benveniste H, Drejer J, Schousboe A, et al.** (1984) "Elevation of the extracellular concentrations of glutamate and aspartate in rat hippocampus during transient cerebral ischemia monitored by intracerebral microdialysis". *J Neurochem* **43**: 1369-1374.

26. **Bernard SA, Gray TW, Buist MD, et al.** (2002) "Treatment of comatose survivors of out-of-hospital cardiac arrest with induced hypothermia". *N Engl J Med* **346**: 557-563.

27. **Bettermann K** (2011) "Biomarkers for stroke: in search of fingerprints". *J Stroke Cerebrovasc Dis* **20**: 173-176.

28. **Bhardwaj A, Northington FJ, Carhuapoma JR, et al.** (2000) "P-450 epoxygenase and NO synthase inhibitors reduce cerebral blood flow response to N-methyl-D-aspartate". *Am J Physiol Heart Circ Physiol* **279**: H1616-1624.

29. **Birks EK, Bousamra M, Presberg K, et al.** (1997) "Human pulmonary arteries dilate to 20-HETE, an endogenous eicosanoid of lung tissue". *Am J Physiol* **272**: L823-829.

30. **Blanco VM, Stern JE, and Filosa JA**. (2008) "Tone-dependent vascular responses to astrocyte-derived signals". *Am J Physiol Heart Circ Physiol* **294**: H2855-2863.

31. **Blewett AJ, Varma D, Gilles T, et al.** (2008) "Development and validation of a high-performance liquid chromatography-electrospray mass spectrometry method for the simultaneous determination of 23 eicosanoids". *J Pharm Biomed Anal* **46**: 653-662.

32. **Bleys RL, and Cowen T**. (2001) "Innervation of cerebral blood vessels: morphology, plasticity, age-related, and Alzheimer's disease-related neurodegeneration". *Microsc Res Tech* **53**: 106-118.

33. **Bottiger BW, Krumnikl JJ, Gass P, et al.** (1997) "The cerebral 'no-reflow' phenomenon after cardiac arrest in rats--influence of low-flow reperfusion". *Resuscitation* **34**: 79-87.

34. **Brown CG, Birinyi F, Werman HA, et al.** (1986) "The comparative effects of epinephrine versus phenylephrine on regional cerebral blood flow during cardiopulmonary resuscitation". *Resuscitation* **14**: 171-183.

35. **Busija DW, Bari F, Domoki F, et al.** (2007) "Mechanisms involved in the cerebrovascular dilator effects of N-methyl-d-aspartate in cerebral cortex". *Brain Res Rev* **56**: 89-100.

36. **Buunk G, van der Hoeven JG, Frolich M, et al.** (1996) "Cerebral vasoconstriction in comatose patients resuscitated from a cardiac arrest?". *Intensive Care Med* **22**: 1191-1196.

37. **Buunk G, van der Hoeven JG, and Meinders AE**. (2000) "Cerebral blood flow after cardiac arrest". *Neth J Med* **57**: 106-112.

38. **Bylund J, Kunz T, Valmsen K, et al.** (1998) "Cytochromes P450 with bisallylic hydroxylation activity on arachidonic and linoleic acids studied with human recombinant enzymes and with human and rat liver microsomes". *J Pharmacol Exp Ther* **284**: 51-60.

39. **Cai H, and Harrison DG**. (2000) "Endothelial dysfunction in cardiovascular diseases: the role of oxidant stress". *Circ Res* **87**: 840-844.

40. **Cambj-Sapunar L, Yu M, Harder DR, et al.** (2003) "Contribution of 5-hydroxytryptamine1B receptors and 20-hydroxyeiscosatetraenoic acid to fall in cerebral blood flow after subarachnoid hemorrhage". *Stroke* **34**: 1269-1275.

41. **Campbell WB, Deeter C, Gauthier KM, et al.** (2002) "14,15-Dihydroxyeicosatrienoic acid relaxes bovine coronary arteries by activation of K(Ca) channels". *Am J Physiol Heart Circ Physiol* **282**: H1656-1664.

42. **Campbell WB, and Falck JR**. (2007) "Arachidonic acid metabolites as endothelium-derived hyperpolarizing factors". *Hypertension* **49**: 590-596.

43. **Cao S, Wang LC, Kwansa H, et al.** (2009) "Endothelin rather than 20-HETE contributes to loss of pial arteriolar dilation during focal cerebral ischemia with and without polymeric hemoglobin transfusion". *Am J Physiol Regul Integr Comp Physiol* **296**: R1412-1418.

44. **Capdevila JH, Falck JR, and Harris RC**. (2000) "Cytochrome P450 and arachidonic acid bioactivation. Molecular and functional properties of the arachidonate monooxygenase". *J Lipid Res* **41**: 163-181.

45. **Caro AA, and Cederbaum AI**. (2006) "Role of cytochrome P450 in phospholipase A2- and arachidonic acid-mediated cytotoxicity". *Free Radic Biol Med* **40**: 364-375.

46. **Centers for Disease C, and Prevention**. (2011) "Million hearts: strategies to reduce the prevalence of leading cardiovascular disease risk factors--United States, 2011". *MMWR Morb Mortal Wkly Rep* **60**: 1248-1251.

47. **Chan PH** (2001) "Reactive oxygen radicals in signaling and damage in the ischemic brain". *J Cereb Blood Flow Metab* **21**: 2-14.

48. **Chan PH, and Fishman RA**. (1984) "The role of arachidonic acid in vasogenic brain edema". *Fed Proc* **43**: 210-213.

49. **Chappell DL, Xiao X, Radziszewski W, et al.** (2011) "Development and validation of a LC/MS/MS method for 6-keto PGF1alpha, a metabolite of prostacyclin (PGI(2))". *J Pharm Biomed Anal* **56**: 600-603.

50. **Chapple DJ, Dusting GJ, Hughes R, et al.** (1980) "Some direct and reflex cardiovascular actions of prostacyclin (PGI2) and prostaglandin E2 in anaesthetized dogs". *Br J Pharmacol* **68**: 437-447.

51. **Chen G, Suzuki H, and Weston AH**. (1988) "Acetylcholine releases endothelium-derived hyperpolarizing factor and EDRF from rat blood vessels". *Br J Pharmacol* **95**: 1165-1174.

52. **Chen JK, Falck JR, Reddy KM, et al.** (1998) "Epoxyeicosatrienoic acids and their sulfonimide derivatives stimulate tyrosine phosphorylation and induce mitogenesis in renal epithelial cells". *J Biol Chem* **273**: 29254-29261.

53. **Chen JK, Wang DW, Falck JR, et al.** (1999) "Transfection of an active cytochrome P450 arachidonic acid epoxygenase indicates that 14,15-epoxyeicosatrienoic acid functions as an intracellular second messenger in response to epidermal growth factor". *J Biol Chem* **274**: 4764-4769.

54. **Cheng J, Ou JS, Singh H, et al.** (2008) "20-hydroxyeicosatetraenoic acid causes endothelial dysfunction via eNOS uncoupling". *Am J Physiol Heart Circ Physiol* **294**: H1018-1026.

55. **Chiamvimonvat N, Ho CM, Tsai HJ, et al.** (2007) "The soluble epoxide hydrolase as a pharmaceutical target for hypertension". *J Cardiovasc Pharmacol* **50**: 225-237.

56. **Cohan SL, Mun SK, Petite J, et al.** (1989) "Cerebral blood flow in humans following resuscitation from cardiac arrest". *Stroke* **20**: 761-765.

57. **Cowart LA, Wei S, Hsu MH, et al.** (2002) "The CYP4A isoforms hydroxylate epoxyeicosatrienoic acids to form high affinity peroxisome proliferator-activated receptor ligands". *J Biol Chem* **277**: 35105-35112.

58. **Della Corte F, Barelli A, Giordano A, et al.** (1993) "CBF determination in post-ischemic-anoxic comatose patients". *Minerva Anestesiol* **59**: 637-641.

59. **Dempsey RJ, Roy MW, Meyer K, et al.** (1986) "Development of cyclooxygenase and lipoxygenase metabolites of arachidonic acid after transient cerebral ischemia". *J Neurosurg* **64**: 118-124.

60. **Denes A, Pinteaux E, Rothwell NJ, et al.** (2011) "Interleukin-1 and stroke: biomarker, harbinger of damage, and therapeutic target". *Cerebrovasc Dis* **32**: 517-527.

61. **Detre JA, Leigh JS, Williams DS, et al.** (1992) "Perfusion imaging". *Magn Reson Med* **23**: 37-45.

62. **Dietrich HH, Kajita Y, and Dacey RG, Jr.** (1996) "Local and conducted vasomotor responses in isolated rat cerebral arterioles". *Am J Physiol* **271**: H1109-1116.

63. **Ding H, Cui G, Zhang L, et al.** (2010) "Association of common variants of CYP4A11 and CYP4F2 with stroke in the Han Chinese population". *Pharmacogenet Genomics* **20**: 187-194.

64. **Donoghue AJ, Nadkarni V, Berg RA, et al.** (2005) "Out-of-hospital pediatric cardiac arrest: an epidemiologic review and assessment of current knowledge". *Ann Emerg Med* **46**: 512-522.

65. **Dorrance AM, Rupp N, Pollock DM, et al.** (2005) "An epoxide hydrolase inhibitor, 12-(3-adamantan-1-yl-ureido)dodecanoic acid (AUDA), reduces ischemic cerebral infarct size in stroke-prone spontaneously hypertensive rats". *J Cardiovasc Pharmacol* **46**: 842-848.

66. **Dos Santos EA, Dahly-Vernon AJ, Hoagland KM, et al.** (2004) "Inhibition of the formation of EETs and 20-HETE with 1-aminobenzotriazole attenuates pressure natriuresis". *Am J Physiol Regul Integr Comp Physiol* **287**: R58-68.

67. **Dringen R** (2000) "Metabolism and functions of glutathione in brain". *Prog Neurobiol* **62**: 649-671.

68. **Dunn KM, Renic M, Flasch AK, et al.** (2008) "Elevated production of 20-HETE in the cerebral vasculature contributes to severity of ischemic stroke and oxidative stress in spontaneously hypertensive rats". *Am J Physiol Heart Circ Physiol* **295**: H2455-2465.

69. **Ellis EF, Police RJ, Yancey L, et al.** (1990) "Dilation of cerebral arterioles by cytochrome P-450 metabolites of arachidonic acid". *Am J Physiol* **259**: H1171-1177.

70. **Fairbanks SL, Young JM, Nelson JW, et al.** (2012) "Mechanism of the sex difference in neuronal ischemic cell death". *Neuroscience* **219**: 183-191.

71. **Fang X, Hu S, Xu B, et al.** (2006) "14,15-Dihydroxyeicosatrienoic acid activates peroxisome proliferator-activated receptor-alpha". *Am J Physiol Heart Circ Physiol* **290**: H55-63.

72. **Faraci FM, Lynch C, and Lamping KG**. (2004) "Responses of cerebral arterioles to ADP: eNOS-dependent and eNOS-independent mechanisms". *Am J Physiol Heart Circ Physiol* **287**: H2871-2876.

73. **Fava C, Montagnana M, Almgren P, et al.** (2008) "The V433M variant of the CYP4F2 is associated with ischemic stroke in male Swedes beyond its effect on blood pressure". *Hypertension* **52**: 373-380.

74. **Ferreiro-Vera C, Mata-Granados JM, Priego-Capote F, et al.** (2011a) "Automated method for targeting analysis of prostanoids in human serum by on-line solid-phase extraction and liquid chromatography-mass spectrometry in selected reaction monitoring". *J Chromatogr A* **1218**: 2848-2855.

75. **Ferreiro-Vera C, Mata-Granados JM, Priego-Capote F, et al.** (2011b) "Automated targeting analysis of eicosanoid inflammation biomarkers in human serum and in the exometabolome of stem cells by SPE-LC-MS/MS". *Anal Bioanal Chem* **399**: 1093-1103.

76. **Filosa JA, and Blanco VM**. (2007) "Neurovascular coupling in the mammalian brain". *Exp Physiol* **92**: 641-646.

77. **Fink EL, Alexander H, Marco CD, et al.** (2004) "Experimental model of pediatric asphyxial cardiopulmonary arrest in rats". *Pediatr Crit Care Med* **5**: 139-144.

78. **Fischer D, Landmesser U, Spiekermann S, et al.** (2007) "Cytochrome P450 2C9 is involved in flow-dependent vasodilation of peripheral conduit arteries in healthy subjects and in patients with chronic heart failure". *Eur J Heart Fail* **9**: 770-775.

79. **Fischer M, and Hossmann KA**. (1995) "No-reflow after cardiac arrest". *Intensive Care Med* **21**: 132-141.

80. **Fisher M, and Brott TG**. (2003) "Emerging therapies for acute ischemic stroke: new therapies on trial". *Stroke* **34**: 359-361.

81. **Fisher M, Feuerstein G, Howells DW, et al.** (2009) "Update of the stroke therapy academic industry roundtable preclinical recommendations". *Stroke* **40**: 2244-2250.

82. **Fleming I** (2007) "Epoxyeicosatrienoic acids, cell signaling and angiogenesis". *Prostaglandins Other Lipid Mediat* **82**: 60-67.

83. **Fornage M, Lee CR, Doris PA, et al.** (2005) "The soluble epoxide hydrolase gene harbors sequence variation associated with susceptibility to and protection from incident ischemic stroke". *Hum Mol Genet* **14**: 2829-2837.

84. **Frykholm P, Andersson JL, Valtysson J, et al.** (2000) "A metabolic threshold of irreversible ischemia demonstrated by PET in a middle cerebral artery occlusion-reperfusion primate model". *Acta Neurol Scand* **102**: 18-26.

85. **Fu Z, Nakayama T, Sato N, et al.** (2008a) "Haplotype-based case study of human CYP4A11 gene and cerebral infarction in Japanese subject". *Endocrine* **33**: 215-222.

86. **Fu Z, Nakayama T, Sato N, et al.** (2008b) "A haplotype of the CYP4F2 gene is associated with cerebral infarction in Japanese men". *Am J Hypertens* **21**: 1216-1223.

87. **Gainer JV, Bellamine A, Dawson EP, et al.** (2005) "Functional variant of CYP4A11 20-hydroxyeicosatetraenoic acid synthase is associated with essential hypertension". *Circulation* **111**: 63-69.

88. **Gando S, Kameue T, Nanzaki S, et al.** (1997) "Massive fibrin formation with consecutive impairment of fibrinolysis in patients with out-of-hospital cardiac arrest". *Thromb Haemost* **77**: 278-282.

89. **Gardiner M, Nilsson B, Rehncrona S, et al.** (1981) "Free fatty acids in the rat brain in moderate and severe hypoxia". *J Neurochem* **36**: 1500-1505.

90. **Gebremedhin D, Lange AR, Lowry TF, et al.** (2000) "Production of 20-HETE and its role in autoregulation of cerebral blood flow". *Circ Res* **87**: 60-65.

91. **Gebremedhin D, Ma YH, Falck JR, et al.** (1992) "Mechanism of action of cerebral epoxyeicosatrienoic acids on cerebral arterial smooth muscle". *Am J Physiol* **263**: H519-525.

92. **Geraghty MC, and Torbey MT**. (2006) "Neuroimaging and serologic markers of neurologic injury after cardiac arrest". *Neurol Clin* **24**: 107-121, vii.

93. **Girouard H, and Iadecola C**. (2006) "Neurovascular coupling in the normal brain and in hypertension, stroke, and Alzheimer disease". *J Appl Physiol* **100**: 328-335.

94. **Goldberg WJ, Kadingo RM, and Barrett JN**. (1986) "Effects of ischemia-like conditions on cultured neurons: protection by low Na+, low Ca2+ solutions". *J Neurosci* **6**: 3144-3151.

95. **Goldstein LB, Adams R, Becker K, et al.** (2001) "Primary prevention of ischemic stroke: A statement for healthcare professionals from the Stroke Council of the American Heart Association". *Circulation* **103**: 163-182.

96. **Golomb MR, Fullerton HJ, Nowak-Gottl U, et al.** (2009) "Male predominance in childhood ischemic stroke: findings from the international pediatric stroke study". *Stroke* **40**: 52-57.

97. **Goplerud JM, Wagerle LC, and Delivoria-Papadopoulos M**. (1989) "Regional cerebral blood flow response during and after acute asphyxia in newborn piglets". *J Appl Physiol* **66**: 2827-2832.

98. **Greenberg S, and Kadowitz PJ**. (1982) "Difference in prostaglandin modulation of arterial and venous smooth muscle responses to bradykinin and norepinephrine". *Methods Find Exp Clin Pharmacol* **4**: 7-24.

99. **Gryglewski RJ** (2008) "Prostacyclin among prostanoids". *Pharmacol Rep* **60**: 3-11.

100. **Gschwendtner A, Ripke S, Freilinger T, et al.** (2008) "Genetic variation in soluble epoxide hydrolase (EPHX2) is associated with an increased risk of ischemic stroke in white Europeans". *Stroke* **39**: 1593-1596.

101. **Hallenbeck JM, Leitch DR, Dutka AJ, et al.** (1982) "Prostaglandin I2, indomethacin, and heparin promote postischemic neuronal recovery in dogs". *Ann Neurol* **12**: 145-156.

102. **Hamel E** (2006) "Perivascular nerves and the regulation of cerebrovascular tone". *J Appl Physiol* **100**: 1059-1064.

103. **Hao CM, and Breyer MD**. (2007) "Physiologic and pathophysiologic roles of lipid mediators in the kidney". *Kidney Int* **71**: 1105-1115.

104. **Harder DR, Alkayed NJ, Lange AR, et al.** (1998) "Functional hyperemia in the brain: hypothesis for astrocyte-derived vasodilator metabolites". *Stroke* **29**: 229-234.

105. **Harder DR, Roman RJ, and Gebremedhin D**. (2000) "Molecular mechanisms controlling nutritive blood flow: role of cytochrome P450 enzymes". *Acta Physiol Scand* **168**: 543-549.

106. **Hardwick JP, Song BJ, Huberman E, et al.** (1987) "Isolation, complementary DNA sequence, and regulation of rat hepatic lauric acid omega-hydroxylase (cytochrome P-450LA omega). Identification of a new cytochrome P-450 gene family". *J Biol Chem* **262**: 801-810.

107. **Hasan N, McColgan P, Bentley P, et al.** (2012) "Towards the identification of blood biomarkers for acute stroke in humans: a comprehensive systematic review". *Br J Clin Pharmacol* **74**: 230-240.

108. **Hayashi S, Park MK, and Kuehl TJ**. (1985) "Relaxant and contractile responses to prostaglandins in premature, newborn and adult baboon cerebral arteries". *J Pharmacol Exp Ther* **233**: 628-635.

109. **Hedlund E, Gustafsson JA, and Warner M**. (2001) "Cytochrome P450 in the brain; a review". *Curr Drug Metab* **2**: 245-263.

110. **Heiss WD, Grond M, Thiel A, et al.** (1998) "Tissue at risk of infarction rescued by early reperfusion: a positron emission tomography study in systemic recombinant tissue plasminogen activator thrombolysis of acute stroke". *J Cereb Blood Flow Metab* **18**: 1298-1307.

111. **Helvig C, Dishman E, and Capdevila JH**. (1998) "Molecular, enzymatic, and regulatory characterization of rat kidney cytochromes P450 4A2 and 4A3". *Biochemistry* **37**: 12546-12558.

112. **Henden T, Strand H, Borde E, et al.** (1993) "Measurements of leukotrienes in human plasma by solid phase extraction and high performance liquid chromatography". *Prostaglandins Leukot Essent Fatty Acids* **49**: 851-854.

113. **Hendrich KS, Kochanek PM, Williams DS, et al.** (1999) "Early perfusion after controlled cortical impact in rats: quantification by arterial spin-labeled MRI and the influence of spin-lattice relaxation time heterogeneity". *Magn Reson Med* **42**: 673-681.

114. **Herlitz J, Engdahl J, Svensson L, et al.** (2005) "Characteristics and outcome among children suffering from out of hospital cardiac arrest in Sweden". *Resuscitation* **64**: 37-40.

115. **Hickey RW, Cohen DM, Strausbaugh S, et al.** (1995) "Pediatric patients requiring CPR in the prehospital setting". *Ann Emerg Med* **25**: 495-501.

116. **Hillered L, Hallstrom A, Segersvard S, et al.** (1989) "Dynamics of extracellular metabolites in the striatum after middle cerebral artery occlusion in the rat monitored by intracerebral microdialysis". *J Cereb Blood Flow Metab* **9**: 607-616.

117. **Hillig T, Krustrup P, Fleming I, et al.** (2003) "Cytochrome P450 2C9 plays an important role in the regulation of exercise-induced skeletal muscle blood flow and oxygen uptake in humans". *J Physiol* **546**: 307-314.

118. **Hoebel BG, and Graier WF**. (1998) "11,12-Epoxyeicosatrienoic acid stimulates tyrosine kinase activity in porcine aortic endothelial cells". *Eur J Pharmacol* **346**: 115-117.

119. **Hofer G, Bieglmayer C, Kopp B, et al.** (1993) "Measurement of eicosanoids in menstrual fluid by the combined use of high pressure chromatography and radioimmunoassay". *Prostaglandins* **45**: 413-426.

120. **Horiuchi T, Dietrich HH, Hongo K, et al.** (2002) "Mechanism of extracellular K+-induced local and conducted responses in cerebral penetrating arterioles". *Stroke* **33**: 2692-2699.

121. **Hornfelt M, Edstrom A, and Ekstrom PA**. (1999a) "Upregulation of cytosolic phospholipase A2 correlates with apoptosis in mouse superior cervical and dorsal root ganglia neurons". *Neurosci Lett* **265**: 87-90.

122. **Hornfelt M, Ekstrom PA, and Edstrom A**. (1999b) "Involvement of axonal phospholipase A2 activity in the outgrowth of adult mouse sensory axons in vitro". *Neuroscience* **91**: 1539-1547.

123. **Hornsten L, Bylund J, and Oliw EH**. (1996) "Dexamethasone induces bisallylic hydroxylation of polyunsaturated fatty acids by rat liver microsomes". *Arch Biochem Biophys* **332**: 261-268.

124. **Hugon J, Vallat JM, and Dumas M**. (1996) "[Role of glutamate and excitotoxicity in neurologic diseases]". *Rev Neurol (Paris)* **152**: 239-248.

125. **Iadecola C, and Gorelick PB**. (2004) "Hypertension, angiotensin, and stroke: beyond blood pressure". *Stroke* **35**: 348-350.

126. **Iliff JJ, and Alkayed NJ**. (2009a) "Soluble Epoxide Hydrolase Inhibition: Targeting Multiple Mechanisms of Ischemic Brain Injury with a Single Agent". *Future Neurol* **4**: 179-199.

127. **Iliff JJ, Jia J, Nelson J, et al.** (2010) "Epoxyeicosanoid signaling in CNS function and disease". *Prostaglandins Other Lipid Mediat* **91**: 68-84.

128. **Iliff JJ, Wang R, Zeldin DC, et al.** (2009b) "Epoxyeicosanoids as mediators of neurogenic vasodilation in cerebral vessels". *Am J Physiol Heart Circ Physiol* **296**: H1352-1363.

129. **Imig JD** (2012) "Epoxides and soluble epoxide hydrolase in cardiovascular physiology". *Physiol Rev* **92**: 101-130.

130. **Imig JD, Falck JR, and Inscho EW**. (1999) "Contribution of cytochrome P450 epoxygenase and hydroxylase pathways to afferent arteriolar autoregulatory responsiveness". *Br J Pharmacol* **127**: 1399-1405.

131. **Imig JD, and Hammock BD**. (2009) "Soluble epoxide hydrolase as a therapeutic target for cardiovascular diseases". *Nat Rev Drug Discov* **8**: 794-805.

132. **Imig JD, Simpkins AN, Renic M, et al.** (2011) "Cytochrome P450 eicosanoids and cerebral vascular function". *Expert Rev Mol Med* **13**: e7.

133. **Imig JD, Zhao X, Zaharis CZ, et al.** (2005) "An orally active epoxide hydrolase inhibitor lowers blood pressure and provides renal protection in salt-sensitive hypertension". *Hypertension* **46**: 975-981.

134. **Ishizuka T, Cheng J, Singh H, et al.** (2008) "20-Hydroxyeicosatetraenoic acid stimulates nuclear factor-kappaB activation and the production of inflammatory cytokines in human endothelial cells". *J Pharmacol Exp Ther* **324**: 103-110.

135. **Ito O, Alonso-Galicia M, Hopp KA, et al.** (1998) "Localization of cytochrome P-450 4A isoforms along the rat nephron". *Am J Physiol* **274**: F395-404.

136. **Iwamoto N, Kobayashi K, and Kosaka K**. (1989) "The formation of prostaglandins in the postmortem cerebral cortex of Alzheimer-type dementia patients". *J Neurol* **236**: 80-84.

137. **Jadhav V, Jabre A, Lin SZ, et al.** (2004) "EP1- and EP3-receptors mediate prostaglandin E2-induced constriction of porcine large cerebral arteries". *J Cereb Blood Flow Metab* **24**: 1305-1316.

138. **Jiang C, and Haddad GG**. (1992) "Differential responses of neocortical neurons to glucose and/or O2 deprivation in the human and rat". *J Neurophysiol* **68**: 2165-2173.

139. **Kaduce TL, Fang X, Harmon SD, et al.** (2004) "20-hydroxyeicosatetraenoic acid (20-HETE) metabolism in coronary endothelial cells". *J Biol Chem* **279**: 2648-2656.

140. **Kagstrom E, Smith ML, and Siesjo BK**. (1983a) "Cerebral circulatory responses to hypercapnia and hypoxia in the recovery period following complete and incomplete cerebral ischemia in the rat". *Acta Physiol Scand* **118**: 281-291.

141. **Kagstrom E, Smith ML, and Siesjo BK**. (1983b) "Local cerebral blood flow in the recovery period following complete cerebral ischemia in the rat". *J Cereb Blood Flow Metab* **3**: 170-182.

142. **Katsuki H, and Okuda S**. (1995) "Arachidonic acid as a neurotoxic and neurotrophic substance". *Prog Neurobiol* **46**: 607-636.

143. **Katz L, Ebmeyer U, Safar P, et al.** (1995) "Outcome model of asphyxial cardiac arrest in rats". *J Cereb Blood Flow Metab* **15**: 1032-1039.

144. **Kee DB, Jr., and Wood JH**. (1984) "Rheology of the cerebral circulation". *Neurosurgery* **15**: 125-131.

145. **Kehl F, Cambj-Sapunar L, Maier KG, et al.** (2002) "20-HETE contributes to the acute fall in cerebral blood flow after subarachnoid hemorrhage in the rat". *Am J Physiol Heart Circ Physiol* **282**: H1556-1565.

146. **Kelly PJ, Hedley-Whyte ET, Primavera J, et al.** (2001) "Diffusion MRI in ischemic stroke compared to pathologically verified infarction". *Neurology* **56**: 914-920.

147. **Kempski O, Shohami E, von Lubitz D, et al.** (1987) "Postischemic production of eicosanoids in gerbil brain". *Stroke* **18**: 111-119.

148. **Keseru B, Barbosa-Sicard E, Schermuly RT, et al.** (2010) "Hypoxia-induced pulmonary hypertension: comparison of soluble epoxide hydrolase deletion vs. inhibition". *Cardiovasc Res* **85**: 232-240.

149. **Kikuta Y, Kasyu H, Kusunose E, et al.** (2000) "Expression and catalytic activity of mouse leukotriene B4 omega-hydroxylase, CYP4F14". *Arch Biochem Biophys* **383**: 225-232.

150. **Kim D, Sladek CD, Aguado-Velasco C, et al.** (1995) "Arachidonic acid activation of a new family of K+ channels in cultured rat neuronal cells". *J Physiol* **484 (Pt 3)**: 643-660.

151. **Kim IH, Morisseau C, Watanabe T, et al.** (2004) "Design, synthesis, and biological activity of 1,3-disubstituted ureas as potent inhibitors of the soluble epoxide hydrolase of increased water solubility". *J Med Chem* **47**: 2110-2122.

152. **Kirino T** (1994) "[Cerebral ischemia and neuronal death]". *No To Hattatsu* **26**: 130-135.

153. **Kishimoto K, Matsumura K, Kataoka Y, et al.** (1999) "Localization of cytosolic phospholipase A2 messenger RNA mainly in neurons in the rat brain". *Neuroscience* **92**: 1061-1077.

154. **Kiss L, Bieniek E, Weissmann N, et al.** (1998) "Simultaneous analysis of 4- and 5-series lipoxygenase and cytochrome P450 products from different biological sources by reversed-phase high-performance liquid chromatographic technique". *Anal Biochem* **261**: 16-28.

155. **Koehler RC, Gebremedhin D, and Harder DR**. (2006) "Role of astrocytes in cerebrovascular regulation". *J Appl Physiol* **100**: 307-317.

156. **Koehler RC, Roman RJ, and Harder DR**. (2009) "Astrocytes and the regulation of cerebral blood flow". *Trends Neurosci* **32**: 160-169.

157. **Koerner IP, Jacks R, DeBarber AE, et al.** (2007) "Polymorphisms in the human soluble epoxide hydrolase gene EPHX2 linked to neuronal survival after ischemic injury". *J Neurosci* **27**: 4642-4649.

158. **Komaba J, Matsuda D, Shibakawa K, et al.** (2009) "Development and validation of an on-line two-dimensional reversed-phase liquid chromatography-tandem mass spectrometry method for the simultaneous determination of prostaglandins E(2) and F(2alpha) and 13,14-dihydro-15-keto prostaglandin F(2alpha) levels in human plasma". *Biomed Chromatogr* **23**: 315-323.

159. **Konkel A, and Schunck WH**. (2011) "Role of cytochrome P450 enzymes in the bioactivation of polyunsaturated fatty acids". *Biochim Biophys Acta* **1814**: 210-222.

160. **Kontos HA, Wei EP, Navari RM, et al.** (1978) "Responses of cerebral arteries and arterioles to acute hypotension and hypertension". *Am J Physiol* **234**: H371-383.

161. **Krep H, Brinker G, Schwindt W, et al.** (2000) "Endothelin type A-antagonist improves long-term neurological recovery after cardiac arrest in rats". *Crit Care Med* **28**: 2873-2880.

162. **Krep H, Fischer M, and Hoeft A**. (2003) "Endothelin-1 elevates regional cerebral perfusion during prolonged ventricular fibrillation cardiac arrest in pigs". *Resuscitation* **57**: 317-318.

163. **Krizanac-Bengez L, Mayberg MR, and Janigro D**. (2004) "The cerebral vasculature as a therapeutic target for neurological disorders and the role of shear stress in vascular homeostatis and pathophysiology". *Neurol Res* **26**: 846-853.

164. **Kroetz DL, and Xu F**. (2005) "Regulation and inhibition of arachidonic acid omega-hydroxylases and 20-HETE formation". *Annu Rev Pharmacol Toxicol* **45**: 413-438.

165. **Kudo I, and Murakami M**. (2002) "Phospholipase A2 enzymes". *Prostaglandins Other Lipid Mediat* **68-69**: 3-58.

166. **Kulik T, Kusano Y, Aronhime S, et al.** (2008) "Regulation of cerebral vasculature in normal and ischemic brain". *Neuropharmacology* **55**: 281-288.

167. **Lasker JM, Chen WB, Wolf I, et al.** (2000) "Formation of 20-hydroxyeicosatetraenoic acid, a vasoactive and natriuretic eicosanoid, in human kidney. Role of Cyp4F2 and Cyp4A11". *J Biol Chem* **275**: 4118-4126.

168. **Lauritzen I, Heurteaux C, and Lazdunski M**. (1994) "Expression of group II phospholipase A2 in rat brain after severe forebrain ischemia and in endotoxic shock". *Brain Res* **651**: 353-356.

169. **Lee HC, Lu T, Weintraub NL, et al.** (1999) "Effects of epoxyeicosatrienoic acids on the cardiac sodium channels in isolated rat ventricular myocytes". *J Physiol* **519 Pt 1**: 153-168.

170. **Lee J, Dahl M, Grande P, et al.** (2010) "Genetically reduced soluble epoxide hydrolase activity and risk of stroke and other cardiovascular disease". *Stroke* **41**: 27-33.

171. **Leffler CW, Busija DW, Mirro R, et al.** (1989) "Effects of ischemia on brain blood flow and oxygen consumption of newborn pigs". *Am J Physiol* **257**: H1917-1926.

172. **Lenaz G** (1979) "The role of lipids in the structure and function of membranes". *Subcell Biochem* **6**: 233-343.

173. **Li DY, Varma DR, and Chemtob S**. (1994) "Ontogenic increase in PGE2 and PGF2 alpha receptor density in brain microvessels of pigs". *Br J Pharmacol* **112**: 59-64.

174. **Li R, Xu X, Chen C, et al.** (2012) "Cytochrome P450 2J2 is protective against global cerebral ischemia in transgenic mice". *Prostaglandins Other Lipid Mediat* **99**: 68-78.

175. **Li W, Wu S, Hickey RW, et al.** (2008) "Neuronal cyclooxygenase-2 activity and prostaglandins PGE2, PGD2, and PGF2 alpha exacerbate hypoxic neuronal injury in neuron-enriched primary culture". *Neurochem Res* **33**: 490-499.

176. **Liachenko S, Tang P, Hamilton RL, et al.** (2001) "Regional dependence of cerebral reperfusion after circulatory arrest in rats". *J Cereb Blood Flow Metab* **21**: 1320-1329.

177. **Liachenko S, Tang P, Hamilton RL, et al.** (1998) "A reproducible model of circulatory arrest and remote resuscitation in rats for NMR investigation". *Stroke* **29**: 1229-1238; discussion 1238-1229.

178. **Lima IV, Bastos LF, Limborco-Filho M, et al.** (2012) "Role of prostaglandins in neuroinflammatory and neurodegenerative diseases". *Mediators Inflamm* **2012**: 946813.

179. **Lindauer U, Megow D, Schultze J, et al.** (1996) "Nitric oxide synthase inhibition does not affect somatosensory evoked potentials in the rat". *Neurosci Lett* **216**: 207-210.

180. **Lippton HL, Paustian PW, Mellion BT, et al.** (1979) "Cardiovascular actions of prostacyclin (PGI2) in the cat". *Arch Int Pharmacodyn Ther* **241**: 121-130.

181. **Lipton P** (1999) "Ischemic cell death in brain neurons". *Physiol Rev* **79**: 1431-1568.

182. **Liu B, Luo W, Zhang Y, et al.** (2012) "Concomitant activation of functionally opposing prostacyclin and thromboxane prostanoid receptors by cyclo-oxygenase-1-mediated prostacyclin synthesis in mouse arteries". *Exp Physiol* **97**: 895-904.

183. **Liu D, Wu L, Breyer R, et al.** (2005a) "Neuroprotection by the PGE2 EP2 receptor in permanent focal cerebral ischemia". *Ann Neurol* **57**: 758-761.

184. **Liu H, Li W, Ahmad M, et al.** (2011) "Modification of ubiquitin-C-terminal hydrolase-L1 by cyclopentenone prostaglandins exacerbates hypoxic injury". *Neurobiol Dis* **41**: 318-328.

185. **Liu H, Li W, Ahmad M, et al.** (2013a) "Increased generation of cyclopentenone prostaglandins after brain ischemia and their role in aggregation of ubiquitinated proteins in neurons". *Neurotox Res* **24**: 191-204.

186. **Liu H, Rose ME, Miller TM, et al.** (2013b) "COX2-derived primary and cyclopentenone prostaglandins are increased after asphyxial cardiac arrest". *Brain Res* **1519**: 71-77.

187. **Liu M, and Alkayed NJ**. (2005b) "Hypoxic preconditioning and tolerance via hypoxia inducible factor (HIF) 1alpha-linked induction of P450 2C11 epoxygenase in astrocytes". *J Cereb Blood Flow Metab* **25**: 939-948.

188. **Liu M, Hurn PD, and Alkayed NJ**. (2004) "Cytochrome P450 in neurological disease". *Curr Drug Metab* **5**: 225-234.

189. **Liu X, Li C, Falck JR, et al.** (2008) "Interaction of nitric oxide, 20-HETE, and EETs during functional hyperemia in whisker barrel cortex". *Am J Physiol Heart Circ Physiol* **295**: H619-631.

190. **Lloyd-Jones D, Adams R, Carnethon M, et al.** (2009) "Heart disease and stroke statistics--2009 update: a report from the American Heart Association Statistics Committee and Stroke Statistics Subcommittee". *Circulation* **119**: 480-486.

191. **Longa EZ, Weinstein PR, Carlson S, et al.** (1989) "Reversible middle cerebral artery occlusion without craniectomy in rats". *Stroke* **20**: 84-91.

192. **Loot AE, Popp R, Fisslthaler B, et al.** (2008) "Role of cytochrome P450-dependent transient receptor potential V4 activation in flow-induced vasodilatation". *Cardiovasc Res* **80**: 445-452.

193. **Lu T, Hoshi T, Weintraub NL, et al.** (2001a) "Activation of ATP-sensitive K(+) channels by epoxyeicosatrienoic acids in rat cardiac ventricular myocytes". *J Physiol* **537**: 811-827.

194. **Lu T, Katakam PV, VanRollins M, et al.** (2001b) "Dihydroxyeicosatrienoic acids are potent activators of Ca(2+)-activated K(+) channels in isolated rat coronary arterial myocytes". *J Physiol* **534**: 651-667.

195. **Ma J, Ayata C, Huang PL, et al.** (1996) "Regional cerebral blood flow response to vibrissal stimulation in mice lacking type I NOS gene expression". *Am J Physiol* **270**: H1085-1090.

196. **Maier KG, and Roman RJ**. (2001) "Cytochrome P450 metabolites of arachidonic acid in the control of renal function". *Curr Opin Nephrol Hypertens* **10**: 81-87.

197. **Manole MD, Foley LM, Hitchens TK, et al.** (2009) "Magnetic resonance imaging assessment of regional cerebral blood flow after asphyxial cardiac arrest in immature rats". *J Cereb Blood Flow Metab* **29**: 197-205.

198. **Manole MD, Hickey RW, Clark RS, et al.** (2008) "Current and future therapies of pediatric cardiopulmonary arrest". *Indian J Pediatr* **75**: 609-614.

199. **Manole MD, Kochanek PM, Foley LM, et al.** (2012) "Polynitroxyl albumin and albumin therapy after pediatric asphyxial cardiac arrest: effects on cerebral blood flow and neurologic outcome". *J Cereb Blood Flow Metab* **32**: 560-569.

200. **Marshall JW, Duffin KJ, Green AR, et al.** (2001) "NXY-059, a free radical--trapping agent, substantially lessens the functional disability resulting from cerebral ischemia in a primate species". *Stroke* **32**: 190-198.

201. **Martin-Venegas R, Casillas R, Jauregui O, et al.** (2011) "Rapid simultaneous analysis of cyclooxygenase, lipoxygenase and cytochrome P-450 metabolites of arachidonic and linoleic acids using high performance liquid chromatography/mass spectrometry in tandem mode". *J Pharm Biomed Anal* **56**: 976-982.

202. **Martin LJ, Al-Abdulla NA, Brambrink AM, et al.** (1998) "Neurodegeneration in excitotoxicity, global cerebral ischemia, and target deprivation: A perspective on the contributions of apoptosis and necrosis". *Brain Res Bull* **46**: 281-309.

203. **Martin LJ, Brambrink A, Koehler RC, et al.** (1997) "Primary sensory and forebrain motor systems in the newborn brain are preferentially damaged by hypoxia-ischemia". *J Comp Neurol* **377**: 262-285.

204. **Marumo T, Eto K, Wake H, et al.** (2010) "The inhibitor of 20-HETE synthesis, TS-011, improves cerebral microcirculatory autoregulation impaired by middle cerebral artery occlusion in mice". *Br J Pharmacol* **161**: 1391-1402.

205. **Masoodi M, and Nicolaou A**. (2006) "Lipidomic analysis of twenty-seven prostanoids and isoprostanes by liquid chromatography/electrospray tandem mass spectrometry". *Rapid Commun Mass Spectrom* **20**: 3023-3029.

206. **Mattammal MB, Strong R, Lakshmi VM, et al.** (1995) "Prostaglandin H synthetase-mediated metabolism of dopamine: implication for Parkinson's disease". *J Neurochem* **64**: 1645-1654.

207. **Matuszewski BK, Constanzer ML, and Chavez-Eng CM**. (2003) "Strategies for the assessment of matrix effect in quantitative bioanalytical methods based on HPLC-MS/MS". *Anal Chem* **75**: 3019-3030.

208. **Mayeux R** (2004) "Biomarkers: potential uses and limitations". *NeuroRx* **1**: 182-188.

209. **McCullough L, Wu L, Haughey N, et al.** (2004) "Neuroprotective function of the PGE2 EP2 receptor in cerebral ischemia". *J Neurosci* **24**: 257-268.

210. **McIntyre M, Bohr DF, and Dominiczak AF**. (1999) "Endothelial function in hypertension: the role of superoxide anion". *Hypertension* **34**: 539-545.

211. **McNally B, Robb R, Mehta M, et al.** (2011) "Out-of-hospital cardiac arrest surveillance --- Cardiac Arrest Registry to Enhance Survival (CARES), United States, October 1, 2005--December 31, 2010". *MMWR Surveill Summ* **60**: 1-19.

212. **Meunier B, de Visser SP, and Shaik S**. (2004) "Mechanism of oxidation reactions catalyzed by cytochrome p450 enzymes". *Chem Rev* **104**: 3947-3980.

213. **Miller TM, Donnelly MK, Crago EA, et al.** (2009) "Rapid, simultaneous quantitation of mono and dioxygenated metabolites of arachidonic acid in human CSF and rat brain". *J Chromatogr B Analyt Technol Biomed Life Sci* **877**: 3991-4000.

214. **Miyata N, Seki T, Tanaka Y, et al.** (2005) "Beneficial effects of a new 20-hydroxyeicosatetraenoic acid synthesis inhibitor, TS-011 [N-(3-chloro-4-morpholin-4-yl) phenyl-N'-hydroxyimido formamide], on hemorrhagic and ischemic stroke". *J Pharmacol Exp Ther* **314**: 77-85.

215. **Mohri I, Kadoyama K, Kanekiyo T, et al.** (2007) "Hematopoietic prostaglandin D synthase and DP1 receptor are selectively upregulated in microglia and astrocytes within senile plaques from human patients and in a mouse model of Alzheimer disease". *J Neuropathol Exp Neurol* **66**: 469-480.

216. **Moncada S, and Vane JR**. (1978) "Pharmacology and endogenous roles of prostaglandin endoperoxides, thromboxane A2, and prostacyclin". *Pharmacol Rev* **30**: 293-331.

217. **Moncada S, and Vane JR**. (1979) "The role of prostacyclin in vascular tissue". *Fed Proc* **38**: 66-71.

218. **Montaner J, Alvarez-Sabin J, Molina C, et al.** (2001) "Matrix metalloproteinase expression after human cardioembolic stroke: temporal profile and relation to neurological impairment". *Stroke* **32**: 1759-1766.

219. **Montaner J, Mendioroz M, Delgado P, et al.** (2012) "Differentiating ischemic from hemorrhagic stroke using plasma biomarkers: the S100B/RAGE pathway". *J Proteomics* **75**: 4758-4765.

220. **Montaner J, Mendioroz M, Ribo M, et al.** (2011) "A panel of biomarkers including caspase-3 and D-dimer may differentiate acute stroke from stroke-mimicking conditions in the emergency department". *J Intern Med* **270**: 166-174.

221. **Montine TJ, Milatovic D, Gupta RC, et al.** (2002) "Neuronal oxidative damage from activated innate immunity is EP2 receptor-dependent". *J Neurochem* **83**: 463-470.

222. **Montine TJ, Sidell KR, Crews BC, et al.** (1999) "Elevated CSF prostaglandin E2 levels in patients with probable AD". *Neurology* **53**: 1495-1498.

223. **Moraes LA, Giner RM, Paul-Clark MJ, et al.** (2004) "An isocratic HPLC method for the quantitation of eicosanoids in human platelets". *Biomed Chromatogr* **18**: 64-68.

224. **Morisseau C, Goodrow MH, Dowdy D, et al.** (1999) "Potent urea and carbamate inhibitors of soluble epoxide hydrolases". *Proc Natl Acad Sci U S A* **96**: 8849-8854.

225. **Morisseau C, Goodrow MH, Newman JW, et al.** (2002) "Structural refinement of inhibitors of urea-based soluble epoxide hydrolases". *Biochem Pharmacol* **63**: 1599-1608.

226. **Mortberg E, Cumming P, Wiklund L, et al.** (2007) "A PET study of regional cerebral blood flow after experimental cardiopulmonary resuscitation". *Resuscitation* **75**: 98-104.

227. **Mu Y, Klamerus MM, Miller TM, et al.** (2008) "Intravenous formulation of N-hydroxy-N'-(4-n-butyl-2-methylphenyl)formamidine (HET0016) for inhibition of rat brain 20-hydroxyeicosatetraenoic acid formation". *Drug Metab Dispos* **36**: 2324-2330.

228. **Muthalif MM, Benter IF, Karzoun N, et al.** (1998) "20-Hydroxyeicosatetraenoic acid mediates calcium/calmodulin-dependent protein kinase II-induced mitogen-activated protein kinase activation in vascular smooth muscle cells". *Proc Natl Acad Sci U S A* **95**: 12701-12706.

229. **Nagao T, Illiano S, and Vanhoutte PM**. (1992) "Heterogeneous distribution of endothelium-dependent relaxations resistant to NG-nitro-L-arginine in rats". *Am J Physiol* **263**: H1090-1094.

230. **Nakano S, Kogure K, Abe K, et al.** (1990) "Ischemia-induced alterations in lipid metabolism of the gerbil cerebral cortex: I. Changes in free fatty acid liberation". *J Neurochem* **54**: 1911-1916.

231. **Narumiya S, Ogorochi T, Nakao K, et al.** (1982) "Prostaglandin D2 in rat brain, spinal cord and pituitary: basal level and regional distribution". *Life Sci* **31**: 2093-2103.

232. **Navarro-Sobrino M, Rosell A, Hernandez-Guillamon M, et al.** (2011) "A large screening of angiogenesis biomarkers and their association with neurological outcome after ischemic stroke". *Atherosclerosis* **216**: 205-211.

233. **Neumar RW, Bircher NG, Sim KM, et al.** (1995) "Epinephrine and sodium bicarbonate during CPR following asphyxial cardiac arrest in rats". *Resuscitation* **29**: 249-263.

234. **Newman JW, Morisseau C, and Hammock BD**. (2005) "Epoxide hydrolases: their roles and interactions with lipid metabolism". *Prog Lipid Res* **44**: 1-51.

235. **Newman JW, Morisseau C, Harris TR, et al.** (2003) "The soluble epoxide hydrolase encoded by EPXH2 is a bifunctional enzyme with novel lipid phosphate phosphatase activity". *Proc Natl Acad Sci U S A* **100**: 1558-1563.

236. **Ng VY, Huang Y, Reddy LM, et al.** (2007) "Cytochrome P450 eicosanoids are activators of peroxisome proliferator-activated receptor alpha". *Drug Metab Dispos* **35**: 1126-1134.

237. **Nieber K** (1999) "Hypoxia and neuronal function under in vitro conditions". *Pharmacol Ther* **82**: 71-86.

238. **Nishida N, Blood AB, Hunter CJ, et al.** (2006) "Role of prostanoids in the regulation of cerebral blood flow during normoxia and hypoxia in the fetal sheep". *Pediatr Res* **60**: 524-529.

239. **Nitatori T, Sato N, Waguri S, et al.** (1995) "Delayed neuronal death in the CA1 pyramidal cell layer of the gerbil hippocampus following transient ischemia is apoptosis". *J Neurosci* **15**: 1001-1011.

240. **Nithipatikom K, DiCamelli RF, Kohler S, et al.** (2001) "Determination of cytochrome P450 metabolites of arachidonic acid in coronary venous plasma during ischemia and reperfusion in dogs". *Anal Biochem* **292**: 115-124.

241. **Nithipatikom K, Gross ER, Endsley MP, et al.** (2004) "Inhibition of cytochrome P450omega-hydroxylase: a novel endogenous cardioprotective pathway". *Circ Res* **95**: e65-71.

242. **Node K, Huo Y, Ruan X, et al.** (1999) "Anti-inflammatory properties of cytochrome P450 epoxygenase-derived eicosanoids". *Science* **285**: 1276-1279.

243. **Nozari A, Rubertsson S, Gedeborg R, et al.** (1999) "Maximisation of cerebral blood flow during experimental cardiopulmonary resuscitation does not ameliorate post-resuscitation hypoperfusion". *Resuscitation* **40**: 27-35.

244. **Nozari A, Rubertsson S, and Wiklund L**. (2000) "Intra-aortic administration of epinephrine above an aortic balloon occlusion during experimental CPR does not further improve cerebral blood flow and oxygenation". *Resuscitation* **44**: 119-127.

245. **Oliw EH, Bylund J, and Herman C**. (1996) "Bisallylic hydroxylation and epoxidation of polyunsaturated fatty acids by cytochrome P450". *Lipids* **31**: 1003-1021.

246. **Oltman CL, Weintraub NL, VanRollins M, et al.** (1998) "Epoxyeicosatrienoic acids and dihydroxyeicosatrienoic acids are potent vasodilators in the canine coronary microcirculation". *Circ Res* **83**: 932-939.

247. **Omura T, and Sato R**. (1964) "The Carbon Monoxide-Binding Pigment of Liver Microsomes. Ii. Solubilization, Purification, and Properties". *J Biol Chem* **239**: 2379-2385.

248. **Omura T, and Sato R**. (1962) "A new cytochrome in liver microsomes". *J Biol Chem* **237**: 1375-1376.

249. **Omura T, Tanaka Y, Miyata N, et al.** (2006) "Effect of a new inhibitor of the synthesis of 20-HETE on cerebral ischemia reperfusion injury". *Stroke* **37**: 1307-1313.

250. **Ortiz de Montellano PR, and Reich NO**. (1984) "Specific inactivation of hepatic fatty acid hydroxylases by acetylenic fatty acids". *J Biol Chem* **259**: 4136-4141.

251. **Panerai RB** (2008) "Cerebral autoregulation: from models to clinical applications". *Cardiovasc Eng* **8**: 42-59.

252. **Panigrahy D, Kaipainen A, Greene ER, et al.** (2010) "Cytochrome P450-derived eicosanoids: the neglected pathway in cancer". *Cancer Metastasis Rev* **29**: 723-735.

253. **Peng X, Zhang C, Alkayed NJ, et al.** (2004) "Dependency of cortical functional hyperemia to forepaw stimulation on epoxygenase and nitric oxide synthase activities in rats". *J Cereb Blood Flow Metab* **24**: 509-517.

254. **Pepicelli O, Fedele E, Bonanno G, et al.** (2002) "In vivo activation of N-methyl-D-aspartate receptors in the rat hippocampus increases prostaglandin E(2) extracellular levels and triggers lipid peroxidation through cyclooxygenase-mediated mechanisms". *J Neurochem* **81**: 1028-1034.

255. **Perez-Chacon G, Astudillo AM, Balgoma D, et al.** (2009) "Control of free arachidonic acid levels by phospholipases A2 and lysophospholipid acyltransferases". *Biochim Biophys Acta* **1791**: 1103-1113.

256. **Phillis JW, and O'Regan MH**. (2004) "A potentially critical role of phospholipases in central nervous system ischemic, traumatic, and neurodegenerative disorders". *Brain Res Brain Res Rev* **44**: 13-47.

257. **Pignataro G, Meller R, Inoue K, et al.** (2008) "In vivo and in vitro characterization of a novel neuroprotective strategy for stroke: ischemic postconditioning". *J Cereb Blood Flow Metab* **28**: 232-241.

258. **Pilitsis JG, Coplin WM, O'Regan MH, et al.** (2003) "Measurement of free fatty acids in cerebrospinal fluid from patients with hemorrhagic and ischemic stroke". *Brain Res* **985**: 198-201.

259. **Pilitsis JG, Diaz FG, O'Regan MH, et al.** (2002) "Differential effects of phospholipase inhibitors on free fatty acid efflux in rat cerebral cortex during ischemia-reperfusion injury". *Brain Res* **951**: 96-106.

260. **Pilitsis JG, Diaz FG, Wellwood JM, et al.** (2001) "Quantification of free fatty acids in human cerebrospinal fluid". *Neurochem Res* **26**: 1265-1270.

261. **Poloyac SM, Zhang Y, Bies RR, et al.** (2006) "Protective effect of the 20-HETE inhibitor HET0016 on brain damage after temporary focal ischemia". *J Cereb Blood Flow Metab* **26**: 1551-1561.

262. **Powell PK, Wolf I, Jin R, et al.** (1998) "Metabolism of arachidonic acid to 20-hydroxy-5,8,11, 14-eicosatetraenoic acid by P450 enzymes in human liver: involvement of CYP4F2 and CYP4A11". *J Pharmacol Exp Ther* **285**: 1327-1336.

263. **Pradelles P, Grassi J, and Maclouf J**. (1990) "Enzyme immunoassays of eicosanoids using acetylcholinesterase". *Methods Enzymol* **187**: 24-34.

264. **Pratt PF, Falck JR, Reddy KM, et al.** (1998) "20-HETE relaxes bovine coronary arteries through the release of prostacyclin". *Hypertension* **31**: 237-241.

265. **Prough DS, Kong D, Watkins WD, et al.** (1986) "Inhibition of thromboxane A2 production does not improve post-ischemic brain hypoperfusion in the dog". *Stroke* **17**: 1272-1276.

266. **Qian L, Ding L, Cheng L, et al.** (2012) "Early biomarkers for post-stroke cognitive impairment". *J Neurol* **259**: 2111-2118.

267. **Ramos-Fernandez M, Bellolio MF, and Stead LG**. (2011) "Matrix metalloproteinase-9 as a marker for acute ischemic stroke: a systematic review". *J Stroke Cerebrovasc Dis* **20**: 47-54.

268. **Rehncrona S, Mela L, and Siesjo BK**. (1979) "Recovery of brain mitochondrial function in the rat after complete and incomplete cerebral ischemia". *Stroke* **10**: 437-446.

269. **Reich NO, and Ortiz de Montellano PR**. (1986) "Dissociation of increased lauric acid omega-hydroxylase activity from the antilipidemic action of clofibrate". *Biochem Pharmacol* **35**: 1227-1233.

270. **Renic M, Klaus JA, Omura T, et al.** (2009) "Effect of 20-HETE inhibition on infarct volume and cerebral blood flow after transient middle cerebral artery occlusion". *J Cereb Blood Flow Metab* **29**: 629-639.

271. **Renic M, Kumar SN, Gebremedhin D, et al.** (2012) "Protective effect of 20-HETE inhibition in a model of oxygen-glucose deprivation in hippocampal slice cultures". *Am J Physiol Heart Circ Physiol* **302**: H1285-1293.

272. **Roger VL, Go AS, Lloyd-Jones DM, et al.** (2012) "Heart disease and stroke statistics--2012 update: a report from the American Heart Association". *Circulation* **125**: e2-e220.

273. **Roggendorf W, and Cervos-Navarro J**. (1977) "Ultrastructure of arterioles in the cat brain". *Cell Tissue Res* **178**: 495-515.

274. **Roman RJ** (2002) "P-450 metabolites of arachidonic acid in the control of cardiovascular function". *Physiol Rev* **82**: 131-185.

275. **Rosenberger TA, Villacreses NE, Hovda JT, et al.** (2004) "Rat brain arachidonic acid metabolism is increased by a 6-day intracerebral ventricular infusion of bacterial lipopolysaccharide". *J Neurochem* **88**: 1168-1178.

276. **Sahu S, Kishore K, and Lata I**. (2010) "Better outcome after pediatric resuscitation is still a dilemma". *J Emerg Trauma Shock* **3**: 243-250.

277. **Saleem S, Ahmad AS, Maruyama T, et al.** (2009) "PGF(2alpha) FP receptor contributes to brain damage following transient focal brain ischemia". *Neurotox Res* **15**: 62-70.

278. **Saleem S, Li RC, Wei G, et al.** (2007) "Effects of EP1 receptor on cerebral blood flow in the middle cerebral artery occlusion model of stroke in mice". *J Neurosci Res* **85**: 2433-2440.

279. **Samuelsson B** (1987) "An elucidation of the arachidonic acid cascade. Discovery of prostaglandins, thromboxane and leukotrienes". *Drugs* **33 Suppl 1**: 2-9.

280. **Satoh T, Ishikawa Y, Kataoka Y, et al.** (1999) "CNS-specific prostacyclin ligands as neuronal survival-promoting factors in the brain". *Eur J Neurosci* **11**: 3115-3124.

281. **Schmued LC, Albertson C, and Slikker W, Jr.** (1997) "Fluoro-Jade: a novel fluorochrome for the sensitive and reliable histochemical localization of neuronal degeneration". *Brain Res* **751**: 37-46.

282. **Schwartzman ML, Falck JR, Yadagiri P, et al.** (1989) "Metabolism of 20-hydroxyeicosatetraenoic acid by cyclooxygenase. Formation and identification of novel endothelium-dependent vasoconstrictor metabolites". *J Biol Chem* **264**: 11658-11662.

283. **Shaffner DH, Eleff SM, Brambrink AM, et al.** (1999) "Effect of arrest time and cerebral perfusion pressure during cardiopulmonary resuscitation on cerebral blood flow, metabolism, adenosine triphosphate recovery, and pH in dogs". *Crit Care Med* **27**: 1335-1342.

284. **Shaffner DH, Eleff SM, Koehler RC, et al.** (1998) "Effect of the no-flow interval and hypothermia on cerebral blood flow and metabolism during cardiopulmonary resuscitation in dogs". *Stroke* **29**: 2607-2615.

285. **Shimizu S, Nagayama T, Jin KL, et al.** (2001) "bcl-2 Antisense treatment prevents induction of tolerance to focal ischemia in the rat brain". *J Cereb Blood Flow Metab* **21**: 233-243.

286. **Shohami E, Rosenthal J, and Lavy S**. (1982) "The effect of incomplete cerebral ischemia on prostaglandin levels in rat brain". *Stroke* **13**: 494-499.

287. **Simard M, Arcuino G, Takano T, et al.** (2003) "Signaling at the gliovascular interface". *J Neurosci* **23**: 9254-9262.

288. **Simpkins AN, Rudic RD, Schreihofer DA, et al.** (2009) "Soluble epoxide inhibition is protective against cerebral ischemia via vascular and neural protection". *Am J Pathol* **174**: 2086-2095.

289. **Simpson AE** (1997) "The cytochrome P450 4 (CYP4) family". *Gen Pharmacol* **28**: 351-359.

290. **Sinal CJ, Miyata M, Tohkin M, et al.** (2000) "Targeted disruption of soluble epoxide hydrolase reveals a role in blood pressure regulation". *J Biol Chem* **275**: 40504-40510.

291. **Smith WS** (2004) "Pathophysiology of focal cerebral ischemia: a therapeutic perspective". *J Vasc Interv Radiol* **15**: S3-12.

292. **Snyder JV, Nemoto EM, Carroll RG, et al.** (1975) "Global ischemia in dogs: intracranial pressures, brain blood flow and metabolism". *Stroke* **6**: 21-27.

293. **Sodhi K, Inoue K, Gotlinger KH, et al.** (2009) "Epoxyeicosatrienoic acid agonist rescues the metabolic syndrome phenotype of HO-2-null mice". *J Pharmacol Exp Ther* **331**: 906-916.

294. **Spector AA, Fang X, Snyder GD, et al.** (2004) "Epoxyeicosatrienoic acids (EETs): metabolism and biochemical function". *Prog Lipid Res* **43**: 55-90.

295. **Spector AA, and Norris AW**. (2007) "Action of epoxyeicosatrienoic acids on cellular function". *Am J Physiol Cell Physiol* **292**: C996-1012.

296. **Spiecker M, and Liao JK**. (2005) "Vascular protective effects of cytochrome p450 epoxygenase-derived eicosanoids". *Arch Biochem Biophys* **433**: 413-420.

297. **STAIR** (1999) "Recommendations for standards regarding preclinical neuroprotective and restorative drug development". *Stroke* **30**: 2752-2758.

298. **Strandgaard S, and Paulson OB**. (1984) "Cerebral autoregulation". *Stroke* **15**: 413-416.

299. **Su P, Kaushal KM, and Kroetz DL**. (1998) "Inhibition of renal arachidonic acid omega-hydroxylase activity with ABT reduces blood pressure in the SHR". *Am J Physiol* **275**: R426-438.

300. **Sun CW, Falck JR, Okamoto H, et al.** (2000) "Role of cGMP versus 20-HETE in the vasodilator response to nitric oxide in rat cerebral arteries". *Am J Physiol Heart Circ Physiol* **279**: H339-350.

301. **Sun GY, Su KL, Der OM, et al.** (1979) "Enzymic regulation of arachidonate metabolism in brain membrane phosphoglycerides". *Lipids* **14**: 229-235.

302. **Sun GY, Xu J, Jensen MD, et al.** (2004) "Phospholipase A2 in the central nervous system: implications for neurodegenerative diseases". *J Lipid Res* **45**: 205-213.

303. **Sun J, Sui X, Bradbury JA, et al.** (2002) "Inhibition of vascular smooth muscle cell migration by cytochrome p450 epoxygenase-derived eicosanoids". *Circ Res* **90**: 1020-1027.

304. **Swanson RA, Morton MT, Tsao-Wu G, et al.** (1990) "A semiautomated method for measuring brain infarct volume". *J Cereb Blood Flow Metab* **10**: 290-293.

305. **Sydserff SG, Borelli AR, Green AR, et al.** (2002) "Effect of NXY-059 on infarct volume after transient or permanent middle cerebral artery occlusion in the rat; studies on dose, plasma concentration and therapeutic time window". *Br J Pharmacol* **135**: 103-112.

306. **Takabatake M, Hishinuma T, Suzuki N, et al.** (2002) "Simultaneous quantification of prostaglandins in human synovial cell-cultured medium using liquid chromatography/tandem mass spectrometry". *Prostaglandins Leukot Essent Fatty Acids* **67**: 51-56.

307. **Takadera T, Yumoto H, Tozuka Y, et al.** (2002) "Prostaglandin E(2) induces caspase-dependent apoptosis in rat cortical cells". *Neurosci Lett* **317**: 61-64.

308. **Takagi K, Ginsberg MD, Globus MY, et al.** (1993) "Changes in amino acid neurotransmitters and cerebral blood flow in the ischemic penumbral region following middle cerebral artery occlusion in the rat: correlation with histopathology". *J Cereb Blood Flow Metab* **13**: 575-585.

309. **Takamatsu H, Tsukada H, Watanabe Y, et al.** (2002) "Specific ligand for a central type prostacyclin receptor attenuates neuronal damage in a rat model of focal cerebral ischemia". *Brain Res* **925**: 176-182.

310. **Takata K, Kitamura Y, Umeki M, et al.** (2003) "Possible involvement of small oligomers of amyloid-beta peptides in 15-deoxy-delta 12,14 prostaglandin J2-sensitive microglial activation". *J Pharmacol Sci* **91**: 330-333.

311. **Tanaka Y, Omura T, Fukasawa M, et al.** (2007) "Continuous inhibition of 20-HETE synthesis by TS-011 improves neurological and functional outcomes after transient focal cerebral ischemia in rats". *Neurosci Res* **59**: 475-480.

312. **Tassoni D, Kaur G, Weisinger RS, et al.** (2008) "The role of eicosanoids in the brain". *Asia Pac J Clin Nutr* **17 Suppl 1**: 220-228.

313. **Taylor SG, and Weston AH**. (1988) "Endothelium-derived hyperpolarizing factor: a new endogenous inhibitor from the vascular endothelium". *Trends Pharmacol Sci* **9**: 272-274.

314. **Terashvili M, Sarkar P, Nostrand MV, et al.** (2012) "The protective effect of astrocyte-derived 14,15-epoxyeicosatrienoic acid on hydrogen peroxide-induced cell injury in astrocyte-dopaminergic neuronal cell line co-culture". *Neuroscience* **223**: 68-76.

315. **Thornhill J, and Asselin J**. (1999) "Temperature and hemodynamic changes associated with increased neural damage to global hemispheric hypoxic ischemia by prior prostaglandin E2, D2 and F2alpha administration". *Prostaglandins Leukot Essent Fatty Acids* **61**: 207-217.

316. **Topjian AA, Berg RA, and Nadkarni VM**. (2008) "Pediatric cardiopulmonary resuscitation: advances in science, techniques, and outcomes". *Pediatrics* **122**: 1086-1098.

317. **Traystman RJ** (2003) "Animal models of focal and global cerebral ischemia". *ILAR J* **44**: 85-95.

318. **Traystman RJ, Kirsch JR, and Koehler RC**. (1991) "Oxygen radical mechanisms of brain injury following ischemia and reperfusion". *J Appl Physiol* **71**: 1185-1195.

319. **Tsai HJ, Hwang SH, Morisseau C, et al.** (2010) "Pharmacokinetic screening of soluble epoxide hydrolase inhibitors in dogs". *Eur J Pharm Sci* **40**: 222-238.

320. **Turner RC, Lucke-Wold B, Lucke-Wold N, et al.** (2013) "Neuroprotection for ischemic stroke: moving past shortcomings and identifying promising directions". *Int J Mol Sci* **14**: 1890-1917.

321. **Unterberg A, Wahl M, Hammersen F, et al.** (1987) "Permeability and vasomotor response of cerebral vessels during exposure to arachidonic acid". *Acta Neuropathol* **73**: 209-219.

322. **Unterwurzacher I, Koal T, Bonn GK, et al.** (2008) "Rapid sample preparation and simultaneous quantitation of prostaglandins and lipoxygenase derived fatty acid metabolites by liquid chromatography-mass spectrometry from small sample volumes". *Clin Chem Lab Med* **46**: 1589-1597.

323. **van den Kerckhoff W, Hossmann KA, and Hossmann V**. (1983) "No effect of prostacyclin on blood flow, regulation of blood flow and blood coagulation following global cerebral ischemia". *Stroke* **14**: 724-730.

324. **VanderNoot VA, and VanRollins M**. (2002) "Capillary electrophoresis of cytochrome P-450 epoxygenase metabolites of arachidonic acid. 1. Resolution of regioisomers". *Anal Chem* **74**: 5859-5865.

325. **Verity MA** (1993) "Mechanisms of phospholipase A2 activation and neuronal injury". *Ann N Y Acad Sci* **679**: 110-120.

326. **Viswanathan CT, Bansal S, Booth B, et al.** (2007) "Quantitative bioanalytical methods validation and implementation: best practices for chromatographic and ligand binding assays". *Pharm Res* **24**: 1962-1973.

327. **Wagerle LC, and Mishra OP**. (1988) "Mechanism of CO2 response in cerebral arteries of the newborn pig: role of phospholipase, cyclooxygenase, and lipoxygenase pathways". *Circ Res* **62**: 1019-1026.

328. **Walton M, Sirimanne E, Williams C, et al.** (1997) "Prostaglandin H synthase-2 and cytosolic phospholipase A2 in the hypoxic-ischemic brain: role in neuronal death or survival?". *Brain Res Mol Brain Res* **50**: 165-170.

329. **Warner M, Kohler C, Hansson T, et al.** (1988) "Regional distribution of cytochrome P-450 in the rat brain: spectral quantitation and contribution of P-450b,e, and P-450c,d". *J Neurochem* **50**: 1057-1065.

330. **Weigl M, Tenze G, Steinlechner B, et al.** (2005) "A systematic review of currently available pharmacological neuroprotective agents as a sole intervention before anticipated or induced cardiac arrest". *Resuscitation* **65**: 21-39.

331. **Whetsell WO, Jr.** (1996) "Current concepts of excitotoxicity". *J Neuropathol Exp Neurol* **55**: 1-13.

332. **Widlansky ME, Gokce N, Keaney JF, Jr., et al.** (2003) "The clinical implications of endothelial dysfunction". *J Am Coll Cardiol* **42**: 1149-1160.

333. **Williams DS, Detre JA, Leigh JS, et al.** (1992) "Magnetic resonance imaging of perfusion using spin inversion of arterial water". *Proc Natl Acad Sci U S A* **89**: 212-216.

334. **Wright DH, Abran D, Bhattacharya M, et al.** (2001) "Prostanoid receptors: ontogeny and implications in vascular physiology". *Am J Physiol Regul Integr Comp Physiol* **281**: R1343-1360.

335. **Wu S, Chen W, Murphy E, et al.** (1997) "Molecular cloning, expression, and functional significance of a cytochrome P450 highly expressed in rat heart myocytes". *J Biol Chem* **272**: 12551-12559.

336. **Xu F, Straub WO, Pak W, et al.** (2002a) "Antihypertensive effect of mechanism-based inhibition of renal arachidonic acid omega-hydroxylase activity". *Am J Physiol Regul Integr Comp Physiol* **283**: R710-720.

337. **Xu SY, and Pan SY**. (2013) "The failure of animal models of neuroprotection in acute ischemic stroke to translate to clinical efficacy". *Med Sci Monit Basic Res* **19**: 37-45.

338. **Xu Y, Liachenko S, and Tang P**. (2002b) "Dependence of early cerebral reperfusion and long-term outcome on resuscitation efficiency after cardiac arrest in rats". *Stroke* **33**: 837-843.

339. **Yang G, Chen G, Ebner TJ, et al.** (1999) "Nitric oxide is the predominant mediator of cerebellar hyperemia during somatosensory activation in rats". *Am J Physiol* **277**: R1760-1770.

340. **Yang ZJ, Carter EL, Kibler KK, et al.** (2012) "Attenuation of neonatal ischemic brain damage using a 20-HETE synthesis inhibitor". *J Neurochem* **121**: 168-179.

341. **Young AR, Ali C, Duretete A, et al.** (2007) "Neuroprotection and stroke: time for a compromise". *J Neurochem* **103**: 1302-1309.

342. **Young KD, Gausche-Hill M, McClung CD, et al.** (2004) "A prospective, population-based study of the epidemiology and outcome of out-of-hospital pediatric cardiopulmonary arrest". *Pediatrics* **114**: 157-164.

343. **Yu M, Cambj-Sapunar L, Kehl F, et al.** (2004) "Effects of a 20-HETE antagonist and agonists on cerebral vascular tone". *Eur J Pharmacol* **486**: 297-306.

344. **Yu M, Sun CW, Maier KG, et al.** (2002) "Mechanism of cGMP contribution to the vasodilator response to NO in rat middle cerebral arteries". *Am J Physiol Heart Circ Physiol* **282**: H1724-1731.

345. **Yu Z, Xu F, Huse LM, et al.** (2000) "Soluble epoxide hydrolase regulates hydrolysis of vasoactive epoxyeicosatrienoic acids". *Circ Res* **87**: 992-998.

346. **Yue H, Jansen SA, Strauss KI, et al.** (2007) "A liquid chromatography/mass spectrometric method for simultaneous analysis of arachidonic acid and its endogenous eicosanoid metabolites prostaglandins, dihydroxyeicosatrienoic acids, hydroxyeicosatetraenoic acids, and epoxyeicosatrienoic acids in rat brain tissue". *J Pharm Biomed Anal* **43**: 1122-1134.

347. **Zangar RC, Davydov DR, and Verma S**. (2004) "Mechanisms that regulate production of reactive oxygen species by cytochrome P450". *Toxicol Appl Pharmacol* **199**: 316-331.

348. **Zhang JP, and Sun GY**. (1995) "Free fatty acids, neutral glycerides, and phosphoglycerides in transient focal cerebral ischemia". *J Neurochem* **64**: 1688-1695.

349. **Zhang L, Ding H, Yan J, et al.** (2008a) "Genetic variation in cytochrome P450 2J2 and soluble epoxide hydrolase and risk of ischemic stroke in a Chinese population". *Pharmacogenet Genomics* **18**: 45-51.

350. **Zhang W, Iliff JJ, Campbell CJ, et al.** (2009) "Role of soluble epoxide hydrolase in the sex-specific vascular response to cerebral ischemia". *J Cereb Blood Flow Metab* **29**: 1475-1481.

351. **Zhang W, Koerner IP, Noppens R, et al.** (2007) "Soluble epoxide hydrolase: a novel therapeutic target in stroke". *J Cereb Blood Flow Metab* **27**: 1931-1940.

352. **Zhang W, Otsuka T, Sugo N, et al.** (2008b) "Soluble epoxide hydrolase gene deletion is protective against experimental cerebral ischemia". *Stroke* **39**: 2073-2078.

353. **Zonta M, Angulo MC, Gobbo S, et al.** (2003) "Neuron-to-astrocyte signaling is central to the dynamic control of brain microcirculation". *Nat Neurosci* **6**: 43-50.

354. **Zordoky BN, Aboutabl ME, and El-Kadi AO**. (2008) "Modulation of cytochrome P450 gene expression and arachidonic acid metabolism during isoproterenol-induced cardiac hypertrophy in rats". *Drug Metab Dispos* **36**: 2277-2286.

355. **Zordoky BN, and El-Kadi AO**. (2010) "Effect of cytochrome P450 polymorphism on arachidonic acid metabolism and their impact on cardiovascular diseases". *Pharmacol Ther* **125**: 446-463.